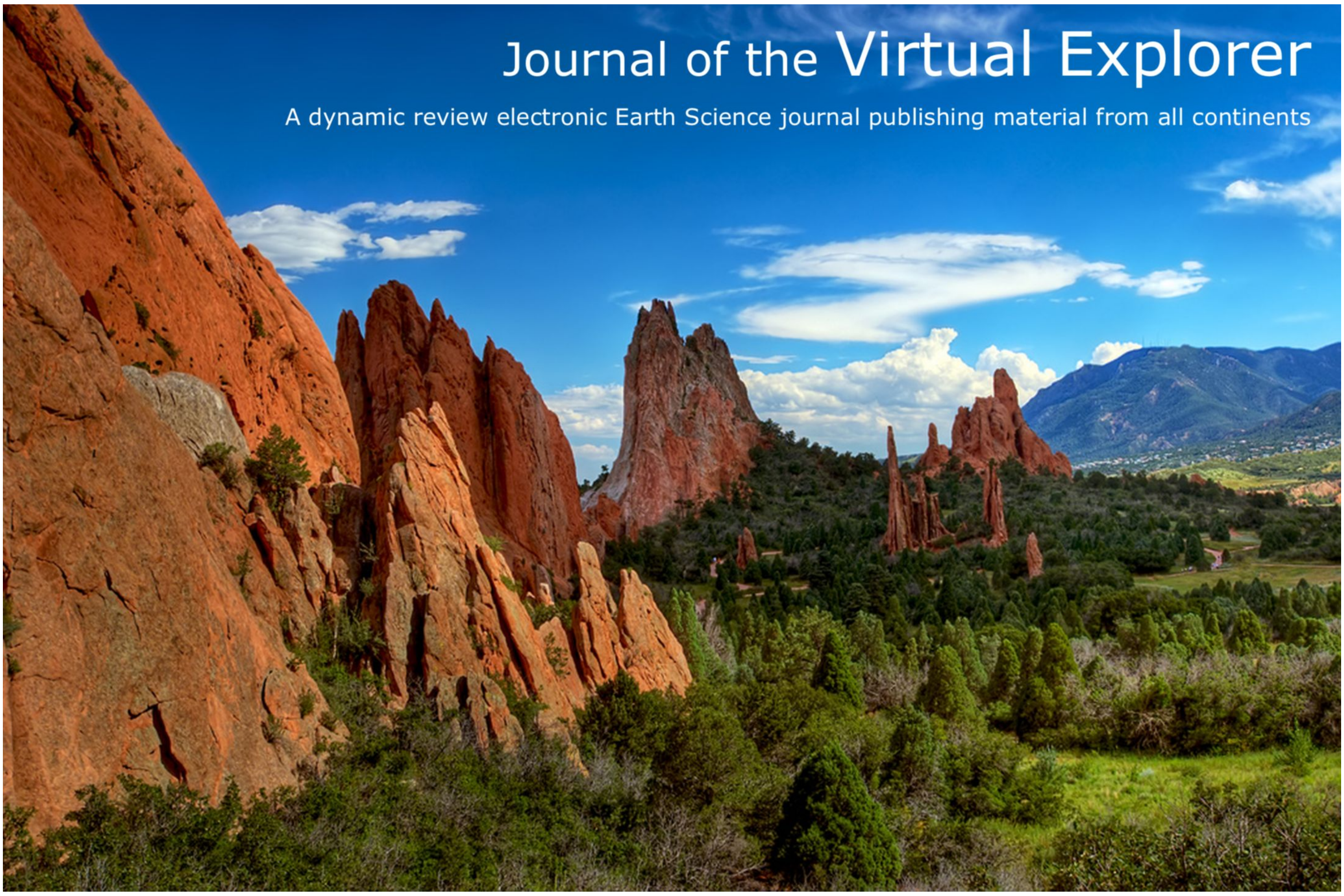

Leucite-bearing (kamafugitic/leucititic) and –free (lamproitic) ultrapotassic rocks and associated shoshonites from Italy: constraints on petrogenesis and geodynamics

Sandro Conticelli, Marinella A. Laurenzi, Guido Giordano, Massimo Mattei, Riccardo Avanzinelli, Leone Melluso, Simone Tommasini, Elena Boari, et al

Journal of the Virtual Explorer, Electronic Edition, ISSN 1441-8142, volume **36**, paper 20
In: (Eds.) Marco Beltrando, Angelo Peccerillo, Massimo Mattei, Sandro Conticelli, and Carlo Doglioni, The Geology of Italy: tectonics and life along plate margins, 2010.

Journal of the Virtual Explorer, 2010
Volume 36
Paper 20
http://virtualexplorer.com.au/

Leucite-bearing (kamafugitic/leucititic) and –free (lamproitic) ultrapotassic rocks and associated shoshonites from Italy: constraints on petrogenesis and geodynamics

Sandro Conticelli

1. Dipartimento di Scienze della Terra, Università degli Studi di Firenze, Via Giorgio La Pira, 4, I-50121, Firenze, Italy. *Email: sandro.conticelli@unifi.it*
2. Istituto di Geoscienze e Georisorse, Consiglio Nazionale delle Ricerche, Via Giorgio La Pira, 4, I-50121, Firenze, Italy.

Marinella A. Laurenzi

Istituto di Geoscienze e Georisorse, Consiglio Nazionale delle Ricerche, Via Moruzzi, 1, I-56124, Pisa, Italy

Guido Giordano

Dipartimento di Scienze Geologiche, Università degli Studi di Roma III, Largo San Leonardo Murialdo, 1, I-00146, Roma, Italy.

Massimo Mattei

Dipartimento di Scienze Geologiche, Università degli Studi di Roma III, Largo San Leonardo Murialdo, 1, I-00146, Roma, Italy.

Riccardo Avanzinelli

Dipartimento di Scienze della Terra, Università degli Studi di Firenze, Via Giorgio La Pira, 4, I-50121, Firenze, Italy.

Leone Melluso

Dipartimento di Scienze della Terra, Università degli Studi di Napoli Federico II, Via Mezzocannone, 8, I-80138, Napoli, Italy

Simone Tommasini

Dipartimento di Scienze della Terra, Università degli Studi di Firenze, Via Giorgio La Pira, 4, I-50121, Firenze, Italy

Elena Boari

Dipartimento di Scienze della Terra, Università degli Studi di Firenze, Via Giorgio La Pira, 4, I-50121, Firenze, Italy

Francesca Cifelli

Dipartimento di Scienze Geologiche, Università degli Studi di Roma III, Largo San Leonardo Murialdo, 1, I-00146, Roma, Italy.

Giulia Perini

Scuola Secondaria di I° Grado Enrico Fermi, Via Enrico Fermi, 4, I-52020, Laterina (AR), Italy.

Abstract: In Italy and surroundings, leucite-free (i.e., lamproites), leucite-bearing (i.e., kamafugites, leucitites, plagioclase-leucitites), and haüyne-bearing (i.e., haüynites, haüyne-leucitites) ultrapotassic igneous rocks have been recorded from Oligocene to present in association with shoshonitic, and high-K calc-alkaline volcanic rocks.

The oldest outcrops of ultrapotassic and related rocks are found within the western Alps in the form of lamprophyric to calc-alkaline dykes intruded during the Oligocene. Four different magmatic provinces, characterised by the association of ultrapotassic igneous rocks with shoshonitic to calc-alkaline series, are also found along the Tyrrhenian margin of the peninsula. These rocks have been produced from Miocene to Holocene with an eastward/southeastward migration with time. Leucite-free silica-rich ultrapotassic lamproitic rocks are restricted to the early stages of magmatism, whereas ultrapotassic leucite-bearing rocks to the middle and late stages.

Mafic ultrapotassic igneous rocks are enriched in incompatible trace elements, with variable fractionation of Ta, Nb, and Ti with respect to Th and Large Ion Lithophile elements, and variable enrichment in radiogenic Sr and Pb and unradiogenic Nd. These characteristics are reconducted to sediment recycling within the upper mantle via subduction. Recycling of carbonate-rich pelites plays an important role in the genesis of leucite-bearing magmas.

Large volume of metasomatic components is predicted to be accommodated within a vein network in the sub-continental lithospheric mantle. Partial melting of the vein generates ultrapotassic magmas, either lamproitic or kamafugitic. Increased interaction between the metasomatic veins and the surrounding mantle dilutes the alkaline component producing shoshonites and high-K calc-alkaline suites. The addition of a further subduction-related component shortly before magma generation is required to explain the isotopic composition of rocks from the Neapolitan district, together with the probable arrival of a within-plate component from the Adria mantle through slab-tear.

Citation: 2010. Leucite-bearing (kamafugitic/leucititic) and –free (lamproitic) ultrapotassic rocks and associated shoshonites from Italy: constraints on petrogenesis and geodynamics. In: (Eds.) Marco Beltrando, Angelo Peccerillo, Massimo Mattei, Sandro Conticelli, and Carlo Doglioni, *Journal of the Virtual Explorer*, volume **36**, paper 20, doi: 10.3809/jvirtex.2010.00251

Journal of the Virtual Explorer, 2010
Volume 36
Paper 20

Dedication

The present paper is dedicated to the memories of Fabrizio Innocenti and Renato Funiciello who passed away on January 27th, 2009 and August 14th, 2009, respectively.

Brief historical outline and lithologic terminology

The potassic magmatism in the Central Mediterranean area developed through time from Oligocene to present, the last eruption of leucite-bearing magmas occurring in 1944 A.D. at Vesuvius. A pioneering comprehensive study performed by Washington (1906) grouped the several magmatic potassic and ultrapotassic suites in three different magmatic regions on the basis of sole mineralogical and petrographic characteristics: the Tuscan, Roman and Apulian regions. These regions were established without any temporal constraints. Washington (1906) did not describe and group the potassic volcanic rocks from Western Alps, Corsica, Tuscan Archipelago, and intra-Apennine area (Umbria). Washington (1906) also used a local lithologic terminology with rocks terms ranging from Vulsinite, Ciminite, Vicoite, Italite, Sommaite, etc.; rock names not used anymore in the international terminology (Le Maitre *et al.*, 2002).

No further comprehensive studies have been performed until the early sixties when Marinelli (1961, 1967) reviewed the rocks of Tuscan Magmatic Region, including both mantle derived igneous rocks and crustal anatectic ones, volcanic and intrusive, cropping out in the same area from Pliocene to Pleistocene. This study has somewhat complicated the general petrogenetic grid for potassic magmas. Some of the mafic Mg-rich rocks from Tuscan region have been subsequently interpreted as the result of complicate processes of enrichment in MgO, Ni, Cr and other compatible elements by gaseous transfert, starting from a granitic parental magma, of ultimate continental crustal origin (Mazzuoli & Pratesi, 1963; Barberi & Innocenti, 1967; Innocenti, 1967; Barberi *et al.*, 1971). This brought also to perpetuate the hypothesis that leucite-free, Mg-rich, ultrapotassic magmas might have been generated by either direct partial melting of the continental crust or by interaction between leucitic magmas and crustal derived granitic melts (e.g., Taylor & Turi, 1976; Turi & Taylor, 1976; Vollmer, 1976, 1977, 1989; Vollmer & Hawkesworth, 1980; Vollmer *et al.*, 1981; Turi *et al.*, 1991; Gasperini *et al.*, 2002).

Figure 1. Distribution of ultrapotassic and related volcanic and sub-volcanic rocks in Italy and surroundings

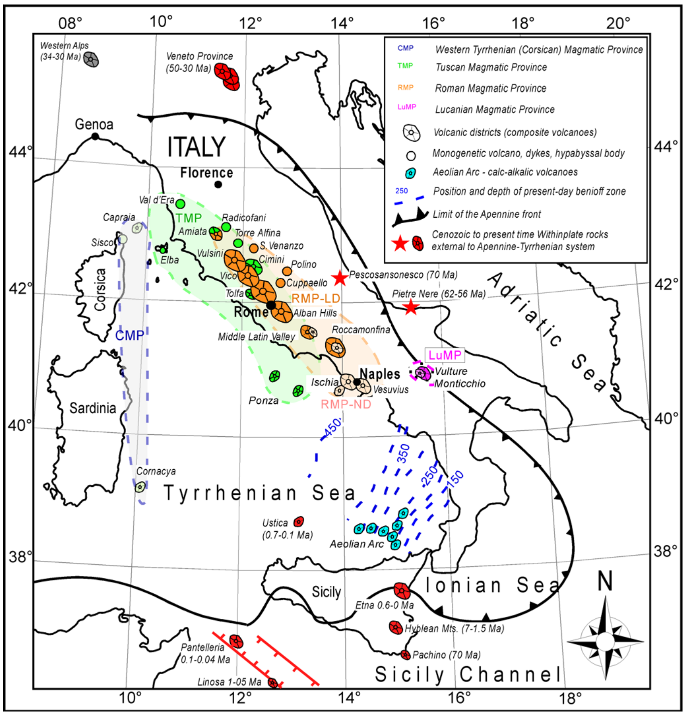

The picture has been modified after Conticelli *et al.*, 2007, 2009b; Avanzinelli *et al.*, 2008, 2009.

Avanzinelli *et al.* (2009) grouped the potassic and associated volcanic rocks of the Central Mediterranean area, by integrating the original division of Washington (1906) with the geochronological and genetic relationships, following the criteria suggested by Turner & Verhoogen (1960). A division in four Magmatic Provinces has been proposed. The Western Tyrrhenian (Corsican) Magmatic Province is the westernmost one, with few magmatic products belonging to volcanic suites ranging from leucite-free ultrapotassic to high-K calc-alkaline of Miocene-Pliocene age (Fig. 1). During Pliocene – Pleistocene, the volcanism migrated eastward to form the Tuscan Magmatic Province (Fig. 1) with emplacement of volcanic rocks belonging to leucite-free ultrapotassic to shoshonitic and calc-alkaline magmatic suites (e.g., Peccerillo *et al.*, 1988; Conticelli & Peccerillo, 1990, 1992; Conticelli *et al.*, 1992, 2001, 2004, 2007, 2009a, 2011a,b; Conticelli, 1998; Peccerillo, 1999, 2005a; Perini *et al.*, 2000, 2003). Coeval intrusive to volcanic silicic rocks of crustal derivation by anatexis have been kept separated because they do not have a common origin, although in some cases hybridization between mantle and crustal derived magmas have been recorded (e.g., Poli *et al.*, 1984;

Pinarelli *et al.*, 1989; Pinarelli, 1991; Innocenti *et al.*, 1992; Poli, 1992, 2004). A further southeastward migration of volcanism during Pleistocene brought to the emplacement of the leucite-bearing ultrapotassic rocks of the Roman Magmatic Province, which in some cases are associated with younger shoshonitic to calc-alkaline suites (e.g., Conticelli *et al.*, 1991, 2002, 2009b; Peccerillo, 2005a,b, and references therein; Boari & Conticelli, 2007; Frezzotti *et al.*, 2007; Boari *et al.*, 2009a). The volcanic activity of the Roman Magmatic Province pierced the boundary with the Holocene in its southernmost district, in the Neapolitan area, where a cluster of four volcanoes with historical volcanic activity occurs(i.e., Ischia, Procida, Phlegrean Fields and Vesuvius volcanoes; Peccerillo, 2005a, and references therein). The Lucanian Magmatic Province is the easternmost volcanic area with the association of Pliocenine haüyne- to leucite-bearing ultrapotassic rocks (e.g., Peccerillo, 2005a and references therein; De Astis *et al.*, 2006; Avanzinelli *et al.*, 2008). A carbonatitic lava has also been found in the activity of the Monticchio volcano, during the final stage of the Lucanian Magmatic Province (e.g. D'Orazio *et al.*, 2007, 2008; Stoppa *et al.*, 2008).

The volcanic suites

Ultrapotassic rocks have been defined using chemical parameters after Carmichael (1971) and Foley *et al.* (1987). A volcanic rock is considered ultrapotassic when it has K_2O > 3 wt. % concomitantly to K_2O/Na_2O = 2 (Le Maitre, 2002). Mineralogical classification of potassic and ultrapotassic rocks is far from being exhaustive and produced a plethora of rock names due also to heteromorphism (Yoder, 1986). Indeed lamproitic rocks on the basis of their mineralogy are made up by a large variety of different rock types; fitzoyite, cedricite, orendite, madupite, wolgidite, cancalite, jumillite, verite, and fortunite are some of the most common lamproitic terms. To avoid this problem and to provide unequivocal classification, Foley *et al.* (1987) suggested a chemical division in three different clans on the basis of chemical parameters: the lamproite, kamafugite, and Roman (plagioclase-leucititic; Foley, 1992a) clans (Fig. 2). In Italy ultrapotassic rocks are associated in time and space also with calc-alkaline lamprophyres, shoshonitic and high-K calc-alkaline volcanic rocks, and at Monticchio volcanic field, within the Lucanian Magmatic Province, with alvikites.

Figure 2. Chemical classification of Ultrapotassic volcanic rocks

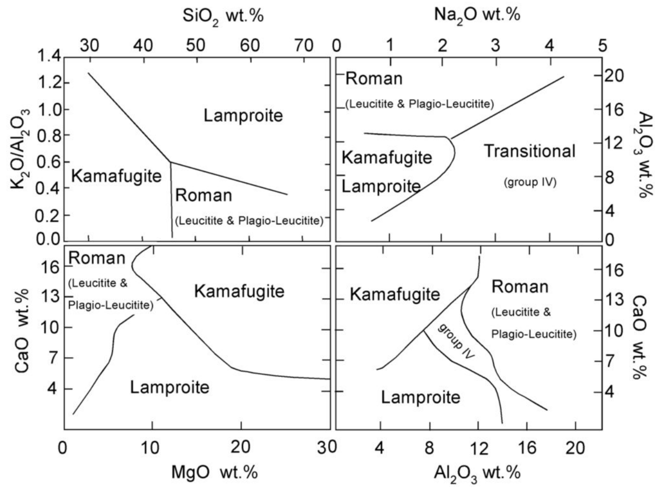

Resemblance classification diagrams after Foley *et al.* (1987), which should be used only with ultrapotassic rocks. In the transitional field fall also some rocks belonging to the shoshonitic series but that matches with the requirements for being considered ultrapotassic.

The **lamproite clan** is made up by Mg-rich alkaline ultrapotassic volcanic to hypabyssal rocks (Foley & Venturelli, 1989). According to Foley *et al.* (1987), the relatively low Al_2O_3, FeO_{Tot}, CaO and Na_2O counterbalanced by extremely high MgO, and extremely variable silica contents, the latter ranging from basic to intermediate compositions are distinctive characteristics (Table 1). Lamproites are invariably plagioclase-free ultrapotassic rocks, characterized by highly forsteritic olivine, chromian spinel, Al-poor clinopyroxene, K-richterite, sanidine, picroilmenite, apatite (Fig. 3); leucite might be present in silica-undersaturated lamproites, but they have never been observed among the lithologies found in the Central Mediterranean (i.e., Corsica, and Tuscany).

The **lamprophyre (calc-alkaline) clan** is an category of sub-volcanic rocks found at convergent plate margins (Rock, 1989). Their names are based on the mineralogy, on the basis of the occurring feldspar and of the possible occurrence of amphibole (Le Maitre, 2002); minette, spessartite, and kersantite are the rock names. They are potassic to ultrapotassic with higher alumina and lime with respect to lamproites (Table 1), but in some cases they are chemically very similar to lamproitic and transitional ultrapotassic rocks (Fig. 2) on the basis of the criteria suggested by Foley *et al.* (1987).

Table 1. Characteristics of the different ultrapotassic, potassic and associate rocks in Central Mediterranean Region.

Clan or series	Type	Chemistry	Mineralogy	Note
Lamproite	Ultrapotassic	CaO < 10 wt.% Na_2O < 1.5 wt.% Al_2O_3 < 12 wt.%	olivine (Fo_{95-85}), clinopyroxene, phlogopite, K-richterite, chromite, sanidine, picroilmenite, magnetite, apatite	Plagioclase-free
Lamprophyre	Ultrapotassic	CaO < 12 wt.% Na_2O < 2 wt.% Al_2O_3 < 14 wt.%	olivine (Fo_{90-85}), clinopyroxene, horneblende, riebeckite-ardvedsonite, phlogopite, chromite, sanidine, plagioclase, magnetite, apatite	Leucite-free
Kamafugite	Ultrapotassic	CaO > 15 wt.% Al_2O_3 < 14 wt.%	olivine (Fo_{95-85}), monticellite, clinopyroxene, phlogopite, chromite, melilite, leucite, kalsilite, perovskite, ilmenite, magnetite, apatite	Feldspar-free
Leucitite Plagio-leucitite	Ultrapotassic	CaO > 15 wt.% Al_2O_3 > 14 wt.%	olivine (Fo_{90-85}), chromite, clinopyroxene, leucite, plagioclase, nepheline, phlogopite, melilite, magnetite, sphene, apatite	
Haüyne-leucitite	Ultrapotassic	CaO > 15 wt.% Al_2O_3 < 12 wt.%	olivine (Fo_{90-80}), chromite, clinopyroxene, leucite, haüyne, nepheline, cancrinite, noseana, melilite, magnetite, apatite	Plagioclase-free
Shoshonite	Potassic	CaO > 15 wt.% Al_2O_3 > 15 wt.%	olivine (Fo_{90-75}), chromite, clinopyroxene, plagioclase, sanidine, biotite, ilmenite, magnetite, apatite	
High-K calc-alkaline	Sub-alkaline	CaO > 15 wt.% Al_2O_3 > 15 wt.%	olivine (Fo_{90-75}), chromite, clinopyroxene, plagioclase, sanidine, biotite, ilmenite, magnetite, apatite	
Alvikites	Carbonatitic	CaO > 30 wt.%	olivine, monticellite, melilite, calcite, clinopyroxene, magnetite	Calcite-bearing

The **kamafugite clan** is a group of rare kalsilite-bearing melilitites described for the first time by Holmes & Harwood (1932) and Holmes (1940). Because of the extreme mineralogical variability each rock recorded has taken the name of the locality where it was discovered, but heteromorphism do also occur as in lamproites (Yoder, 1986); Sahama (1974) suggested to keep the old names (i.e., katungite, mafurite, ugandite) for each single rock, but to collect them in a unique clan with a root name from the acronym of the African members: **Ka**tungite – **Maf**urite – **Ug**andite. Gallo *et al.* (1984) suggested the inclusion in the kamafugite clan also of the Italian terms, such as the coppaellite and the venanzite. Kamafugitic rocks are ultrapotassic but strongly silica and alumina undersaturated; with this respect they are larnite normative. According to the definition of Foley *et al.* (1987), kamafugite clan is made up by Mg-rich alkaline ultrapotassic volcanic rocks characterised by relatively low SiO_2, Al_2O_3 and FeO_{Tot} but extremely high CaO and Na_2O contents (Fig. 2; Table 1). Kamafugites are feldspar-free rocks although dominated by kalsilite, nepheline, and sometimes leucite as felsic phases and olivine, clinopyroxene, phlogopite, and melilite (Fig. 3) among the mafic ones (Sahama, 1952, 1954, 1960; Gragnani, 1972; Yoder 1976, 1979; Gallo *et al.*, 1984; Cundari & Ferguson, 1991; Conticelli & Peccerillo, 1992).

The **Roman rocks** are leucite-bearing silica undersaturated ultrapotassic rocks and they are known worldwide since the original work by Washington (1906). Originally, a plethora of names has been used also for this group of rocks. These names recall the occurrence locality for the specific rock type (e.g., vulsinite, ciminite, cecilite, vicoite, italite, etc.). Le Maitre (2002) suggested a classification based on mineralogical and chemical parameters (Total Alkali Silica), thus leucite-bearing basanite, tephrite, phonolitic tephrite, tephritic phonolite, and phonolite are presently the basic names beside the term leucitite. All these rocks might be classified in a group name termed **leucitite and plagio(clase)-leucitite clan** on the base of the frequent occurrence of modal plagioclase (Foley, 1990a). According to the definition of Foley *et al.* (1987) the leucitite and plagio(clase)-leucitite clan (i.e., Roman rocks) is made up by alkaline ultrapotassic volcanic rocks characterised by widely variable MgO, with relatively low SiO_2, and FeO_{Tot}, but relatively high CaO, Al_2O_3, and Na_2O contents (Fig. 2; Table 1). This group of rocks was also defined by Appleton (1972) as high potassium series. The relative acronym, HKS, has been widely used in the specific scientific literature about Roman rocks. We prefer the use of the leucitite and plagioleucitite clan because self explanatory of the main mineralogical characteristics of these rocks, and not locally related to the Italian magmatism. Leucite is ubiquitously present with plagioclase missing only in the most silica undersaturated terms (Fig. 3).

The **haüyne-bearing clan** is made up by highly silica undersaturated volcanic rocks characterised by high levels of both K_2O and Na_2O (De Fino *et al.*, 1987; Beccaluva *et al.*, 2002). Haüyne is also found as phenocryst along with leucite and rarely nepheline (Table 1; Fig. 3). These rocks are confined in the Lucanian Magmatic Province and have low silica contents. They are found associated to melilite-bearing rocks and alvikites.

All rocks with approximately 50 % vol. of carbonate minerals can be classified as **carbonatite**. Calcium-, Magnesium- and Iron carbonatite are divided on the basis of the main carbonate phase in the mode of the rock; namely calcite, dolomite, ankerite. Alvikites is a silica-rich calcium-carbonatite that is distinguished by Sövite on the basis of trace element contents (Le Bas, 1999). A hot debate about the occurrence of primary carbonatite clan in Italy is open since the end of the last century. Stoppa & Woolley (1997) made a review of the possible occurrence of carbonatite-like rocks in Italy, but some of them have been questioned to be real carbonatites. In some cases they have been classified as pyrometamorphic rocks due to either natural or anthropogenic combustion of marly sedimentary rocks (e.g. Melluso *et al.*, 2003, 2005a, 2005b; Capitanio *et al.* 2004; Stoppa *et al.*, 2005), in other cases some of them have been questioned as the result of carbonate sintexis to provide a wide spectrum of minerals, according to the findings of Tilley (1952), resulting in a dilution of major and trace element contents, but not of CaO (Peccerillo 1998; Peccerillo, 2004, 2005b, Wolley *et al.*, 2005). Unquestioned mantle-derived alvikitic rocks have been documented at Monticchio monogenetic field (e.g., Jones *et al.*, 2000; D'Orazio *et al.*, 2007).

The **shoshonitic series** is a magmatic sequence of rocks mildly enriched in potassium, with variably silica saturated terms in the most evolved rocks. The rock types range from potassic trachybasalt (shoshonitic basalt) to trachyte, passing through shoshonite s.s. and latite. These rocks have variable enrichment in K_2O in the most primitive terms. No definitive boundary between ultrapotassic clans and shoshonitic series has been drawn on the K_2O vs. silica diagram (Peccerillo & Taylor, 1976); in some cases shoshonites are ultrapotassic rocks as well (e.g., Conticelli *et al.*, 2011b,c) and they fall within the field of transitional group IV ultrapotassic rocks (Fig. 2) according to the classification scheme of Foley *et al.* (1987). In Italy this group of rocks has been originally recognised by Appleton (1972) at Roccamonfina volcano, who distinguished them as a low potassium series (LKS) group from the leucite-bearing ultrapotassic series (high potassium series; HKS). Later Civetta *et al.* (1981) renamed them as potassic series (KS) keeping the Appleton's (1972) name for the leucite-bearing terms. Conticelli & Peccerillo (1992) interpreted the rocks belonging to this series as transitional (TRANS) from ultrapotassic series to calc-alkaline series. Conticelli *et al.* (2004) preferred the use of shoshonite the official names provided by IUGS (Le Maitre, 2002).

Figure 3. Microphotographs of thin sections of ultrapotassic and related volcanic and sub-volcanic rocks in Italy and surroundings

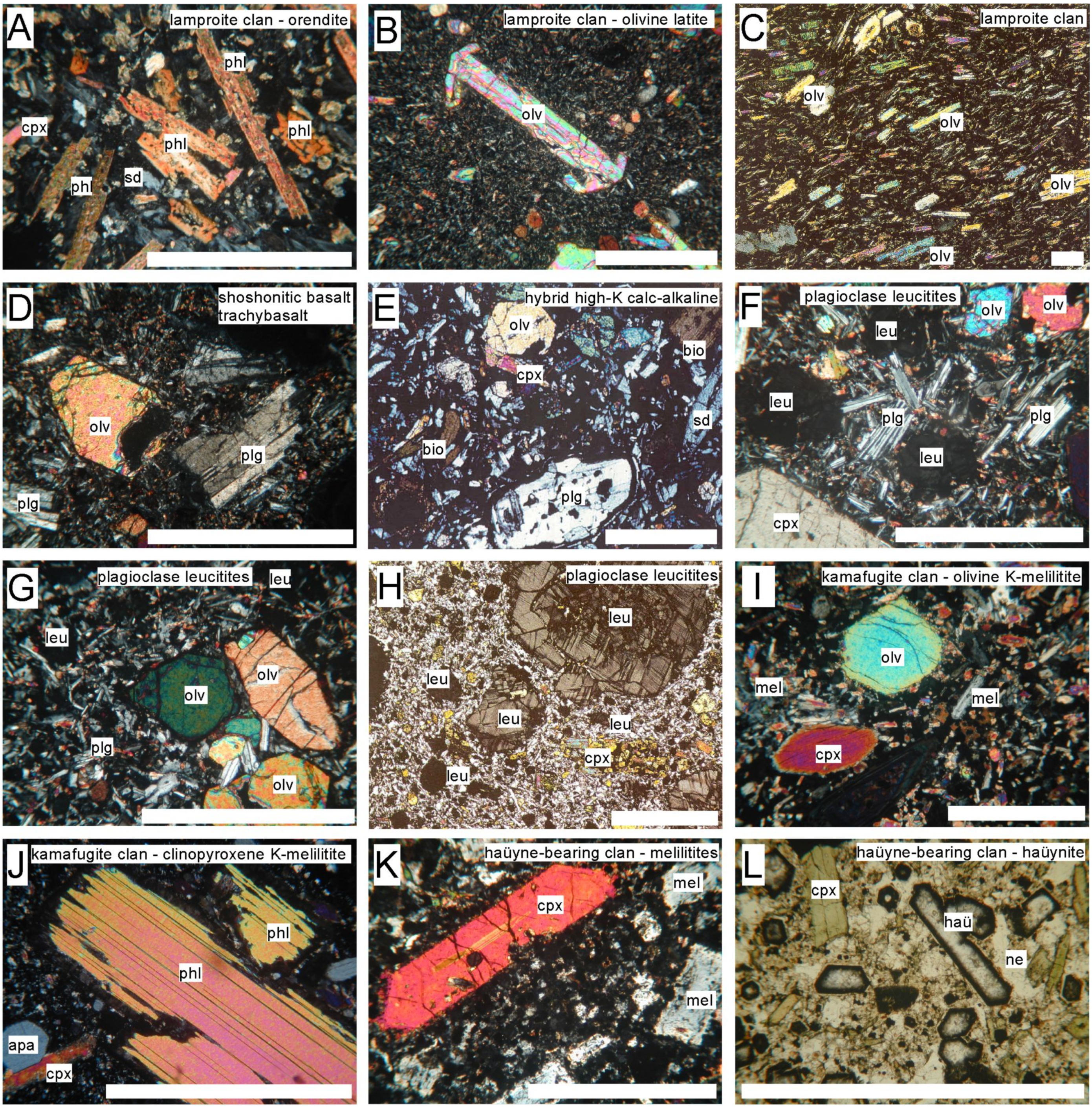

Photos have been performed at polarized microscope by Sandro Conticelli and Leone Melluso. White bar is 2 mm long. Legend: apa = apatite; bio = biotite; cpx = clinopyroxene; haü = haüyne; leu = leucite; mel = melilite; ne = nepheline; olv = olivine; phl = phlogopite; plg = plagioclase; sd = sanidine. Localities and Magmatic Provinces: A) Orciatico, Tuscan Magmatic Province; B) Torre Alfina, Tuscan Magmatic Province; C) Torre Alfina, Tuscan Magmatic Province; D) Radicofani, Tuscan Magmatic Province; E) Monte Amiata, hybrid volcano; F) Vesuvius, 1631-1944 A.D., Roman Magmatic Province – Neapolitan District (ND); G) Roccamonfina, Roman Magmatic Province; H) Vulsini, Roman Magmatic Province; I) San Venanzo, Roman Magmatic Province; J) Cupaello, Roman Magmatic Province; K) Pedra della Scimmia - Vulture, Lucanian Magmatic Province; L) Melfi - Vulture, Lucanian Magmatic Province.

The **high-K calc-alkaline** and **calc-alkaline series** are defined on the basis of K_2O contents with respect to silica (Peccerillo & Taylor, 1976). They also match the chemical and mineralogical parameters provided by Arculus (2003). They are sub-alkaline rock with terms ranging from basalts to rhyolites, passing through basaltic andesite, andesite, and dacite (Le Maitre, 2002). The pre-fix high-K is added when needed according to the Peccerillo & Taylor's (1976) scheme (Fig. 8b). These rocks are more represented within the ultrapotassic association of the Italian pensula than previously though (Di Girolamo *et al.*, 1976; Perini *et al.*, 2000; Conticelli *et al.*, 2004, 2009a, 2010a,b; Boari & Conticelli, 2007; Frezzotti *et al.*, 2007; Boari *et al.*, 2009a).

The Geodynamic framework

The present-day structure of the Central Mediterranean region derives from the convergence of Africa and Eurasia, which over the Tertiary occurred at about 1-2 cm/yr on average, with a total value estimated in about 400-500 km (Dewey *et al.*, 1989). During such time, the Ionian-Adriatic lithosphere continuously subducted toward west and northwest underneath the Eurasia plate. This process led to the progressive closure of the intervening Mesozoic oceanic basins of the Tethyan domain, with the formation of a complex arcuate orogenic belt (Apennine- Maghrebide belt) and extensional back-arc basins (Ligure-Provençal and Tyrrhenian basin) (Dewey *et al.*, 1989; Horvath & Berckheimer, 1982). The subducting slab is still recognizible beneath the Calabrian arc, where deep seismicity is detected along a narrow (~ 200 km) and steep (70°) Benioff plane dipping northwestward down to about 500 km. Continental collision is probably still active in the central-northern Apennines, where intermediate earthquakes occur down to 90 km (Selvaggi & Amato, 1992; Carminati *et al.*, 2005).

The Africa-Eurasia convergence and the consequent subduction of the Ionian-Adriatic lithosphere, resulted in the building of the Alps-Apennine belts. The main geological evidence of such process within the Apennine chain are the deposition of thick siliciclastic deposits in the foredeep basins and the HP/LT metamorphism, in the internal part of the orogenic wedge (Jolivet *et al.*, 1998). In the Apennines, the migration of the orogenic front is marked by the onset of siliciclastic deposits, which are progressively younger toward the Adriatic-Ionian foreland. The onset of siliciclastic deposition occurred in northern Apennines during the Late Cretaceous in the Ligurian oceanic domain, which was deformed during Late Cretaceous to Early Eocene time, and formed a double vergent accretionary wedge, now outcropping from Corsica to the Italian peninsula (Treves, 1984; Carmignani *et al.*, 1994). Starting from the Oligocene onwards, foredeep basins migrated eastward and formed on the top of continental crust, pertaining to the passive margin of Apulia. Their incorporation into the Apenninic orogenic wedge marked the subduction of Adriatic continental lithosphere underneath Europe. Afterwards, during the Neogene, the foredeep basins further migrated toward the Apulia foreland ahead of the eastward migrating orogenic front. Foredeep basins formed on top of progressively more external units, with an eastward migration and during the Quaternary reached the configuration in the Adriatic foreland, where the foredeep deposition ceased (Cipollari & Cosentino, 1995, and references therein). During the Quaternary the southeastward rollback of the subducting Ionian plate was expressed in the southern Apennines by the progressive southeastward shifting (parallel to the longitudinal axis of the chain) of the Bradanic foredeep basin (Tropeano *et al.*, 2002, and references therein) and of the Apenninic outer thrust front, which is presently located off-shore, in the Ionian Sea (Doglioni *et al.*, 1999 and references therein).

In the central-western Mediterranean, differential trench retreat of the Ionian-Adriatic slab caused the formation of the Liguro-Provençal and Tyrrhenian back arc basins (Malinverno & Ryan, 1986; Lonergan & White, 1997; Faccenna *et al.*, 2001; 2004). The Liguro-Provençal spreading took place simultaneously with the eastward drift of the Corsica-Sardinia block, which rotated counterclockwise about a pole located north of Corsica (e.g., Van der Voo, 1993; Speranza *et al.*, 2002 and references therein). Rifting and drifting processes in the Corsica-Sardinia were related to the southeastward retreat of the subducting Ionian slab, and were accompanied by arc-related volcanism, which appeared first in Sardinia (~32My) and in Provençe and continued until ~14 My in southwestern Sardinia (i.e., Beccaluva *et al.*, 1985; Lustrino *et al.*, 2004).

After the end of the Corsica-Sardinia drifting, back-arc extension continued in the southern Tyrrhenian Sea. In this basin, oceanic crust formed diachronously in two sub-basins: between ~4.3 and 2.6 Ma the Vavilov basin was formed, whereas the Marsili basin developed after

~2 Ma (Marani & Trua, 2002; Nicolosi *et al.*, 2006). Seismic, structural and stratigraphic data on the on-shore western Calabria-Peloritani terrane (Mascle *et al.*, 1988; Sartori, 1990; Mattei *et al.*, 2002) suggest that rifting started along the western margin of the southern Tyrrhenian Sea (Sardinian margin) during Serravallian, and progressively migrated south-eastward in the Vavilov (late Messinian-Early Pliocene) and Marsili (Late Pliocene-Early Pleistocene) basin. In the northern Tyrrhenian Sea lithospheric extension caused the formation of Neogene sedimentary basins. N-S to NW-SE oriented extensional basins developed on the previously thickened Alpine crust in the hinterland, contemporary with flexural basins in the foreland (e.g., Kastens *et al.*, 1988) which get younger eastward as well documented by the age of the infilling sedimentary sequences. In the westernmost Tyrrhenian sea these sedimentary sequences are Lower Miocene in age and are characterized by N-S trending east-dipping normal faults (Bartole, 1995) while they are Pleistocene in age in the Umbrian region, where extensional tectonics is presently active and most of the normal faults strike NW-SE and dip westward (Jolivet *et al.*, 1998; Collettini *et al.*, 2006).

Present day tectonics and kinematics

Space geodesy investigations, the distribution of seismicity, geological, structural and paleomagnetic data provide a framework of the recent tectonic evolution of the Italian geodynamics, which is substantially different from that active during the Neogene and Pleistocene (until about 1 Ma), where the processes of subduction and opening of backarc basins do not appear active anymore (D'Agostino & Selvaggi, 2004; Goes *et al.*, 2004; Mattei *et al.*, 2007). The GPS data show that in Italy the current convergence between Eurasia and Nubia (the African plate with the exception of the region east of the East African Rift) is about 5-6 mm / year and oriented NW (Fig. 4) (Sella *et al.*, 2002; D'Agostino & Selvaggi, 2004). The study of earthquakes and tectonics, however, has recently suggested that the manner in which this convergence is absorbed along the margin between the two plates is extremely complex, given the coexistence of compressive and extensional deformation along a wide area stretching from north Africa to Greece, and affecting also the entire Italian peninsula (McKenzie, 1972; Pondrelli *et al.*, 1995; Goes *et al.*, 2004). The existence of areas with low or no seismicity has suggested the possible presence of kinematically independent microplates between Eurasia and Africa. In particular, the distribution of earthquakes (Anderson & Jackson, 1987) and recent geodetic data (Ward, 1994; D'Agostino and Selvaggi, 2004; Goes *et al.*, 2004) shows that the Adriatic region currently moves to NE respect to Eurasia, and has therefore an independent motion relative to both the Nubia and European plates (Fig. 4).

Figure 4. GPS velocities relative to Eurasia of continuous stations in Italy.

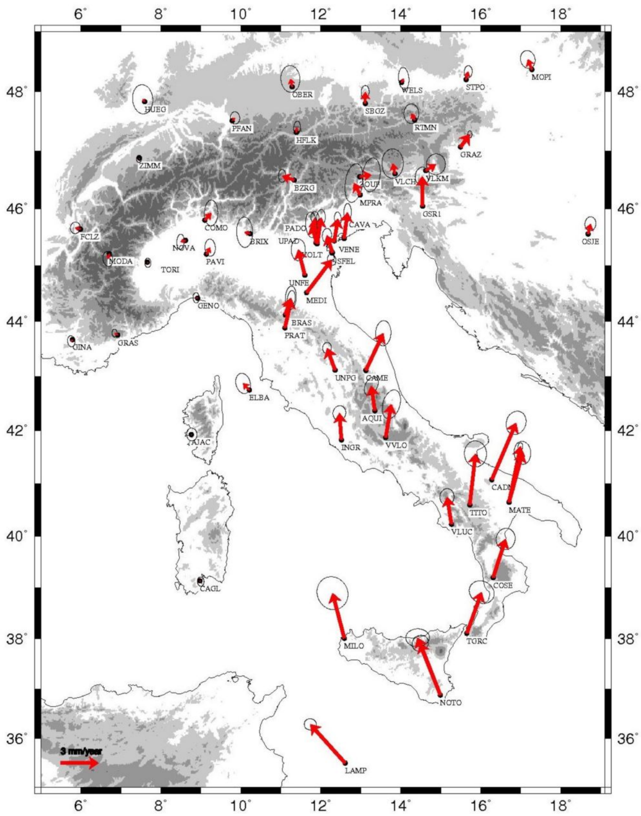

Velocities relative to Eurasia defined from continuous stations in Italy of Global Positioning Systems. Error ellipse represents the 95% confidence interval (drawn after D'Agostino & Selvaggi, 2004 and Mattei *et al.*, 2008).

These results are consistent with several geological and paleomagnetic data that show a gradual deactivation of the compressional outer fronts of the Apennines and Sicily, the gradual decrease of the subduction processes in the Italian region and the end of the curvature processes of the Northern Apennines and the Calabrian Arc (Mattei *et al.*, 2004; Cifelli *et al.*, 2007; Mattei *et al.*, 2007). These data suggest that the convergence between

Africa and Eurasia is currently absorbed by the motion of the Adriatic microplate, rather than by subduction of Adriatic-Ionian lithosphere. At the same time geodetic data show that the Adriatic area is kinematically independent from the Apennine area, which shows velocity vectors oriented NNW respect to Eurasia, confirming the existence of a band of active deformation in the axis of the chain already highlighted by the study of seismicity and geological analysis (Valensise & Pantosti, 2001 and references cited). In this same area studies of deformation based on geodetic triangulation shows that the region is currently subject to an extension rate of about 3-5 mm/year NE-SW oriented (Hunstad *et al.*, 2003), which is consistent with the focal mechanisms and the distribution of the major historical and instrumental earthquakes which occurred in the axial zone of the Apennine chain.

D'Agostino *et al.* (2008), on the base of GPS observations and earthquake slip vectors, suggest that the kinematics of the Adriatic region is controlled by the presence of two distinct microplates: Adria (corresponding with the northern Adriatic region) and Apulia (corresponding with the southern Adriatic, Ionian and Hyblean regions), whose relative motion controls the active deformation in the central Adriatic Sea. The opposite rotations (counterclockwise for Adria and clockwise for Apulia) of these two microplates respect to Europe are able to explain the present-day deformation pattern in the central Adriatic region and represent the way in which the relative motion between Nubia and Eurasia is presently accommodated in the Central Mediterranean region.

Structural and geological features of the extensional Tyrrhenian margin

In the westernmost northern Tyrrhenian Sea, where the Western Tyrrhenian (Corsican) Magmatic Province occur (Fig. 1), the sedimentary sequences that infill the extensional sedimentary basins are Lower Miocene in age and they are bounded by N-S trending east-dipping normal faults (Bartole, 1995), whilst in the Apennine region they are Pleistocene in age, where extensional tectonics is presently active and most of the normal faults strike NW-SE.

In the central Tyrrhenian margin, the onset of extensional tectonics can be dated at the Late Miocene because syn-rift sedimentary sequences have been recognized in extensional basins located between the Tolfa-Cerite-Manziana and Roccamonfina volcanoes (Fig. 1). In the Southern Tyrrhenian margin, south of the Roccamonfina area, extensional tectonics started more recently than in the northern and central Tyrrhenian margin, with similar eastward temporal migration. In this region the onset of the extension is marked by Late Pliocene syn-rift sedimentary marine deposits that crop out along the Tyrrhenian coast of the Campania region. Extension later progressed toward the axis of the Apennine chain, where sedimentary basins are filled by lower-middle Pleistocene continental sequences (Cinque *et al.*, 1993), and the largest ($M > 6.7$) historical and instrumental seismicity ever recorded occurred.

In Northern Apennines extensional tectonics is mostly controlled by NW-SE oriented, east-dipping low-angle normal faults and associated high-angle east-dipping normal faults. Low-angle normal faults gently dipping toward the east, show evidence of present-day activity along the axial part of the Apennine chain, whereas their old equivalents are now outcropping along the western part of the margin. Here exhumed normal faults have been widely recognized in the Alpine metamorphic units in the Elba and Giglio Island, offshore Tuscany (Jolivet *et al.*, 1998; Collettini *et al.*, 2006). Toward the south, the existence of low-angle normal faults is less evident and active extension is mainly given by high-angle normal faults, NW-SE oriented. In Central Apennines high-angle active normal faults are mostly dipping toward the west. Such faults show a long term tectonic activity, which is responsible for the formation of large intermontane extensional basins, infilled by Late Pliocene-Quaternary continental sedimentary sequences (D'Agostino *et al.*, 2001; Cavinato *et al.*, 2002). High-angle NW-SE oriented, west dipping, normal faults are especially evident along the axis of the Apennine chain. Conversely, toward the west normal faults are covered by Quaternary volcanic deposits and their existence has been recognized by means of geophysical investigations and deep boreholes drilled for geothermal research (Barberi *et al.*, 1994).

In Southern Apennine, active normal faults are at high-angle and NW-SE oriented and they are either dipping toward the east or toward the west. In particular, field observations and seismological data show that the fault responsible of the Irpinia 1981 $M = 6.5$ earthquake occurred along a NW-SE oriented east-dipping normal fault (Westaway & Jackson, 1984; Pantosti *et al.*, 1993), whereas, some of the most important intermontane Quaternary extensional basins are bounded by NW-SE west dipping oriented normal faults.

All along the extensional Tyrrhenian margin an important role is exerted by transverse tectonic structures, NE-SW oriented, which either bound some of the major extensional sedimentary basins in the area, or represent the tectonic elements along which the main segments of the NW-SE oriented normal faults reverse their dip directions (Faccenna *et al.* 1994a; Acocella & Funiciello 2006; Barchi *et al.*, 2007). In some cases NE-SW oriented faults also bound major NE-SW oriented extensional sedimentary basins (i.e., Baccinello-Cana, Cerite, Ardea, Garigliano), which formed parallel to the main, NE-SW oriented, stretching direction and play a major role to transfer extension to the different segments of the NW-SE oriented normal faults. The NE-SW normal faults system is particularly important along the western side of the extensional Tyrrhenian margin, whereas assume a minor importance within the axis of the Apennine chain, where extensional basins are NW-SE oriented. In particular, NE-SW tectonic lineaments represent a major factor to control the location of Quaternary volcanoes all along the western Italian peninsula. Most of the Quaternary volcanoes formed where NW-SE normal faults intersect transverse tectonic lineaments, which represent a preferential structure for magma upwelling and fluids emissions (Funiciello & Parotto 1978; Acocella & Funiciello 2006).

Extensional tectonics along the Tyrrhenian margin of the Italian peninsula has produced significant crustal thinning, high thermal flow, mantle fluids, and a characteristic distribution of seismic activity along the Italian Tyrrhenian margin. Crustal thickness has been recently defined in detail along a transect from Northern Corsica to the Adriatic Sea in the framework of the CROP 03 project (Pialli *et al.* 1998; Collettini *et al.* 2006) and using receiver functions from teleseismic data (Piana Agostinetti *et al.*, 2002; Di Bona *et al.*, 2008). Results converge to show the upwelling of Moho in the Tyrrhenian area, where Moho depth is about 22 km, and a progressive westward thickening of the continental crust as far as the Apennine chain, with a maximum crustal thickness of about 35-38 km observed toward the Adriatic foreland. To the west, data indicate a partial overlapping between the deep Adriatic Moho and the shallower Tuscan Moho, with a mantle slice embedded between two crustal slices.

Thermal flow is generally characterized by very high values all along the Tyrrhenian border of the central-northern peninsula, from Tuscany to Campania, but discontinuously distributed. Southern Tuscany and northern Latium have high heat flow (>100 mW/m^2), with localised peaks (>600 mW/m^2), which produce several geothermal fields, with the Larderello one being the most famous worldwide (Mongelli *et al.*, 1991) (Fig. 5). Toward the south-east, thermal flow values are drastically reduced within the Middle Latin Valley, the area comprised between the Colli Albani and the Roccamonfina volcanoes, as a consequence of the presence of thick carbonatic sedimentary sequences hosting huge karstic reservoirs, which buffer heat flow to values lower than standard (30 mW/m^2). It is also noteworthy that the presence of convective support to topography and strong attenuation of seismic waves consistently suggest that a positive thermal structure of the crust-mantle boundary is characteristic of a large region including the Apennine chain and its Tyrrhenian border from southern Tuscany to the Vulture area (Mele *et al.*, 1997; D'Agostino & McKenzie, 1999).

Figure 5. Heat flow and seismicity in Central Italy.

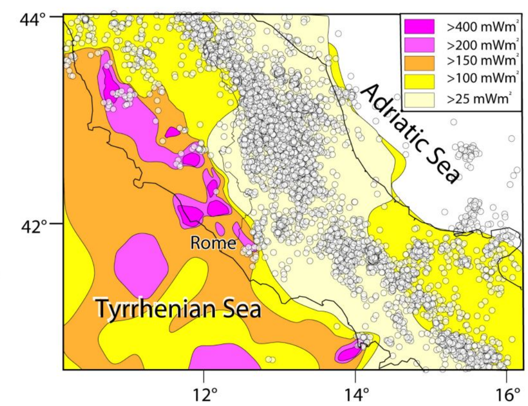

Heat flow and seismicity in Central Italy. Heat flow values are generally very high along the Central-Northern Tyrrhenian margin of the Italian peninsula (Mongelli & Zito, 1991). High values of heat flow correspond to a decrease in seismic activity, which is concentrated along very small areas corresponding to recent or active volcanoes or geothermal fields.

The extensional Tyrrhenian margin of the Apennine chain is also affected by extensive CO_2 degassing, mostly derived from a mantle source and representing a significant amount of the estimated global CO_2 emitted from sub aerial volcanoes (Collettini & Barchi, 2002; Chiodini *et al.*, 2004; Miller *et al.*, 2004). The anomalous flux of CO_2 decreases toward the axis of the Apennine chain. Here fluid overpressures, documented at depth by deep boreholes, suggest that CO_2-rich fluids can be trapped by stratigraphic or structural seals and released to shallow reservoirs at hydrostatic fluid pressure, triggering the main seismic events in the Apenninic chain (Miller *et al.*, 2004). Strong historical and instrumental earthquakes have occurred along the axis of the Apennine chain, and represent the most important effect of active deformation in the Italian peninsula. In this region the extensional active stress field is NE-SW oriented, with extension rate of 2.5-3.0 mm/yr. Here, M>6.5 earthquakes nucleate in the upper crust at depth between 5 and 12 km with extensional focal mechanisms, in agreement with geodetic data (Hunstad *et al.*, 2003) and borehole breakouts results (Montone *et al.*, 2004). Toward the Tyrrhenian margin seismicity decreases dramatically in correspondence with the abrupt increase of positive heat flow anomalies. In this region seismic activity generally nucleates at very shallow level and is mostly concentrated along the active volcanoes and geothermal fields of the area (Fig 5).

Geochronology and time of magmatism

The first geochronological data related to the potassic magmatism in the Central Mediterranean area date back to many decades ago (Evernden & Curtis, 1965). Several data were accumulated with time, with variable geological confidence, with different accuracy and with an uneven distribution on the various volcanic centers (e.g., Marra *et al.*, 2004 and Laurenzi, 2005 and references therein). K/Ar and ^{40}Ar-^{39}Ar data constitute almost the bulk of the age data on the Italian ultrapotassic and associated magmatic rocks, being data obtained with all other methods, as Rb/Sr, U-Th disequilibrium, Fission Tracks subordinated. ^{14}C dating is quite widespread on products younger than 50 kyr, obviously limited to organic material found in and within volcanic products.

During this long period of time the technological progress led to instrumental improvements which enabled precise analyses on very small samples, at least for conventional K/Ar method and, above all, for ^{40}Ar-^{39}Ar method. It is sufficient to compare the weights of mineral separates used for the Ar analyses listed in Table 7 of Evernden & Curtis (1965) with the single crystal laser total fusion age data appeared in literature at the end of last century (Alvarez *et al.*, 1996; Karner & Renne, 1998). Quite often published age data related to the same volcanic units disagree. This is particularly true for several old K/Ar data, and there are many reasons to explain the observed discrepancies. K/Ar ages are in fact model ages, because an atmospheric initial isotopic ratio is assumed in their calculation, and if this is not the case the obtained "age" value is older than the true one. Other "wrong" ages likely derive from the use of altered mineral phases, as revealed by their non-stoichiometric K contents. A further possibility of biased younger K/Ar ages is limited to sanidines, which have difficulties to melt completely (McDowell, 1983), with consequent underestimate of ^{40}Ar concentration. It is clear from the above consideration that ^{40}Ar-^{39}Ar data, when available, will be preferred to K/Ar data.

Sometimes only age data obtained several years ago with the K/Ar method are available for the geochronological reconstruction. And rarely the whole set of products of a volcanic district has been dated and/or ages were inferred from stratigraphic reconstructions. The geochronological discussions on the various volcanoes and volcanic districts have different levels of deepening. Those areas having wide and recent geochronological data have on average short descriptions, whereas areas having few and/or old data have often much longer discussions, and sometimes new age calculations. There are many critical points and open questions on the majority of volcanic districts, and several data are needed to constrain these volcanic activities. Within the limits of published data, an effort was done at least to confine the beginning and the end of the known volcanic activity in each area. Pyroclastic products are widespread and likely overwhelming by volume among products of the potassic volcanism. These products are often found as distal tephra within marine and continental sedimentary succession. Their use and their ages are beyond the scopus of this paper, due also to the difficulty to identify precisely their provenance. Hence only pyroclastic deposits of consistent width and clearly assigned to a volcanic district will be considered. Within the limits of published data, we'll try at least to confine the beginning and the end of the known volcanic activity in each area. Mentioned age data published before 1977 have been recalculated with Steiger & Jäger (1977) constants. ^{40}Ar-^{39}Ar ages, which are relative to monitor ages that might not be strictly comparable, have not been normalised to a unique monitor and monitor age. Consequent incidental age biases are well below the degree of detail of the following discussion, which aims to give a chronological framework for the ultrapotassic volcanism. For the same reason, on average age errors are not shown.

In the following paragraphs we will report a description of the different magmatic provinces occurring in Italy. This scheme follows the geographic location of Magmatic Provinces and then of Volcanic Districts from Northwest to Southeast, which broadly correspond to the onset of ultrapotassic magmatism (Fig. 6 - data used for drawing figure are from the following selected list: Evernden & Curtiss, 1965; Krummenacher & Evernden, 1965; Barberi *et al.*, 1967; Borsi *et al.*,1967; Carraro & Ferrara, 1968; Nicoletti, 1969; Hunziker, 1974; Lombardi *et al.*, 1974; Basilone & Civetta, 1975; Civetta *et al.*, 1978; Bigazzi *et al.*, 1981; Radicati *et al.*, 1981; Cassignol & Gillot, 1982; Gillot *et al.*, 1982; Metzeltin & Vezzoli, 1983; Pasquarè *et al.*, 1983; Sollevanti, 1983; Fornaseri, 1985a, b; Laurenzi & Villa, 1985, 1987; Poli *et al.*, 1987; Metrich *et al.*, 1988; Savelli, 1983, 1988; Ballini *et al.*, 1989a; Villa *et al.*, 1989; D'Orazio *et al.*, 1991; Turbeville, 1992; Cioni *et al.*, 1993; Barberi *et al.*, 1994; Laurenzi *et al.*, 1994; Nappi *et al.*, 1995; Laurenzi & Deino, 1996; Bellucci *et al.*, 1999; Pappalardo *et al.*, 1999; Villa *et al.*, 1999; Brocchini *et al.*, 2000, 2001; Giannetti & De Casa, 2000; Conticelli *et al.*, 2001; De Vivo *et al.*, 2001; Giannetti, 2001; Karner *et al.*, 2001a, b, c; Mascle *et al.*, 2001; Altaner *et al.*, 2003; Marra *et al.*, 2003, 2009; Rolandi *et al.*, 2003; Deino *et al.*, 2004; Cadoux *et al.*, 2005; Freda *et al.*, 2006; Florindo *et al.*, 2007; Rouchon *et al.*, 2008; Scaillet *et al.*, 2008; Boari *et al.*, 2009b; Cadoux & Pinti, 2009; Gasparon *et al.*, 2009; Giaccio *et al.*, 2009; Sottili *et al.*, 2010). They are: i) the Oligocene Magmatism in the Western Alps; ii) the Miocene Magmatic events of the Western Tyrrhenian Magmatic Province (Corsican); iii) the Plio-Pleistocene Magmatic events of the Tuscan Magmatic Province; iv) the Monte Amiata, a Middle Pleistocene "hybrid" volcano; v) the Pleistocene Magmatic events I: the Roman Magmatic Province including the Latian districts (e.g., Vulsini, Vico, Sabatini, Colli Albani, Middle Latin Valley, and Roccamonfina), the intramontane Umbrian district (found within the Apennine chain), and the Neapolitan district (i.e., Ischia, Procida, Campi Flegrei, and Somma-Vesuvius volcanoes); vi) the Pleistocene Magmatic events II: the Lucanian Magmatic Province including the Monte Vulture volcano and the nested Monticchio lakes monogenetic field.

Figure 6. Age distribution of ultrapotassic and related volcanic and sub-volcanic rocks in Italy and surroundings.

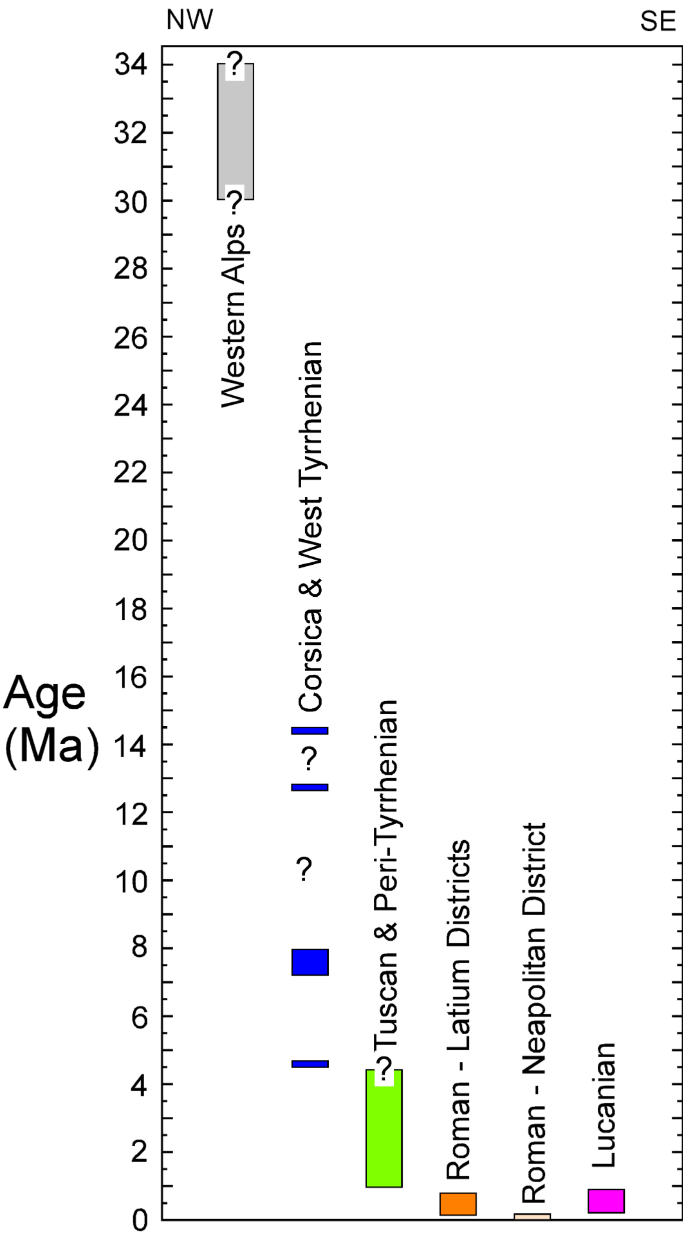

Age distribution of ultrapotassic and related volcanic and sub-volcanic rocks in Italy and surroundings. For data source of geochronological data see text.

In each of these sections the ages reported are from a thoughtful evaluation of the original geochronologic data.

Oligocene Magmatism in the Western Alps

Syn to post-collisional magmatism related to the building of the Alpine chain is recorded in the southern portion of the Alps, with emplacement and formation of hypabissal dykes, small plutons and volcano-sedimentary rocks. They are widespread and petrologically diverse with a clear compositional geographical polarity, with tholeiitic to calc-alkaline igneous rocks in Southeastern Alps, high-K calc-alkaline to calc-alkaline in Central Alps, and ultrapotassic, shoshonitic to high-K calc-alkaline in Western Alps (e.g., Beccaluva *et al.*, 1983). Post-collisional ultrapotassic and related shoshonitic to high-K calc-alkaline igneous rocks are found within a restricted area in the internal zone of the North-Western Alps (e.g., Dal Piaz *et al.*, 1979; Callegari *et al.*, 2004; Peccerillo & Martinotti, 2006; Owen, 2008). They are found mostly within the Sesia-Lanzo and Combin Units North of the Canavese Line (Fig. 7). It has been argued that these dykes are the hypabissal manifestation of a more intense volcanic activity, nowday totally removed, witnessed by the occurrence of calc-alkaline to shoshonitic volcano-sedimentary unit in the internal portion of the cover series of the Sesia Zone (Callegari *et al.*, 2004). The Traversella, Valle del Cervo and Biella calc-alkaline plutonic rocks are though to represent shallow level intrusion of the differentiated magmas derived by the calc-alkaline to shoshonitic parental magmas (Callegari *et al.*, 2004).

Figure 7. Distribution of Oligocene ultrapotassic dykes and related sub-volcanic bodies in Western Alps.

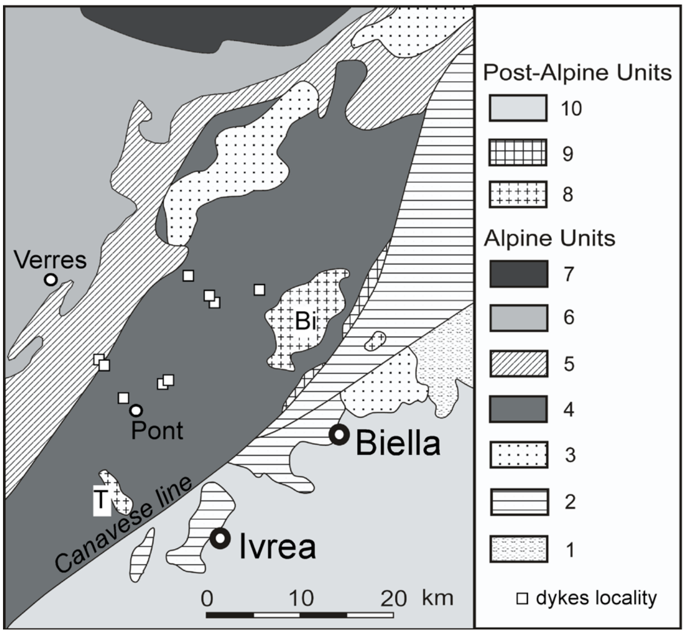

Oligocene ultrapotassic dykes and related sub-volcanic bodies occurr in the Western Alps in the area between Val d'Aosta and Piemonte Region and developed in the forms of dyke but some plutonic bodies and volcanoclastics sediments have been also found. Legend: 1) low grade Permian granites and granodiorites; 2) Ivrea zone mafic complex; 3) Ivrea zone knzigitic rocks; 4) Internal Sesia-Lanzo zone (eclogitic micaschists); 5) external Sesia-Lanzo zone (gneiss complex); 6) Schistés Lustrés and ophiolitic complex; 7) Monte Rosa and Gran Paradiso Nappe (orthogneisses); 8) Oligocenic plutonic bodies (T = Traversella; Bi = Biella); 9) Oligocenic volcanoclastic cover series; 10) Pleistocene-Holocene coves. Open squares represent sample localies of the work of Conticelli *et al.* (2009a). Modified after Dal Piaz *et al.* (1979); Venturelli *et al.* (1984); Callegari *et al.* (2004); Owen (2008); Conticelli *et al.* (2009a).

The age of the ultrapotassic and related magmatism in the Western Alps has been found to be within the range 34-30 Ma (Krummenacher & Evernden, 1962; Carraro & Ferrara, 1968; Hunziker, 1974), which is coeval with the peak of post-collisional magmatism of the entire Alps (von Blanckenburg *et al.*, 1998).

Ultrapotassic rocks of the western Alps have a lamproitic affinity; they are plagioclase-free micaceous dykes characterised by intersertal textures with phlogopite, clinopyroxene, and K-feldspar, accompanied by minor altered olivine, and riebckite-arfvedsonite amphibole with accessory apatite, sphene, and Fe-Ti oxides (Venturelli *et al.*, 1984). Shoshonitic to high-K calc-alkaline plagioclase-bearing lamprophyric rocks (kersantite to spessartite) are found associated in space and time with ultrapotassic rocks.

The lamproite-like samples have consistently high MgO contents (8.6-13.6 wt. %; Venturelli *et al.*, 1984; Peccerillo & Martinotti, 2006; Owen, 2008; Prelevic *et al.*, 2008; Conticelli *et al.*, 2009a) (Table 2). In the SiO_2-K_2O diagram (Peccerillo & Taylor, 1976; Fig. 8b) they plot on its top end, within the ultrapotassic rock field with a positive correlation between K_2O and silica, but not with MgO (Conticelli *et al.*, 2009a). Shoshonitic rocks have strongly variable MgO content (1.9-10.9; Venturelli *et al.*, 1984; Peccerillo & Martinotti, 2006; Owen, 2008; Prelevic *et al.*, 2008; Conticelli *et al.*, 2009a), which well correlate with silica and K_2O. High-K calc-alkaline rocks show also fairly variable MgO (1.1-7.6; Venturelli *et al.*, 1984; Peccerillo & Martinotti, 2006; Owen, 2008; Prelevic *et al.*, 2008; Conticelli *et al.*, 2009a), with data plotting on the potassium-rich basaltic andesite to rhyolite fields. Low-K calc-alkaline rocks have been found by Owen (2008).

Table 2. Chemical (major and trace) and Sr-Nd-Pb isotopic values for Western Alps rocks.

Reference	1	2	3	1	1	1	1	1	1	1	4
Locality	*Rio Rechantez*	*Rio Rechantez*	*Rio Rechantez*	*Plan d'Albard*	*Plan d'Albard*	*Cora Road*	*Cervo Valley*	*Stolen Valley*	*Gressoney Valley*	*Lake La Vecchia*	
Latitude	45°36'59"N	45°36'59"N	-	45°36'64"N	-	45°39'97"N	-	-	-	-	-
Longitude	07°49'57"E	07°49'57"E	-	07°45'36"E	-	07°51'51"E	-	-	-	-	-
Series	LMP	LMP	LMP	LMP	LMP	SHO	SHO	SHO	HKCA	HKCA	CA
Sample	**VDA 15**	**05RR02**	**WA05avb**	**VDA 03**	**MEC 247**	**VDA 14**	**MEC 241**	**MEC 216**	**KAW697**	**MEC 240**	**WA 107**
SiO_2 (wt.%)	48.77	49.61	50.64	55.10	56.00	52.21	60.00	60.40	53.69	63.07	50.22
TiO_2	1.188	1.18	1.17	1.312	1.24	0.935	0.53	0.54	0.86	0.42	0.637
Al_2O_3	10.94	11.30	11.98	10.20	11.00	13.89	17.30	17.40	17.60	17.06	10.26
Fe_2O_3	7.10	7.31	4.67	4.68	2.21	7.25	2.14	2.06	2.96	0.69	7.95
FeO	-	-	1.93	-	2.65	-	3.39	3.12	3.50	3.97	-
MnO	0.115	0.11	0.13	0.081	0.09	0.125	0.10	0.11	0.15	0.11	0.138
MgO	11.34	11.82	11.15	8.94	9.27	7.31	2.10	2.04	2.55	1.08	16.19
CaO	7.78	8.35	6.92	4.02	3.11	7.40	3.76	4.34	7.77	3.23	7.52
Na_2O	1.41	1.29	0.70	1.13	1.29	2.47	3.37	3.59	3.09	3.63	2.23
K_2O	6.47	6.13	7.36	9.24	9.07	3.75	4.38	4.09	1.89	3.18	0.37
P_2O_5	1.33	1.16	1.14	1.13	1.09	0.92	0.37	0.37	0.37	0.22	0.14
LOI	2.04	1.26	2.25	3.53	1.80	3.24	2.30	2.10	5.24	3.56	3.02
Sum	98.48	99.52	100.04	99.36	98.82	99.50	99.74	100.16	99.67	100.22	98.68
Mg-V	78.83	79.03	79.22	81.66	80.74	70.15	45.31	46.24	46.46	33.04	82.60
Sc (ppm)	29	32.7	24	13	16.6	27	11.7	11.2	16.7	2.26	33.2
V	181	270.6	156	83	95.0	182	88.9	85.0	142	15.6	163
Cr	560	932.8	630	470	571	310	23.4	21.1	-	-	665
Co	34	-	35	25	41.1	26	52.9	64.9	-	-	44.8
Ni	270	356.4	281	280	260	140	46.3	59.4	55.4	12.8	326
Cu	20	-	-	30	40.0	50	3.84	6.67	12.7	3.2	39
Zn	80	-	-	90	79.7	90	54.1	46.6	73.2	58.3	57
Ga	16	-	-	19	-	19	-	-	-	-	-
Rb	321	317	436	555	646	172	222	193	58.0	103	292
Sr	756	790	570	799	750	882	695	687	563	605	680
Y	31.9	28.1	28	30.8	28.9	29.3	26.5	26.4	23.5	18.5	24
Zr	472	359	399	665	638	334	370	353	187	199	236
Nb	28.3	32.3	29	34.4	36.4	24.2	38.6	35.4	12.8	12.38	16.2
Cs	10.4	9.10	10.7	28.4	13.2	6.0	3.75	5.48	1.39	0.86	22.1
Ba	4213	4400	3494	3797	3533	2592	2400	2388	1622	1315	3250
La	107	123.6	66.15	106	97.6	55.7	63.9	62.2	36.5	54.4	53.9
Ce	256	291.7	152	260	256	127	131	130	72.5	101	121
Pr	35.7	37.62	20.3	37.1	36.8	16.9	16.1	15.9	8.57	10.4	16.0
Nd	159	166.3	92.0	169	168	75.0	57.1	57.1	32.8	34.7	70.7
Sm	32.4	31.63	21.4	33.6	34.0	16.2	13.2	13.1	6.37	5.35	16.0
Eu	6.07	5.34	3.88	5.88	5.24	3.32	1.80	1.79	1.51	1.23	3.43
Gd	18.8	16.4	14.1	19.0	18.7	10.4	7.31	7.33	5.52	4.34	12.5
Tb	2.00	-	1.50	1.85	1.77	1.28	0.90	0.90	0.75	0.55	1.30
Dy	7.67	7.02	6.67	7.29	6.61	5.89	4.78	4.69	4.32	3.07	5.31
Ho	1.21	-	1.02	1.18	1.00	1.03	0.91	0.92	0.86	0.64	0.82
Er	2.97	2.35	2.61	2.77	2.34	2.89	2.64	2.67	2.45	1.92	2.20
Tm	0.38	-	0.35	0.34	0.28	0.40	0.39	0.39	0.35	0.29	0.284
Yb	2.19	1.84	2.19	1.93	1.58	2.46	2.61	2.61	2.32	2.01	1.71
Lu	0.28	0.25	0.28	0.25	0.22	0.36	0.42	0.41	0.37	0.33	0.212
Hf	13.0	9.81	10.1	18.1	16.6	9.2	9.09	9.35	3.68	4.43	6.6
Ta	1.97	1.60	1.68	2.73	2.28	1.74	2.92	2.39	0.83	0.79	0.83
Pb	34.0	32.0	91	105	132.0	36.0	28.0	26.0	16.7	15.7	40
Th	127	125.6	84	134	135	72.3	137	135	21.3	20.1	45.8
U	22.6	22.3	17.6	22.4	24.2	22.0	29.0	30.0	6.11	5.69	10.4
$^{87}Sr/^{86}Sr$ m	0.717280	0.718180	0.716310	0.718024	0.717894	0.712412	0.712135	0.711099	0.710258	0.709197	0.705920
$^{87}Sr/^{86}Sr$ i	0.716756	0.717685	0.715367	0.717168	0.716832	0.712172	0.711741	0.710753	0.710131	0.708987	0.705391
$^{143}Nd/^{144}Nd$ m	0.512020	0.512014	0.512090	0.512026	0.512034	0.512125	0.512118	0.512118	0.512325	0.512313	0.512440
$^{143}Nd/^{144}Nd$ i	0.511996	0.511992	0.512063	0.512002	0.512010	0.512099	0.512091	0.512091	0.512302	0.512295	0.512413
$^{206}Pb/^{204}Pb$ m	18.879	18.878	18.686	18.690	18.724	18.847	18.993	19.037	18.706	18.723	18.895
$^{206}Pb/^{204}Pb$ i	18.678	18.667	18.628	18.626	18.669	18.663	18.680	18.687	18.597	18.615	18.818
$^{207}Pb/^{204}Pb$ m	15.719	15.718	15.688	15.717	15.719	15.681	15.693	15.694	15.672	15.679	15.605
$^{207}Pb/^{204}Pb$ i	15.710	15.708	15.685	15.714	15.716	15.672	15.679	15.678	15.666	15.674	15.601
$^{208}Pb/^{204}Pb$ m	39.351	39.472	38.979	39.093	39.095	39.031	39.278	39.490	38.909	38.868	38.224
$^{208}Pb/^{204}Pb$ i	38.980	39.081	38.889	38.967	38.993	38.832	38.792	38.973	38.783	38.742	38.112

Legend: LMP = lamproite like; SHO = shoshonite series; HKCA = High-K calc-alkaline; CA = Calc-Alkaline; Mg-V = [MgO]/([MgO]+0.85*[FeOtot]); - = not analyzed; m = measured; i = initial calculated at 30 ma;
Data from: 1 = Conticelli *et al.* (2009a); 2 = Prelević *et al.* (2008); 3 = Peccerillo and Mattinotti. (2006); 4 = Owen (2008).

Figure 8. Classification and incompatible trace element characteristics of Western Alps Oligocene ultrapotassic and related rocks

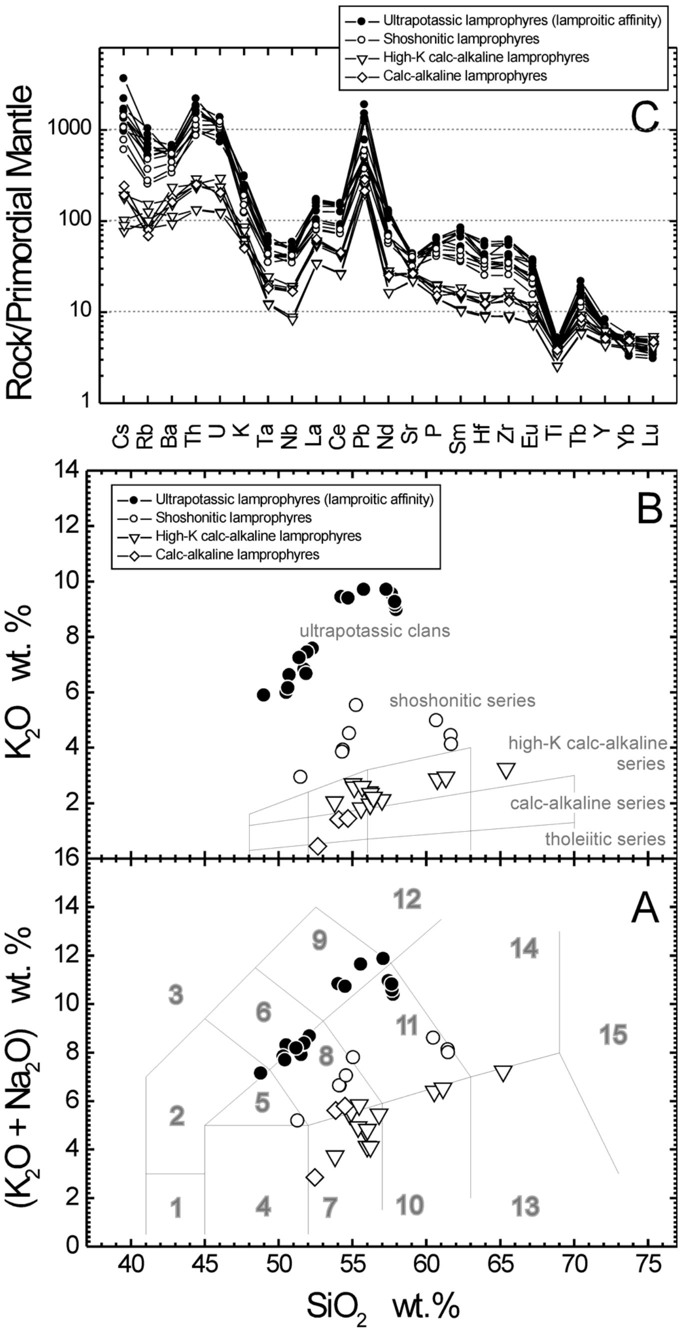

Classification and geochemical characteristics of the Western Alps leucite-free ultrapotassic and associated rocks. A) Total Alkali-Silica (TAS - Fields are: 1 = picritic basalt, 2 = basanite/tephrite, 3 = foidite (leucitite, haüynite, nephelinite, kalsilitite, etc.), 4 = basalt, 5 = potassic trachybasalt; 6 = phonolitic tephrite, 7 = basaltic andesite, 8 = shoshonite, 9 = tephritic phonolite, 10 = andesite, 11 = latite, 12 = phonolite, 13 = dacite, 14 = trachyte/trachydacite, 15 = rhyolite) classification diagram (Le Maitre, 2002). For TAS field names see text; B) K_2O wt.% vs. SiO_2 wt.% classification diagram with reported the grid for orogenic volcanic rock suites (Peccerillo & Taylor, 1976). C) Incompatible trace element patterns for mafic volcanic rocks normalised to the primordial mantle values of Sun & McDonough (1989). Data from Venturelli *et al.* (1984); Peccerillo & Martinotti (2006); Owen (2008); Prelevic *et al.* (2008); Conticelli *et al.* (2009a).

The Western Alps ultrapotassic (lamproite-like) and related rocks are variably enriched in incompatible trace elements, which positively correlate with K_2O at almost constant high MgO contents (Conticelli *et al.*, 2009a). These rocks on the Total Alkali Silica diagram (TAS, Le Maitre *et al.*, 2002) align along three different trends at different alkali contents (Fig. 8a), as well as on the K_2O vs SiO_2 diagram (Fig. 8b). Lamproites have the highest levels of incompatible trace elements, including lanthanides, but with characteristic fractionation of large ion lithophile elements (LILE) with respect to high field strength elements (HFSE). Passing from ultrapotassic to high-K calc-alkaline mafic rocks, through shoshonites, no significant deviations from this behaviour are observed but just a total decrease of incompatible trace element abundances (Fig. 8c). Throughs at Ba, Ta, Nb, and Ti with peaks at Th, U and Pb are the most important characteristics that are typical of the incompatible trace element distributions of orogenic type magmas (e.g. Hoffman, 1995; Hoefs, 2010). Among HFSE it is worth-noting the normalized Ta/Nb > 1, coupled to the normalized Nd/Sr > 1 that inverted to a value < 1 passing from lamproite to shoshonitic and calc-alkaline rocks (Fig. 8c).

The Miocene Magmatic events of the Western Tyrrhenian Magmatic Province (Corsican)

Miocene ultrapotassic, shoshonitic and high-K calc-alkaline igneous rocks are found in close temporal association distributed along the Eastern margin of the Sardinia-Corsica micro-plate, although a small monogenetic volcano at Zenobito volcano was produced during the Pliocene (Fig. 9). Ultrapotassic rocks, with lamproitic affinity, are found in the Northeastern portion of the Corsica Island, 15 km north of Bastia, in the form of a sill intruded into the Alpine terranes belonging to the “Schistes Lustrés” (i.e., Serie of the Castagniccia; e.g., Velde, 1967; Wagner & Velde, 1986; Peccerillo *et al.*, 1988); shoshonitic to high-K calc-alkaline sub-volcanic to volcanic rocks are found few kms offshore from Sardinia and Corsica islands, at Sarcya seamount (Cornacya) and

Capraia Island, respectively (e.g., Mascle *et al.*, 2001; Chelazzi *et al.*, 2006; Conticelli *et al.*, 2007, 2009a, 2011a; Gasparon *et al.*, 2008; Avanzinelli *et al.*, 2009). The Punta dello Zenobito volcano is a small monogenetic center lying on the southwestern edge of the Capraia Island, and it is made up by a cinder cone and few lava flows.

Figure 9. Distribution of Miocene ultrapotassic igneous rocks (dykes and volcanic rocks) and associated shoshonites and calc-alkaline rocks from western Tyrrhenian Sea (Corsica Magmatic Province)

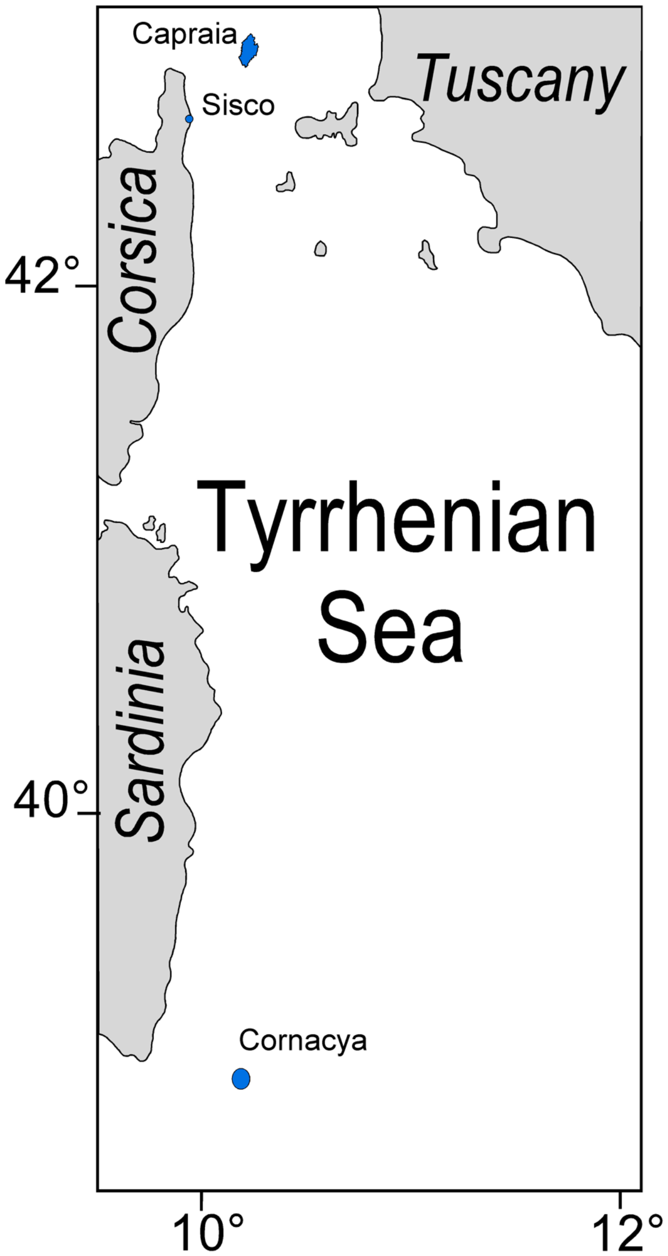

Ultrapotassic rocks are found exclusively along the northeastern edge of the Corsica island, whereas shoshonites are from submarine centers offshore of the southeastern edge of Sardinia Island. High-K calc-alkaline are from the Capraia volcano, located within the northen Tyrrhenian Sea (Conticelli *et al.*, 2011a).

The oldest sampled product of the Corsica Magmatic Province is the Sisco lamproite: one whole rock, one K-feldspar and two phlogopites of different grain-size, for a total of six analyses, have been used to calculate a K/Ar isochron plot of 14.58 ± 0.2 Ma (Civetta *et al.*, 1978). Mascle *et al.* (2001) report a ^{40}Ar-^{39}Ar total age of 12.6 ± 0.3 Ma (± 1s) for a dredged andesitic pebble from Cornacya. This age was calculated from 15 in-situ ^{40}Ar-^{39}Ar analyses performed on a single automorph crystal of biotite; a weighted average calculation on the same data points, carried out in this paper, gives an age of 13.07 ± 0.5 Ma (95% conf. lev., MSWD=1.5), slightly older but equal within error to the total age. It is worth to note that both Sisco and Cornacya age data are related to a unique sample, hence there aren't data that allow to infer the time span of magmatic activity, if any.

The dating of volcanic products of Capraia Island displays a noticeable disagreement among K/Ar, Ar-Ar and Rb/Sr data. Whereas K/Ar (9.8-5.0 Ma: Borsi, 1967; Pierattini, 1978) and Rb/Sr biotite-whole rock data (6.9-3.5 Ma: Barberi *et al.*, 1986, abstract only) evidence a quite long volcanic history, Ar-Ar data (Gasparon *et al.*, 2009) show that the majority of the actually subaerial samples are comprised in a narrow interval of time (7.8-7.2 Ma). Age data related to Punta dello Zenobito monogenetic volcano, whose orogenic affinity has been questioned (Chelazzi *et al.*, 2006; Conticelli *et al.*, 2007, 2009a, 2011a) disagree as well. K/Ar and Ar-Ar data are quite concordant within error (4.93 Ma, Borsi, 1967, and 4.76 Ma, Gasparon *et al.*, 2009, respectively), while either the 2.72 Ma K/Ar datum of Pierattini (1978) or the 3.92 Ma Rb/Sr datum of Barberi *et al.* (1986) are younger. Ar-Ar ages are on average preferred relative to K/Ar model ages, but the spread registered also by Rb/Sr biotite ages might be indicative of hidden problems in dating Capraia samples.

The Sisco lamproite is a leucite- and plagioclase-free ultrapotassic rocks with intersertal texture and a parageneses made of phlogopite, clinopyroxene, olivine, sanidine, and K-richterite associated to subordinate abundance of chromian spinel, ilmenite, pseudobroockite and priderite. Rare roedderite has also been found. Si+Al tetrahedral deficiency has been also observed in the chain silicate minerals (Wagner & Velde, 1986). Shoshonitic (Cornacya) and high-K calc-alkaline rocks (Capraia) range from shoshonites, to olivine latites, trachytes, high-K andesites, trachy-dacites, and rhyolites (Fig. 10a), and they are characterised by the occurrence of modal plagioclase, with sanidine and horneblende restricted to the most differentiated terms (Mascle *et al.*, 2001; Gagnevin *et al.*, 2007; Conticelli *et al.*, 2011a). The Punta dello Zenobito volcanic rocks are made up by porphyritic trachy-andesites with olivine and clinopyroxene phenocrysts set in a groundmass made up by abundant plagioclase.

The Sisco lamproite has a peralkaline index > 1, with high MgO (6.4-7.1 wt.%, Peccerillo *et al.*, 1988). Sisco lamproite has the highest K_2O and the lowest Al_2O_3 among the whole Central Mediterranean lamproites (Prelevic *et al.*, 2008; Conticelli *et al.*, 2009a). Shoshonitic rocks from Cornacya show a wide compositional range from mafic to felsic commons (Mascle *et al.*, 2001). High-K calc-alkaline rocks from Capraia volcano are intermediate to felsic in compositions, with MgO between 1.38 and 3.91 wt. % (Table 3), overlapping the trend of high-K calc-alkaline rocks from Western Alps and Murcia-Almeria (Conticelli *et al.*, 2009a, 2011a). The Punta dello Zenobito volcanic rocks, which are youngest ones of this region show peculiar compositional characteristics with mild enrichment in TiO_2, a characteristic not observed in the older Cornacya and Capraia rocks (Table 3; Chelazzi *et al.*, 2006).

Similarly to the the Western Alps ultrapotassic and related rocks, all mafic rocks of this association are enriched in incompatible trace elements, at different levels for the different magmatic series, with a clear positive correlation with K_2O contents (Conticelli *et al.*, 2009a). Throughs at Ba Ta, Nb, P and Ti are observed, although with some characteristic difference, with peaks at Th, U, Pb, and Sm (Fig. 10c). Sisco lamproite are distinguished by all other ultrapotassic Mediterranean rocks for their high Hf and Zr contents, and for their lowest enrichments in Cs, Pb, and U (Fig. 10c). The youngest volcanic episode of Punta dello Zenobito volcano is also characterised by the smallest LILE/HFSE fractionation with an almost flat pattern for incompatible trace elements (Fig. 10c), a characteristic that speak for the occurrence of an important within plate signature in its mantle source.

Figure 10. Classification and incompatible trace element characteristics of Western Tyrrhenian Miocene ultrapotassic and related rocks

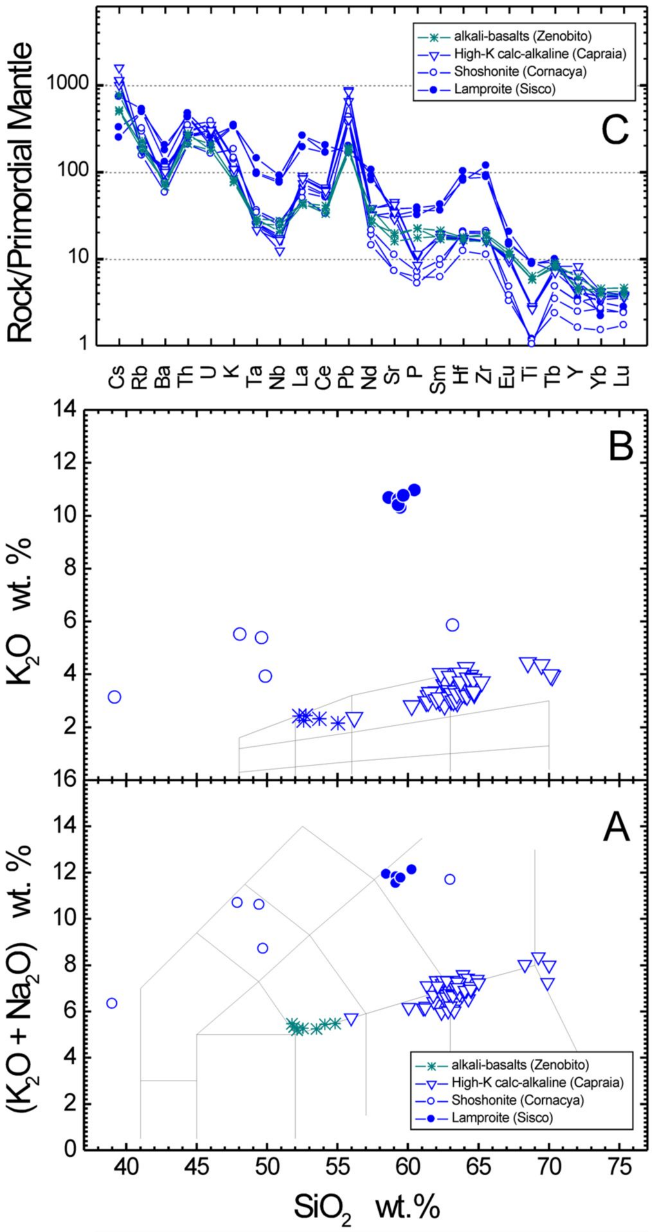

Classification and geochemical characteristics of Western Tyrrhenian (Corsican) Miocene ultrapotassic (lamproites) and related rocks. A) Total Alkali-Silica (TAS) classification diagram (Le Maitre, 2002). B) K_2O wt.% vs. SiO_2 wt.% classification diagram with reported the grid for orogenic volcanic rock suites (Peccerillo & Taylor, 1976). C) Incompatible trace element patterns for mafic volcanic rocks normalised to the primordial mantle values of Sun & McDonough (1989). Data from Peccerillo *et al.* (1988); Conticelli and Peccerillo (1992); Mascle *et al.* (2001); Conticelli *et al.* (2002, 2007, 2009a, 2011a); Prelevic *et al.* (2008).

Table 3. Chemical (major and trace) and Sr-Nd-Pb isotopic values for Western Tyrrhenian Sea (Corsica Magmatic Province) and Tuscan magmatic Province rocks.

Reference	1 – 2	3	2 - 4	2 – 4	2 - 5	2 - 6	2 - 6	7	2 - 5	8	9
Province	*Corsica*	*Corsica*	*Corsica*	*Corsica*	*Tuscany*	*Tuscany*	*Tuscany*	*Tuscany*	*Tuscany*	*Tuscany*	*Tuscany*
Locality	Sisco	Cornacya	Capraia	Zenobito	T. Alfina	Orciatico	Montecatini	Cimino	TorreAlfina	Campiglia	Tolfa
Latitude	40°35'25"N	39°04'48"N	43°03'02"N	-	-	43°26'10"N	-	42°23'13"N	-	-	-
Longitude	07°45'21"E	10°17'40"E	09°50'35"E	-	-	10°44'22"E	-	12°12'39"E	-	-	-
Series	LMP	SHO	HKCA	Alk-Bas	MRX	Orendite	Minette	SHO	HKCA	HKCA	CA
Sample	**SIS 04**	**SAR1.05B**	**CP10 bis**	**CP 54 bis**	**VS 76**	**ORC 01**	**MVC100**	**VS 232**	**VS 27**	**AE10A1**	**TMR 97**
SiO_2 (wt.%)	58.50	30.08	60.70	50.56	48.47	57.79	56.86	56.39	57.67	58.39	54.37
TiO_2	2.27	0.64	0.70	1.65	2.40	1.51	1.37	1.12	1.21	0.70	0.88
Al_2O_3	10.84	17.62	15.60	15.49	11.95	11.79	12.61	16.01	14.94	13.84	18.82
Fe_2O_3	0.81	7.93	5.24	9.31	2.77	2.24	3.25	1.07	0.10	2.90	6.87
FeO	2.42	-	-	0.80	5.20	3.12	2.84	3.99	5.54	4.36	1.52
MnO	0.06	0.06	0.09	0.13	0.11	0.08	0.10	0.09	0.10	0.53	0.10
MgO	6.63	12.43	4.38	6.41	15.75	8.23	7.15	7.98	7.52	5.84	2.22
CaO	3.12	3.07	5.99	7.92	5.47	3.46	3.47	5.55	4.36	3.12	5.69
Na_2O	1.02	2.38	2.90	2.83	0.33	1.31	1.20	1.27	1.15	0.64	1.43
K_2O	10.73	2.46	3.22	2.42	6.70	8.06	7.91	5.87	5.90	6.64	4.27
P_2O_5	0.67	0.39	0.23	0.48	0.58	0.85	0.92	0.26	0.46	0.23	0.47
LOI	2.09	22.61	1.15	1.13	0.27	1.55	2.43	0.88	1.07	2.80	3.31
Sum	99.16	99.67	100.20	99.10	100.00	99.99	100.11	100.48	100.02	99.99	99.95
Mg-V	81.54	78.51	66.08	59.41	81.11	77.07	72.23	77.16	73.69	63.73	37.68
Sc (ppm)	11.5	10.12	16.5	22.8	15.0	18.5	20.2	-	17.0	17.0	-
V	84	112.5	136	166	169	116	137	144	131	-	-
Cr	340	5.34	180	400	1983	500	380	401	457	418	-
Co	19.0	-	13.7	30	59	28.1	27	27	32	25.9	-
Ni	230	130.16	11	69	1379	280	140	175	250	145	-
Cu	30	-	7	25	-	50	340	-	-	-	-
Zn	100	-	71	87	-	80	90	-	-	-	-
Ga	23	-	19	18	-	21	21	-	-	-	-
Rb	318	132.09	113	115	454	612	768	363	334	267	205
Sr	640	811.01	966	399	399	577	408	427	565	453	572
Y	19.4	19.19	38	20	22	23.8	28	24	35	28	24
Zr	1040	149.64	184	221	353	749	491	444	572	166	296
Nb	54.8	10.00	9	15	16	39	30.1	26	32	15	7
Cs	2.00	-	9.0	4.0	-	25.2	14.0	5.5	-	18	-
Ba	1450	825.14	821	540	990	1400	1370	682	1089	1210	1107
La	183	54.08	63	29	59	148	79.8	88.4	88	33.0	57.0
Ce	367	109.08	119	68	131	352	206	197	200	61	114
Pr	41.6	12.50	13.0	10.9	-	47.4	29.8	26.0	-	-	-
Nd	146	46.50	51.6	51.9	69	193	133	99.8	93	27	47.0
Sm	19.1	7.48	8.7	9.6	14.4	26.9	23.5	15.3	19.2	5.9	8.2
Eu	3.5	1.57	1.78	2.09	2.12	4.32	4.02	2.37	2.69	1.01	1.70
Gd	11.3	5.69	5.7	6.2	-	14.4	13.6	8.71	-	-	6.8
Tb	1.09	0.70	0.90	1.00	0.69	1.27	1.31	1.11	1.03	0.60	-
Dy	4.64	3.67	4.2	4.9	-	5.23	5.87	5.25	-	-	4.5
Ho	0.79	0.70	0.79	0.99	-	0.89	0.99	0.79	-	-	-
Er	2.1	1.96	2.40	2.70	-	2.42	2.67	2.37	-	-	2.3
Tm	0.276	0.29	0.30	0.40	-	0.32	0.36	0.26	-	-	-
Yb	1.59	1.90	2.10	2.30	1.40	1.85	2.19	2.00	2.79	2.10	1.90
Lu	0.211	0.31	0.29	0.35	0.16	0.25	0.30	0.30	0.39	0.27	0.37
Hf	32.1	4.60	5.5	5.6	7.70	21.4	13.4	13.5	13.1	3.9	-
Ta	3.96	0.66	1.00	1.20	0.96	2.93	2.17	2.00	1.70	0.79	-
Pb	12.0	45.61	63	12	29	30.0	19.0	40	-	-	53.0
Th	37.9	21.85	22	24	29.9	119	112	61.8	58.0	13.0	26.0
U	4.61	1.68	6.6	3.8	7.1	14.9	18.2	9.91		3.90	6.30
$^{87}Sr/^{86}Sr$ m	0.71256	0.704733	0.70876	0.70819	0.71599	0.71597	0.71704	0.715647	0.71649	0.709700	0.711780
$^{87}Sr/^{86}Sr$ i	0.71227	0.704650	0.70872	0.70813	0.71595	0.71579	0.71672	0.715610	0.71647	0.709579	0.711686
$^{143}Nd/^{144}Nd$ m	0.512156	0.512650	0.512347	0.512258	0.512074	0.512096	0.512089	0.512055	0.512113	0.512210	-
$^{143}Nd/^{144}Nd$ i	0.512149	0.512642	0.512342	0.512255	0.512073	0.512094	0.512086	0.512054	0.512112	0.512202	-
$^{206}Pb/^{204}Pb$ m	18.841	-	-	-	18.631	18.717	18.663	18.727	-	-	18.796
$^{206}Pb/^{204}Pb$ i	18.786				18.629	18.697	18.624	18.725	-	-	18.788
$^{207}Pb/^{204}Pb$ m	15.695	-	-	-	15.642	15.699	15.640	15.663	-	-	15.721
$^{207}Pb/^{204}Pb$ i	15.692				15.642	15.698	15.638	15.663	-	-	15.721
$^{208}Pb/^{204}Pb$ m	39.330	-	-	-	38.771	39.116	39.026	39.022	-	-	39.031
$^{208}Pb/^{204}Pb$ i	39.181				38.768	39.062	38.947	39.017	-	-	39.021

Legend: LMP = lamproite like; MRX = Mica Rich Xenolith with lamèproitic composition enclosed in lamproite like rocks of Torre Alfina (Conticelli and Peccerillo, 1990; Conticelli, 1998); SHO = shoshonite series; HKCA = High-K calc-alkaline; CA = Calc-Alkaline; Mg-V = [MgO]/([MgO]+0.85*[FeOtot]); - = not analyzed; m = measured; i = initial calculated at the age of emplacement (see text);

Data from: 1 = Peccerillo *et al.* (1988); 2 = Conticelli *et al.* (2007); 3 = Mascle *et al.* (2001); 4 = Conticelli *et al.* (2010b); 5 = Conticelli (1998); 6 = Conticelli *et al.* (1992); 7 = Perini *et al.* (2003); 8 = Conticelli *et al.* (2002); 9 = Pinarelli (1991).

The Pliocene-Pleistocene Magmatic events: Tuscan Magmatic Province

The Tuscan Region has been the site of bimodal igneous activity during the Pliocene and Pleistocene (Fig. 11). Crustal-derived magmas, formed by anatexis of lower to intermediate continental crust occurred to form granitic to granodioritic plutonic bodies (Fig. 11) and some hybrid products that have intermediate characteristics between mantle- and crustal-derived magmas have been also produced (Poli *et al.* 1984, 1989; Peccerillo *et al.*, 1987; Pinarelli *et al.*, 1989; Poli 1992, 1996; Westermann *et al.*, 1993; Gagnevin *et al.*, 2004, 2005a, 2005b; Poli *et al.*, 2004). For the purpose of the present work we are not going to include here igneous rocks that are generated dominantly by magmas of continental crust derivation. They are usually treated separately from mantle derived ultrapotassic and related rocks.

Figure 11. Distribution of Plio-Pleistocene ultrapotassic igneous rocks and associated shoshonites and calc-alkaline rocks from Eastern Tyrrhenian Sea and Italian Peninsula (Tuscan, Roman and Lucanian Magmatic Provinces)

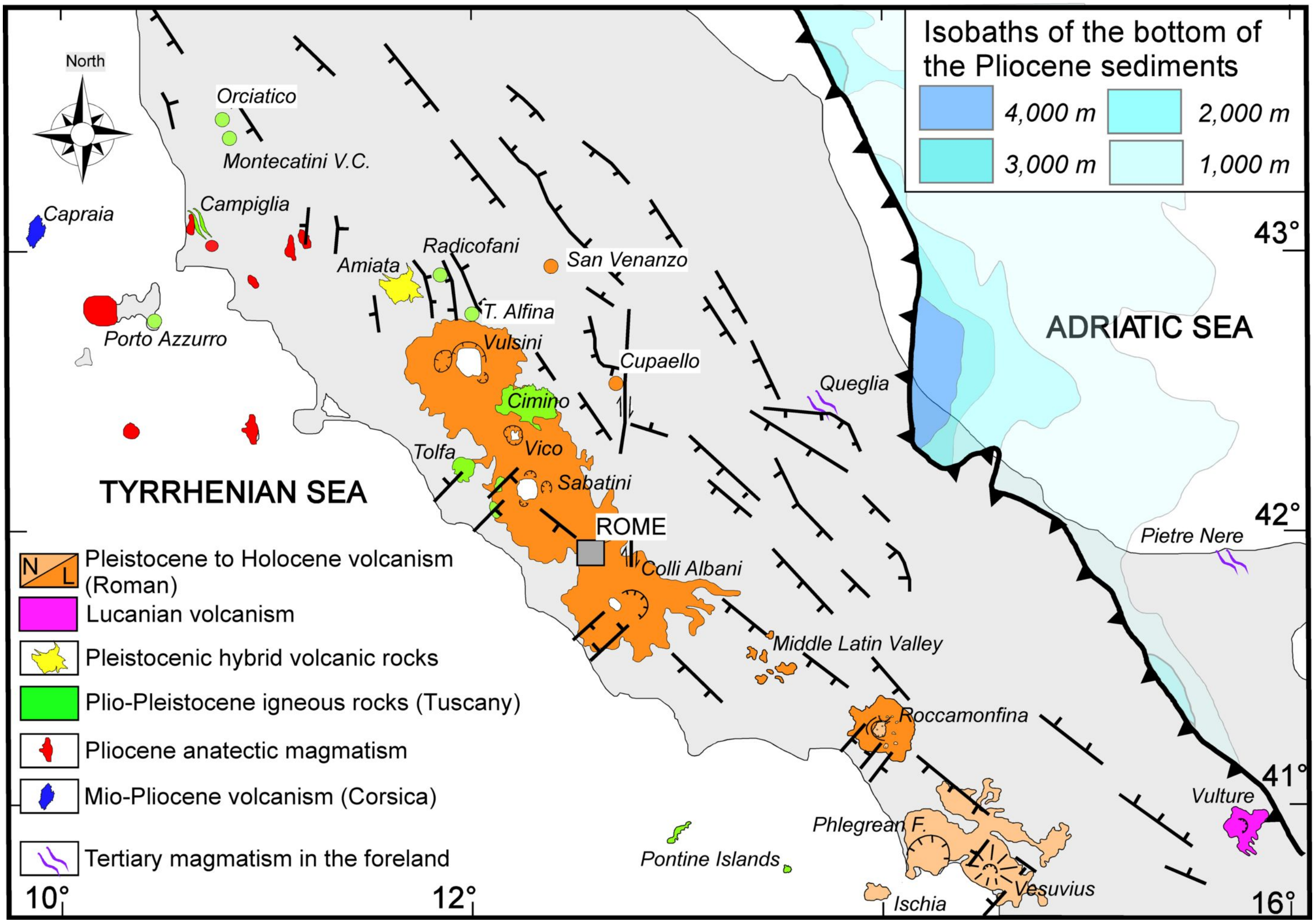

Ultrapotassic rocks are found distributed along the Tyrrhenian border of the Italian peninsula, and in some cases offshore within the eastern Tyrrhenian Sea and on the other hand in the intra-apennine setting. Tuscan, Roman and Lucanian magmatic provinces can be efficiently divided on the basis of mineralogy of the ultrapotassic rocks, timing of magmatism and location with respect to the Italian peninsula. Tuscan Magmatic rocks are Pliocenic in ages and ultrapotassic terms are always leucite-free; they are distributed in the westernmost portions of the region. Roman Magmatic rocks are Pleistocenic to holocenic in ages and ultrapotassic terms are always leucite-bearing; they are distributed in the central portions of the region. Lucanian Magmatic rocks are Pleistocenic in ages with leucite/haüyne-bearing ultrapotassic terms; they are distributed locally in the southeasternmost area of the the region. The only deviation from this rule is represented by the Monte Amiata volcano. See text for further explanation. Redrawn after Avanzinelli *et al.* (2009); Mattei *et al.* (2010).

The Pliocene mantle-derived ultrapotassic and related rocks are made up by high-potassium calc-alkaline, shoshonitic, and plagioclase- and leucite-free alkaline ultrapotassic rocks (i.e., lamproite) generated by magmas of ultimate mantle-origin (Conticelli *et al.*, 2009a). They are found as scattered outcrops straddling the Tyrrhenian border of the Italian Peninsula (Fig. 11). Traditionally the Tuscan Magmatic Province has been considered to be confined a little beyond the administrative border of the Tuscany region (Peccerillo *et al.*, 1987; Innocenti *et al.*, 1992; Poli *et al.*, 2004), but coeval leucite-free potassic to sub-alkaline magmatic rocks are found along the entire Tyrrhenian border of the peninsula (Avanzinelli *et al.*, 2009). Therefore, in this chapter we have also included the descriptions of the coeval volcanic rocks that have been either intruded and erupted few kms north of Rome (i.e., Tolfa, Manziana, Ceriti; Fig. 11), and offshore at Ponza Island, within the Pontinian Archipelago (Fig. 11). Indeed these volcanic rocks have high-K calc-alkaline and shoshonitic affinities, although silicic terms prevail over mafic ones.

The oldest volcanic rocks of the Tuscan Magmatic Province are found at Elba Island, Tuscan Archipelago (Fig. 11) with an ^{40}Ar-^{39}Ar age of 5.8 Ma (Conticelli *et al.*, 2001), followed by the emplacement in the mainland, Val d'Era area, of the hypabissal minette of Montecatini Val di Cecina, 4.2 Ma (K/Ar; Borsi *et al.*, 1967), of the orendite of Orciatico (4.1 Ma, Capaldi G. Personal Communication in Conticelli *et al.*, 1992) (Fig. 11), and of the olivine latitic dikes at Campiglia (Conticelli, 1989). Almost coevally are erupted the products of the Tolfa-Manziana-Ceriti dome complexes (Fig. 11). They are made up of trachytic to rhyodacitic domes, massive lava flows, and welded ignimbrites, but latitic to olivine latitic mafic enclaves are also found to testify the occurrence of mafic magmas in their genesis (Fazzini *et al.*, 1972; Clausen & Holm, 1990; Pinarelli, 1991; Bertagnini *et al.*, 1995). Several K/Ar dates are available for the Tolfa-Manziana-Ceriti volcanic rocks spread from 4.3 to 1.9 Ma, excluding a datum from a xenolith (Evernden & Curtis, 1965; Bigazzi *et al.*, 1973; Lombardi *et al.*, 1974; Villa *et al.*, 1989). Villa *et al.* (1989) performed a new mineral separation on four rocks previously analysed by Lombardi *et al.* (1974), and obtained ages overlapping within error for Tolfa and Manziana samples, all around 3.5 Ma, either older (3) and younger (1) than previous data. Villa *et al.* (1989) explain the discrepancies observed among the old and new analyses with the use of mixed mineral phases by Lombardi *et al.* (1974), as testified by K-feldspars non-stoichiometric K contents. A fairly young age, 2.36 Ma, on a sanidine with a stoichiometric K% is reported also by Evernden & Curtis (1965). The data since now available do not allow to identify a precise time length for this volcanism.

The Pontine Islands are placed offshore of the Southern Latium coast (Fig. 11). Ponza and Ventotene Islands are placed at the same distance from the Apennine front of Tolfa-Manziana-Ceriti dome comeplexes, due to the arcuate morphology of the Northern Apennine chain. Only K/Ar data are available in literature for the Pontine Islands volcanic rocks. The recent paper by Cadeaux *et al.* (2005) gives an age interval from 4.2 to 3.7 Ma for the outcropping rhyolitic dykes and associated hyaloclastites of Ponza Island. Previous authors indicate older ages for the same products (5.1-4 Ma: Barberi *et al.*, 1967; Savelli, 1983, 1988; Altaner *et al.*, 2003). Cadeaux *et al.* (2005) recognise a second episode at about 3 Ma in the central-southern part of the island, and indicates an age around 1 Ma for the final subaerial activity of the Southern portion of the Island. Barberi *et al.* (1967) and Savelli (1988) report slightly older ages for the final activity of Ponza. Furthermore, K/Ar ages of illite-smectite of hydrotermally altered rocks constrain the alteration event at about 3.4 Ma (Altaner *et al.*, 2003). At Palmarola Island K/Ar ages obtained from different laboratories are less discordant than in Ponza, and are comprised between 1.8-1.6 Ma (Barberi *et al.*, 1967; Savelli, 1988) and 1.6-1.5 Ma (Cadeaux *et al.*, 2005). The Ventotene Island is the subaerial remnant of post caldera volcanic rocks emplaced along an old calderic rim. The Ventotene stratovolcano is well below sea level. K/Ar ages on Ventotene oldest outcropping products disagree, ranging from 1.75 Ma (Barberi *et al.*, 1967) to 0.92 Ma (Bellucci *et al.*, 1999); the volcanic activity then continues till an undefined recent time (< 0.15 Ma for a pumice form the uppermost pyroclastic floe unit, Metrich *et al.*, 1988). Santo Stefano Island appears as a lava dome, emplaced on a flank of Ventotene submerged sratovolcano, which is covered by pyroclastic products: K/Ar model ages are comprised between 1.2 and 0.6 Ma (Barberi *et al.*, 1967; Fornaseri, 1985a; Metrich *et al.*, 1988; Bellucci *et al.*, 1999). A bit more southeast, in the Campanian Plain (Fig. 11), thick sequences of altered volcanites of calc-alkaline affinity were found in drillings (Parete 2 and Villa

Literno 1 wells; Di Girolamo *et al.*, 1976). K/Ar age of the deepest sample of Parete 2 well (2.0 ± 0.4 Ma, Barbieri *et al.*, 1979) is devoid of analytical details. ^{40}Ar-^{39}Ar analyses of plagioclases separated from both wells failed to give reliable results (Brocchini, 1999). Hence, the age of this volcanism remains uncertain.

Figure 12. Classification and incompatible trace element characteristics of Tuscan Magmatic Province

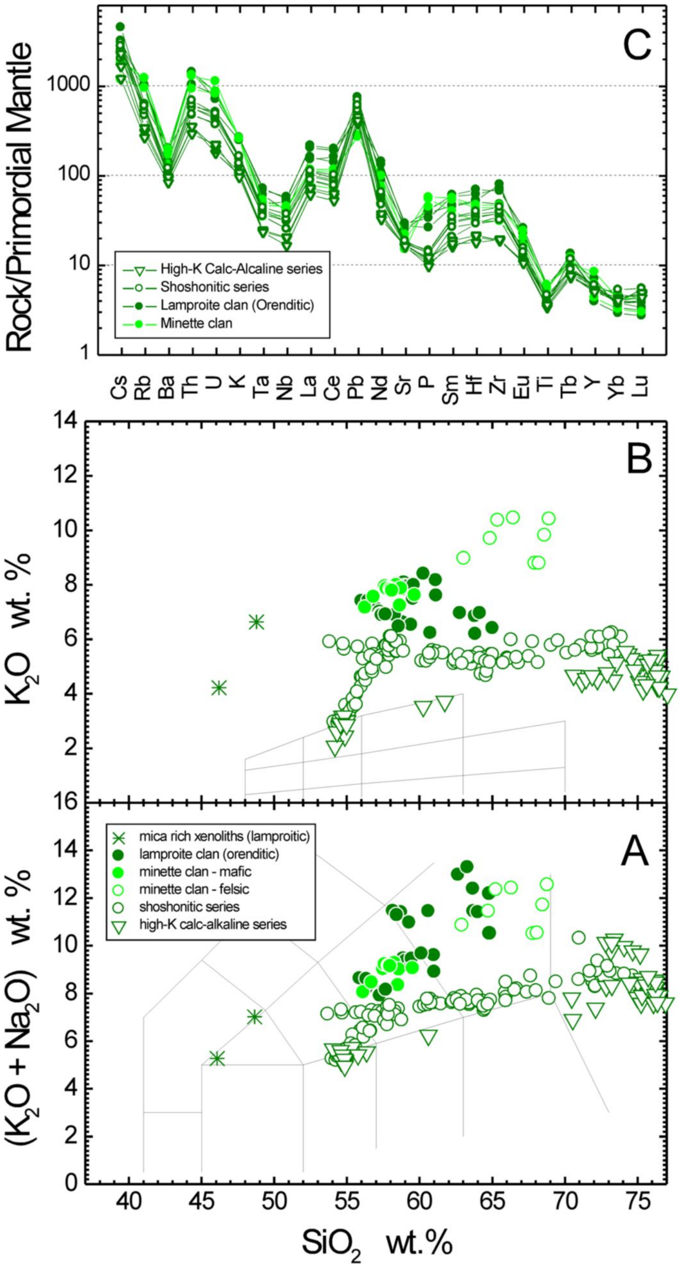

Classification and geochemical characteristics of Tuscan Plio-Pleistocene ultrapotassic (lamproites) and related rocks. A) Total Alkali-Silica (TAS) classification diagram (Le Maitre, 2002). B) K_2O wt.% vs. SiO_2 wt.% classification diagram with reported the grid for orogenic volcanic rock suites (Peccerillo & Taylor, 1976). C) Incompatible trace element patterns for mafic volcanic rocks normalised to the primordial mantle values of Sun & McDonough (1989). Data from Metrich *et al.* (1988); Peccerillo *et al.* (1988); Pinarelli (1991); Conticelli & Peccerillo (1992); Conticelli *et al.* (1992, 2002, 2007, 2009a, 2011b, 2011c); Conticelli (1998); D'Antonio *et al.* (1989a); Cadeaux *et al.* (2005); Prelevic *et al.* (2008).

The youngest Leucite-free ultrapotassic rocks of the Tuscan Magmatic Province are found a bit more east, erupted along the NNW-SSE extensional basin that will be occupied later, during the Pleistocene, by the Roman leucite-bearing volcanic rocks. The emplacement of the basaltic andesitic to shoshonitic lavas of Radicofani center (Fig. 11) is placed around 1.3 Ma: the ^{40}Ar-^{39}Ar age of one Radicofani lava flow and the K/Ar model ages of the neck agree within error (Pasquarè *et al.*, 1983; D'Orazio *et al.*, 1991). K/Ar model ages on the olivine latite with lamproitic affinity and latite to trachytes with shoshonitic affinity of Monte Cimino Volcanic Complex are comprised in the interval 1.43-0.97 Ma (Evernden & Curtis, 1965; Nicoletti *et al.*, 1969; Puxeddu, 1971; Sollevanti, 1983), partially overlapping with Radicofani volcanic rocks. There are also two ^{40}Ar-^{39}Ar age spectra on a sanidine megacryst from the Faggeta quartz-latitic dome, without a clear age calculation (Villa, 1988: the paper was centered on Ar geochemistry). The flattish parts of the two spectra give a weighted average of about 1.1 and 1.16 Ma (new calculation from Table 1 of Villa, 1988). Only a K/Ar model age of 0.82 Ma is available for the olivine latite with lamproite affinity of Torre Alfina (Nicoletti *et al.*, 1981a; Conticelli, 1998).

The rocks of this period range in composition from ultrapotassic (i.e., lamproite-like) to shoshonitic and high-K calc-alkalic rocks (Table 3; Fig. 12b). Shoshonitic rocks are represented by the overall spectrum of compositions, from trachybasalt to trachyte, as well as high-K calc-alkalic rocks with terms ranging from high-K basaltic andesites to rhyolites (Fig. 12a). Lamproite-like rocks are few and mostly mafic with phenocrysts of Al-poor clinopyroxene, and olivine with chromite inclusions (Fig. 3a-c), set in a groundmass made up of clinopyroxene, phlogopite, sanidine, K-richterite, apatite, picroilmentite and Ti-magnetite and accessory perrierite/chevkinite (Wagner & Velde, 1986; Conticelli *et al.*, 1992; Cellai *et al.*, 1993, 1994; Conticelli, 1998). The aluminium content in clinopyroxene increases from lamproite to shoshonite with contemporaneous appearance of plagioclase

(Fig. 3d; Conticelli *et al.*, 2010b). Two pyroxene high-K calc-alkaline rocks are strongly differentiated products, at Cimino, Tolfa, Manziana, and Ponza, which are associated at younger mafic lamproite-like shoshonitic rocks (Clausen & Holm, 1990; Pinarelli, 1991; Perini *et al.*, 2003; Conte & Dolfi, 2002; Paone, 2004; Cadeaux *et al.*, 2005; Conticelli *et al.*, 2010d). Equilibrium clinopyroxene and orthopyroxene is the main petrographic characteristic of the most differentiated terms, which are associated to biotite, sanidine, plagioclase, apatite, zircon, ilmenite, Ti-magnetite.

The mafic Plio-Pleistocene magmatic rocks of the peri-tyrrhenian area positively correlate with K_2O contents (see Fig. 8 in Conticelli *et al.*, 2009a), showing a temporal decrease in the contents of this oxide. High-MgO volcanic rocks, irrespectively of their K_2O content, display strong depletions in Ti, Ta, and Nb relative to Th and LILE (Fig. 12c). When compared to Corsican rocks, Plio-Pleistocenic volcanic rocks show higher peaks at Th, U, Pb, Zr and Hf, and deeper troughs of Ba, Ta, Nb, P, and Ti (Fig. 12c). These rocks still dispay normalized Ta/Nb and Nd/Sr lower than unity. Conticelli & Peccerillo (1992) argued that incompatible trace element concentrations and their distribution and fractionation are primary characteristics derived directly from their mantle source(s) due to sediment recycling within the upper mantle.

The Monte Amiata: a Quaternary “hybrid” volcano

The Monte Amiata volcano, Late Pleistocene in age, is located in Southern Tuscany, well within the area of the Tuscan Magmatic Province (Fig. 11). The Monte Amiata volcano is a small linear volcano that produced few lava flows, domes and dome collapse (Fig. 13) with a high-K calc-alkaline to shoshonitic character (Fig. 14). Its chronology relies on several K/Ar and Fission Tracks data that cover the whole volcanic activity (Evernden & Curtis, 1965; Bigazzi *et al.*, 1981; Pasquaré *et al.*, 1983; Cadeaux & Pinti, 2009), and few ^{40}Ar-^{39}Ar data on the oldest products (Laurenzi & Villa, 1991; Barberi *et al.*, 1994). The initial known activity start at about 300 ka (Barberi *et al.*, 1994; Cadeaux & Pinti, 2009), hence all older ages reported in literature are problematic. The end of Amiata volcanic activity is quite undefined: Bigazzi *et al.* (1981) gave ages around 200 ka for the final lava domes, but Cadoux & Pinti (2009) dispute that conclusion and affirm that sanidine ages are “magmatic ages” and not eruption ages, leading to uncertain age assignment for all products. In spite of disputes on the time length of Amiata activity, this volcano is much younger of any other volcanic center belonging to the Tuscan Magmatic rocks (leucite-free ultrapotassic rocks) and well within the time span of Roman volcanic rocks (lecite-bearing ultrapotassic rocks).

Figure 13. Geological sketch map of the Monte Amiata volcano a hybrid volcanic center transitional between Tuscan and Roman Magmatic provinces

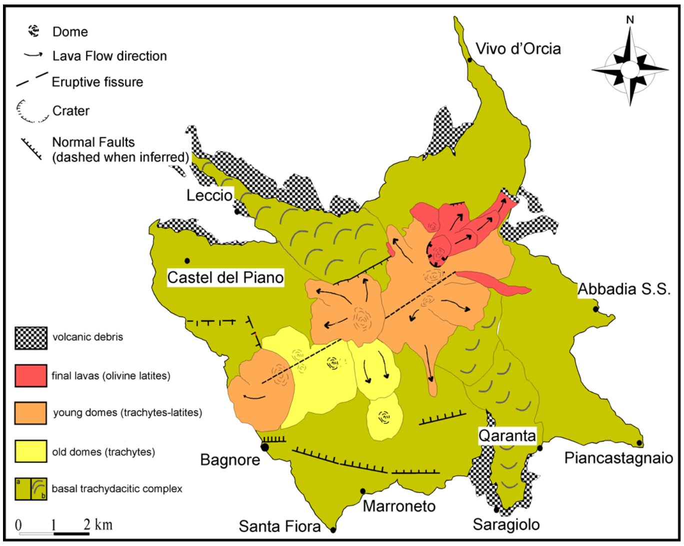

Geological sketch map of the Monte Amiata linear volcano. Redrawn after Ferrari *et al.* (1996).

The Monte Amiata volcanic rocks range from Two-Pyroxene trachydacites to olivine-bearing, orthopyroxene-free olivine latite to trachyte (Fig. 14a) (Ferrari *et al.*, 1996). The oldest products belonging to the Basal trachytic complex are made up of biotite, plagioclase, sanidine, clinopyroxene and orthopyroxene, amphibole, Ti-magnetite and rarely by interstitial quartz (van Bergen, 1984; Ferrari *et al.*, 1996). The youngest ones have a slightly bimodal composition with early emplacement of trachytic to latitic lavas (Fig. 14a), in the form of exogenous lava domes and short massive lava flows, and the final emplacement of olivine-latitic to shoshonitic lava flows (Fig. 14a). In addition Monte Amiata volcanic rocks are characterised by the occurrence of abundant magmatic enclaves and metasedimentary xenoliths ranging from centimetre to decimetre size. Metasedimentary xenoliths, ranging from angular to irregularly-rounded, are mostly flattened in shape and predominate in Basal

Trachydacitic rocks. Fine-grained magmatic enclaves have ellipsoidal shape with cuspidate margins convex toward the hosts. The amount of fine-grained magmatic enclaves increases with decreasing ages of host rocks, from Basal Trachytic Complex to Final Lavas. Fine-grained magmatic enclaves range from porphyritic to aphyric and invariably display chilled margin texture, ranging in compositions from trachybasaltic to shoshonitic and latitic. Petrographic and compositional characteristics of fine-grained magmatic enclaves suggest that they were molten at the moment of the inclusion by the host trachytic magma. Their characteristics are strongly suggestive for the occurrence of interaction between different types of magmas prior to eruption (Ferrari *et al.*, 1996; Cadoux & Pinti, 2009). This hypothesis is also supported by the occurrence of disequilibria texture among the mineral assemblages of the dome complex (intermediate volcanic activity) (Fig. 3e).

From a petrological point of view the Monte Amiata volcanic rocks were produced by the crystallization of strongly differentiated shoshonitic magma with trachytic to trachydacitic compositions (Ferrari *et al.*, 1996; Cadoux & Pinti, 2009; Conticelli *et al.*, 2009c). This magma produced the early eruption of the basal trachytic complex and of the trachytic to latitic dome complex (Fig. 14a). Conticelli *et al.* (2009c, 2010b) suggested that the early Monte Amiata magma derived by the fractional crystallization plus crustal contamination starting from a parental magma similar in composition to the Radicofani shoshonitic trachybasalt. The intermediate and final eruptions of the Monte Amiata have been produced by the mingling between this extremely differentiated high silica magma and ultrapotassic silica-undersaturated magmas (Roman) (van Bergen *et al.*, 1983). The arrival in the shallow level magmatic reservoir of newly formed leucite-bearing hot magma from the source region triggered Monte Amiata eruptions. Mafic enclaves represent the evidence of the mingling between leucite-bearing Roman magmas and the relic high-K calc-alkaline magmas of the previous Tuscan episode. Leucite crystallization from Roman magma has been suppressed by the strong silica activity of the stagnant differentiated Tuscan magmas, crystallizing in the magma reservoir at shallow depth. These processes well explain the characteristic composition of the Monte Amiata rocks and the very young time span of volcanic activity, suggesting that the Monte Amiata is neither a Tuscan nor a Roman volcano, but just a “hybrid” volcano due to the interaction between leucite-free and -bearing potassic to ultrapotassic magmas (Conticelli *et al.*, 2009c).

Figure 14. Classification and incompatible trace element characteristics of Quaternary Monte Amiata volcanic rocks

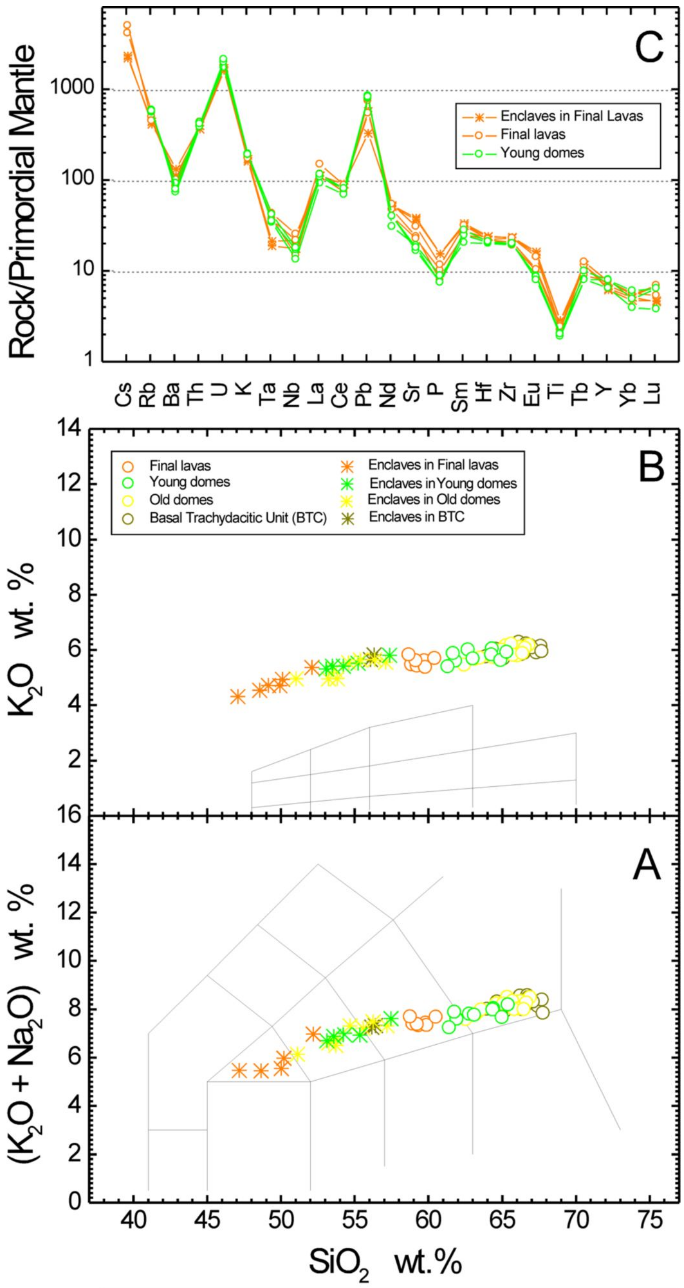

Classification and geochemical characteristics of the Monte Amiata volcanic rocks and mafic enclaves. A) Total Alkali-Silica (TAS) classification diagram (Le Maitre, 2002). B) K_2O wt.% vs. SiO_2 wt.% classification diagram with reported the grid for orogenic volcanic rock suites (Peccerillo & Taylor, 1976). C) Incompatible trace element patterns for mafic volcanic rocks normalised to the primordial mantle values of Sun &

McDonough (1989). Data from Ferrari *et al.* (1996), and authors' unpublished data.

The mingling hypothesis is also testified by the incompatible trace element distribution shown in figure 14c. Indeed mafic Final Lavas display normalized patterns very similar to those of the Tuscan rocks, with troughs at Ba, Ta, Nb, P, and Ti, and peaks at Cs, U, and Pb. The strong peak at U with extremely high U/Th ratios is peculiarly different, and it is much higher than in the rest of the Tuscan rocks (Fig. 14c). Incompatible trace element patterns of mafic enclaves differ greatly from those of the lavas in terms of normalized Ta/Nb, Nd/Sr, and Zr/Hf, although no differences have been observed among U/Th ratios (Fig. 14c).

The Quaternary Magmatic events: Roman and Lucanian Magmatic provinces

Early in the twentieth century, Washington (1906) defined the Roman Magmatic Province as a unique magmatic association characterized by leucite-bearing ultrapotassic volcanic rocks, extending from Northern Latium to the Neapolitan area. Since then several authors re-defined the Roman Province limits on the basis of different criteria (e.g., Hawkesworth & Vollmer, 1979; Vollmer & Hawkesworth, 1980; Ayuso *et al.*, 1998; Paone, 2004; Peccerillo, 2005a). In the present paper we keep the original definition using the petrographic criterium adopted by Washington (1906) and later resurrected by Turner & Verhoogen (1960), because this is coherent with an easy recognition from other timely close volcanic association worldwide, and because this division correlates with main mechanisms of magma genesis and geodynamic events in the area (Conticelli *et al.*, 2004; Avanzinelli *et al.*, 2009). Indeed the Roman Province is characterized by Pleistocene to Holocene leucite-bearing ultrapotassic igneous rocks, whereas the Tuscan Magmatic Province by Pliocene to Pleistocene leucite-free ultrapotassic igneous rocks, the Lucanian Magmatic Province by Pleistocene haüyne/leucite-bearing ultrapotassic rocks. This would be a simple, but consistent, criterium to assess magmatic domains. With an eye to the geochemical and isotopic characteristic we further divide internally the Roman rocks between the Latian districts, in which ultrapotassic leucite-bearing volcanic rocks dominate over shoshonites, and the Neapolitan one, where shoshonite volcanic rocks are more abundant than ultrapotassic leucite-bearing volcanic rocks (Fig. 11).

The Roman Magmatic Province

The Roman Magmatic Province comprises several volcanic districts that can be made up by a cluster of two/three volcanic apparata (e.g., Vulsini, Sabatini, and Neapolitan, Fig. 11), by a monogenetic volcanic field (e.g., Middle Latin Valley, and Campi Flegrei, Fig. 11), or just by a single volcanic apparatus with a summit caldera and a post-caldera monogenetic activity (e.g., Vico, Colli Albani, and Roccamonfina volcanoes, Fig. 11). The Roman Magmatic Province, in Northern Latium, overlaps the volcanic rocks belonging to the Tuscan Magmatic Province (Fig. 11). The volcanism of the Roman Magmatic Province begun at about 760 ka (Florindo *et al.*, 2007) and protracted till the present time, being the last eruption at Vesuvius of 1944 A.D., with a maximum production of volcanic rocks between 400 and 200 ka in the Latian districts and between 200 ka and the present for the Neapolitan district. Minor centers of the Roman Magmatic Province are found in Umbria, in an intramontane region, at San Venanzo and Cupaello.

The Latian districts

The Latian volcanic districts occupy prevalently the Latium region although the Roccamonfina volcano is well within the campanian region. They have been active coevally during the Pleistocene and presently most of them are just quiescent. On the basis of petrographic data the Latian districts are prevalently made up by leucite-bearing ultrapotassic magmas, in some cases preceeded by hybrid Tuscan-Roman magmas, as in the cases of early activity at Vulsini, Vico, Sabatini (see below), and followed by less alkaline leucite-bearing and leucite-free shoshonitic volcanic rocks in the post caldera activity. The Leucite-bearing ultrapotassic magmas are predominat over the late leucite-free magmas (i.e., shoshonitic to calc-alkaline magmas; Avanzinelli *et al.*, 2009, and references therein).

1. Vulsini district

The Vulsini district is the northernmost volcanic cluster of the Roman Province and it is formed by the coalescence of four large volcanic apparata: the Palaeo-Bolsena, Bolsena, Montefiascone and Latera volcanoes (Nappi *et al.*, 1987, 1998; Palladino *et al.*, 2010) (Fig. 15). The volcanic rocks cover an area larger than 2,000 km^2, filling up a depressed area represented by the Siena-Radicofani and Paglia-Tevere grabens. The coalescence of the four volcanic apparatus formed a shield-like area with a central depressed zone occupied today by the Bolsena lake (Fig. 15). All four volcanic complexes are made up mainly of ignimbrites with subordinate lava flows, although a lava plateau has been recorded in the early history of the Latera volcano (e.g., Conticelli *et al.*, 1987, 1989; Vezzoli *et al.* 1987).

Figure 15. Geological sketch map of the Vulsini district (Roman Magmatic Province).

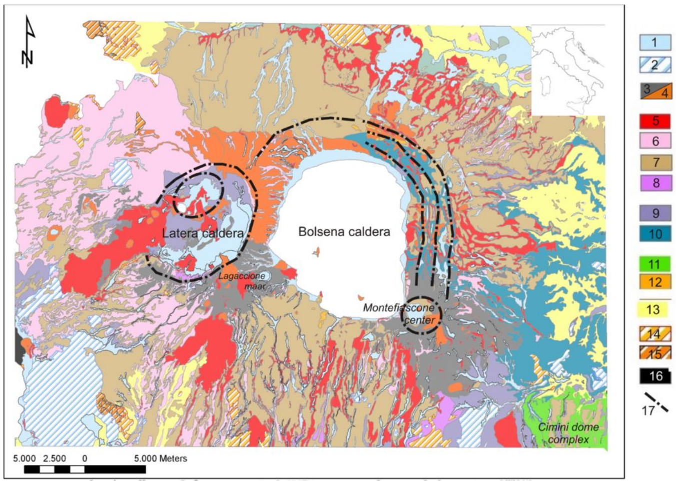

Geological sketch map of the Vulsini district. Legend: 1) Holocene alluvial and lacustrine deposits; 2) travertine; 3-9) Bolsena, Latera and Montefiascone calderas; 3) scoria cones; 4) phreatomagmatic deposits; 5) leucite-bearing lavas; 6) pozolanaceous ignimbrites; 7) fallout and reworked pyroclastics; 8) spatter-rich ignimbrites; 9) lithoidal ignimbrites; 10) PaleoBolsena volcano welded to unwelded ignimbrites and leucite-bearing tuffs; 11) rhyodacite Peperino Tipico ignimbrite (Cimini dome complex); 12) rhodacitic domes; 13) post-orogeny Pliocene-Pleistocene marine sediments; 14) Allochtonous Flysch; 15) Meso-Cenozoic pre-syn-orogenic successions; 16) Paleozoic basement; 17) caldera.

Palaeo-Bolsena volcanic apparatus has been supposed to be the oldest volcanic center and it is made up by the large trachytic, partly welded, ignimbrite called “Nenfro”, associated to leucititic to tephri-phonolitic lava flows and plinian pyroclastic fall horizons (Nappi *et al.*, 1987, 1991, 1994, 1995). Volcanic activity begun with a plinian fall layer dated at 0.59 Ma (^{40}Ar-^{39}Ar, Barberi *et al.*, 1994) and 0.58 Ma (K/Ar, Nappi *et al.*, 1995). Several conflicting age data are published on “Nenfro” ignimbrite that likely caused the Paleo-Bolsena calderic collapse: 0.88 to 0.4 Ma (K/Ar, Nicoletti *et al.*, 1981), 0.5 Ma (^{40}Ar-^{39}Ar, Barberi *et al.*, 1994) and 0.51 Ma (K/Ar, Nappi *et al.*, 1995). Single crystal, laser total fusion ^{40}Ar-^{39}Ar dating performed on a new mineral separation from the original six samples of Barberi *et al.* (1994) gives a well constrained age for this formation of 0.498 Ma (Laurenzi & Deino, 1996). The Bolsena volcanic complex begun its activity after the formation of the Palaeo-Bolsena caldera and lasted for few hundred thousand years (Palladino *et al.*, 2010, and references included). It developed mainly in the eastern sector of the Vulsinisan district with the formation of a large caldera depression partly occupied by the Bolsena Lake, and produced two thick ignimbrite sheets, fall deposits and lava flows which built an ignimbrite shield (Freda *et al.*, 1990; Nappi *et al.*, 1998; Palladino *et al.*, 2010). Fissural lava flows formed a lava plateau south of Bolsena Lake in the Marta-Tuscania area (Palladino *et al.*, 1994). The Montefiascone volcano (~0.29 - ~0.23 Ma: Nappi *et al.*, 1995; Brocchini *et al.*, 2000) evolved within the period of activity of Bolsena and partially overlapped with the Latera Volcano, developed in the western sector (~0.28 - ~0.15 Ma: Metzeltin & Vezzoli, 1983; Turbeville, 1992). Both Montefiascone and Latera volcanoes are characterized by different activities that brought to the formation of a small stratovolcano with a small summit caldera (ca. 2.5 km wide) at Montefiascone, compared to a large flat ignimbritic volcanic plateau with a large central polyphasic nested caldera (ca. 9 km wide) at Latera (Sparks, 1975; Varekamp, 1980; Conticelli *et al.*, 1986, 1987, 1991; Vezzoli *et al.*, 1987; Coltorti *et al.*, 1991; Turbeville 1992, 1993; Di Battistini *et al.*, 1998, 2001). The final activity is represented by the Bisentina and Martana Islands, and likely other centers below the Bolsena Lake, tentatively still active around 0.13 Ma (K/Ar, Nappi *et al.*, 1995).

The volcanic products are mainly characterised by leucite-bearing ultrapotassic rocks (Tables 4 and 5) with few leucite-free shoshonitic rocks confined in the post-caldera activity of the Latera volcano (Table 6; e.g., Conticelli *et al.*, 1991) and some melilite-bearing leucitites (kamafugites) in the early stages of the Montefiascone volcano (di Battistini *et al.*, 2001).

The ultrapotassic rocks range in composition from leucite-bearing basanites, leucitites, tephrites, phonolitic-tephrites, tephritic-phonolites, and phonolites (Fig. 16a). Extremely differentiated products dominated volumetrically over mafic terms, but in some cases syn-depositional formation of analcite after leucite allow the K_2O and alkalis loss, a characteristic capable to drive the juvenile

Figure 16. Classification and incompatible trace element characteristics of Pleistocene volcanic rocks from Monti Vulsini volcanoes.

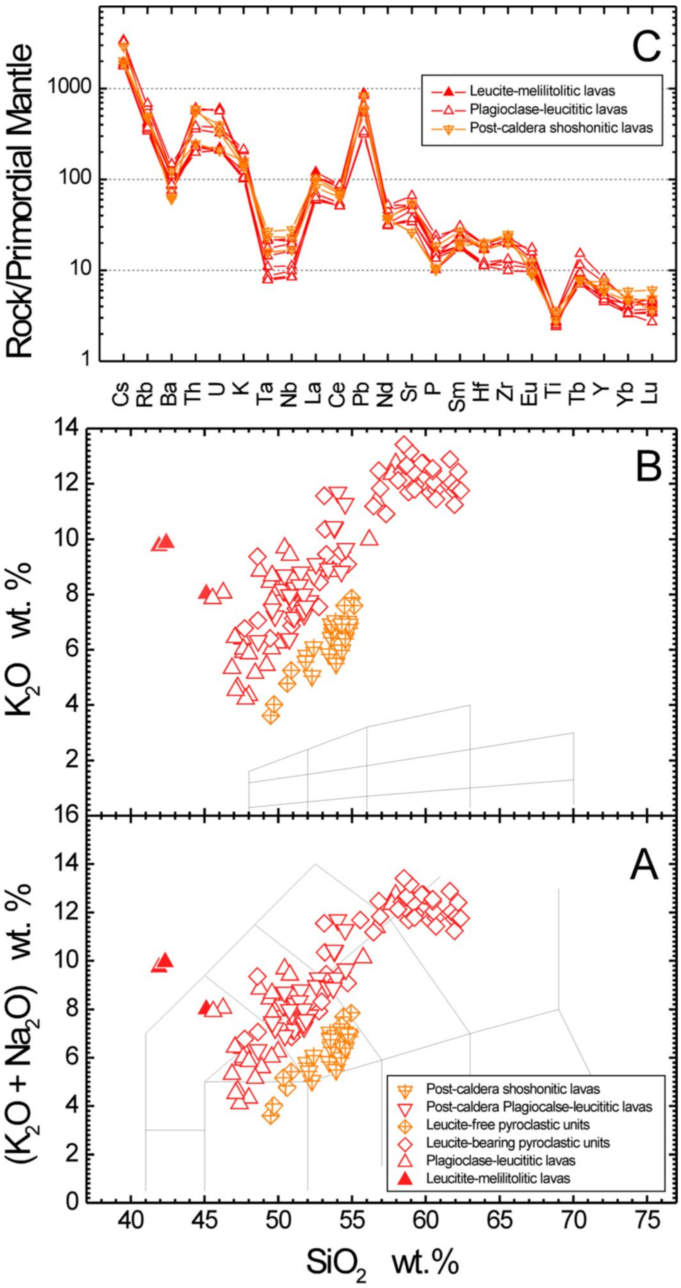

Classification and geochemical characteristics of the Vulsini leucite-bearing ultrapotassic rocks and associated shoshonitic ones. A) Total Alkali-Silica (TAS) classification diagram (Le Maitre, 2002). B) K_2O wt.% vs. SiO_2 wt.% classification diagram with reported the grid for orogenic volcanic rock suites (Peccerillo & Taylor, 1976). C) Incompatible trace element patterns for mafic volcanic rocks normalised to the primordial mantle values of Sun & McDonough (1989). Data from Holm *et al.* (1982); Civetta *et al.* (1984); Rogers *et al.* (1986); Conticelli *et al.* (1987, 1991, 2002, 2007); Coltorti *et al.* (1991); Di Battistini *et al.* (2001, 2002); Gasperini *et al.* (2002).

clasts (pumice) in ignimbrite toward a trachy-phonolitic to trachytic compositions (Conticelli *et al.*, 1987; Parker, 1989) (Fig. 16a). The most mafic compositions are always found among lava flows and they are found mainly in the plateau-like structure of the southern sector of the Vulsinian district and of Montefiascone volcano where leucite-bearing basanitic to tephritic lavas do occur (Civetta *et al.*, 1984; Rogers *et al.*, 1985; Conticelli *et al.*, 2002). Post caldera activity was particularly intense at the Latera volcano with bimodal magmatism both leucite-bearing and –free lavas (Fig. 15). Leucite-bearing post-caldera Latera lavas have compositions ranging from tephritic to tephri-phonolitic (Fig. 16a), whereas leucite-free lavas are particularly abundant within and external to the caldera in the southern eastern sector of the volcano with the Selva del Lamone lava flow (Fig. 15) and they have a clear shoshonitic affinity with lavas ranging in composition from K-trachybasalts to latites (Figs. 16a,b).

The shoshonitic trachy-basalts have mineralogy assemblages made up of abundant olivine, clinopyroxene and plagioclase, but they differ significantly in terms of geochemistry with respect to other post-caldera shoshonitic rocks from other volcanic districts of the Roman Province (e.g., Holm *et al.*, 1982; Varekamp & Kalamarides, 1989; Conticelli *et al.*, 1991, 2009b; Turbeville, 1993). The most abundant mafic mineral in the Roman rocks is the clinopyroxene, which differ significantly from volcanic rocks crystallized in equilibrium with leucite or not. Indeed, clinopyroxene from lamproite-like ultrapotassic rocks are generally aluminium poor, with Si +Al not sufficient to fill completely the tetrahedral site, whereas clinopyroxene from Roman rocks, either leucite-free or –bearing ones, are characterized by excess Al that patitioned between tetrahedral and octahedral sites (Barton *et al.*, 1982; Holm, 1982; Cellai *et al.*, 1994; Bindi *et al.*, 1999; Chelazzi *et al.*, 2006). Clinopyroxene in shoshonite from Latera volcano are transitional between those typical of leucite-free (Tuscan lamproites) and Roman rocks, whereas those from shoshonites in other Roman districts have also Al excess (Perini & Conticelli, 2002; Boari & Conticelli, 2007; Cellai *et al.*, 1994). Leucite is found both as phenocryst and as groundmass phase in plagioclase leucitites and leucitites (Fig. 3h). Sanidine is present both in the most evolved phonolitic and trachy-phonolitic terms, and it is also found also in leucite-free rocks of the Palaeo-Bolsena volcano and of the post-caldera Latera volcano.

Table 4 Chemical (major and trace) and Sr-Nd-Pb isotopic values for Roman Magmatic Province Kamafugitic rocks and melilitites.

Reference	1	1	1	2 - 1	2	2	2	3	3	4 - 5	4 - 5
District:	MLV	MLV	MLV	Umbrian	Umbrian	Umbrian	Umbrian	Vulsini	Vulsini	Albani	Albani
Locality	Colle Morrone	Colle Castellone	Colle Castellone	Polino	Polino	Cupaello	San Venanzo	Monte-fiascone	Monte-fiascone	Osa	Capo di Bove
Latitude	41°33'28"N	41°34'02"N	40°33'49"N	-	-	-	-	-	-	41°54'00"N	41°47'28"N
Longitude	13°18'11"E	13°18'07"E	12°18'08"E	-	-	-	-	-	-	12°42'24"E	12°34'59"E
Series	limestone	Kam	kam	limestone	Karb ??	Kam	kam	kam	kam	Melilitite	Melilitite
Sample	**ERN57**	**ERN56**	**ERN84**	**AM 7**	**AM 6**	**SVK 07**	**SVK 01**	**EI 27**	**CM 207**	**VLS 25**	**VLS 17**
Age:	602 ka	602 ka	602 ka	465 ka	465 ka	465 ka	465 ka	250 ka	250 ka	297 ka	291 ka
SiO_2 (wt.%)	7.66	46.03	46.54	0.23	19.33	44.49	41.88	41.70	44.90	44.10	47.81
TiO_2	0.07	1.06	1.10	0.00	0.61	1.11	0.69	0.91	0.74	0.71	0.73
Al_2O_3	2.09	16.46	16.64	0.04	4.70	7.92	12.28	14.90	12.90	15.84	16.01
Fe_2O_3	0.62	4.59	5.33	0.03	2.54	5.27	1.95	8.93	8.54	3.11	2.10
FeO	0.13	3.18	2.83	0.00	2.68	2.44	4.45	0.00	0.00	5.62	5.45
MnO	0.03	0.14	0.15	0.00	0.07	0.11	0.11	0.16	0.13	0.14	0.14
MgO	1.05	4.61	4.07	0.41	11.40	10.38	12.78	4.90	7.88	6.95	4.84
CaO	47.59	10.55	10.26	56.03	37.28	14.68	15.21	15.20	15.40	11.02	9.55
Na_2O	0.55	2.17	1.56	0.05	0.14	0.32	1.06	1.67	1.25	2.18	1.74
K_2O	0.28	9.77	9.53	0.01	0.52	9.55	8.36	8.21	6.59	8.10	9.93
P_2O_5	0.08	0.97	0.92	0.00	0.62	1.34	0.39	0.77	0.37	0.77	0.78
LOI	39.85	0.47	1.07	43.20	20.11	2.48	0.83	2.30	1.50	1.46	0.95
Sum	100.00	100.00	100.00	100.00	100.00	100.09	99.99	99.65	100.20	100.00	100.02
Mg-V	76.11	56.82	52.68	96.96	82.80	75.19	81.20	56.1	68.3	63.38	58.04
Sc (ppm)	1.2	20.1	20.4	<1	<1	16.6	21.4	-	-	20.1	17
V	17	223	228	-	50	72	110	-	-	290	287
Cr	-	13	13	21	691	65	880	7	234	29	19
Co	1.90	28.5	29.0	5.8	37.0	34.7	41.8	32.0	32.0	37.1	30
Ni	-	34.0	30.9	19	357	87	141	39	39	48	46
Cu	3.10	93.6	87.8	-	-	-	-	114	114	133	135
Zn	14.7	71.2	73.4	-	-	-	-	104	104	74	71
Ga	-	-	-	-	-	-	-	22	22	-	13
Rb	15	491	504	3	46	509	432	635	635	425	463
Sr	386	2500	1870	645	1903	3758	1706	2547	2547	1673	1487
Y	4.5	43.2	42.8	9	26	44	27	43	43	45	48
Zr	10	547	512	<10	372	848	319	429	429	302	317
Nb	1.62	35.2	35.2	3	14	47	18	19	19	16	17
Cs	0.59	53.9	60.8	-	-	74	33	-	-	-	38.5
Ba	56	4010	3930	35	4053	3980	501	1628	1628	1721	1743
La	4.30	241	226	7.5	116	257	77	161.5	161.5	148	115
Ce	7.14	478	452	11	248	526	176	336.0	336.0	267	227
Pr	0.97	52.7	50.8	-	-	-	-	40.1	40.1	-	27.3
Nd	3.84	196	189	8.8	111	248	94	152.2	152.2	120	102
Sm	0.78	33.7	32.4	1.6	22.1	38.9	16.6	26.7	26.7	27.0	18.1
Eu	0.19	7.03	6.76	0.37	3.70	6.79	3.01	21.60	21.60	4.19	3.51
Gd	0.84	28.8	27.8	-	-	-	-	17.5	17.5	-	14.1
Tb	0.13	3.02	2.92	0.2	1.3	2.5	1.4	-	-	1.70	1.47
Dy	0.72	11.9	11.5	-	-	-	-	9,97	9,97	-	6.74
Ho	0.15	1.84	1.79	-	-	-	-	1.34	1.34	-	1.13
Er	0.42	4.81	4.62	-	-	-	-	3.75	3.75	-	2.80
Tm	0.06	0.50	0.49	-	-	-	-	0.42	0.42	-	0.35
Yb	0.36	3.01	2.91	0.89	1.40	2.90	2.37	3.19	3.19	2.82	2.20
Lu	0.06	0.42	0.42	0.09	0.26	0.59	0.45	0.37	0.37	0.42	0.32
Hf	0.34	14.9	12.3	0.5	10.0	22.9	8.3	9.8	9.8	8.9	8.0
Ta	0.10	0.97	0.84	0.1	0.6	3.30	0.92	1.00	1.00	0.89	0.81
Pb	0.20	133	134	-	-	36.2	16.5	-	-	83	77
Th	1.00	93.5	90.5	1.7	46.3	112.4	36.9	76.0	76.0	50.5	50
U	2.26	7.57	6.07	-	-	28.0	9.13	16.4	16.4	9.8	5.1
$^{87}Sr/^{86}Sr$ m	0.708841	0.711176	0.711156	0.707460	0.710440	0.711280	0.710419	0.71042	0.71042	0.710291	0.710336
$^{87}Sr/^{86}Sr$ i	0.708840	0.711171	0.711149	0.707460	0.710440	0.711277	0.710414	0.71042	0.71042	0.710288	0.710333
$^{143}Nd/^{144}Nd$ m	0.512151	0.512120	0.512119	0.511848	0.512035	0.512124	0.512080	0.51213	0.51213	0.512102	0.512105
$^{143}Nd/^{144}Nd$ i	0.512151	0.512120	0.512119	0.511848	0.512035	0.512124	0.512080	0.51213	0.51213	0.512102	0.512105
$^{206}Pb/^{204}Pb$ m	-	18.7258	18.7362	-	-	18.740	18.728	-	-	18.768	18.763
$^{206}Pb/^{204}Pb$ i	-	18.725	18.736	-	-	18.736	18.725	-	-	18.768	18.763
$^{207}Pb/^{204}Pb$ m	-	15.6704	15.6823	-	-	15.663	15.648	-	-	15.683	15.680
$^{207}Pb/^{204}Pb$ i	-	15.670	15.682	-	-	15.663	15.648	-	-	15.683	15.680
$^{208}Pb/^{204}Pb$ m	-	38.9686	39.0089	-	-	38.953	38.877	-	-	39.012	39.005
$^{208}Pb/^{204}Pb$ i	-	38.967	39.008	-	-	38.948	38.874	-	-	39.011	39.004

Legend: MLV = Middle Latin Valley; kam = kamafugite; Karb = either carbonatite (Lupini and Stoppa, 1993) or diluted kamafugite after limestone assimilation (Peccerillo, 1998); Mg-V = [MgO]/([MgO]+0.85*[FeOtot]); - = not analyzed; m = measured; i = initial calculated at the age of emplacement (see age in the headings of the table).

Data from: 1 = Boari *et al.* (2009b); 2 = Conticelli *et al.* (2007); 3 = di Battistini *et al.* (2001); 4 = Boari *et al.* (2009a); 5 = Conticelli *et al.* (20010a).

Table 5 **Chemical (major and trace) and Sr-Nd-Pb isotopic values for Roman Magmatic Province (Latian districts) Plagio-leucititic and leucititic rocks.**

Reference	1	2	2	3	4	4	5	5	5	6	6
District:	Vulsini	Vico	Vico	Sabatini	Sabatini	Sabatini	MLV	MLV	MLV	Rocca-monfina	Rocca-monfina
Locality	Fiordini	C.le Montagna	Poggio Nibbio	Bracciano	M.te Maggiore	Vigna Orsini	Sant'Ar-cangelo	Celleta Schiappa	Tecchiena Convento	?	Caldera wall
Latitude	-	-	-	-	00°01'27"O	00°15'02"O	41°33'42"N	41°34'00"N	41°41'09"N	?	41°19'00"N
Longitude	-	-	-	-	42°08'16"N	42°09'11"N	13°18'29"E	13°17'23"E	13°19'20"E	?	13°58'18"E
Series	Plagio leucitites	Plagio leucitites	Plagio leucitites	Plagio leucitites	Plagio leucitites	Plagio leucitites	Plagio leucitites	Plagio leucitites	Plagio leucitites	Plagio leucitites	Plagio leucitites
Sample	**VS 189**	**VCO 99**	**VCO 8**	**DMS 983**	**BR 29**	**BR 11**	**ERN86**	**ERN58**	**ERN34**	**R-35**	**RMN 44**
Age:	250 ka	300 ka	100 ka	400 ka	390 ka	250 ka	260 ka	410 ka	412 ka	400 ka	390 ka
SiO_2 (wt.%)	49.86	53.37	49.65	49.52	48.36	57.79	46.83	46.78	48.47	45.30	46.33
TiO_2	0.61	0.68	0.76	0.67	0.70	0.30	0.83	0.84	0.82	1.04	0.97
Al_2O_3	15.39	18.35	15.24	16.55	16.80	20.74	18.25	17.47	18.06	16.75	15.26
Fe_2O_3	1.33	1.58	4.50	2.64	2.55	1.22	4.93	4.31	4.37	6.85	4.73
FeO	4.78	4.23	3.68	4.33	4.40	0.92	3.24	3.05	2.86	3.28	4.10
MnO	0.15	0.11	0.15	0.13	0.13	0.12	0.16	0.14	0.14	0.14	0.15
MgO	9.93	3.92	7.16	6.73	6.57	0.24	3.63	5.49	4.46	6.12	6.61
CaO	10.40	7.05	11.46	10.03	9.85	2.72	9.64	11.26	10.08	11.03	12.59
Na_2O	1.86	1.94	1.82	1.43	1.30	4.87	2.17	1.97	2.85	1.84	1.60
K_2O	4.47	7.97	4.56	6.71	8.33	9.70	9.14	7.62	6.90	5.24	6.63
P_2O_5	0.30	0.38	0.23	0.62	0.61	0.08	0.50	0.41	0.31	0.70	0.62
LOI	0.91	0.43	0.79	0.64	0.40	1.30	0.70	0.67	0.69	1.29	0.58
Sum	99.99	100.02	100.00	100.00	100.00	100.00	100.00	100.00	100.00	99.58	100.18
Mg-V	77.7	59.3	66.0	67.8	67.3	20.0	49.7	62.3	57.8	57.6	62.4
Sc (ppm)	26.3	18.6	-	-	29.4	0.8	11.0	18.7	17.4	30.0	-
V	202	174	246	326	-	87	275	236	211	271	312
Cr	476	48	228	34	162	6	26	124	71	78	164
Co	37.0	20	34	34.7	33.0	2.9	26.7	26.1	23.2	-	34.5
Ni	180	37	74	15	74	2	27.0	47.0	42.0	51	72
Cu	56	48	97	-	-	-	71.8	70.7	64.6	-	109
Zn	63	62	69	-	-	-	74.2	66.1	64.9	-	83
Ga	11	-	-	-	-	-	-	-	-	-	18
Rb	266	493	339	488	636	265	447	377	395	502	322
Sr	1085	1339	1064	2178	1812	1583	2260	2130	1920	1606	1784
Y	22	55	33	40.5	26	49	40.0	35.0	29.8	-	38.9
Zr	225	369	231	419	266	696	417	293	269	262	226
Nb	15	19	13	10.1	14	37	20.9	13.7	15.2	8	10.5
Cs	27	-	-	36.0	-	-	41.0	36.1	33.6	-	31.0
Ba	824	1431	531	1835	1202	760	1470	1630	1320	1022	1460
La	83	122	-	136	88	175.0	129	108	96.4	-	105.4
Ce	156	235	-	277	202	323.0	279	227	205	202.6	210.8
Pr	-	-	-	33.0	-	-	32.5	26.5	23.0	-	24.9
Nd	52.0	87	-	129	90	101	125	101	86.0	91.4	90.0
Sm	10.9	19.0	-	24.2	17.5	16.7	22.6	18.9	15.8	15.7	18.4
Eu	2.10	3.02	-	4.96	3.20	2.70	4.63	4.01	3.38	3.43	3.70
Gd	-	-	-	15.2	-	-	19.6	16.6	14.0	11.7	12.9
Tb	1.00	1.60	-	1.95	1.5	1.80	2.23	1.92	1.62	-	1.81
Dy	-	-	-	9.71	-	-	9.66	8.53	7.23	-	7.32
Ho	-	-	-	1.49	-	-	1.62	1.44	1.24	1.36	1.19
Er	-	-	-	3.53	-	-	4.33	3.81	3.37	3.45	2.96
Tm	-	-	-	0.44	-	-	0.51	0.46	0.41	-	0.367
Yb	2.10	2.40	-	2.70	2.20	4.10	3.12	2.79	2.54	2.32	2.16
Lu	0.36	0.77	-	0.37	0.38	0.70	0.45	0.41	0.38	0.34	0.311
Hf	5.2	8.5	-	10.1	6.2	10.2	10.5	7.60	7.08	-	6.38
Ta	0.91	1.34	-	1.21	0.6	1.90	0.99	0.59	0.76	-	0.54
Pb	63	122	33	78.4	46.0	131	79.4	61.6	69.1	-	50.6
Th	48.4	74.4	-	63.4	45.0	-	53.5	41.0	37.5	-	36.7
U	12.7	12.0	5.12	11.0	10.2	-	11.2	9.91	8.88	-	8.68
$^{87}Sr/^{86}Sr$ m	0.71029	0.711158	0.708185	0.710782	0.710048	0.710188	0.710071	0.709815	0.709421	0.70965	0.709533
$^{87}Sr/^{86}Sr$ i	0.71028	0.711153	0.708184	0.710778	0.710042	0.710186	0.710069	0.709812	0.709418	0.70964	0.709530
$^{143}Nd/^{144}Nd$ m	0.512093	0.512108	0.512214	0.512117	0.512094	-	0.512127	0.512121	0.512142	-	0.512152
$^{206}Pb/^{204}Pb$ m	18.731	18.737	18.827	18.754	18.705	-	18.7796	18.8018	18.8153	-	18.788
$^{207}Pb/^{204}Pb$ m	15.657	15.619	15.659	15.657	15.640	-	15.6811	15.6884	15.6883	-	15.689
$^{208}Pb/^{204}Pb$ m	38.938	38.985	39.078	39.018	38.988	-	39.0168	39.0464	39.0475	-	39.048

Legend: MLV = Middle Latin Valley; Plagio-leucitites include also leucitites s.s.; Mg-V = [MgO]/([MgO]+0.85*[FeOtot]); - = not analyzed; m = measured; i = initial calculated at the age of emplacement (see age in the headings of the table).

Data from: 1 = Conticelli *et al.* (2002); 2 = Perini *et al.* (2004); 3 = Gasperini *et al.* (2002); 4 = Conticelli *et al.* (1987); 5 = Boari *et al.* (2009a); 6 = Conticelli *et al.* (2009b).

Apparently normalized incompatible trace element patterns of plagioclase leucititic rocks of the Vulsinian district are similar to those of earlier magmatisms (Fig. 16c) characterized by leucite-free ultrapotassic rocks (i.e., lamproite) and associated shoshonites and calc-alkaline rocks (i.e. Western Alps, Western Tyrrhenian Sea, Tuscany). Vulsinian plagioclase leucititic rocks and associated shoshonites, however, display larger throughs at Nb, Ta, and Ti, the appearance of a small through at Hf, and a small peak at Sr, concomitantly to the inversion of the U/Th and Ta/Nb normalized ratios (Fig. 16c), with respect to the older leucite-free ultrapotassic and associated shoshonites and calc-alkaline rocks (Figs. 8c, 10c, 12c).

2. Vico district

The Vico district consists of a single Pleistocene volcanic edifice built in the form of a conic stratovolcano cut by a summit polygenetic caldera (Mattias & Ventriglia, 1970; Perini *et al.*, 1997, 2004). Post-caldera activity, subordinate in volume, both within and on the edge of the caldera do occur (Fig. 17; Perini *et al.* 1997, 2004). The Vico volcano like the other Roman volcanoes North of Rome (Fig. 11) developed within the NW–SE Siena-Radicofani and Paglia-Tevere extensional basin (Barberi *et al.*, 1994), and it covers almost completely an older volcanic apparatus belonging to the Tuscan Magmatic Province, the Monte Cimino Volcanic Complex.

Figure 17. Geological sketch map of the Vico district (Roman Magmatic Province).

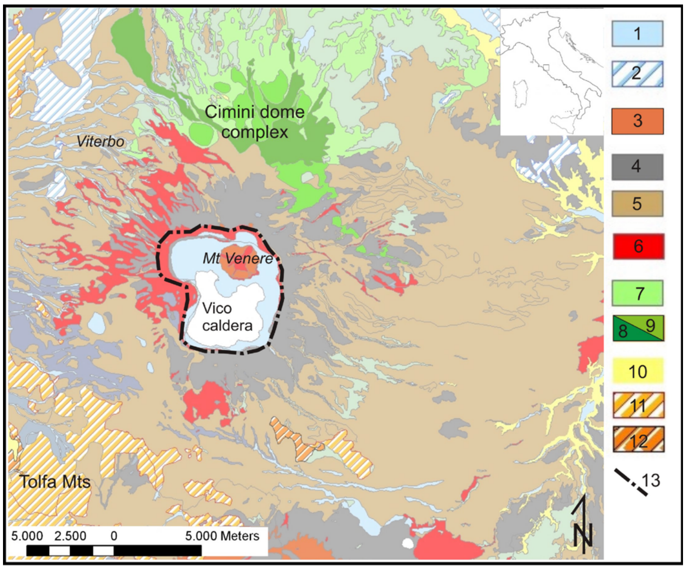

Geological sketch map of the Vico volcano. Legend: 1) Holocene alluvial and lacustrine deposits; 2) travertine; 3) Monte Venere period: post-caldera scoria cones (third period); 4-6) Lago di Vico period (second period): 4) Carbognano phreatomagmatic ignimbrite; 5) caldera forming phonolitic ignimbrites; 6) stratocone building leucite-bearing lavas; 7-9) Cimini dome complex (1300-900 ka): 7) rhyodacitic Peperino Tipico ignimbrite; 8) rhyodacitic domes; 9) lamproitic lava; 10) post-orogeny Pliocene-Pleistocene marine sediments; 11) Allochtonous Flysch; 12) Macigno Flysch; 13) caldera.

The stratigraphy of Vico volcano is divided into three main rock successions: the Rio Ferriera, the Lago di Vico, and the Monte Venere successions (Perini *et al.*, 1997, 2004). The early activity, during the Rio Ferriera period (I^{st}) produced pyroclastic fall and flow units interbedded to minor lava flows (Cioni *et al.*, 1987; Barberi *et al.*, 1994; Perini *et al.*, 1997, 2000). The onset of the Rio Ferriera period is constrained by the age of the basal plinial fall at about 0.42 Ma (Sollevanti, 1983; Barberi *et al.*, 1994). All K/Ar model ages older than 0.42 Ma (Nicoletti, 1969) are clearly biased. The Lago di Vico period (II^{nd}) involved an early stratovolcano-building phase (0.30–0.26 Ma; Sollevanti, 1983; Laurenzi & Villa, 1987; Barberi *et al.*, 1994) with emplacement of leucite-bearing lava flows (~ 50 km^3; Bertagnini & Sbrana, 1986; Perini *et al.*, 1997, 2004). Villemant & Fléhoc (1989) report a K/Ar age of 0.18 Ma and a U-Th isochron age of 0.21 (+0.028/-0.022) Ma for the final episode of the stratovolcano building period. Towards the end of the Lago di Vico period four explosive ignimbrite-forming eruptions caused the destruction of the Vico edifice and the formation of an 8 km diameter polygenetic caldera (Perini *et al.*, 1997, 2004). These were the Farine, Ronciglione (0.16 Ma), Sutri (*Tufo Rosso a scorie nere*, 0.15 Ma) and Carbognano (0.14 ka) eruptions (Sollevanti, 1983; Laurenzi & Villa, 1987; Barberi *et al.*, 1994; Perini *et al.*, 1997, 2004; Bear *et al.*, 2009a,b). The post caldera activity (i.e., Monte Venere period - III^{rd}) comprises the so called "*Tufi Finali*", several monogenetic cones, and minor lava flows. The Monte Venere is an intra-caldera cinder cone, whereas other three cinder cones are found along the northern caldera rim from Poggio Nibbio to Poggio Varo (Fig. 17). A small shoshonitic lava flow has been vented from a fracture on the caldera margin flowing down both into the caldera and along the external northern flank of the volcano (Perini *et al.*, 1997, 2004). K/Ar ages comprised between 0.095 and 0.085 Ma are from Monte Venere rocks (Laurenzi & Villa, 1985; Villemant & Fléhoc, 1989); a ^{40}Ar-^{39}Ar age equal within error to K/Ar ones was obtained on scoriaceous deposits drilled into the Vico lake sediments (Magri & Sadori, 1999; Laurenzi, unpublished datum).

The Rio Ferriera volcanic rocks have a mild potassic nature, resembling closely previous Tuscan rocks of the underlying Cimino volcano, but leucite appears randomly. They range in composition from latite to trachyte and rhyodacite (Fig. 18a, 18b). Large sanidine phenocrysts are also found but they are not in equilibrium with Vico magmas, corroborating the hypothesis that Rio Ferriera formations represent hybrid rocks due to magma mixing between differentiated Tuscan high-K calc-alkaline magmas and newly arrived ultrapotassic silica-undersaturated leucite-bearing Roman magmas (Perini *et al.*, 2000, 2003). The Lago di Vico period of activity was dominated by plagioclase-leucititic lavas and pyroclastic rocks, ranging in compositions from leucite-bearing tephrites to leucite-bearing phonolites, passing through phonolitic-tephrites and tephritic-phonolites (Fig. 18a). Syn-depositional alkali loss in pyroclastic rocks is observed at Vico volcano similarly to Vulsinian district (Fig. 18a).

Vico post caldera activity, analogously to what observed at Latera volcano, diplays a clear bimodal petrologic affinity (Tables 5 and 6). Leucite-bearing tephrites (Monte Venere scoria and lavas) beside leucite-free olivine latites with a shoshonitic affinity (Poggio Nibbio lavas) and olivine trachybasalts (Poggio Nibbio scoria), the latter showing seldom leucite both as phenocrysts and in the groundmass, occur in the post caldera period (Fig. 18a).

Normalized incompatible trace element patterns of leucite-bearing Vico rocks differs significantly from those of Vulsinian ones (Fig. 18c). Apart the general pattern with HFS elements fractionated with respect to LIL elements, which is a general rule for the overall western Mediterranean ultrapotassic and associated rocks (e.g., Conticelli *et al.*, 1986, 1997, 2002, 2004, 2007, 2009a), the Vico rocks show larger troughs at Ba, P, and Ti but smaller ones at Ta and Nb, with larger peaks at Pb than Vulsinian plagio-leucititic rocks. Other differences with Vulsinian rocks are observed in the normalized Th/U, Ta/Nb, Nd/Sr, Zr/Hf ratios (Fig. 18c). Fractionation of Th/U has been found to be a peculiar characteristic of the Vico volcano with respect to the other Roman volcanoes (Villemant & Palacin, 1987; Villemant & Fléhoc, 1989; Avanzinelli *et al.*, 2008).

Figure 18. Classification and incompatible trace element characteristics of Pleistocene volcanic rocks from Vico volcano.

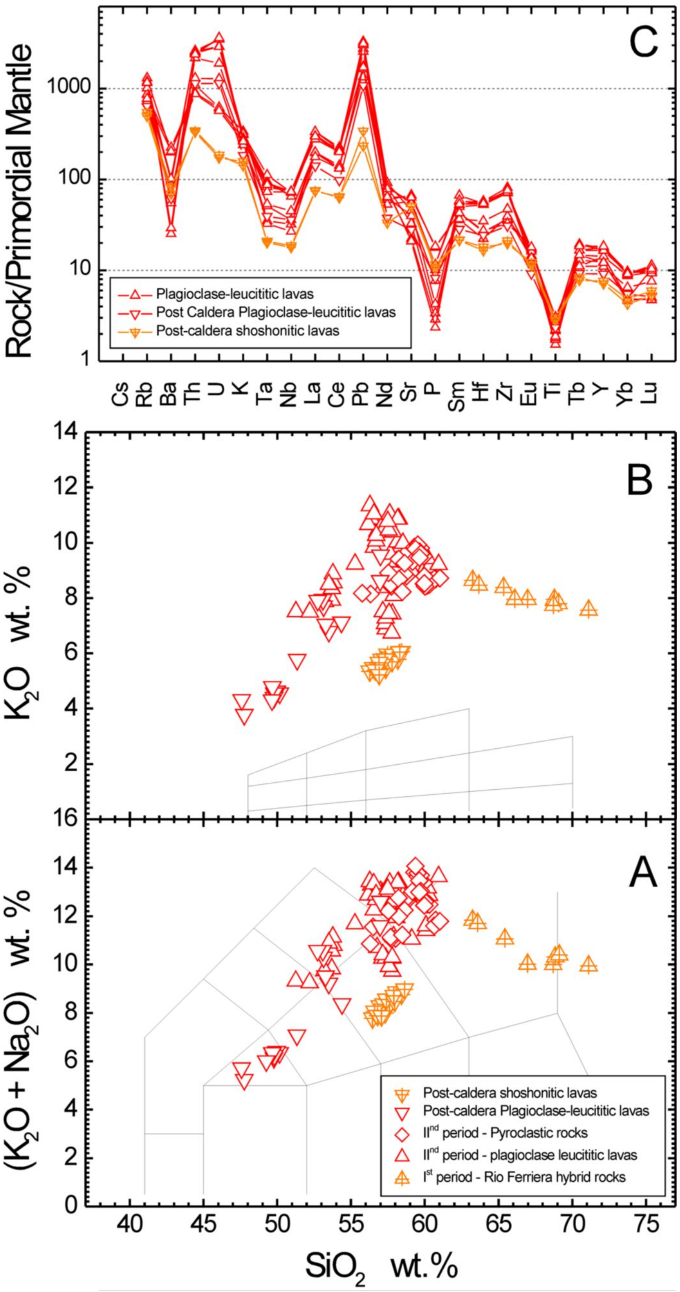

Classification and geochemical characteristics of the Vico leucite-bearing ultrapotassic rocks and associated shoshonitic ones. A) Total Alkali-Silica (TAS) classification diagram (Le Maitre, 2002). B) K_2O wt.% vs. SiO_2 wt.% classification diagram with reported the grid for orogenic volcanic rock suites (Peccerillo & Taylor, 1976). C) Incompatible trace element patterns for mafic volcanic rocks normalised to the primordial mantle values of Sun & McDonough (1989). Data from Barbieri *et al.* (1988); Perini *et al.* (1997, 2000, 2003, 2004).

Table 6 **Chemical (major and trace) and Sr-Nd-Pb isotopic values for Roman Magmatic Province (Latian districts) shoshonitic, high-K calc-alkalic and calc-alkalic volcanic rocks**

Reference	1 - 2	3	4	5	5	5	5	6	6	6	6
District:	Vulsini	Vulsini	Vico	MLV	MLV	MLV	MLV	Rocca-monfina	Rocca-monfina	Rocca-monfina	Rocca-monfina
Locality	Selva del Lamone	?	P.gio Nibbio	spinazzeta	Selva Piana	La Badia	Case Scolopi	Masseri Robetti	Monte Lattani	Monte S.Croce	Poggio Molara
Latitude			-	41°33'13"N	41°31'35"N	41°32'35"N	41°32'09"N	41°18'59"N	41°18'03"N	41°17'59"N	41°18'08"N
Longitude	-	-	-	13°21'00"E	13°21'21"E	13°19'19"E	13°21'20"E	13°58'24"E	13°58'42"E	13°57'43"E	13°58'24"E
Series	Sho	Sho	Sho	Sho	Sho	CA	CA	Sho	Sho	Sho	HKCA
Sample	**Bols 301**	**TrB 6701**	**VCO 155**	**ERN77**	**ERN91**	**ERN83**	**ERN94**	**Rmn 11**	**RMN 24**	**RMN 30**	**RMN 33**
Age:	150 ka	150 ka	100 ka	345 ka	357 ka	269 ka	269 ka	327 ka	169 ka	148 ka	130 ka
SiO_2 (wt.%)	53.37	53.37	57.07	48.66	49.57	48.70	50.25	47.28	54.38	55.19	53.40
TiO_2	0.72	0.75	0.62	0.74	0.81	0.82	0.77	0.91	0.73	0.73	0.80
Al_2O_3	17.89	15.85	16.66	17.03	17.84	17.36	18.53	15.80	18.25	18.96	18.65
Fe_2O_3	1.57	2.12	2.30	2.40	3.50	3.91	3.45	2.48	2.09	4.14	1.92
FeO	3.92	3.60	2.63	4.99	4.28	4.57	4.19	5.96	4.37	2.46	6.09
MnO	0.11	0.12	0.10	0.15	0.15	0.16	0.15	0.15	0.14	0.16	0.15
MgO	7.00	7.03	5.67	8.47	6.55	8.08	7.00	9.35	3.14	3.04	4.44
CaO	7.60	8.87	6.05	11.88	11.02	12.06	10.39	12.05	7.25	6.24	8.58
Na_2O	2.53	2.52	2.71	2.19	2.48	2.98	3.37	1.32	2.86	2.89	2.16
K_2O	4.55	4.33	5.74	2.76	3.39	0.54	0.74	1.29	4.93	4.45	3.00
P_2O_5	0.21	0.23	0.16	0.24	0.22	0.22	0.24	0.30	0.30	0.24	0.18
LOI	0.53	0.65	0.30	0.49	0.20	0.89	0.93	3.22	1.75	1.36	0.63
Sum	100.00	99.44	100.00	100.00	100.00	100.28	100.00	100.11	100.18	99.86	100.00
Mg-V	73.4	72.8	71.65	71.20	64.79	67.57	66.70	70.53	51.30	50.76	54.36
Sc (ppm)	23.4	-	20.3	27.5	25.7	32.3	27.6	43.8	-	-	-
V	-	156	138	209	226	221	215	-	205	189	202
Cr	508	233	247	408	167	319	217	350	14	9	43
Co	30.0	-	21	32.6	31.9	34.3	32.8	43	20.3	19.9	23.8
Ni	128	111	108	69.0	41.0	58.0	47.0	74	10	11	17
Cu	-	-	40	74.7	84.1	63.6	44.5	-	43	51	15
Zn	-	-	55	60.2	66.3	60.0	61.5	-	68	81	99
Ga	-	-	-	-	-	-	-	-	19	20	19
Rb	315	319	423	173	160	130	134	189	207	162	132
Sr	548	563	601	1058	1076	808	1007	819	1060	898	892
Y	29	37	53	18	21	19	19	30	32.0	30.8	26.2
Zr	279	247	349	124	132	112	114	146	205	199	139
Nb	20	18	26	9.10	9.45	6.88	7.87	16	16.2	16.6	10.6
Cs	16.0	-	-	9.11	10.6	7.40	8.11	18.0	10.8	4.98	7.67
Ba	442	543	425	533	566	454	520	841	752	656	580
La	71.7	72.5	104.533	39.1	42.1	30.8	37.1	40.7	63.0	53.2	39.0
Ce	129.0	149.0	185.6	82.2	88.7	66.8	78.8	77	128.6	108.9	78.7
Pr	-	-	-	9.81	10.5	8.21	9.43	-	13.4	11.2	8.72
Nd	50	53.2	58	38.8	41.2	33.4	37.7	36	52.5	42.7	34.1
Sm	9.1	8.6	14.2	7.71	8.17	7.08	7.60	7.66	10.5	8.65	6.91
Eu	1.50	1.66	1.65	1.94	2.02	1.77	1.91	1.88	2.40	1.97	1.65
Gd	-	-	-	7.45	7.79	6.69	7.29	-	8.12	6.85	5.72
Tb	0.85	1.05	1.2	0.99	1.03	0.91	0.96	0.7	1.21	1.07	0.91
Dy	-	-	-	5.13	5.36	4.82	5.06	-	5.92	5.44	4.59
Ho	-	-	-	0.96	1.00	0.91	0.95	-	1.08	1.06	0.90
Er	-	-	-	2.63	2.77	2.47	2.63	-	3.08	3.10	2.61
Tm	-	-	-	0.35	0.37	0.33	0.35	-	0.441	0.441	0.378
Yb	2.90	1.91	2.60	2.15	2.27	2.02	2.15	1.73	2.84	2.80	2.51
Lu	0.45	0.25	0.43	0.33	0.35	0.31	0.33	-	0.414	0.424	0.373
Hf	6.2	6.3	8.0	3.68	3.79	3.17	3.50	2.8	5.20	5.04	3.72
Ta	1.10	0.83	1.77	0.53	0.62	0.45	0.51	0.90	0.94	0.96	0.70
Pb	59	-	101	17.1	21.2	13.0	16.1	8.71	22.5	25.3	17.8
Th	46.89	53.0	103	13.1	13.7	8.72	10.7	7.8	18.6	19.1	9.2
U	8.36	-	25	3.49	4.34	2.69	2.94	1.7	5.3	5.6	2.2
$^{87}Sr/^{86}Sr$ m	0.70993	0.70990	0.710136	0.706981	0.706973	0.706604	0.706779	0.706663	0.707455	0.707031	0.707476
$^{87}Sr/^{86}Sr$ i	0.70993	0.70990	0.710133	0.706978	0.706971	0.706602	0.706778	0.706660	0.707454	0.707030	0.707475
$^{143}Nd/^{144}Nd$ m	0.512189	0.512160	0.512177	0.512361	0.512341	0.512374	0.512360	0.512377	0.512371	0.512369	0.512265
$^{206}Pb/^{204}Pb$ m	18.668	18.728	18.728	18.9344	18.8987	18.9218	18.9167	19.153	19.069	19.008	18.896
$^{207}Pb/^{204}Pb$ m	15.670	15.676	15.674	15.6773	15.6811	15.6883	15.6948	15.680	15.694	15.693	15.700
$^{208}Pb/^{204}Pb$ m	39.025	39.000	39.007	39.0360	39.0250	39.0533	39.0898	39.199	39.212	39.168	39.118

Legend: MLV = Middle Latin Valley; sho = shoshonitic series; HKCA = High-K calc-alkaline series; CA = calc-alkaline series; Mg-V = [MgO]/([MgO]+0.85*[FeOtot]); - = not analyzed; m = measured; i = initial calculated at the age of emplacement (see age in the headings of the table).
Data from: 1-2 = Conticelli *et al.* (1991, 2002, 2007); 3 = Rogers *et al.* (1985); 4 = Perini *et al.* (2004); 5 = Boari *et al.* (2009a); 6 = Conticelli *et al.* (2009b).

3. Sabatini district

The volcanic style of the Sabatini volcanoes was mainly explosive but lava flows are also abundant and vented from several different centers spread out over the entire district area (Fig. 19; Conticelli *et al.*, 1997). There are three caldera depressions, which are from east to west: Sacrofano, Baccano and Bracciano caldera (Fig. 19; De Rita *et al.*, 1983, 1988 1993a, 1993b; De Rita & Zanetti, 1986; De Rita & Sposato, 1986). The Sabatini district developed within the southeastern prosecution of the NW–SE Siena-Radicofani and Paglia-Tevere extensional basin (e.g., Baldi *et al.*, 1974; Locardi *et al.*, 1976; Barberi *et al.*, 1994). Analogously to the Vico district also the Sabatini overlap partially, on its western portion an older volcanic complex belonging to the Tuscan Magmatic Province, which is the Tolfa-Ceriti Dome Complex (Figs. 11, 19), made of leucite-free shoshonitic to high-K calc-alkaline rocks belonging to the Pliocene lamproite-shoshonite-calc-alkaline suite of the Tuscan Magmatic Province (Fig. 12b). These pre-Sabatini volcanic rocks outcrop within the volcanic cover of the Sabatini district at Manziana and Monte Calvario areas, and define the southwestern and northwestern edges of the district (Fig. 19). On the basis of geological and volcanological records the volcanic activity of Sabatini district has been divided in five different periods (e.g., Conticelli *et al.*, 1997; Karner *et al.*, 2001a).

Figure 19. Geological sketch map of the Sabatini district (Roman Magmatic Province).

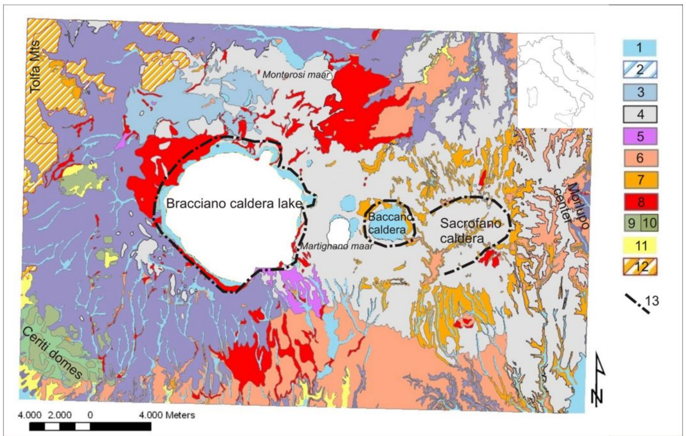

Geological sketch map of the Sabatini district. Legend: 1) Holocene alluvial and lacustrine deposits; 2) travertine; 3) scoria cones; 4) phreatomagmatic deposits from the final Sacrofano caldera phase and the recent maars; 5) pozolanaceous ignimbrites; 6) fall deposits; 7) lithoidal ignimbrites; 8) undersaturated lavas; 9-10) Manziana-Ceriti rhyodacitic domes, lavas and ignimbrites; 11) Messinian-Pliocene post-orogenic marine deposits; 12) Allochtonous Flysch.

All ages mentioned in the following discussion are ^{40}Ar-^{39}Ar ages, unless otherwise stated. Distal tephra layers probably related to the early Sabatini history, found in well cores, are dated between 0.8 and 0.76 Ma (Florindo *et al.*, 2007), followed by other pyroclastic deposits, always in distal sections, that cover the time span from 0.65 Ma (Karner *et al.*, 2001a) till the emplacement of Morlupo block and ash deposit (0.59 Ma, Cioni *et al.*, 1993). Continuous volcanic activity, characterized by large volumes of products, started at about 0.59 Ma and lasted till about 0.4 Ma. The activity of the first period continued in the eastern sector (Fig. 19) with the emplacement of the “*Tufo Giallo della Via Tiberina*” ignimbrite (0.55 Ma, Karner *et al.*, 2001a), and then moved also to the western sector of the district where strong parossistic eruptions produced the “*Prima Porta*” ignimbrite (0.51 Ma: Karner *et al.*, 2001a), the “*Grottarossa* ” pyroclastic sequence (0.52 Ma: Karner *et al.*, 2001a), the “*Tufo Terroso con Pomici Bianche*” (0.49 Ma: Karner *et al.*, 2001a), the “*Tufo Grigio Sabatino*” (also called “*Tufo Rosso a Scorie Nere Sabatino*”) a red tuff with black pumice (0.43 Ma, K/Ar: Evernden & Curtis, 1965; 0.45 Ma: Cioni *et al.*, 1993, Karner *et al.*, 2001a), the “*Peperini Listati*” ignimbrite (0.45 Ma: Cioni *et al.*, 1993). The third period of activity was mainly characterised by effusive eruptions with lava flows alternated to large volume of fallout and surges deposits, the latter grouped in the “*Tufi Varicolori della Storta*” (0.41 Ma: Karner *et al.*, 2001a), and the “*Tufi Stratificati Varicolori di Sacrofano*” pyroclastic sequences (Fig. 19). The activity of this period was concluded by the “*Tufo Giallo di Sacrofano*” ignimbrite (0.29 Ma: K/Ar, Fornaseri, 1985; ^{40}Ar-^{39}Ar, Karner *et al.*, 2001a; Sottili *et al.*, 2010). During this period both the Bracciano and Sacrofano calderas were formed (De Rita *et al.*, 1983, 1993a). The fourth period of activity produced several monogenetic centers widely distributed over the entire district (Fig. 19). Most of them produced a single lava flow associated to scoria cones. The most intense monogenetic activity was concentrated in the Rocca Romana - Trevignano area, in the northwestern sector, but cinder cones have been also found in the eastern sector as well (Monte Maggiore, Colle Aguzzo, Casale Francalancia; Fig. 19), and at the border of the Bracciano caldera (Trevignano, Vigna di Valle). The fifth period of activity concentrated in the central sector of the district, in the area between the Bracciano and Sacrofano calderas (Fig. 19), with hydromagmatic activity that produced the tuff ring and tuff cones of Stracciacappe, Martignano, and Baccano. Age data just out clarify the more recent activity of this volcanic district, with the hydromagmatic centres concentrated at about 0.1-0.09 Ma (Sottili *et al.*, 2010); these ages confirm the previous youngest recorded age, 0.09 Ma (K/Ar, Fornaseri, 1985a).

Apart the Morlupo trachyte, which represents a very small outcrop of hybrid products at the very beginning of activity, and the Vigna di Valle leucite-bearing latite, a Bracciano post caldera lava, the rest of the Sabatini volcanic rocks are made up exclusively by silica-undersaturated volcanic rocks (Cundari, 1979; Conticelli *et al.*, 1997), ranging in composition from leucite-bearing tephrites to phonolites (Fig. 20a). Alkali and potassium lost (Fig. 20a,b) during syn-depositional transformation of leucite in analcite is observed in pyroclastic juvenile fragments of the Sabatini volcanoes (Parker, 1989). Clinopyroxene and leucite are the most abundant phenocryst phases with olivine restricted to the most evolved terms. Groundmasses are made up of leucite, clinopyroxene, plagioclase, nepheline, phlogopite, magnetite, and apatite. Titanite and haüyne have been found as accessory minerals in the most extreme differentiated phonolites (authors' unpublished data). The Vigna di Valle lavas are the less silica undersaturated lavas, and beside the centimetric leucite megacrysts/xenocrysts the rocks is made up of hyalophane and Barium-phlogopite crystals as well. Clinopyroxene are salitic in composition with strong zoning and abundant aluminium, enough to fill completely the tetrahedral site and to partition it in the octahedral (Cundari & Ferguson, 1982; Dal Negro *et al.*, 1985; Cellai *et al.*, 1994).

Incompatible trace element contents of Sabatini volcanic rocks have similar distribution and fractionation to leucite-bearing rocks of other volcanoes of the Roman Province (Fig. 20c), with negative spikes at Ba, Ta, Nb, P, Hf, and Ti, and peaks at Rb, Pb, Sr. Although mostly ultrapotassic rocks are observed in the Sabatini volcanic activity, a slight decrease in K_2O and incompatible element is observed passing from pre-caldera to post-calderas periods (Conticelli *et al.*, 1997). The observed decrease in the total amount of incompatible trace elements at the same level of differentiation has been already seen

Figure 20. Classification and incompatible trace element characteristics of Pleistocene volcanic rocks from Sabatini volcanoes.

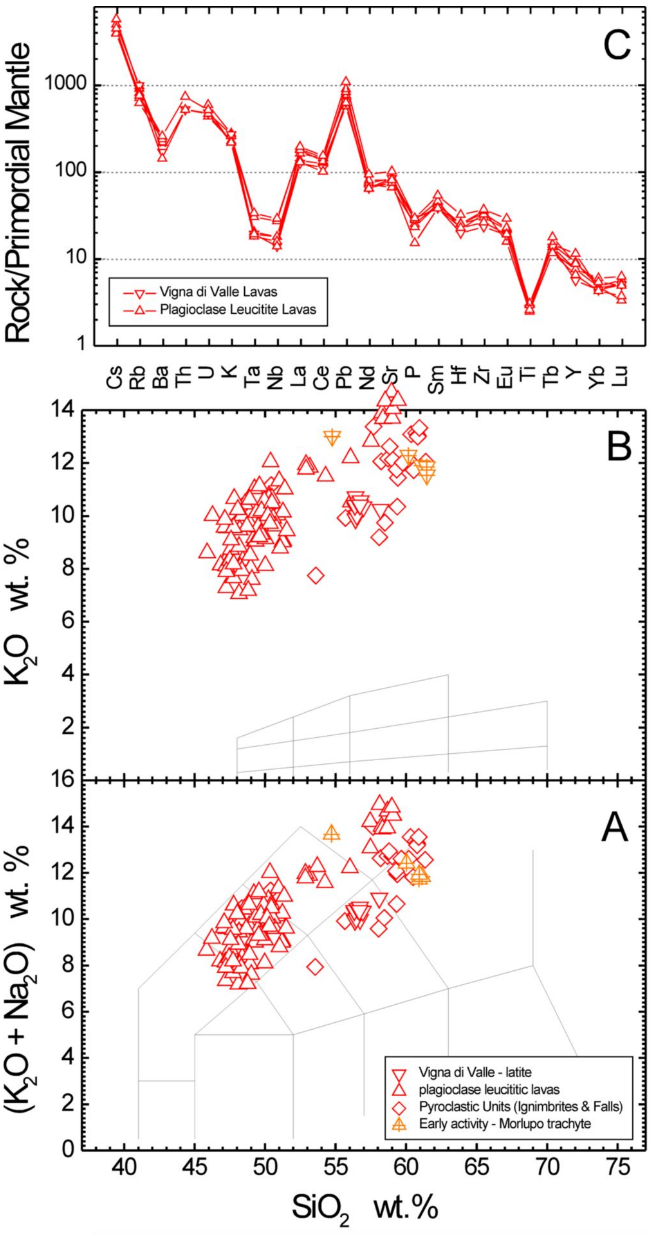

Classification and geochemical characteristics of the Sabatini leucite-bearing ultrapotassic rocks. A) Total Alkali-Silica (TAS) classification diagram (Le Maitre, 2002). B) K_2O wt.% vs. SiO_2 wt.% classification diagram with reported the grid for orogenic volcanic rock suites (Peccerillo & Taylor, 1976). C) Incompatible trace element patterns for mafic volcanic rocks normalised to the primordial mantle values of Sun & McDonough (1989). Data from Conticelli *et al.* (1997).

at the passage from pre- to post-caldera activity in the leucite-bearing series of Vulsinian volcanoes and Vico ones. In the latter cases, however, beside these leucite-bearing post-caldera series, leucite-free rocks have been erupted in the very last phases of volcanism. Indeed at Latera volcano (Vulsinian district) and at Poggio Nibbio (Vico district) leucite-free olivine-bearing shoshonitic trachybasalts are observed as the last eruption of the volcanic cycle in these two districts (Figs. 16 and 18). At the Sabatini district none of these mildly alkaline compositions have been observed, but it might not be excluded that magmas involved in the final hydromagmatic activity of Baccano-Martignano-Stracciacappe might have a shoshonitic affinity rather than ultrapotassic.

Figure 21. Geological sketch map of the Colli Albani (Alban Hills) district (Roman Magmatic Province).

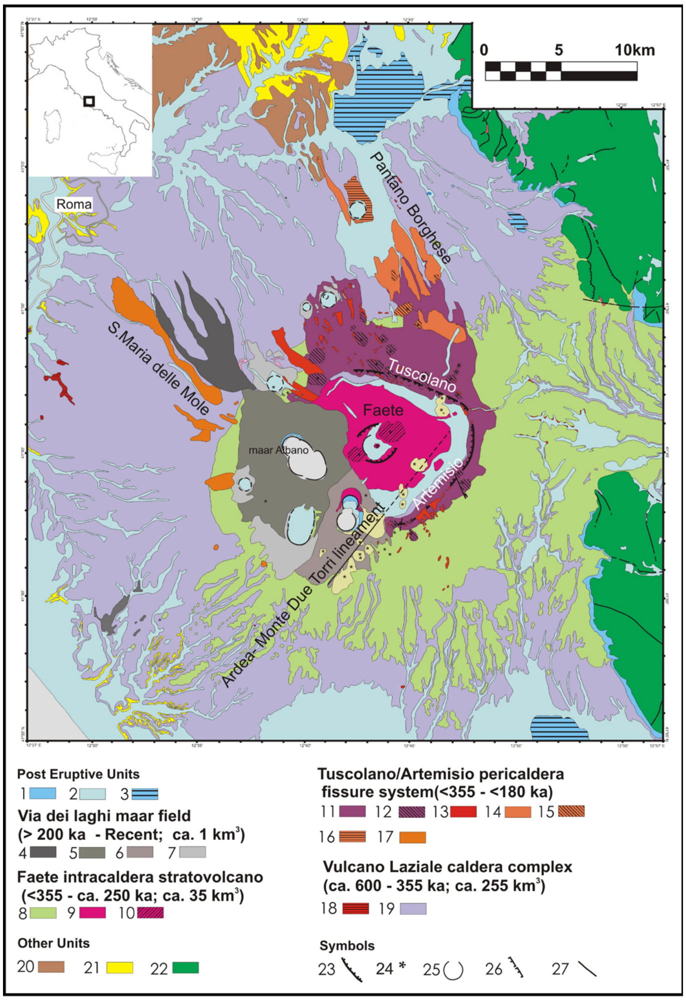

Geological sketch map of Colli Albani volcano with reported the three main periods of activity: I) Vulcano Laziale Period (pre-caldera), characterised by central activity with predominant paroxysmal explosive eruptions and fissural lava flows; II) Tuscolano Artemisio – Monte delle Faete period (post-caldera), characterised by the occurrence of six different sectors of volcanic activity: a) external to the caldera rim, with the Santa Maria della Mole lavas, the Pantano-Borghese centers and the Monte Due Torri cones and lavas; b) caldera-rim monogenetic activity that occurred along the northern and western edges of the Caldera (Tuscolano and Artemisio alignements); c) internal to the caldera, with the formation of the composite volcano of Monte delle Faete; III) The Via dei Laghi period, characterised by phreatomagmatic activity with little magmatic activity.

Legend: 1 & 2) alluvial deposits; 3) travertine; 4) Tavolato formation; 5) Albano maar; 6) Nemi maar; 7) other maars; 8) subplinian fall; 9) lower Faete succession; 10) upper Faete succession; 11) Tuscolano Artemisio (T.A.) scoria; 12) T.A. welded scoria; 13) T.A. lavas; 14 & 15) Pantano Borghese scoria & lavas; 16 & 17) Santa Maria delle Mole scoria & lava; 18 & 19) plateau lavas & ignimbrites; 20) Sabatini volcanic products; 21 & 22) sedimentary sequences; 23) caldera rim; 24) cinder cones; 25) maars; 26) inferred caldera rim; 27) fault. Re-drawn after Giordano *et al.* (2006), and Boari *et al.* (2009a).

4. Alban Hills (Colli Albani) district

The Colli Albani (Alban Hills) is a large flat stratovolcano with a central polygenetic caldera, and a dispersed post-caldera activity (Fig. 21). It was active from 0.6 Ma till recent times (e.g., Giordano *et al.*, 2006, 2010; Marra *et al.*, 2008, and references therein). It is located immediately south of Rome, some 15 km from the center of the city, on whose rocks the Ethernal city was built on and by (Funiciello *et al.*, 2008). Volcanic activity occurred at the intersection of a NW-SE extensional basin, the Latin Valley, which represent the natural southward prosecution of the Siena-Radicofani-Paglia extensional basin, with a NE-SW and N-S systems of extensional and strike-slip faults (Faccenna *et al.*, 1994a, 1994b, 1994c; De Rita *et al.*, 1995). Volcanic rocks lie over Pliocene-Pleistocene marine sands and clays, and over the bordering horsts made of Triassic/Miocene platform carbonate units (Funiciello & Parotto, 1978; Danese & Mattei, 2010).

According to Giordano *et al.* (2006, 2010), volcanic activity of the Colli Albani volcano can be divided into three main periods: i) the “Vulcano Laziale” period, ii) the “Tuscolano Artemisio – Monte delle Faete” period, and iii) the “Via dei Laghi” period (Fig. 21). Polygenetic caldera collapse is the main volcano-tectonic characteristic delimiting the activity of the first period. The volume of the erupted volcanic rocks decreases greatly with time: from some 300 km^3 during the first period to ca. 1 km^3

during the last period. The Vulcano Laziale volcanic edifice cover an area of about 1,600 km^2, with an ignimbrite plateau associated with a piece-meal caldera complex, with over 300 km^3 of dominantly pyroclastic products and subordinate lava (Fornaseri *et al.*, 1963; De Rita *et al.*, 1995; Giordano *et al.*, 2006, 2010). Early volcanic activity generated the Pisolitic Tuffs succession (0.6-0.5 Ma; De Rita *et al.*, 2002 and reference therein), which is interbedded with distal early pyroclastic from Sabatini volcanoes (Karner *et al.*, 2001a, 2001b; Marra *et al.*, 2009). All ages mentioned in the following discussion are ^{40}Ar-^{39}Ar ages, unless otherwise stated. The largest volumetric units are represented by the Pozzolane Tuffs succession (0.46-0.35 Ma, Giordano *et al.*, 2010 and references therein), a sequence of three large ignimbrites with intermediate compositions (Fig. 23a). The "*Pozzolane Rosse*" (0.457 Ma, Karner *et al.*, 2001a), the "*Pozzolane Nere*" (0.407 Ma, Karner *et al.*, 2001a; 0.405±0.003 Ma, K/Ar, Karner *et al.*, 2001c) and the "*Tufo Lionato-Pozzolanelle*" are the main ignimbrites (Watkins *et al.*, 2002; Giordano *et al.*, 2006, 2010). The "*Tufo Lionato-Pozzolanelle*" forms the "*Villa Senni*" Formation, related to the last caldera collapse of the Colli Albani volcano, and responsible for the present day configuration of the caldera. Several ages are present in literature for the "*Tufo Lionato*" (0.355 Ma, Karner *et al.*, 2001a; 0.365 Ma, Marra *et al.*, 2009) and "*Pozzolanelle*" [0.35±0.03 Ma, average of 3 Rb/Sr isochron ages, and 0.34 (0.35 Ma updating the age of the used monitor) ±0.007 Ma, average of 7 ^{40}Ar-^{39}Ar ages on leucites, Radicati *et al.*, 1981; 0.357 Ma, Karner *et al.*, 2001a]. Indeed, today the caldera has an 8 km diameter and it is asymmetric with a horse-shaped wall. Between major caldera forming eruptions volcanic activity was intra-caldera and localised along peri/extra-caldera fissures: the Vallerano lavas (0.46 Ma, Bernardi *et al.*, 1982, K/Ar; Karner *et al.*, 2001a, ^{40}Ar-^{39}Ar), Corcolle and Fontana Centogocce units, which, are dominantly made up of tephra fall units and lava flows.

With the formation of the caldera in its present day morphology, the volcano changed drastically its volcanic style and feeding system, with arrival to the surface of magmas through several different pathways. Lavas of the post caldera period have been dated between 0.35 and 0.15 Ma (K/Ar, Bernardi *et al.* 1982; ^{40}Ar-^{39}Ar, Karner *et al.* 2001a, Marra *et al.* 2003). Five main sectors of post-caldera vocanic activity have been recognized (Giordano *et al.* 2006, 2010 and Boari *et al.*, 2009a) and produced ca. 40 km^3 of erupted products: i) the Monte delle Faete, which is a stratovolcano (944 m a.s.l.) built up in the middle of the caldera; ii) the Tuscolano Artemisio composite edifice, which is made of coalescent scoria cones and lava flows aligned along circum- and extra-caldera fracture; iii) the Pantano Borghese monogentic alignement, which is external to the caldera rims on the NE sector of the district; iv) the Santa Maria della Mole monogenetic alignement, which is external to the caldera rims on the NW sector of the district; v) the Monte Due Torri-Ardea monogenetic alignment, which is made of an alignement of scoria cone across the caldera alon a NE-SW trending fracture.

The most recent period of volcanic activity (i.e., “Via dei Laghi” period) was concentrated on the south-western flank of the volcano (Giordano *et al.*, 2006; Freda *et al.*, 2006) with prevalent but small phreatomagmatic eruptions (Fig. 21), for the interaction with shallow productive aquifers (e.g., De Benedetti *et al.*, 2008). The phreatomagmatic activity brought about the disruption of the SW rim of the caldera, with the formation of several coalescent maars aligned along both NNW-SSE and NS regional trends (e.g., de Rita *et al.*, 1988, 1995; Funiciello *et al.*, 2003). The temporal extent of the last activity of the Alban Hills has been matter of debate for years and involved U/Th and ^{40}Ar-^{39}Ar datings: an experiment performed with the two methods on the same samples gave on average discordant ages, being U/Th data below ~ 0.025 Ma, noticeably younger than ^{40}Ar-^{39}Ar data (Villa, 1992; Voltaggio *et al.*, 1994). The polygenetic Albano maar is the last formed and produced phreatic activity since about 0.07 Ma (Marra *et al.*, 2003; Freda *et al.*, 2006; Giaccio *et al.*, 2009). The end of the Albano activity is debated too: Freda *et al.* (2006) and Giaccio *et al.* (2009) established the last volcanic episode at ~0.04 and ~0.03 Ma, respectively, while other authors extend the activity throughout the Holocene (Villa *et al.*, 1999; Funiciello *et al.*, 2003; De Benedetti *et al.*, 2008).

The most stricking feature of the Colli Albani rocks is their more silica-undersaturated character with respect to the other leucitites and plagio-leucitites of the Roman Province (Fig. 22a, 22b), which is accompayned by higher MgO and CaO contents of volcanic rocks (Tables 4 and 5). Also the four main ignimbrites have chemical compositions of the juvenile fragments, representing the composition of the magma triggering the eruption, never exceeding tephritic-phonolite compositions, but with

Figure 22. Classification and incompatible trace element characteristics of Pleistocene volcanic rocks from Colli Albani volcano.

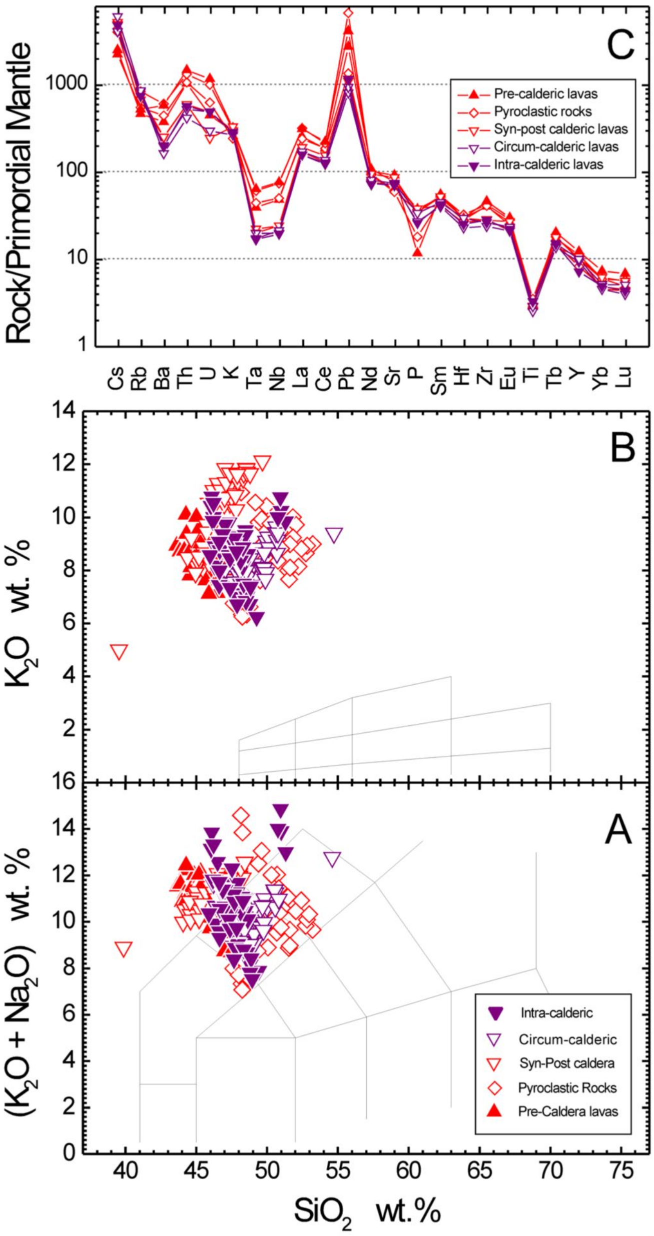

Classification and geochemical characteristics of the Colli Albani volcanic rocks. A) Total Alkali-Silica (TAS) classification diagram (Le Maitre, 2002). B) K_2O wt.% vs. SiO_2 wt.% classification diagram with reported the grid for orogenic volcanic rock suites (Peccerillo & Taylor, 1976). C) Incompatible trace element patterns for mafic volcanic rocks normalised to the primordial mantle values of Sun & McDonough (1989). Data from Fornaseri & Scherillo (1963); Laurenzi (1980); Peccerillo *et al.* (1984); Ferrara *et al.* (1985); Francalanci *et al.* (1987); Trigila *et al.* (1995); Freda *et al.* (1997); Palladino *et al.* (2001); Conticelli *et al.* (2002, 2007, 2010); Freda *et al.* (2006); Gaeta *et al.* (2006); Giordano *et al.* (2006); De Benedetti *et al.* (2008); Boari *et al.* (2009a).

some ignimbrites (i.e., Pozzolane Rosse, and Pozzolanelle) with phonolitic tephritic and tephritic compositions as well (Figs. 22a, 22b). This is the major compositional difference with other Latium volcanoes, where ignimbrites have invariably a phonolitic to trachyphonolitic compositions (Figs. 16a, 18a, 20a). This has been thought to represent a problem for the passive enrichment of volatites needed to trigger parossistic eruptions, and for this reason Freda *et al.* (1997) claimed for a supply of CO_2 to early trigger eruptions from carbonate syntexis. This process has been widely discussed by several authors who found in some specific cases the evidence to support it, but in other cases questioned the abuse of this differentiation process (e.g., Freda *et al.*, 2007; Iacono Marziano *et al.*, 2007, 2008; Boari *et al.*, 2009a; Gaeta *et al.*, 2009; Conticelli *et al.*, 2010; Peccerillo *et al.* 2010). These compositional differences indicate that Colli Albani magmas have lower silica activity and alumina saturation than other Roman magmas, such to stabilize melilite in many silica undersaturated volcanic rocks, to prevent crystallization of either plagioclase or K-feldspar (Conticelli *et al.*, 2010). Among phenocrysts, Leucite is among the most abundant mineral in pre-caldera pyroclastic rocks, and in the Monte delle Faete lavas and pyroclastic rocks, whereas is confined in the groundmasses of Pre-caldera plateau melilititic lavas, and post-caldera ones. Clinopyroxene is a ubiquitous phenocryst mineral, often showing complex zoning (Aurisicchio *et al.*, 1988; Gaeta *et al.*, 2005). Olivine is confined in the most mafic pre- and post-caldera lavas, and like in all other ultrapotassic volcanoes it has euhedral chromite inclusions. In the groundmasses beside minerals found as phenocrysts, Ba-phlogopite, Ti-magnetite, nepheline, Ca-Fe olivines and apatite are also found (e.g., Gaeta *et al.*, 2000; Conticelli *et al.*, 2010; Melluso *et al.*, 2010). Akermanitic melilite crystals are confined to the groundmasses of most silica-undersaturated foidites of the pre- and post-caldera periods. The Capo di Bove (e.g., Cecilite, Washington, 1906) and the Osa foidites are the best examples among post-caldera lavas. Melanite garnet, gehlenitic melilite and Al-spinel are typical minerals of skarn ejecta (Federico & Peccerillo, 2002), and they are found as xenocrysts in pyroclastic rocks of the Via dei Laghi hydromagmatic activity (Conticelli *et al.*, 2010).

The primordial mantle normalized patterns (Figs. 22c) show significant differences between mafic MgO-rich magmas from pre- to post-caldera. Indeed, pre-caldera leucititic and melilititic magmas show smaller throughs at Ba, and Hf, with respect to post-caldera ones. In additions differences in LIL elements total abundances are also observed (Figs. 22c). Boari *et al.* (2009a) explained this characteristic as due to a different supply of magma from a slightly different mantle source. Pre-caldera magmas should have been produced by smaller degrees of partial melting, at higher pressure, of a veined metasomatised upper mantle than post-caldera parental magma.

Figure 23. Geological sketch map of the Middle Latin Valley district (Roman Magmatic Province).

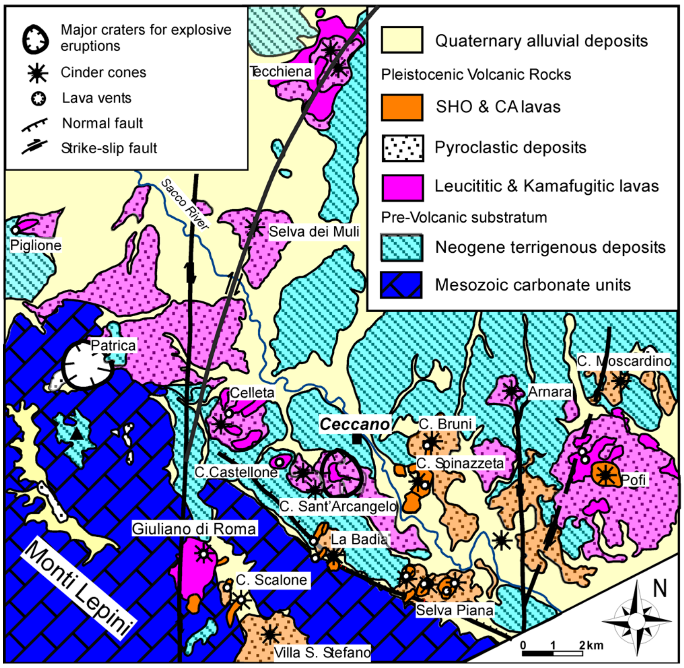

Geological sketch map of the Middle Latin District. Redrawn after Pasquaré *et al.* (1985), Sani *et al.* (2004), Boari & Conticelli (2007), Boari *et al.* (2009b). Main monogenetic volcanoes are represented by cinder cones, tuff rings and small plateau-like lava flows.

5. Middle Latin Valley district

The Middle Latin Valley district is located in the Southern Latium area (Fig. 11), some 100 km south of Rome, and some 60 km from Ernici Mounts, the locality to which this volcanism refers to with the name of Hernican District in the early scientific literature (Branco, 1877; Viola, 1899, 1902; Washington, 1906). Being the volcanic field developed well within the Latin Valley, in its middle sector, several authors (e.g., Angelucci *et al.*, 1974; Dolfi, 1981; Acocella *et al.*, 1996; Boari, 2005; Boari & Conticelli, 2007; Frezzotti *et al.*, 2007) used that the name “Middle Latin Valley” to refer the volcanic rocks of this district; a name that better defines the outcrop locality and the geographic area than Hernican, the original name choosen for this volcanic field and kept for several years in the Earth Science literature.

The volcanism of the Middle Latin Valley district developed during the Pleistocene (Basilone & Civetta, 1975; Fornaseri, 1985a; Boari *et al.*, 2009b). Among the Roman districts the Middle Latin Valley is the only one that lacks a large volcanic edifice; only small volumes of primitive magmas erupted from small scattered volcanic centers (Civetta *et al.*, 1979, 1981; Pasquaré *et al.*, 1985; Boari, 2005; Boari & Conticelli, 2007; Frezzotti *et al.*, 2007; Boari *et al.*, 2009b; Nikokossian & van Bergen, 2010). The total volume of erupted magma is significantly lower than that observed in all the other volcanic districts of the Roman Magmatic Province, probably due to the distinctive geological and geodynamic evolution of the Apennine chain and Adriatic foreland in this area. The volcanic field is clustered in a narrow area well within the Sacco River valley, the median sector of the Latin Valley, located between the Apennine chain and the Monti Lepini (Fig. 11). The Latin Valley is a NNW-SSE extensional basin. The volcanic field is made up of cinder cones, small lava plateau, short lava flows, and tuff rings with associated small volume of hydromagmatic pyroclastic flows (Patrica pyroclastic flows, Fig. 23). The vents are arranged along the NNW-SSE fault at the foot of Monti Lepini, which delimited the southwestern edge of the Latin Valley, and the N-S and NNE-SSW dextral strike-slip faults (Sani *et al.*, 2004) (Fig. 23), both tectonic systems provided preferential pathways for the mafic low viscosity magmas uprise (Acocella *et al.*, 1996).

The absence of a large central volcanic edifice and of a large area covered by pyroclastic deposits, which might be used as stratigraphic markers, makes it difficult to reconstruct a reliable stratigraphic succession. Therefore the volcanic history of the Middle Latin Valley volcanic fields has been reconstructed using geochronologic data on each single volcanic center (Basilone & Civetta, 1975; Cortesi C. reported as personal communication in Fornaseri, 1985a; Boari *et al.*, 2009b). In addition, because the grouping has been made on the basis of geochemical and petrological informations, the time succession is strongly integrated with compositional characteristics change (Boari *et al.*, 2009b).

Figure 24. Classification and incompatible trace element characteristics of Pleistocene volcanic rocks from Middle Latin Valley monogenetic volcanoes.

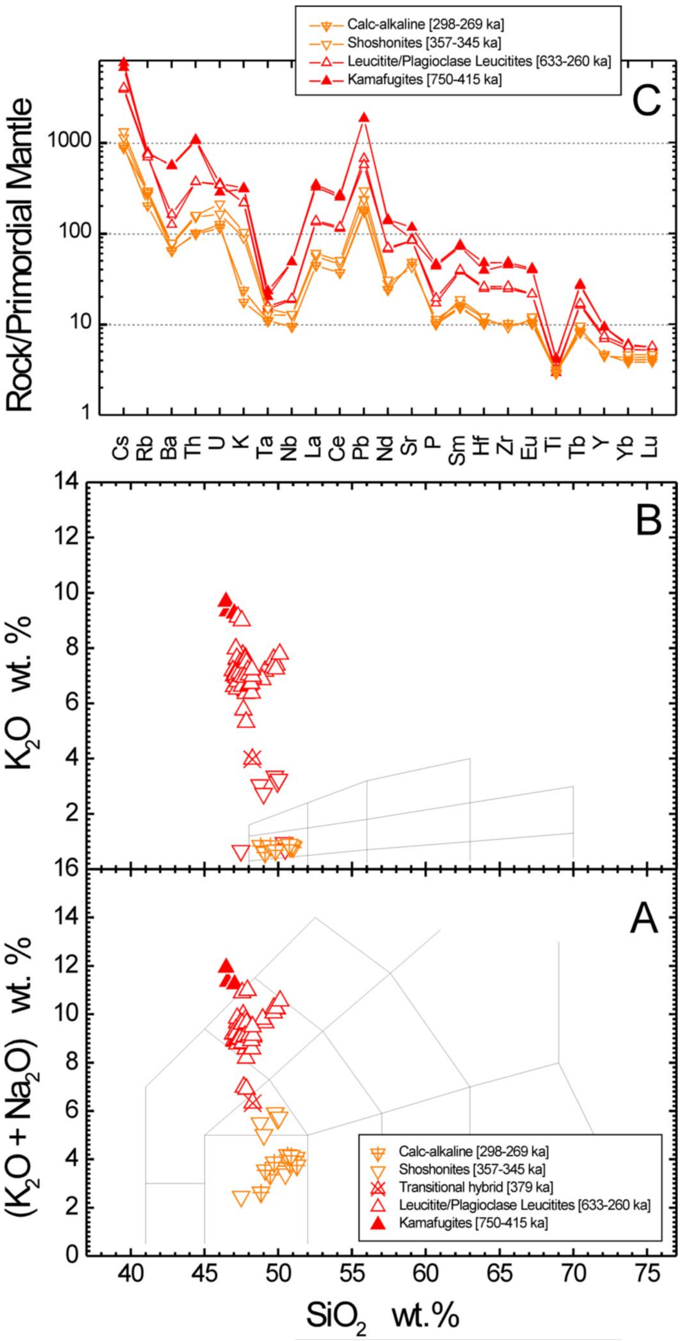

Classification and geochemical characteristics of the Middle Latin Valley volcanic rocks. A) Total Alkali-Silica (TAS) classification diagram (Le Maitre, 2002). B) K_2O wt.% vs. SiO_2 wt.% classification diagram with reported the grid for orogenic volcanic rock suites (Peccerillo & Taylor, 1976). C) Incompatible trace element patterns for mafic volcanic rocks normalised to the primordial mantle values of Sun & McDonough (1989). Data from Boari *et al.* (2009b).

Kamafugites are the early magmatic rocks to appear on surface in the volcanic field (0.7-0.6 Ma; Basilone & Civetta, 1975; Boari *et al.*, 2009b); they are represented by leucite-bearing melilitites with a paragenesis made of melilite, olivine, clinopyroxene, phlogopite, Ti-magnetite, nepheline and apatite; secondary calcite is also found to fill vesicles and fractures. The Patrica hydromagmatic tuffs have neither juvenile fragments nor glass shards as large as to perform whole rock or EPM analyses, respectively, thus their evolved kamafugitic nature was established on the basis of mineral compositional data on loose crystal fragments (Boari & Conticelli, 2007). Patrica pyroclastic units display a much younger ^{40}Ar-^{39}Ar age, ~0.42 Ma (Boari *et al.*, 2009b), which matches the K/Ar value of 0.4 Ma given by Fornaseri (1985a). All ages mentioned since now in the following discussion are ^{40}Ar-^{39}Ar ages, unless otherwise stated. Leucitites appears as early as kamafugites at Piglione center at about 0.61 Ma (Boari *et al.*, 2009b). Plagioclase leucitites appears slightly later (Giuliano di Roma, and Tecchiena), between 0.41 and 0.39 Ma (Boari *et al.*, 2009b), although a younger age of 0.25 Ma has been found for the Colle Sant'Arcangelo leucitite (Boari *et al.*, 2009b). The leucitites and plagio-leucitites are mostly phonolitic tephrites (Fig. 24a), with no or limited differentiation (Figs. 24a, 24b). Few tephrites are also found at Selva dei Muli cinder cone and Pofi volcano. Mineralogy of leucitites and plagio-leucitites is made preferentially by leucite + clinopyroxene ± olivine ± plagioclase ± Ti-magnetite ± apatite ± phlogopite. Monogenetic volcanoes that produced leucitites and plagioclase leucitites are generally located along the N-S and NNE-SSW dextral strike-slip faults (Fig. 23). Volcanic rocks with shoshonitic affinity (Fig. 24b) appear as late as 0.36 and 0.35 Ma (Boari *et al.*, 2009b). These volcanic rocks have trachy-basaltic compositions (Fig. 25a) with phenocrysts of olivine and clinopyroxene, set in a groundmass made of clinopyroxene, olivine, plagioclase, and Ti-magnetite; in some samples leucite crystals are also found in the groundmass (Boari & Conticelli, 2007). Basalts with calc-alkaline affinity (Boari, 2005; Boari & Conticelli, 2007; Frezzotti *et al.*, 2007) have been vented from the same centers of soshonitic products at Colle Spinazzeta, Selva Piana, and La Badia, where basalts are stratigraphically younger than shoshonitic ones. Basaltic scoriae from the Pofi scoria cone has given an age of 0.29 Ma (Boari *et al.*, 2009b), which disagrees with the K/Ar ages on the underlying lava flows of the plateau, 0.11 and 0.08 Ma (Fornaseri, 1985a). The leucititic lavas that gave these very young K/Ar ages show stratigraphic correlation with the lavas of the Pofi plateau (Angelucci & Negretti, 1963), dated at 0.40 Ma, (K/Ar, Basilone & Civetta, 1975). A basaltic lava from Colle Vescovo, a final center in the Selva Piana area, gave an age of 0.3 Ma (Boari *et al.*, 2009b), coherent with the scoria sample of Pofi. These calcalkaline-like basalts (Fig. 24a) have significantly lower K_2O than any other Middle Latin Valley rocks, overlapping partially with altered shoshonites where K_2O has been removed by secondary processes (Fig. 24b). These altered rocks are also characterized by secondary minerals and weathering textures (Boari, 2005; Boari & Conticelli, 2007). Basalts with calc-alkaline affinity are characterized by sub-porphyritic textures with olivine and clinopyroxene phenocrysts with groundmass made of plagioclase + glass + clinopyroxene Ti-magnetite + olivine (Boari, 2005; Boari & Conticelli, 2007; Boari *et al.*, 2009b). Monogenetic volcanoes and centres that vented lavas with shoshonitic and calc-alkalic petrologic affinities are generally located along the NNW-SSE normal fault delimiting the Monti Lepini-Monti Ausoni ridge (Fig. 23).

The lack of a large volcanic apparatus and therefore of a structured system of magma chambers beneath the Middle Latin Valley volcanic field is probably the reason for missing magmatic differentiation at shallow depth, and therefore for outcropping of mafic primitive igneous compositions (Tables 4, 5, and 6). This characteristics permit to observe a large compositional spectrum in terms of silica and K_2O contents (Fig. 24b) that might be present also in the other volcanoes of the Roman province, hidden by shallow level differentiation and compositional buffering of the different magmas produced with time in the mantle source. This permits also to observe the variation of trace element contents with time and potassium contents of primitive MgO-rich magmas (Fig. 24c). Indeed as already shown for other magmatic provinces of the Mediterranean region it is possible to argue a direct and positive correlation between incompatible trace element contents and potassium enrichment in mafic primitive MgO-rich volcanic rocks (Conticelli *et al.*, 2009a). The same holds true for the Italian ultrapotassic volcanic rocks, from Western Alps (Fig. 8) to Corsica (Fig. 10), Tuscany (Fig. 12), and Roman Province (Figs. 16, 18, 20, and 22). Indeed, the most K_2O enriched mafic rocks of the Middle Latin Valley (i.e., kamafugites), have also the highest abundance in incompatible trace elements, and the normalized incompatible trace element patterns recall closely those of pre-caldera melilitites and leucitites of the Colli Albani district (Fig. 22c), with peculiar smaller negative spikes at Ba, and larger at Ta, Nb, P, and Zr with respect to younger magmas (Fig. 24c). Passing from kamafugite to leucitite/plagio-leucitite mafic rocks with time, it is observed also an increase of the negative spikes at Ba, Sr and P, which is coupled to a decrease of the troughs at Ta, Nb, and Ti (Fig. 24c). This trend is continuous with time passing also from leucitites to shoshonite and calc-alkaline mafic rocks. In addition, it is worthy to note the normalized Ta/Nb ratio that pass from a value <<1 in kamafugites to values > 1 in the youngest volcanic rocks (i.e., calc-alkaline; Fig. 24c).

Figure 25. Geological sketch map of the Roccamonfina district (Roman Magmatic Province).

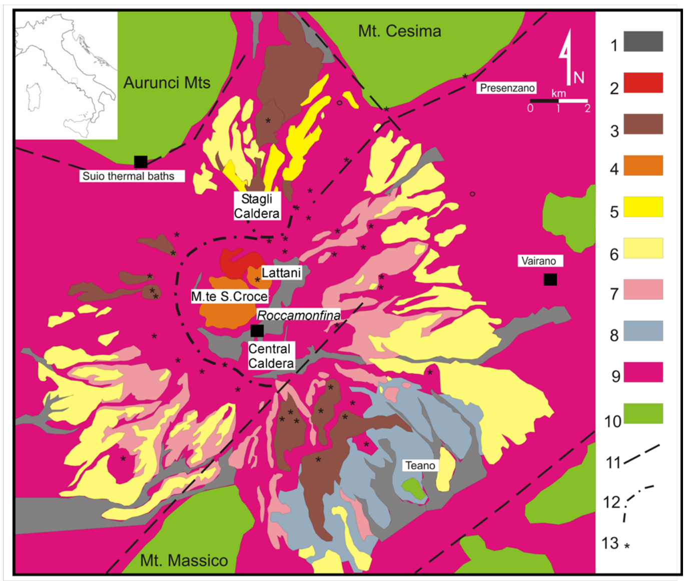

Geological sketch map of the Roccamonfina volcano (redrawn after: Giannetti, 1964, 2001; Taylor *et al.*, 1979; Cole *et al.*, 1992; Giordano *et al.*, 1998a, 1998b; Conticelli *et al.*, 2009b). Legend. 1 - Campanian Ignimbrite (erupted from Campi Flegrei); 2-5 Late phase of post-caldera activity (Vezzara synthem; 155-50 ka); 2 – HKCA final lavas; 3 – Shoshonitic mafic lava and pyroclastics from monogenetic centers; 4 – Shoshonitic domes; 5 – Yellow Trachytic Tuff; 6-8 - Early phase of post-caldera activity (Riardo synthem; 385-230 ka); 6 – White Trachytic Tuffs; 7 – Teano pyroclastic succession; 8 – Brown Leucitic Tuff; 9 – Pre-caldera activity Leucite-bearing lava and pyroclastics (HKS) (Roccamonfina synthem; 630-385 ka); 10 – Mesozoic-Cenozoic pre-orogenic carbonatic-terrigenous succession; 11 – Main extensional faults; 12 – caldera rim; 13 – scoria cones.

6. Roccamonfina district

The volcano of Roccamonfina is stratovolcano characterized by sector collapses and an apical central caldera (Fig. 25) (Cole *et al.*, 1992; De Rita & Giordano, 1996; Giannetti, 2001; Rouchon *et al.*, 2008). It belongs to the Roman Magmatic Province (Washington, 1906; Avanzinelli *et al.*, 2009). It was the first volcano in which a "low potassium series" accompanying leucite-bearing ultrapotassic rocks was recognized (Appleton, 1972).

The Roccamonfina volcano is located at the intersection of a NNW-SSE extensional basin with important NE-SW and N-S tectonic lineaments, which cut the Mesozoic-Cainozoic Apennine carbonatic sequences (Accordi, 1963; Incoronato *et al.*, 1985; Accordi & Carbone, 1988; Mattei *et al.*, 1995; Giordano *et al.*, 1995; Bosi & Giordano, 1997). The volcanic succession lies on transgressive marine sedimentary sequence that filled the NE-SW Garigliano Graben (Ippolito *et al.*, 1973; Watts, 1987; Giordano *et al.* 1995). The Roccamonfina volcano is made up by lavas and pyroclastic rocks erupted in three main periods of activity (Ballini *et al.*, 1989a; De Rita & Giordano 1996; Giannetti, 2001; Rouchon *et al.*, 2008). The beginning of the volcanic activity relies on the dating of the oldest products found in the well Gallo 85-1, above the sedimentary substratum: whereas K/Ar ages of the deepest lava are slightly discordant, the ^{40}Ar-^{39}Ar age on a lava sample lying ~50 m above the bottom of the volcanic pile gives 0.59 Ma, (Ballini *et al.*, 1989a). All ages older than about 0.6 Ma present in literature are likely biased at some extent (Gasparini & Adams, 1969; Cortini *et al.*, 1973; Giannetti *et al.*, 1979; Radicati *et al.*, 1988). The first period of activity was dominated by leucite-bearing lava flows interbedded to minor ash fall and mud-flow deposits (San Carlo lavas), peripheral dikes, parasitic monogenetic centres, and eccentric domes on the flank of the volcano were also emplaced (Di Girolamo *et al.* 1991). The volcanic rocks emitted during this period have leucititic to plagioclase-leucititic affinity, ranging form basanite to phonolite (Fig. 26a), and with a mineralogy made up of olivine, clinopyroxene, leucite, plagioclase, Ba-phlogopite, apatite, Ti-magnetite and amphibole, with sanidine and rare sodalite. A first stratocone destroying event occurred at 0.44 Ma with the formation of a lateral sector collapse (Rouchon *et al.*, 2008), but leucite-bearing volcanic activity did not interrupt and continue with the building up of a new stratocone, which covered almost completely the old volcano-tectonic depression (Cole *et al.*, 1992a; De Rita & Giordano, 1996; Giannetti, 2001).

Figure 26. Classification and incompatible trace element characteristics of Pleistocene volcanic rocks from Roccamonfina volcano.

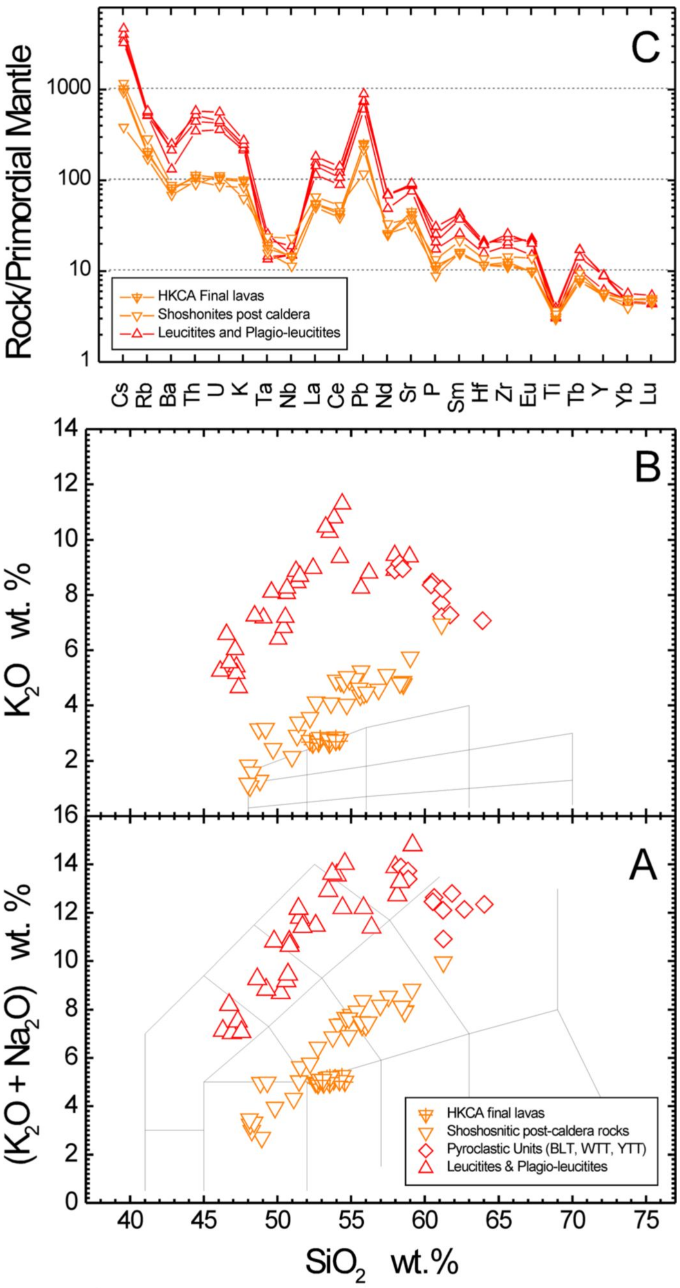

Classification and geochemical characteristics of the Roccamonfina volcanic rocks. A) Total Alkali-Silica (TAS) classification diagram (Le Maitre, 2002). B) K_2O wt.% vs. SiO_2 wt.% classification diagram with reported the grid for orogenic volcanic rock suites (Peccerillo & Taylor, 1976). C) Incompatible trace element patterns for mafic volcanic rocks normalised to the primordial mantle values of Sun & McDonough (1989). Data from Ghiara *et al.* (1973) Ghiara & Lirer (1977), Hawkesworth & Vollmer (1979), Vollmer & Hawkesworth (1981), Rogers *et al.* (1985); Giannetti & Luhr (1983), Luhr & Giannetti (1987), Conticelli & Peccerillo (1992); Giannetti & Ellam (1994); Conticelli *et al.* (2002, 2007, 2009b), Rouchon *et al.* (2008).

The beginning of the formation of the summit caldera marked the passage to the second period of activity (De Rita & Giordano, 1996), which was characterised by plinian activity, with the eruption of five main, caldera forming pyroclastic flow units (Giannetti & Luhr, 1983; Luhr & Giannetti, 1987; Ballini *et al.*, 1989b; Cole *et al.*, 1993; Giannetti, 1996; Giordano 1998a, 1998b; Giannetti & De Casa, 2000), which are namely the Brown Leucitic Tuff and the succession of the White Trachytic Tuffs (Cole *et al.*, 1992, 1993; De Rita *et al.*, 1998; Giannetti & De Casa, 2000). Pyroclastic units have a variable composition from phonolitic to trachytic. Recent K/Ar and ^{40}Ar-^{39}Ar ages of the Brown Leucitic Tuff agree at 0.35 Ma (Rouchon *et al.*, 2008; Scaillet *et al.*, 2008). The White Trachytic Tuff succession is stratigraphically much more complicated. Giannetti & De Casa (2000) present a range of ages comprised between 0.31 Ma for the lower unit till 0.23 Ma for the upper one. Laurenzi *et al.* (1990) suggested an interval between 0.32 Ma and <0.28 Ma for the whole serie, whereas Quidelleur *et al.* (1997) present an age of 0.33 Ma for the Lower Unit of the White Trachytic Tuff. The largest compositional range is observed among the juvenile clasts of the Brown Leucitic Tuff, which is thought to be made by a single eruption, and thus that variability might be interpreted as well as due to syn-depositional alkali-loss due to leucite and glass transformation (Giannetti & Masi, 1989; Parker, 1989). The White Trachytic Tuff falls well within the trachytic field (Fig. 26a).

The third and last period of post-caldera activity was characterized by dome to monogenetic volcanism within the caldera, along the caldera edge, and on the flanks of the primordial Roccamonfina volcano (Fig. 25). The geochronological data on the rocks of this period do not permit to define exatly the last lava flow eruption which is vented from a fracture on the western flank of Monte Santa Croce Dome and flowed down the miffle of the caldera at the foot of Monte Lattani intra-caldera dome. Indeed the Monte Santa Croce dome yielded the youngest ages found at Roccamonfina (K/Ar, 0.16 Ma, Radicati *et al.*, 1988; 0.15 Ma, Rouchon *et al.*, 2008). Samples from cinder, scoria cones and lava flows on the caldera rim and external to the caldera range between 0.33 Ma (Casale Robetti; ^{40}Ar-^{39}Ar; Laurenzi's unpublished data) and 0.27 Ma (Colle Friello; K/Ar, Rouchon *et al.*, 2008). Post caldera volcanic rocks are leucite-free, and mostly belonging to the shoshonitic series (Fig. 26b). The youngest leucite-free lava flows, which have been vented from a fracture on a flank of Monte Santa Croce dome, have revealed compositional variations pointing to the HK-calc-alkaline field (Fig. 26b).

Beccaluva *et al.* (1991) pointed out that ultrapotassic rocks outcropping below the 41st parallel display clear difference in trace element distribution with respect to those from above this parallel (Tables 5 and 6). The Roccamonfina volcano, is just few degree north from the 41st parallel and then ultrapotassic leucite-bearing rocks have incompatible trace element distribution similar to the other Latian districts. On the other hand, the post-caldera shoshonitic rocks from Roccamonfina have significantly lower LIL elements with respect to any other Roman rocks, and in particular with the other post-caldera shoshonites of the northernmost Latian districts (Fig. 16c). Shoshonitic rocks from the nearby Middle Latin Valley district (Fig. 24c) display significant differences with respect to shoshonitic rocks from Roccamonfina both in terms of total enrichments and of fractionation of HFS with respect to LIL elements (Fig. 26c). With this respect, the Roccamonfina post-caldera shoshonites display trace element distribution similarities with volcanic rocks from the Neapolitan district (Tables 6 and 7) and at a certain scale with those from Lucanian Magmatic Province (Conticelli *et al.*, 2009b). As a corollary the leucite-bearing pre-caldera ultrapotassic rocks have no significant compositional differences with other Roman volcanic rocks from either Latium or Umbria regions. In summary, the leucite-bearing ultrapotassic volcanism of Roccamonfina is well within the chronological, mineralogical and compositional limits of the Latian districts of the Roman Magmatic Province.

7. Umbrian District

Washington (1906) fails to describe the ultrapotassic rocks found in the intra-apennine area. The monogenetic volcano of San Venanzo and the lava center of Cupaello are the major volcanic outcrops of the Umbria districts (Rodolico, 1937; Mittempergher 1965; Sartori, 1965) and they were already known in the Italian scientific literature since the end of the XIXth century (Verri, 1880; Sabatini, 1899). Several other sites in intra-apenninic areas with occurrence of volcanic rocks have been reported recently (e.g., Accordi & Angelucci, 1962; Durazzo *et al.*, 1984; Bellotti *et al.*, 1987; Stoppa, 1988; Michetti & Serva, 1991; Traversa *et al.*, 1991; Brunamonte *et al.*, 1992; Stoppa & Lavecchia, 1992; Cipollari *et al.*, 1998; Tallini *et al.*, 2002). In some cases these outcrops are just ancient volcanoclastic levels (e.g., Peglio and Petrasecca; Cipollari *et al.*, 1998), in other cases are levels of airfall tuffs from either the main Roman volcanoes or Etna (Sabatini, Colli Albani, Neapolitan volcanoes, Mirco, 1990; Tallini *et al.*, 2002; Wulf *et al.*, 2004), and eventually they are pyrometamorphic rocks originate either by carchoal pit burning or by natural coal combustion (e.g., Melluso *et al.*, 2003, 2005a, b; Capitanio *et al.*, 2004; Grapes, 2006). Only for Monte Autore, La Queglia, and Polino outcrops the magmatic and the provenance nature have not been questioned. In the first case, the strong alteration allows the obtaining neither of a petrographic description nor of a bulk chemical analysis; based on clinopyroxene composition the Roman nature of the Monte authore dyke was inferred (Mirco, 1990). The La Queglia dyke is a typical alkaline lamprophyre intruded in a carbonate platform during the Eocene, much earlier than orogenic processes involved this unit in the Apennine chain (Durazzo *et al.*, 1982; Mirco, 1990). The Polino rock has a clear alvikitic bulk composition although a hot debate within the scienfic literature questioned its primary mantle nature versus carbonate contamination with surrounding limestones (e.g., Stoppa & Lupini, 1993; Peccerillo, 1998, 2004, 2005b; D'Orazio *et al.*, 2008).

In the lights of the strong diversity on emplacement mechanisms, nature and genesis of the rocks found within the Apennine chain we focus and limit our attention only on the classical outcrops that present a wide consensus about their ultimate magmatic nature and local venting: the San Venanzo, Cupaello, and Polino centers.

San Venanzo and Cupaello monogenetic volcanic centers (Fig. 11) are the only ones in which compositional features of volcanic rocks are unaltered and testify the original characteristics of ultrapotassic magmatism (Gallo *et al.*, 1984; Taylor *et al.*, 1984; Peccerillo *et al.*, 1988; Conticelli, 1989; Stoppa & Cundari, 1995; Stoppa, 1996; Zanon, 2005). They are located within the Apennine orogenic chain. The San Venanzo lies on a horst bordering the western sector of the Tiber River Valley extensional basin, whereas the Cupaello lava vented from a NW-SE normal fault bordering the southeastern foot of the Monti Reatini at the edge of the Rieti extensional basin (Cavinato *et al.*, 1989; Zanon, 2005).

Figure 27. Geological sketch map of the San Venanzo volcanic field (Roman Magmatic Province).

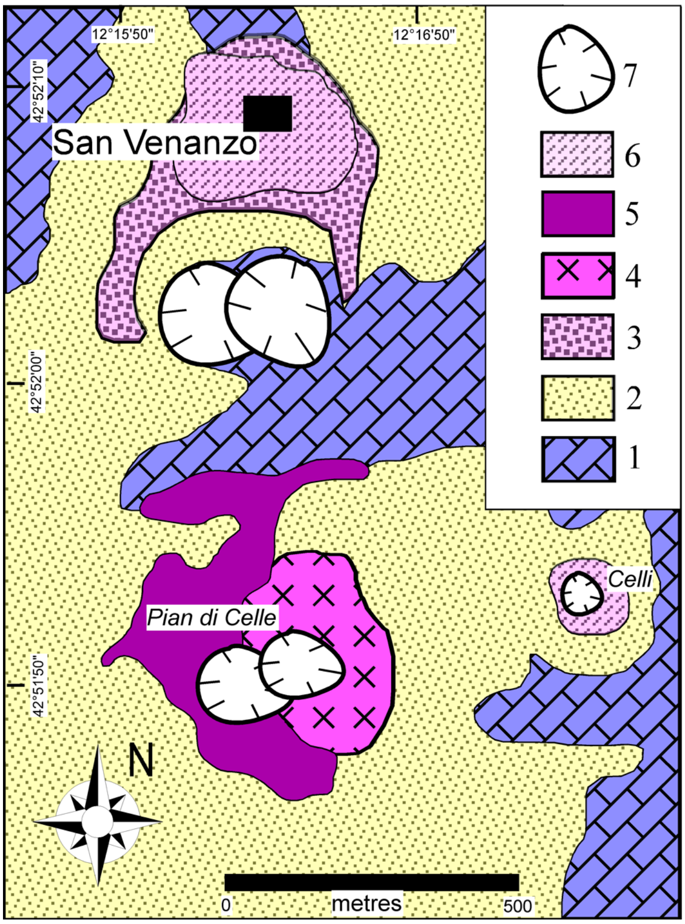

Geological sketch map of the San Venanzo volcanic field (Umbria district). Legend: 1) Miocene sandstones and marly flysh of the Umbrian sedimentary sequence; 2) Plio-Pleistocene clay and sand; 3) San Venanzo maar – breccia flow deposit; 4) Pian di Celle tuff cone – pyroclastic deposits; 5) kalisilite-bearing olivine melilitoite; 6) pyroclastic fall deposits of the San Venanzo and Celli volcanic centers; 7) volcanic centers. Redrawn after Stoppa (1996) and Zanon (2004).

The San Venanzo volcanic field includes three distinct eruptive vents: the San Venanzo maar, the Pian di Celle tuff ring, and the Celli tuff cone (Fig. 27). A K/Ar age of 0.46 Ma on leucite separated from a pegmatoid facies was provided by Laurenzi & Villa (1984). After, a more detailed chronological study gave a much younger ^{40}Ar-^{39}Ar age of 0.27 Ma for a sanidine from the basal tephra (Pian di Celle) (Laurenzi *et al.*, 1994). Both phlogopite and leucite of the pegmatoid veinlets showed saddle-shaped age spectra, which account for the difference between K/Ar and Ar-Ar ages (Laurenzi *et al.*, 1994).

Figure 28. Classification and incompatible trace element characteristics of Pleistocene volcanic rocks from Umbrian monogenetic volcanoes.

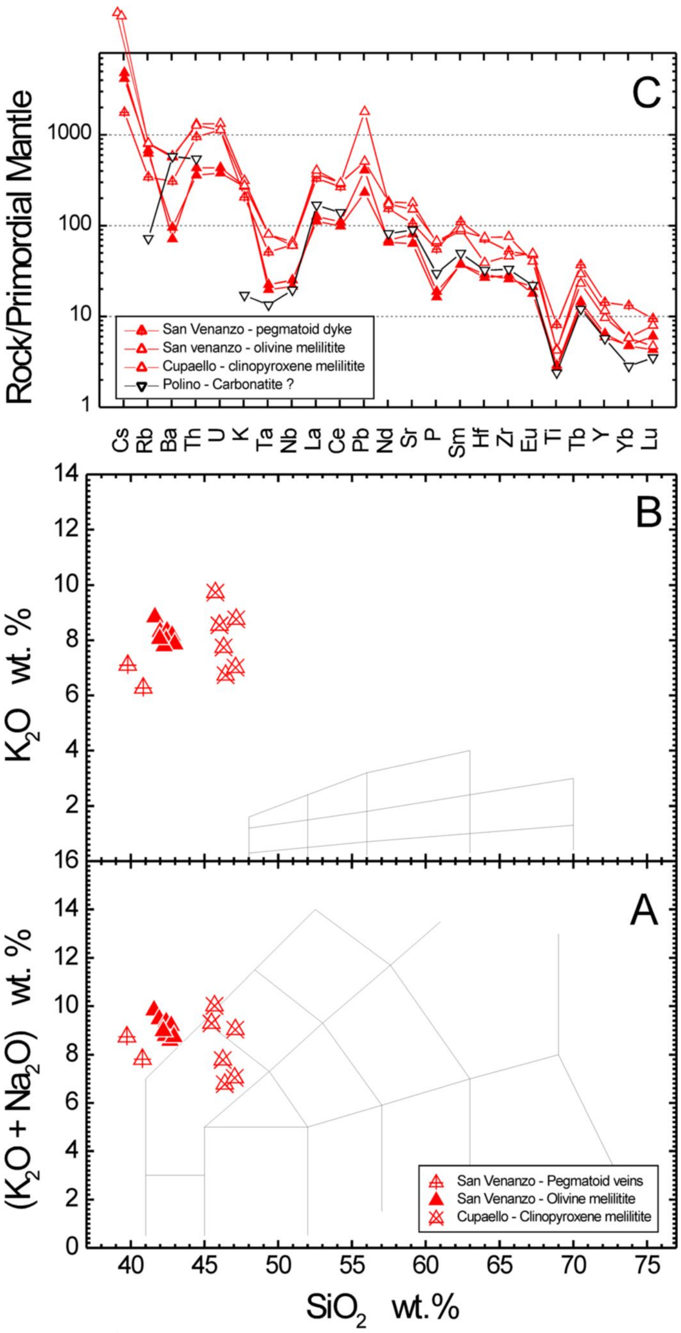

Classification and geochemical characteristics of the Umbrian kamafugitic rocks. A) Total Alkali-Silica (TAS) classification diagram (Le Maitre, 2002). B) K_2O wt.% vs. SiO_2 wt.% classification diagram with reported the grid for orogenic volcanic rock suites (Peccerillo & Taylor, 1976). C) Incompatible trace element patterns for mafic volcanic rocks normalised to the primordial mantle values of Sun & McDonough (1989). Data from Peccerillo *et al.* (1988); Conticelli (1989), Conticelli & Peccerillo (1992); Conticelli *et al.* (2002, 2007).

The Cupaello is a small lava tongue that has flowed down for few hundred meters above the lacustrine deposits of the Rieti valley (Rodolico, 1937; Gragnani, 1972; Cavinato *et al.*, 1989; Stoppa & Cundari, 1995). For the Cupaello lavas, a kalsilite-enriched separate gave a saddle shaped spectrum with the only indication of a maximum age of ~ 0.64 Ma (Villa *et al.*, 1991). The Polino outcrop is a narrow plug, some two meters in diameter, embedded in a heavy limestone sequence (ca. 6,000 meters; Michetti, 1990). Two ^{40}Ar-^{39}Ar ages are available for the Polino outcrop: ~ 0.4 Ma on sanidine from pyroclastic deposits and of 0.28 Ma on a massive block (Laurenzi *et al.*, 1994).

The three outcrops of melilitites are characterized by different mineralogical assemblages of the relatively restricted whole rock compositional range (Table 4). Indeed all the samples from Umbria fall in the foiditic field (Fig. 28a) if exception is made for some Cupaello samples in which the weathering have decreased the total K_2O with consequent slight increase of SiO_2 (Fig. 28a, 28b). On the other hand, the samples from Polino rock do not fall within the range of the diagrams of figures 28a and 28b, but it has consistently lower silica, K_2O and Na_2O (Table 4) to claim for a possible carbonatitic nature (Stoppa & Lupini, 1993; Stoppa & Woolley, 1997; D'Orazio *et al.*, 2008; Stoppa *et al.*, 2008).

On the basis of major element chemistry and mineralogy the Umbrian rocks belongs to the kamafugitic clan (Table 1). Åkermatite-rich melilite is the most characteristic mineral of Umbrian rocks (Fig. 3), which reflects the very low silica activity, which is a consequence of the strong silica-undersaturation of the magma. Melilite-bearing rocks display the lowest silica and the highest CaO among volcanic rocks such to determine the appearance of larnite in their CIPW norm. Melilite coexists with a limited number of common minerals and appears to be equally stable with K-rich and Na-rich minerals. In igneous rocks melilite has never been found in equilibrium with either plagioclase or K-feldspar (Yoder, 1972). In the Umbrian rocks melilite is found in equilibrium with feldspatoids, both leucite and kalsilite. In the San Venanzo rocks large phenocrysts of olivine are found, whereas clinopyroxene is restricted to the groundmass together with melilite, phlogopite, kalsilite, magnetite, and nepheline, with accessory perovskite, apatite, chromite, and monticellite (Conticelli, 1989; Cundari & Ferguson, 1992). On the other hand, in the Cupaello melilitites, olivine is replaced by monticellite within the groundmass, which is found in equilibrium with melilite, clinopyroxene, phlogopite, and kalsilite. Clinopyroxene and phlogopite are present as large phenocrysts. The Polino rock is far from being an exhaustive and clear carbonatite. Indeed, phlogopite and olivine are the only phenocrysts phases, and the groundmass is made of melilite, clinopyroxene, phlogopite, kalsilite, perowskite and monticellite. Calcite is also found but its primary nature is still strongly debated (Lupini & Stoppa, 1993; Barker, 1996; Peccerillo, 1998; Wolley *et al.*, 2005; Peccerillo, 2005b; D'Orazio *et al.*, 2008).

Incompatible trace element concentration is among the highest total abundances observed in Roman rocks. The same distribution of other Mediterranean ultrapotassic rocks is observed for normalised patterns with high field strength element, but not Th, fractionated with respect to large ion lithophile elements, a characteristic typical of orogenic magmatic rocks (Fig. 28c). Apart this general rule, San Venanzo, Cupaello and Polino display some differences from each other. The San Venanzo olivine melilitites display a pattern strongly similar to those of ultrapotassic leucitites and plagioclase-leucitites of the Roman rocks (Figs. 16c, 18c, 20c, 22c, 24c and 26c) with comparable Ta/Nb, Nd/Sr, and Zr/Hf normalized ratios. Indeed the Cupaello clinopyroxene melilitites have the highest incompatible trace element abundances, but they do not show negative anomaly at Ba, and have reverse Ta/Nb normalized ratios (Fig. 28c). The Polino ailvikite have the lowest incompatible trace element abundances among the overall Umbrian rocks with very low K, which is a noticeable exception for carbonatite and melilite pairs, where usually the carbonatite has more than three times the incompatible trace element contents of the companion silicate rocks (e.g., Le Bas, 1987; Green *et al.*, 1992; Kjarsgaard *et al.*, 1995; Le Roex & Lanyon, 1998). D'Orazio *et al.* (2008) have shown that Polino ailvikite is strongly depleted in incompatible trace elements with respect to other similar primary mantle carbonatites.

The Neapolitan district

The Neapolitan district is the southernmost cluster of volcanoes of the Roman Magmatic Province, just south of the 41st parallel, and it is formed by four main volcanic apparata: the Ischia, Procida, Campi Flegrei and Somma-Vesuvius (Fig. 29). Most of the Neapolitan district volcanoes developed during the Upper Pleistocene but with an intense volcanic activity piercing the Pleistocene-Holocene boundary (Brocchini *et al.*, 2001; De Vivo *et al.*, 2001; Deino *et al.*, 2004), and important historical eruptions recorded (e.g., Ischia, Campi Flegrei, Vesuvius; e.g., Santacroce, 1987; Rosi & Sbrana, 1987; Vezzoli, 1987). A wealth of data regarding the recent phases of activity of these volcanoes is available, but we know little about the Middle Pleistocene history of Neapolitan volcanoes, because most of them buried by Holocene volcanic activity, or just beneath the sea level. It is clear that shoshonitic volcanic products dominate over leucite-bearing ultrapotassic rocks. In addition, in most of the Neapolitan volcanoes, the silica-undersaturated ultrapotassic rocks are completely missing in the geological records, with the exception of Mt. Vesuvius, where they appears lately, after a long period characerized by either leucite-free or –poor volcanic rocks (e.g., Peccerillo, 2005a; Avanzinelli *et al.*, 2009, and references therein).

Figure 29. Geological sketch map of the Neapolitan district (Roman Magmatic Province).

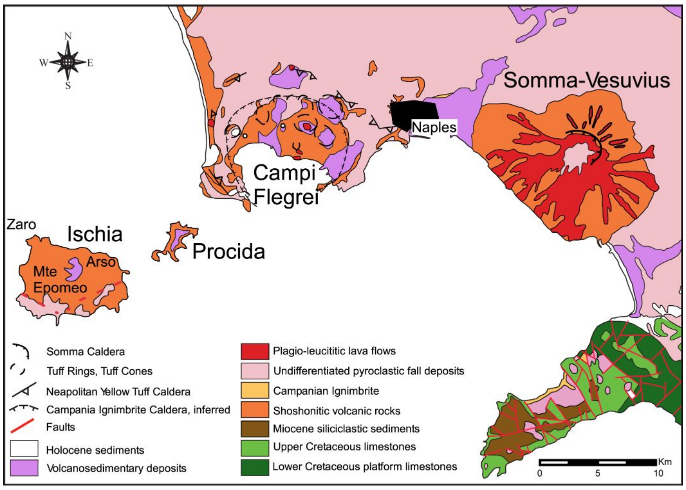

Geological sketch map of the Neapolitan volcanic district (redrawn after Bonardi *et al.*, 1988.

The absence of Pliocene marine sediments in the drills of the Campanian Plain, indicate that the southern part of the plain was above sea level during the Middle Pleistocene (Brancaccio *et al.*, 1991; Cinque *et al.*, 1993), the period to which are dated back the older potassic and ultrapotassic rocks of the district (330 ka; Brocchini *et al.*, 2001).

The volcanic rocks cover an area as large as the entire Campanian plain, and some tephra levels originated from the largest eruptions of the Campi Flegrei and Ischia can be found throughout the Mediterranean basin and over. The geological evolution of the Campanian plain and the relationships with volcanic activity have been studied in detail by several authors (Ippolito *et al.*, 1973; Cinque *et al.*, 1987, 1993; Albore Livadie *et al.*, 1989; Brancaccio *et al.*, 1991; Romano, 1992). The volcanic complexes are made up maily of pyroclastic rocks with subordinate lava flows but their structures and morphological appearance vary widely.

1. Ischia Island

The Ischia volcanic complex emerges from the sea with a height of 787 m. a.s.l. at Monte Epomeo and with an extension of about 40 km^2 (Fig. 29). The island is made up prevalently by volcanic rocks, with pyroclastic ones predominant over lavas, and lava domes. The morphology and geological setting of the island is controlled by the regional geology, and local features related to dome resurgence that built the Mt. Epomeo horst (Orsi *et al.* 1991, 1992a; Acocella & Funiciello, 1999; Acocella *et al.*, 2001). The subaerial volcanic activity has been divided in five main phases (Vezzoli, 1988). The eruption of the Mt. Epomeo Green Tuff marked the distinction between the old (first two periods) and the young cycle of activity.

The oldest outcropping products have not been dated and are made up by a thick sequence of pyroclastic rocks and lava flows (subordinate). Their source is unknown, and they are considered to preceed the oldest dated activity, 0.15 Ma of the lava flow of "*Punta della Guardiola*", outcropping in the southeastern and southwestern edges of the island (Poli *et al.*, 1987). The former, as well as all the other ages reported for Ischia are K/Ar model ages. During the first cycle, scattered volcanic activity developed on the island with the emplacement mainly of lava domes and pyroclastic rocks, with subordinate lava flows. The cycle ended with the "*Parata*" lavas dated at 0.07 Ma (Poli *et al.*, 1987). The second cycles started with the eruption of the "*Monte Epomeo*" Green Tuff at 0.055 Ma (Cassignol & Gillot, 1982; Gillot *et al.*, 1982), followed by an intense pyroclastic activity that brought to the emplacement of the "*Pignatiello*" and "*Citara*" (0.033 Ma; Gillot *et al.*, 1982) pyroclastic units, which are interbedded with deposits of several minor pyroclastic eruptions. At the end of this intense period of pyroclastic activity, whose emission centers have not been recognized, volcanism moved in the south-western sector of the island where several monogenetic centers produced an intense but scattered strombolian activity with formations of cinder cones and lava flows. This phase protracted till about 0.018 Ma (Poli *et al.*, 1987). The last phase of activity, which started from 0.010 Ma b.p. and continued till historical times (1302 A.D.), developed in the northeastern and northwestern sectors of the island through several small monogenetic eruptive centers that erupted lava flows and pyroclastic deposits (Poli *et al.* 1987; Chiesa *et al.*, 1988).

The volcanic rocks of Ischia island range in composition from shoshonites through latite to alkali trachyte and trachyphonolite (Fig. 30a), these latter rarely having a weak peralkaline affinity (Poli *et al.* 1987, 1989; Crisci *et al.*, 1988; Di Girolamo *et al.* 1995; Avanzinelli *et al.* 2008; Tommasini's unpublished data). Trachytic rocks are dominant throughout the volcanic sequence, whereas mafic rocks (shoshonites and latites) are more frequent in the late stage of activity (<0.01 Ma), in the form of scoria cones aligned along preexisting structures (*Vateliero*, *Molara* and *Cava Nocelle*, Fig. 29). Moreover, several eruptions produced volcanic rocks varying in composition from mafic to intermediate/evolved rocks (latite/trachyte; e.g., 1302 A.D., *Arso* lava flow, Fig. 29). Mingling processes are also noticed in some recent lava flows (e.g. *Zaro*; Di Girolamo *et al.*, 1995). The parageneses contain clinopyroxene ± plagioclase ± olivine, with inclusions of chromiferous spinel, and rare phlogopite. Latites have less olivine, less An-rich plagioclase and more Fe-rich clinopyroxene, whereas typical trachytes have sanidine phenocrysts, to which hedenbergitic clinopyroxene, sodalite, magnetite and several accessory phases complete the mineral assemblages. Trachytes and trachyphonolites have also aenigmatite and sodic clinopyroxene within the groundmasses, thus demonstrating their peralkaline nature (Melluso's unpublished data).

Table 7 Chemical (major and trace) and Sr-Nd-Pb isotopic values for Roman Magmatic Province – the Neapolitan district volcanic rocks

Reference:	1	2 - 3	2 - 3	1 - 4	5 - 3	6	7	8	9 - 10	10	3
Volcano	Ischia	Ischia	Ischia	Procida	Procida	Phlegrean Fields	Phlegrean Fields	Somma	Vesuvius	Vesuvius	Vesuvius
Locatlity:	Epomeo	Grotta di Terra	Zaro	Procida	fiumicelo	Ponti Rossi	Ponti Rossi	Pollena Quarry	Pompei	-	North of OV tongue
series	Sho	Sho	Sho	Sho	Sho	Sho	Sho	Sho	Pl-leucitite	Pl-leucitite	Pl-leucitite
type	green tuff	lava	lava	lithic	lava	pre-CI	NYT	dyke	pumice	pumice	lava
Sample:	P38.Ea	I 109	I 2SF	AP 16	FAM	ME043	PrB5s*	VES 14	S19 (1)b	R10	VES 17
Age:	*55 ka*	*28 ka*	*6 ka*	*75 ka*	*55 ka*	*58 ka*	*12 ka*	*25 ka*	*79 A.D.*	*1631 A.D.*	*1944 A.D.*
SiO_2 (wt.%)	63.29	52.14	52.01	48.89	52.10	58.03	54.75	51.39	51.90	47.90	48.91
TiO_2	0.40	1.34	1.36	1.23	1.27	0.38	0.60	0.98	0.49	0.95	1.03
Al_2O_3	19.13	18.20	18.09	15.65	15.80	18.11	18.13	17.61	19.10	16.40	19.30
Fe_2O_3	-	7.99	7.23	1.48	10.20	3.85	6.28	7.43	4.30	8.30	1.10
FeO	2.36	-	-	6.75	-	-	-	-	-	-	6.71
MnO	0.09	0.13	0.14	0.14	0.15	0.13	0.13	0.12	0.13	0.15	0.16
MgO	0.68	3.32	5.44	8.89	4.71	0.74	1.92	4.65	1.83	5.26	3.72
CaO	1.76	7.59	8.16	11.64	9.08	2.81	5.15	8.46	5.70	10.80	8.46
Na_2O	5.03	4.68	3.78	2.88	2.82	3.70	3.24	2.15	4.29	2.27	1.54
K_2O	7.23	4.01	3.22	1.52	3.42	7.61	7.84	5.85	8.72	6.36	8.24
P_2O_5	0.03	0.67	0.48	0.31	0.44	0.16	0.36	0.74	0.24	0.83	0.84
LOI	0.10	0.96	0.31	0.61	3.65	4.68	1.62	0.31	2.89	0.62	0.24
Sum	100.10	101.03	100.22	99.99	103.64	100.21	100.03	99.69	99.59	99.84	100.25
Mg-V	37.7	49.2	63.7	69.8	51.8	30.8	41.6	59.3	49.8	59.6	50.3
Sc (ppm)	4.0	16.2	20.8	38.2	20.1	-	8.8	23	7.0	25.4	-
V	39	229	166	192	237	57	147	206	-	-	230
Cr	7	23	145	406	5	11	-	50	22	66	48
Co	7.0	17.7	20.1	43.8	27.4	3.1	-	22	8.7	29.0	22.7
Ni	-	16	57	164	23	5	-	30	10	30	26
Cu	-	61	20	61	56	6	-	170	10	92	101
Zn	-	-	-	58	-	84	-	70	80	81	-
Ga	-	15	14	22	15	-	-	18	-	-	15
Rb	232	57	118	47	131	232	302	238	360	230	307
Sr	191	648	475	474	814	633	1055	793	870	960	885
Y	55	24	24	23	24	31	31	24.9	26	34	23.0
Zr	230	143	137	104	133	314	249	217	280	215	206
Nb	44	30	37	13	20	45	32	35.4	52	26	40.0
Cs	7.4	6.9	6.9	-	5.5	-	-	11.9	21.6	13.8	17.5
Ba	197	1390	600	464	1310	1000	2075	1663	960	1900	2090
La	56	42.4	37.9	16.6	40.7	80.0	65.4	41.7	78.1	47.6	51.3
Ce	102	80.9	66.7	33.0	79.1	149.9	122.6	88.6	130.8	94.2	102
Pr	-	9.66	8.31	-	9.88	15.7	-	10.5	-	-	12.5
Nd	53	36.8	30.3	20	37.6	53.4	51.7	40.0	41.2	47.0	47.1
Sm	7.5	7.3	6.0	5.1	7.6	9.4	10.3	8.75	7.6	10.1	9.40
Eu	1.20	2.25	1.70	1.68	2.29	2.22	2.60	2.15	1.60	2.28	2.36
Gd	-	6.81	5.77	5.3	7.09	7.5	8.4	7.04	-	-	7.76
Tb	0.80	0.81	0.72	0.67	0.86	1.00	-	0.96	0.69	1.01	0.85
Dy	-	4.40	4.25	4.4	4.54	5.61	5.80	4.79	-	-	4.25
Ho	-	0.90	0.81	-	0.81	1.08	-	0.82	-	-	0.75
Er	-	2.56	2.41	1.84	2.31	2.83	3.30	2.26	-	-	2.13
Tm	-	0.31	0.33	-	0.28	0.39	-	0.333	-	-	0.260
Yb	2.0	2.30	2.20	2.20	1.90	2.51	2.50	2.04	1.85	2.03	1.90
Lu	0.36	0.33	0.31	0.26	0.28	0.37	0.50	0.304	0.26	0.29	0.250
Hf	5.6	3.0	3.0	2.2	3.0	-	-	5.3	4.7	4.5	4.0
Ta	2.7	1.60	2.10	0.79	1.00	-	-	2.08	2.35	1.55	1.90
Pb	-	15.0	10.8	-	14.8	48.3	38.7	30	70	21	-
Th	15.3	9.6	7.79	5.0	9.27	-	25.0	21.3	35.6	16.3	19.45
U	4.6	1.9	2.58	-	2.62	-	-	7.67	11.4	4.8	6.30
$^{87}Sr/^{86}Sr$ m	0.70688	0.706122	0.705503	0.705060	0.706556	0.706810	0.707521	0.707647	0.707610	0.707105	0.707228
$^{143}Nd/^{144}Nd$ m	0.512481	0.512598	0.512683	0.512726	0.512536	0.512610	0.512510	0.512487	0.512507	0.512490	0.512474
$^{206}Pb/^{204}Pb$ m	-	-	-	18.836	19.305	19.246	19.044	-	19.089	18.954	19.0213
$^{207}Pb/^{204}Pb$ m	-	-	-	15.634	15.798	15.693	15.695	-	15.687	15.617	15.6956
$^{208}Pb/^{204}Pb$ m	-	-	-	38.790	39.445	39.324	39.205	-	39.185	38.915	39.1506

Legend: sho = shoshonitic series; Pl-leucitite = plagioclase leucitites and leucitites; pre-CI = pre Campanian Ignimbrite; NYT = Neapolitan Yellow tuff; Mg-V = [MgO]/([MgO]+0.85*[FeOtot]); - = not analyzed; m = measured.

Data from: 1 = Poli *et al.* (1987); 2 = Di Girolamo *et al.* (1995); 3 = Avanzinelli *et al.* (2008); 4 = Conticelli *et al.* (2002); 5 = Fedele *et al.* (1996); 6 = Pappalardo *et al.* (1999, 2002); 7 = Orsi *et al.* (1995); 8 = authors' unpublished data; 9 = Civetta *et al.* (1991); 10 = Ayuso *et al.* (1998).

Figure 30. Classification and incompatible trace element characteristics of Pleistocenic to Holocenic rocks from Ischia volcano.

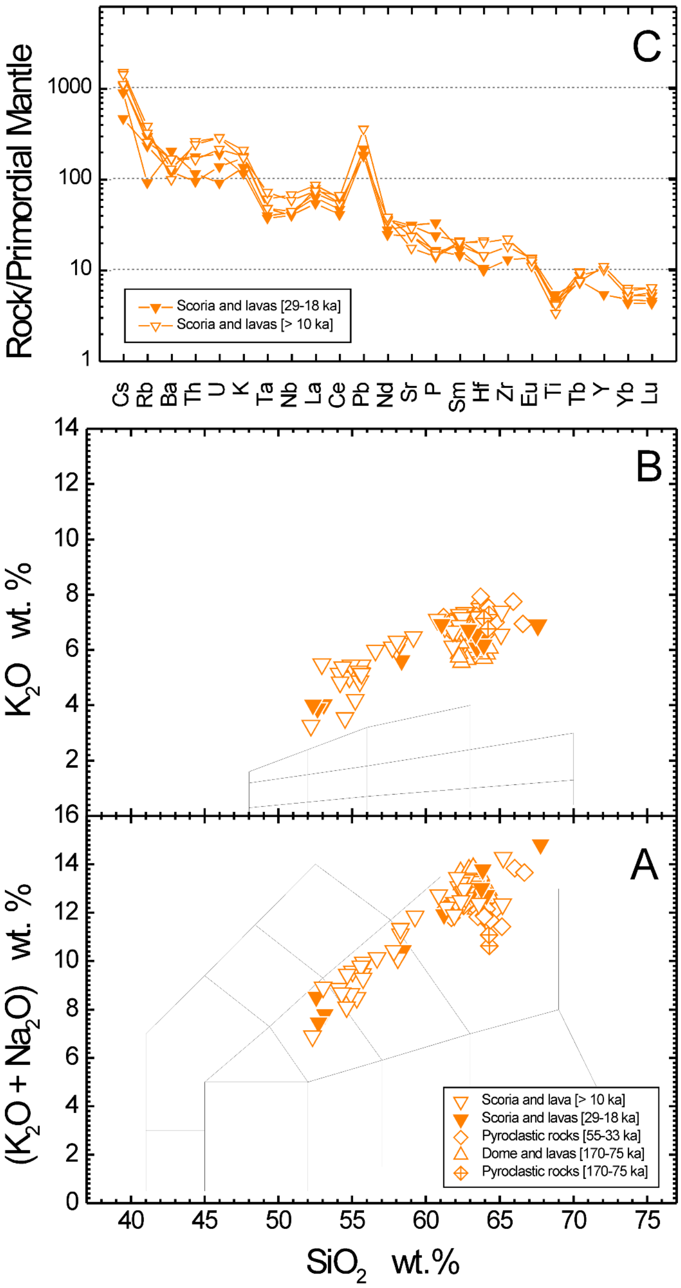

Classification and geochemical characteristics of the Ischia volcanic rocks. A) Total Alkali-Silica (TAS) classification diagram (Le Maitre, 2002). B) K_2O wt.% vs. SiO_2 wt.% classification diagram with reported the grid for orogenic volcanic rock suites (Peccerillo & Taylor, 1976). C) Incompatible trace element patterns for mafic volcanic rocks normalised to the primordial mantle values of Sun & McDonough (1989). Data from Poli *et al.* (1987, 1989), Crisci *et al.* (1988), Di Girolamo *et al.* (1995), Avanzinelli *et al.* (2008) Tommasini's unpublished data).

No ultrapotassic rocks have been observed at Ischia (Fig. 30b), The Ischia mafic rocks display the lowest abundances in incompatible trace elements among the whole Roman and Italian shoshonites, but surprisingly is also the fractionation of HFE with respect to LIL elements is very weak (Fig. 30c). Troughs at Ta, Nb, and Ti as well as peaks at Th and U are negligible with respect to adjacent normalized elements (Fig. 30c). These geochemical characteristics are argued to testify the channelling of a within-plate component into the upper mantle source of Italian magmas (Avanzinelli *et al.*, 2008).

2. Campi Flegrei and Procida Island

The Campi Flegrei volcanic field, including Procida and Vivara islands, is a volcanic area formed by small volcanic apparata and several monogenetic volcanoes, in the form of tuff rings, tuff cones and rarely cinder cones and lava domes, cropping out outside, on the borders, and within a large polygenetic caldera formed by the eruptions of the Campanian Ignimbrite and the Neapolitan Yellow Tuff (e.g., Rosi *et al.*, 1983; Armienti *et al.*, 1983; Di Girolamo *et al.*, 1984; Rosi & Sbrana, 1987; Orsi *et al.*, 1992, 1995, 1996a, 1999; Cole & Scarpati, 1993; Di Vito *et al.*, 1999; De Vivo *et al.*, 2001; Ort *et al.*, 2003).

The oldest volcanic activity is represented by the pre-Campanian Ignimbrite deposits, which are found as loose remnant cropping out outside and on the borders of the Campanian Ingnimbrite caldera, and it dates back till ~0.08 Ma (Pappalardo *et al.*, 1999) (Fig. 29). Other ignimbritic deposits are found in the Campanian Plain with ^{40}Ar-^{39}Ar ages of ~0.21 Ma (De Vivo *et al.*, 2001) and ~0.29 Ma (Rolandi *et al.*, 2003). The large volume Campanian ignimbrite (Fisher *et al.*, 1993; Rosi *et al.*, 1996: ca. 300 km^3 of dense rock equivalent magma - D.R.E.), whose proximal products are found at Procida, Monte di Procida, Giugliano, Quarto, Cuma, bottom of Camaldoli and San Martino Hills have been produced by a large eruption, on which several age data were published (^{40}Ar-^{39}Ar ages: ~0.037 Ma, Deino *et al.*, 1994; ~0.039 Ma, De Vivo *et al.*, 2001; ~0.038 Ma, weighted average of 10 samples in Fedele *et al.*, 2008). An intense volcanic activity occurred after the formation of the Campanian Ignimbrite caldera, with the formation of pyroclastic deposits from several volcanic centers. A second large eruption dates back at 0.015 Ma (Deino *et al.*, 2004) with the emplacement of the Neapolitan Yellow Tuff (Cole & Scarpati, 1993; Wohletz *et al.*, 1996), which has been estimated at 12 km^3 D.R.E (Rosi & Sbrana, 1987). The most recent volcanic activity, placed within the Neapolitan Yellow Tuff caldera and on its borders, dates back to 1538 A.D. with the eruption of *Monte Nuovo* (e.g., de Vita *et al.*, 1999; Isaia *et al.*, 2004; D'Oriano *et al.*, 2005). At present, only fumarolic and bradeyseismic activity is ongoing.

The Campi Flegrei volcanic rocks are predominantly of pyroclastic nature and vary in composition from shoshonitic basalts to trachytes and trachyphonolites (Fig. 31a), belonging to the shoshonitic series (Fig. 31b); some trachyphonolites are weakly peralkaline (e.g., Armienti *et al.*, 1983; Villemant, 1988; Beccaluva *et al.*, 1990; Civetta *et al.*, 1991a; Melluso *et al.*, 1995; Pappalardo *et al.*, 1999, 2002; D'Antonio *et al.*, 1999b; Paone, 2004). The most mafic compositions are present at Procida volcano as lava clasts in phreatomagmatic eruptions and scoriae from monogenetic activity (e.g., D'Antonio *et al.*, 1999a; De Astis *et al.*, 2004; Fedele *et al.*, 2006). Differentiated compositions are rarely found in the mainland within the Campi Flegrei volcanic field (e.g., Concola, Cigliano, Montagna Spaccata, Nisida) and they have been achieved by open system shallow level differentiation processes (e.g., Pappalardo *et al.*, 2002). The majority of the Campi Flegrei volcanic rocks are trachytes and trachyphonolites, including the chemically zoned Campanian Ignimbrite and Neapolitan Yellow Tuff deposits (e.g., Scarpati *et al.*, 1993; D'Antonio *et al.*, 1999a, Fedele *et al.*, 2008). Evidence of interaction between mafic and evolved magmas is clearly seen in most pyroclastic eruptions (Fedele *et al.*, 2009), and is more frequent in the latest stage of activity (<0.015 Ma), where less evolved compositions are frequently found.

Mineralogically, the primitive basalts have typical phenocryst assemblage formed mainly by Fo-rich olivine with chromiferous spinel inclusions, with Mg-rich clinopyroxene, and Ca-rich plagioclase. Latites have more Na-rich plagioclase, with clinopyroxene, phlogopite, magnetite phenocrysts and microlites, whereas trachytes have the typical assemblage K- to Na-rich sanidine, Na-plagioclase, Fe-rich clinopyroxene, Fe-rich amphibole and several accessoriy phases, with additional groundmass or microphenocryst sodalite ± nepheline. Mixed phenocryst assemblages are frequently found in both lava domes and pyroclastic rocks (e.g., Fedele *et al.*, 2008).

Figure 31. Classification and incompatible trace element characteristics of Holocenic volcanic rocks from Campi Flegrei and Procida.

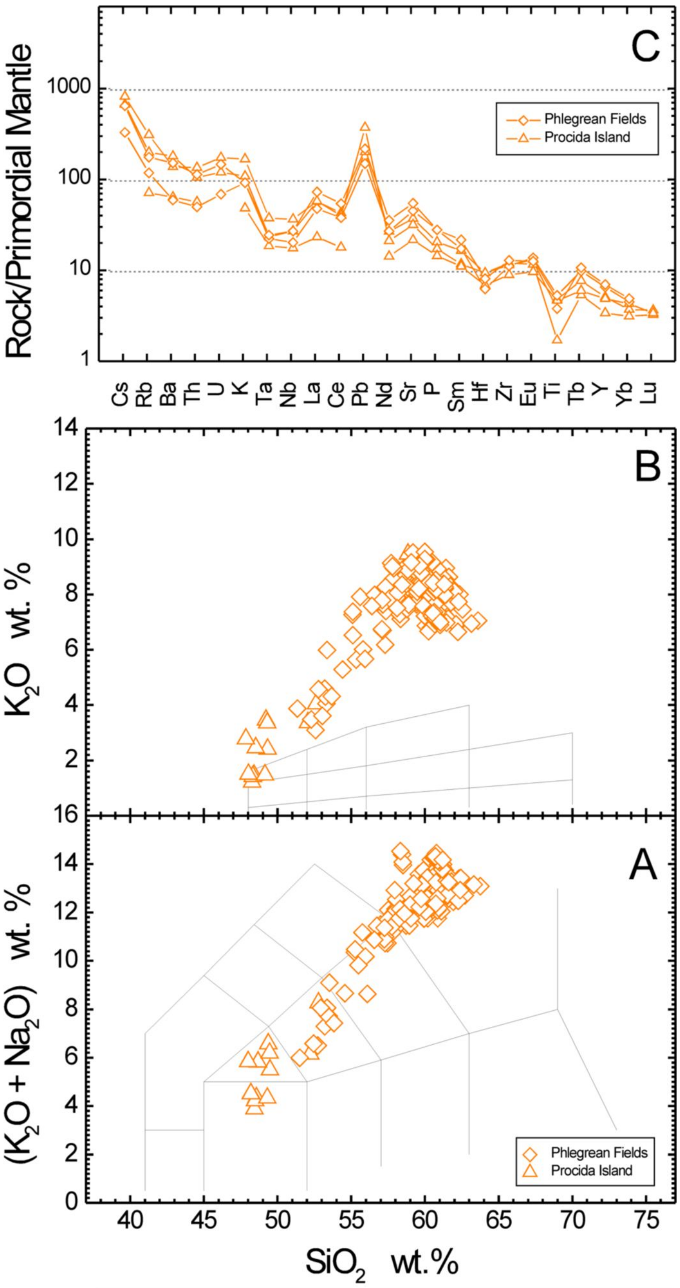

Classification and geochemical characteristics of the Campi Flegrei and Procida volcanic rocks. A) Total Alkali-Silica (TAS) classification diagram (Le Maitre, 2002). B) K_2O wt.% vs. SiO_2 wt.% classification diagram with reported the grid for orogenic volcanic rock suites (Peccerillo & Taylor, 1976). C) Incompatible trace element patterns for mafic volcanic rocks normalised to the primordial mantle values of Sun & McDonough (1989). Data from Pappalardo *et al.* (1999, 2002), D'Antonio *et al.* (1999b), Fedele *et al.* (2006, 2008), Avanzinelli *et al.* (2006, 2008).

Figure 32. Classification and incompatible trace element characteristics of Pleistocenic to Holocenic volcanic rocks from Somma-Vesuvius volcano.

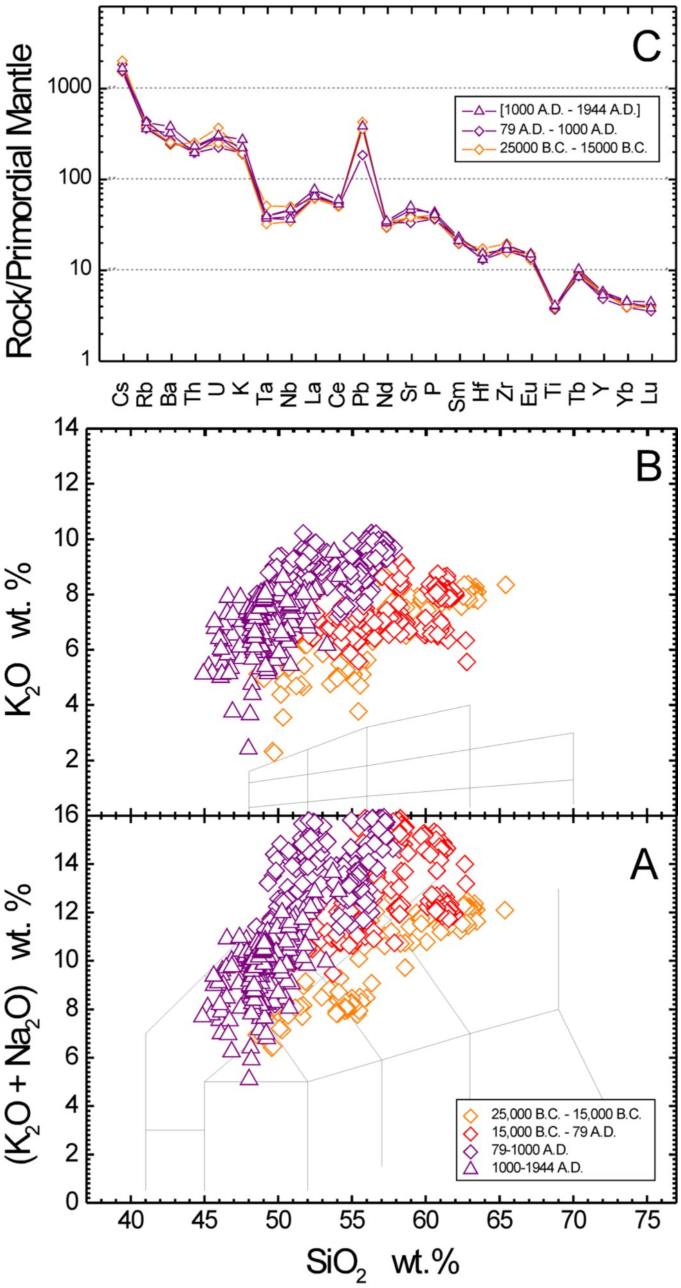

Classification and geochemical characteristics of the Somma-Vesuvius volcanic rocks. A) Total Alkali-Silica (TAS) classification diagram (Le Maitre, 2002). B) K_2O wt.% vs. SiO_2 wt.% classification diagram with reported the grid for orogenic volcanic rock suites (Peccerillo & Taylor, 1976). C) Incompatible trace element patterns for mafic volcanic rocks normalised to the primordial mantle values of Sun & McDonough (1989). Data from Joron *et al.* (1987), Ayuso *et al.* (1998), Di Rienzo *et al.* (2007), Avanzinelli *et al.* (2008) Melluso's unpublished data).

Incompatible normalized trace element patterns of the mafic volcanic rocks from Campi Flegrei and Procida have mild enrichment with smooth fractionation of large ion lithophile with respect to high field strength elements (Fig. 31c). Indeed Ta and Nb troughs are extremely smoother with respect to other Roman volcanoes. The Ba trough is absent, whereas the Hf trough is more pronounced (Fig. 31c). It is important to note, as in the rest Neapolitan district the relatively low U and Th abundances with respect to the other Italian ultrapotassic and related igneous rocks, with also peculiar U/Th ratios (Avanzinelli *et al.*, 2008).

3. Somma-Vesuvius

The Somma-Vesuvius volcanic complex is actually formed by two main volcanic edifices separated by two calderas: the Monte Somma composite volcano, disrupted by several pyroclastic eruptions which formed at least two calderas in the last 0.022 Ma (the Somma caldera s.s. and the Piano delle Ginestre calderas), and the Vesuvius s.s., a cone mostly formed by juxtaposition (and disruption) of volcanic rocks erupted from the 79 A.D. (Pompei eruption) and the 1944 A.D. last eruption. Some eccentric cones and lava domes are recorded throughout the activity (e.g., Santacroce, 1987; Rosi *et al.*, 1993; Principe *et al.*, 2004; Di Renzo *et al.*, 2007; Cioni *et al.*, 2008; Santacroce *et al.*, 2008). The oldest volcanic activity has been found as leucitite-bearing lavas in a drill at Trecase and dated at about 0.4 Ma (Brocchini *et al.*, 2001).

The Vesuvius rocks lack of primitive magma compositions (Table 7), due to a more or less efficient stoping in several shallow depth reservoirs (e.g., Civetta *et al.*, 1991b, 2004; Santacroce *et al.*, 1993; Cioni *et al.*, 1995; Del Moro *et al.*, 2001; Fulignati *et al.*, 2004; Gurioli *et al.*, 2005; Morgan *et al.*, 2006; Scaillet *et al.*, 2008). There is clear evidence of shift of magmatic compositions with time (Joron *et al.*, 1987; Cioni *et al.*, 2008, and references therein). The bulk of the Somma volcanic rocks are less undersaturated in silica, and range in composition from leucite-bearing trachybasalts to leucite latites to trachytes, whereas the more recent volcanic rocks, in the form of lava flows and juvenile products of plinian eruptions, range in composition from leucite basanite and leucite tephrite to phonolite (Fig. 32a). All the Somma-Vesuvius mafic volcanic rocks are silica undersaturated, and belong to the ultrapotassic plagioclase-leucititic volcanic series (Fig. 32b), differently from the volcanic rocks of Campi Flegrei volcanic field and Ischia volcanic complex, indicating completely independent magma reservoirs and feeding systems (e.g., Cortini & Hermes, 1981; Joron *et al.*, 1987; Caprarelli *et al.*, 1993; Villemant *et al.*, 1993; Ayuso *et al.*, 1998; Paone, 2006; Cioni *et al.*, 2008 and references therein). Recently, Iacono Marziano *et al.* (2007), resurrected the old hypothesis by Rittman (1933) of shallow level carbonate assimilation to explain the transition from leucite-free shoshonitic Somma compositions to ultrapotassic leucite-bearing recent activity.

Similarly to the other Neapolitan district volcanoes, incompatible normalized trace element patterns of Somma-Vesuvius mafic rocks still have a very marked fractionation of LILE with respect to HFSE (Fig. 32c), with troughs Ta, Nb, and Ti, no Ba anomaly and inversion of Th enrichment with occurrence of a very small trough (Fig. 32c). In terms of trace element distribution the volcanic rocks of the Neapolitan district display some similarities with the volcanic rocks of the Lucanian Magmatic Province (i.e., Monte Vulture, see below), but Peccerillo (2001, 2005a) and Peccerillo & Alagna (2010, this volume) suggested a geochemical connection with Stromboli volcanic rocks (Aeolian Islands), which are, however, characterized by distinctly lower silica undersaturation.

Lucanian Magmatic Province: the Mt. Vulture and Monticchio lakes volcanoes

The Lucanian Magmatic Province is made up by the Monte Vulture and Monticchio nested volcanoes, with few small eccentric explosive monogenetic centres along the Ofanto valley and at Ripacandida. The volcanism of this province is located east of the Apennine system, not far from the Apulian foreland (Fig. 11). The Monte Vulture volcano lies on a structural high made up by Meso-Cenozoic units of the substratum with Pliocene continental sediments on their top (Schiattarella & Beneduce, 2006; Giannandrea *et al.*, 2006). The volcanic activity at Vulture-Monticchio nested volcanoes (Fig. 33) developed entirely within the Pleistocene starting at about 0.74 Ma (Villa & Buettner, 2009). The main stratovolcano represented by the Rionero and, mainly, by the Vulture-San Michele subsynthems (Principe & Giannandrea, 2006) was built up between ~0.67 and ~0.6 Ma (Brocchini *et al.*, 1994; Villa & Buettner, 2009). At the end of this period volcanic activity produced lava flows from parasitic vents along the north and north-eastern side of the volcano, with the emission of the Melfi haüynophire (0.56 Ma, Bonadonna *et al.*, 1998; 0.57 Ma, Villa & Buettner, 2009) and Piano di Croce lavas, and the beginning of the sector collapse along the curved faults of the Valle dei Grigi (Guest *et al.*, 1988; Principe & Giannandrea, 2006). The volcanic and tectonic activity of the Vulture area has been sealed by a thick paleosoil (Schiattarella *et al.*, 2005). Volcanic activity renewed later in small centres along fractures and it is characterised by small carbonatitic lava flows and explosion craters with formation of the Lago Grande and Lago Piccolo maars (Stoppa & Principe, 1997; Principe & Giannandrea, 2006). The magmatic fraction of a surge from the Laghi di Monticchio volcanic field gives an age of about 0.13 Ma (Brocchini *et al.*, 1994). The Toppo del Lupo lavas are likely part of this monogenetic activity (D'Orazio *et al.*, 2007, 2008). All reported ages for this magmatic Province are ^{40}Ar-^{39}Ar ages.

Figure 33. Geological sketch map of the Monte Vulture volcano (Lucanian Magmatic Province).

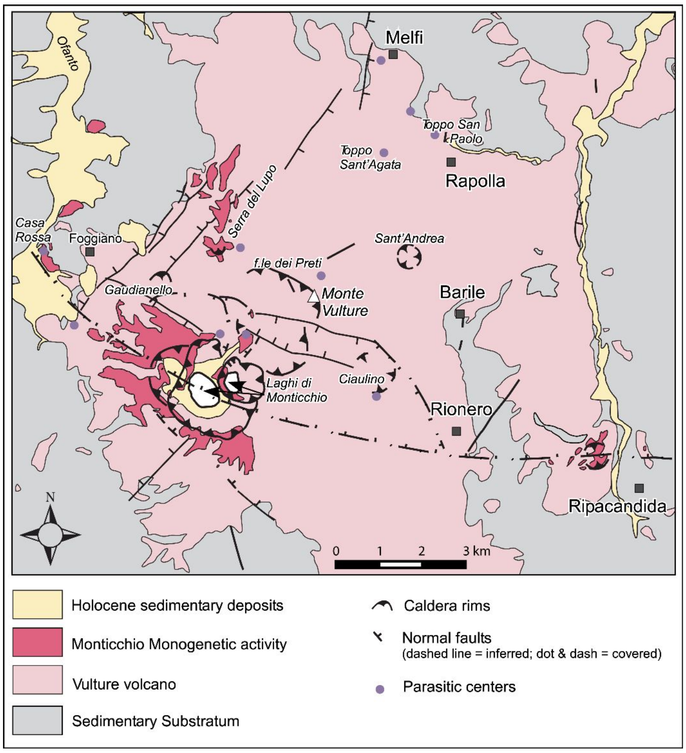

Geological sketch map of the Lucanian volcanic district redrawn after Giannandrea *et al.*, 2006..

Table 8 **Chemical (major and trace) and Sr-Nd-Pb isotopic values for Lucanian Magmatic Province volcanic rocks: Vulture and Monticchio nested volcanoes.**

Reference	1	2	3	1 - 4	3	3	1 – 4 - 5	3	3	6	6
Volcano:	Vulture	Vulture	Vulture	Vulture	Vulture	Vulture	Monticchio	Monticchio	Monticchio	Monticchio	Monticchio
Locality	Toppo San Paolo	Toppo Capraro	Summit Monte Vulture	Pedra della Scimmia	Foggiano	Melfi	Case Renzoni	Toppo del Lupo	Toppo del Lupo	Monticchio lakes	Monticchio lakes
Rock type	*Phonolite*	*mafitite aut.*	*haüyne foidite*	*melilitite*	*basanite*	*haüynite*	*rounded lapilli*	*rounded lapilli*	*upper lava*	*Harz-burgite*	*Wehrlite*
Sample	**VLT 02**	**VU 621**	**VV 13**	**VLT 14**	**VV6**	**VTR 4**	**VLT 99**	**VM 7**	**VM 8**	**Aj6H**	**Aj8W**
Age:	*673 ka*	*629 ka*	*629 ka*	*629 ka*	*629 ka*	*573 ka*	*132 ka*	*132 ka*	*132 ka*	*132 ka*	*132 ka*
SiO_2 (wt. %)	55.66	37.12	42.50	39.79	45.9	40.4	40.87	18.00	16.30	43.83	38.38
TiO_2	0.23	2.45	1.17	2.39	1.47	0.97	1.64	0.50	0.46	0.03	0.13
Al_2O_3	22.12	16.08	16.80	14.53	15.0	18	11.83	6.10	5.41	1.14	2.57
Fe_2O_3	1.95	8.70	9.45	4.56	8.54	8.69	10.58	6.59	6.51	8.17	13.88
FeO	0.78	2.02	-	5.74	-	-	-	-	-	-	-
MnO	0.13	0.17	0.19	0.22	0.13	0.23	0.25	0.35	0.35	0.11	0.13
MgO	0.29	5.61	4.69	4.37	6.75	3.05	11.36	2.77	2.96	45.27	43.62
CaO	3.35	18.06	12.70	16.41	12.2	12.5	14.42	36.60	40.20	0.85	1.31
Na_2O	7.45	4.65	4.00	4.01	3.26	6.15	0.86	0.71	0.47	0.01	0.00
K_2O	5.94	2.05	5.08	4.87	4.29	3.79	2.40	0.39	0.17	0.01	0.00
P_2O_5	0.02	0.86	1.13	1.04	1.08	0.69	1.61	2.21	2.18	0.01	0.02
LOI	2.08	2.11	1.39	1.97	1.05	3.75	4.19	24.50	22.40	0.00	0.00
Sum	100.00	99.88	99.10	99.89	99.67	98.22	100.01	98.72	97.41	99.43	100.04
Mg-V	19.35	54.43	53.63	48.19	64.82	45.00	71.45	49.49	51.45	92.81	87.99
CO_2 (wt. %)	-	-	-	-	-	-	-	20.80	17.40	-	-
Sc (ppm)	-	9.9	15	-	24	5	32.7	7	7	8.7	3.4
V	69	274	271	303	212	249	218	373	316	33	65
Cr	1.5	2.7	7	12	105	5	309	7	7	2585	13958
Co	1.98	47.5	30	26.9	30	21	38.2	19	19	-	-
Ni	2	15	20	19	38	11	182	20	22	2407	1799
Cu	6	-	61	72	52	57	47	43	40	2	5
Zn	91	-	-	160	-	-	89	-	-	51	131
Ga	29	-	-	27	-	-	15	-	-	1.0	4.1
Rb	150	65	153	94.5	133	117	27.8	11.1	21.2	0.57	0.31
Sr	2980	2,510	2537	2540	2029	4228	2130	7357	10486	5.4	13.5
Y	17.1	49	69	75	55	58	48.5	91	87	0.202	0.94
Zr	392	406	478	487	433	466	312	175	210	1.30	4.36
Nb	154	76	112	131	80	176	107	320	332	0.366	0.630
Cs	14.6	2.32	10.3	6.12	6.9	12.2	1.4	1.38	5.3	0.024	0.012
Ba	3220	1,617	2777	2290	2240	2329	2900	7167	6450	15.6	16.1
La	323	173	277	213	166	323	268	619	604	0.37	1.07
Ce	480	318	512	412	330	554	449	1051	1027	0.68	2.50
Pr	41.9	-	55	47.4	38	54	49.7	100	98.9	0.079	0.329
Nd	106	123	199	170	143	188	163	318	313	0.326	1.530
Sm	11.7	25.4	34	33.7	24.9	28.2	26.9	43	42	0.068	0.363
Eu	2.36	5.73	7.3	7.63	5.3	6.4	6.62	9.2	9.2	0.018	0.009
Gd	3.77	-	23.8	24.8	18.2	18.5	22.0	28.3	28.2	0.061	0.343
Tb	0.59	2.1	3.15	3.61	2.42	2.44	2.25	3.5	3.4	0.009	0.046
Dy	2.83	-	14.8	15.4	11.2	12	10.2	16.5	16.1	0.047	0.264
Ho	0.43	-	2.39	2.40	1.88	1.97	1.70	2.8	2.88	0.009	0.044
Er	1.15	-	5.4	6.00	4.4	4.7	4.57	6.6	6.8	0.026	0.112
Tm	0.156	-	0.65	0.728	0.56	0.63	0.510	0.96	1.03	0.004	0.015
Yb	1.02	4.42	3.8	4.09	3.27	3.7	3.50	5.4	5.6	0.031	0.091
Lu	0.151	0.57	0.53	0.558	0.45	0.49	0.430	0.72	0.76	0.007	0.015
Hf	5.43	7.11	-	10.3	-	-	6	-	-	0.038	0.151
Ta	7.77	5.43	5.80	6.91	4.6	8.4	5.0	9.7	10.2	-	-
Pb	99.9	-	67	34.1	31	120	55.1	72	70	0.40	0.99
Th	99.0	40.5	72	49.2	38	82	44.57	85	85	0.054	0.132
U	14.2	11.2	18.7	17.6	8.5	23.4	10.14	43	56	0.017	0.026
$^{87}Sr/^{86}Sr$ m	0.705712	0.705864	0.705918	0.706397	0.705227	0.705791	0.705786	0.706159	0.706147	0.70424	0.70501
$^{87}Sr/^{86}Sr$ i	0.705710	0.705863	0.705916	0.706396	0.705225	0.705790	0.705786	0.706159	0.706147	0.70424	0.70501
$^{143}Nd/^{144}Nd$ m	0.512699	0.512564	0.512709	0.512591	0.512712	0.512699	0.512636	0.512586	0.512579	0.512800	0.512710
$^{206}Pb/^{204}Pb$ m	-	19.211	19.280	19.4996	19.389	19.290	19.2582	19.231	19.231	-	-
$^{207}Pb/^{204}Pb$ m	-	15.683	15.718	15.7138	15.693	15.707	15.6929	15.669	15.667	-	-
$^{208}Pb/^{204}Pb$ m	-	39.192	39.351	39.5521	39.389	39.289	39.2513	39.181	39.174	-	-

Legend: aut. = autoctonous name (Hieke Merlin, 1967); Mg-V = [MgO]/([MgO]+0.85*[FeOtot]); - = not analyzed; m = measured; i = initial calculated at the age of emplacement (see age in the headings of the table).
Data from: 1 = Avanzinelli *et al.* (2010); 2 = Heike Merlin (1967), De Fino *et al.* (1986), De Astis *et al.* (2006); 3 = D'Orazio *et al.* (2007); 4 = Bindi *et al.* (1999) ; 5 = Avanzinelli *et al.* (2008); 6 = Downes *et al.* (2002).

Figure 34. Classification and incompatible trace element characteristics of Pleistocenic rocks from Lucanian Magmatic Province.

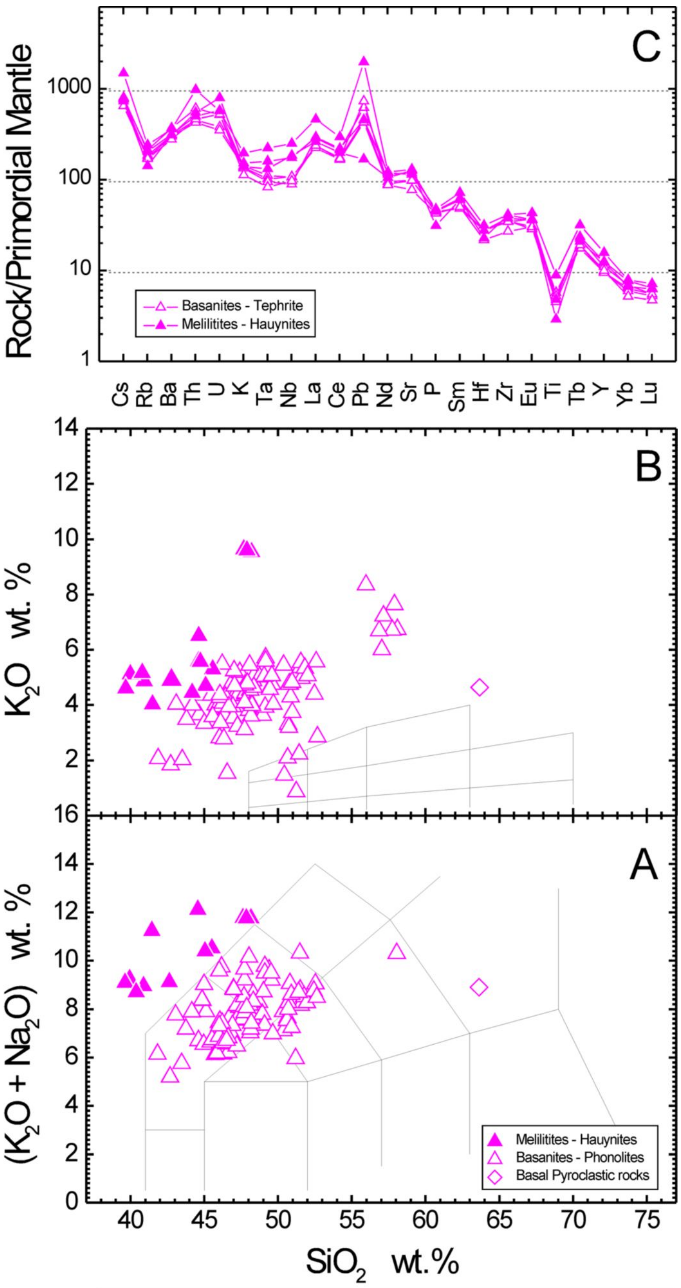

Classification and geochemical characteristics of the Lucanian volcanic rocks. A) Total Alkali-Silica (TAS) classification diagram (Le Maitre, 2002). B) K_2O wt.% vs. SiO_2 wt.% classification diagram with reported the grid for orogenic volcanic rock suites (Peccerillo & Taylor, 1976). C) Incompatible trace element patterns for mafic volcanic rocks normalised to the primordial mantle values of Sun & McDonough (1989). Data from Hieke Merlin (1967), De Fino *et al.* (1986), Melluso *et al.* (1996), Beccaluva *et al.* (2002), Downes *et al.* (2002), De Astis *et al.* (2006), D'Orazio *et al.* (2007, 2008), Stoppa *et al.* (2008), Avanzinelli *et al.* (2008, 2010).

The bulk of the erupted products mostly belong to a basanite-tephrite-phonolite series (Fig. 34a; Table 8), with mafic products (basanites and tephrites) dominating in both lavas and pyroclastic rocks (e.g., De Fino *et al.*, 1986; Beccaluva *et al.*, 2002). More silica undersaturated rocks, though minor in volume, are typical of this volcanic complex (Hieke Merlin, 1964, 1967). Melilitites, haüynites, haüyne-bearing leucitites are also found at the end of the Monte Vulture volcanic activity in the form of dikes, plugs and lava flows in the north-western flank of the volcano (Fig. 33). On the other hand, trachyphonolites are found as dykes in the neighbourings of the volcanic complex, and may be representatives of an earlier, and less silica undersaturated stage of activity (Melluso *et al.*, 1996; Beccaluva *et al.*, 2002). The typical phenocryst mineralogy of basanites and tephrites is composed by Fo-rich olivine (with chrome spinel inclusions), Ca-rich clinopyroxene, haüyne and leucite, to which Ca-rich plagioclase, amphibole, biotite and Fe-Ti oxides can be associated (Melluso *et al.*, 1996; Caggianelli *et al.*, 1990). Typical phonolites have phenocrysts of sanidine, haüyne, Fe-rich clinopyroxene, magnetite and garnet in a groundmass with additional nepheline. The melilite-bearing rocks are plagioclase-free rocks with clinopyroxene and haüyne phenocrysts; melilite is present as phenocryst or as groundmass phase, along with leucite, nepheline, Ti-rich garnet, magnetite, mica and perovskite (Melluso *et al.*, 1996).

The Monticchio lakes volcanic activity was mainly characterized by pyroclastic deposits related to explosive and hydromagmatic activity. A small carbonatitic lava flow has been also found at Toppo del Lupo (e.g., Stoppa and Principe, 1997; D'Orazio *et al.*, 2007, 2008; Stoppa *et al.*, 2008). Within the hydromagmatic units round lapilli tuffs units with ejecta of intrusive carbonatites and mantle nodules are also found (e.g., Jones *et al.*, 2000; Rosatelli *et al.*, 2000; Downes *et al.*, 2002). The carbonatic lava flows and pyroclastic rocks have olivine, monticellite, clinopyroxene, melilite, magnetite, amphibole and phlogopite, along with primary calcite laths (D'Orazio *et al.*, 2007). K_2O contents of the volcanic products decrease with time passing from Monte Vulture to Monticchio volcanoes. Sodic compositions are also found among lapilli tuffs of the Monticchio lake activity (Avanzinelli *et al.*, 2008, 2010). In addition the Lucanian volcanic rocks have an increasing content of incompatible elements, coupled to a decreasing fractionation of HFSE with respect to LILE, with time passing from Monte Vulture to Monticchio products (Fig. 34c). This feature has been interpreted by De Astis *et al.* (2006) as an increasing contribution of asthenospheric foreland mantle in the genesis of Lucanian rocks from slab tears in the Adriatic plate subducted beneath the Italian Peninsula. A partial melting during adiabatic ascent of the upper mantle source has been evidenced for the final Monticchio lake rocks (Avanzinelli *et al.*, 2008, 2010).

Volcanic structures of the Roman and Lucanian Magmatic Provinces

Monogenetic volcanism and dyking prevails in the Western Alps, Corsica and Tuscan Magmatic provinces, whereas volcanic edifices, ranging from flat ignimbrite shields to steep stratovolcanoes, prevail within the Roman and Lucanian magmatic provinces. This characteristic is a direct consequence of the volume of magma produced by the mantle source(s) but also of the tectonic regime acting during magma emplacement. There is a general consensus about the fact that Pleistocene volcanoes of the Roman and Lucanian Magmatic Provinces are favoured by the extensional post-orogenic tectonics. Indeed, locations and spacing on a crustal scale of the Roman volcanoes is ubiquitously related to intersection between NW-trending and NE-trending transverse extensional structures. This has been recorded in almost all volcanic districts of the Roman province: Vulsini (Barberi *et al.* 1984), Vico (Sollevanti 1983; Bear *et al.*, 2009a,b), Sabatini (De Rita *et al.*, 1983, 1996), Colli Albani (Giordano *et al.*, 2006), Middle Latin Valley (Sani *et al.*, 2006; Boari *et al.*, 2009b), Roccamonfina (Giordano *et al.*, 1995; De Rita & Giordano, 1996), Campi Flegrei (Scandone *et al.* 1991; Orsi *et al.*, 1996a), and Somma-Vesuvius (Santacroce, 1987; Bianco *et al.*, 1998) volcanoes. Furthermore, NE-trending faults are transfer structures of the regional NW-trending extensional faults, and seldom inherited from NE-trending transfer structure formed during the Apennine compression. For this reason NE-trending faults are thought to bear a more vertical dip than NW-trending faults which instead have been highlighted as low-angle normal faults in several seismic studies (Collettini *et al.*, 2006). NE-trending fractures and faults may play therefore a determinant role to magmatic melts upwelling through the upper crust (Acocella & Funiciello, 2006).

Middle-Upper Pleistocene volcanoes of the Tyrrhenian margin, belonging to the Roman and Lucanian Magmatic provinces, show a variety of morphologies and eruption styles. Volumes involved are in the order of several hundreds of km^3 for each volcanic complex and of several thousands of cubic kilometres for the whole volcanic belt (Table 9). All volcanoes, apart the Middle Latin Valley monogenetic ones, are associated with calderas, which are formed almost coevally, then suggesting a further structural and geodynamic control on volcanism. Very highly explosive volcanoes erupted several intermediate to large volume ignimbrites and are characterised by large, polyphased calderas and large ignimbritic plateaux. These complexes have been classified as caldera complexes and they are, from north to south: the Bolsena and Latera volcanoes in the Vulsinian district, the Bracciano and Sacrofano volcanoes in the Sabatian district, the Vulcano Laziale volcano in the Colli Albani district, the Campi Flegrei volcano in the Neapolitan district. On the other hand, several composite volcanoes characterized by a well formed stratocone are also present either as main edifice or as a secondary edifice during post caldera activity. At the former category belong the Vico, Roccamonfina, Ventotene, Ischia, Somma, and Vulture volcanoes, whereas to the latter one belong the Monte delle Faete, the intracaldera stratocone of Colli Albani, and the Vesuvius (Table 9).

Almost all the Roman and Lucanian volcanoes erupted intermediate volume ignimbrites, which brought to the formation of small summit collapse composite calderas (e.g., Vico, Roccamonfina, Ischia, Somma-Vesuvius and Vulture). Ischia volcanic complex hosts the only resurgent caldera (Orsi *et al.*, 1991; Acocella & Funiciello 1999). Sector collapses associated with gravitational instability of the stratovolcanoes have also been described at Roccamonfina (De Rita & Giordano, 1996) and Vulture (Guest *et al.*, 1988) volcanoes.

Latest stages of activity of many of the Roman and Lucanian volcanoes are associated to phreatomagmatism, which produced tuff rings and tuff cones, but maar volcanism has been also recorded (e.g., Albano lake and Monticchio lakes, Figs. 21 and 33).

Table 9. Summary scheme for the volcanic edifices related with silica-undersaturated ultrapotassic magmas of the Roman and Lucanian Magmatic Provinces

Volcanic District	Edifice	Type	Epochs of activity	Dominant style of activity	Magmatic series	Product volume (km^3)	Time period (ka)	References
Amiata		Dome		Effusive	Hybrid		200-300	Ferrari *et al.* 1995
Vulsini	Latera	Alkaline ignimbrite shield and caldera complex	4 - Hydromagmatic	Phreatomagmatic	Shoshonitic		55-180	Vezzoli *et al.*, 1987 Nappi *et al.*, 1991 Palladino *et al.* 2010
			3 - Latera	Explosive	Shoshonitic Leucititic	20	140-300	
	Bolsena	Alkaline ignimbrite shield and caldera complex	2 – Bolsena-Montefiascone	Explosive/effusive	Leucititic Kamafugitic	280	250-500	
			1 - Paleobolsena	Explosive/effusive	Hybrid		500-600	
Vico		Stratovolcano	3 - Monte Venere	Effusive/explosive	Shoshonitic Leucititic	1.5	95-140	Sollevanti 1983 Perini *et al.*, 2000, 2004 Bear *et al.*, 2009a,b
			2 - Lago di Vico	Explosive	Leucititic	15	140-200	
			1 - Rio Ferriera	Effusive	Leucititic	50	200-350	
				Effusive-explosive	Hybrid	?	≥ 400	
Sabatini	Sacrofano	Alkaline ignimbrite shield and caldera complex		Explosive/ phreatomagmatic	Leucititic	180±45	<50 - >590	Cioni *et al.*, 1993 Di Filippo 1993 De Rita *et al.*, 1996 Conticelli *et al.*. 1997 Karner *et al.*, 2001
	Bracciano	Alkaline ignimbrite shield and caldera complex		Effusive/explosive	Leucititic		<150 - >433	
Colli Albani	Via dei Laghi	Maar field	3 – Via dei Laghi	Phreatomagmatic	Leucititic	1	quiescent (<23) - ?200	Karner *et al.*, 2001 Funiciello *et al.*, 2003 Giordano *et al.*, 2006, 2010 Boari *et al.*, 2009a Conticelli *et al.*, 2010a
	Faete	Stratovolcano	2 – Tuscolano-Artemisio-Faete	Effusive/esplosive	Leucititic	35	?180-<355	
	Tuscolano-Artemisio	Fissure system		Effusive	Leucititic			
	Vulcano Laziale	Alkaline ignimbrite shield and caldera complex	1- Vulcano Laziale	Explosive/effusive	Leucititic Kamafugitic	255	355-600	
Middle Latin Valley (former Ernici)		Monogenetic field		Explosive/effusive	Calc-alkaline Shoshonitic Leucititic Kamafugitic		750-250 ka	Civetta *et al.* 1981 Boari and Conticelli, 2007 Frezzotti *et al.* 2007 Boari *et al.* 2009b
Roccamonfina	Vezzara	Stratovolcano	Epoch III	Effusive/explosive	High-K CA Shoshonitic Leucititic	1.5	55-200	Giannetti & Luhr 1983 Cole *et al.*, 1993 De Rita, Giordano, 1996 Conticelli *et al.*. 2009b Rouchon, *et al.*, 2008
	Riardo	Caldera forming	Epoch II	Explosive	Shoshonitic Leucititic	30	230-385	
	Roccamonfina	Stratovolcano	Epoch I	Effusive	Leucititic	100	400-630	
Ventotene		Submarine-emergent stratovolcano		Effusive/explosive	Shoshonitic		200 - >900	Perrotta *et al.* 1996
Ischia		Emergent stratovolcano		Explosive/effusive	Shoshonitic		historical (1302 C.E.) - >55	Acocella,Funiciello 1999 Orsi *et al.*, 1991, 1996
Campi Flegrei-Procida		Alkaline ignimbrite shield and caldera complex		Explosive	Shoshonitic	>600	historical (1538 C.E.) - > 47	Cole and Scarpati 1993 Fisher *et al.*, 1993 Rosi *et al.*, 1996 Wholetz *et al.*, 1996 Piochi, *et al.* 2004
Vesuvio-Somma	Vesuvio	Stratovolcano		Effusive/explosive	Leucititic Shoshonitic	100	Historical (1944 C.E.) - 17	Sigurdsson *et al.*, 1985 Santacroce 1987 De Vivo *et al.*, 2003
	Somma						>17 - >35	
Vulture	Monticchio	Monogenetic maar, tuff ring, lavas	Monticchio	Phreatomagmatic/effusive	Carbonatitic Na-alkali basalts	?	141-132	De Fino *et al.*, 1986 Melluso *et al.*, 1996 Beccaluva *et al.*, 2002 De Astis *et al.*, 2006 Buettner *et al.*, 2006 D'Orazio *et al.*, 2007, 2008
	Monte Vulture	Stratovolcano	Monte Vulture	Effusive/esplosive	Haüyne-bearing leucititic		540 - 740	

The Mt. Amiata volcano, which is the northernmost Pleistocene volcanoes of this belt (Fig. 11), is somewhat intriguing. For long time it was thought to belong to the Tuscan Magmatic Province (e.g., Marinelli, 1961; Peccerillo *et al.*, 1987; Innocenti *et al.*, 1992; Peccerillo, 2005a), but a series of petrologic and geochemical evidence related the triggering of the Mt. Amiata volcanic activity to the arrival of leucite-bearing Roman magmas at shallow level (van Bergen *et al.*, 1983; Conticelli *et al.*, 2010c).

Figure 35. Nd-Sr isotopic variations for the Western Alps, Western Tyrrhenian Sea (Corsica) and Tuscan Magmatic provinces.

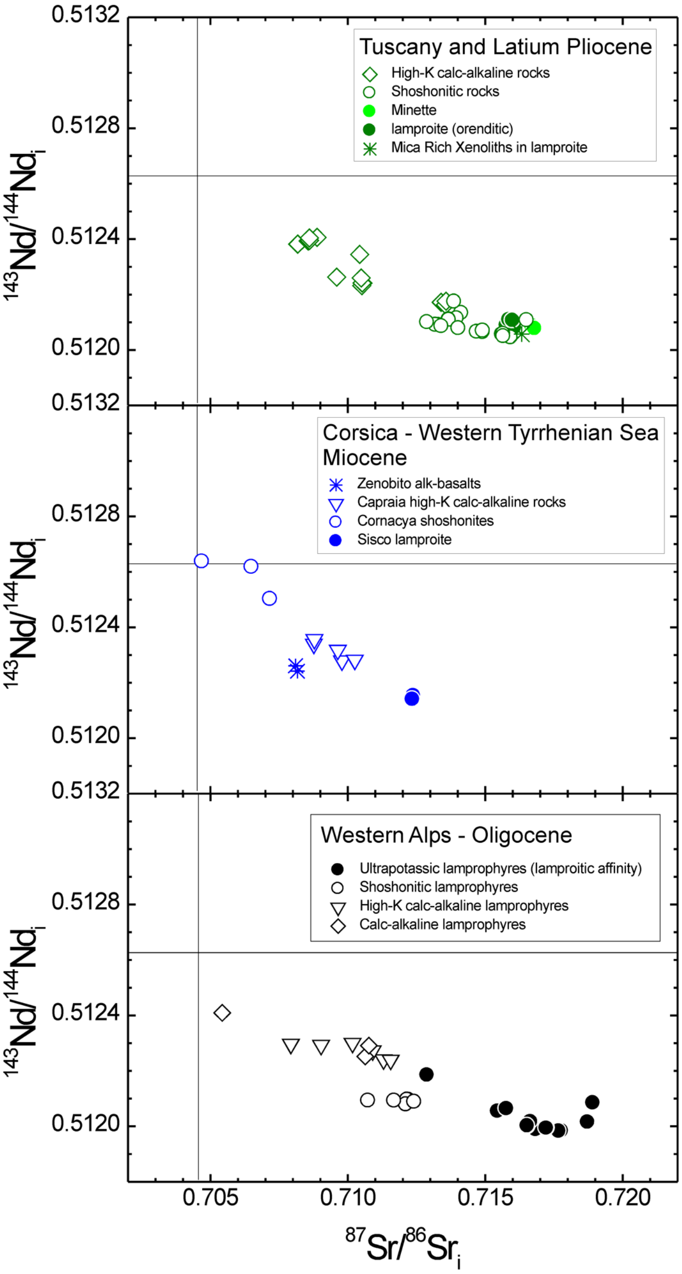

Data from Venturelli *et al.* (1984), Peccerillo *et al.* (1988), Pinarelli (1991), Conticelli *et al.* (1992, 2002, 2007, 2009a, 2010c, 2010d), Conticelli (1998), Cadeaux *et al.* (2005), Peccerillo & Martinotti (2006), Owen (2007), Prelevic *et al.* (2008), Avanzinelli *et al.* (2008).

Uprising silica-undersaturated magmas, potentially leucite-bearing, have been intercepted by long-living magma chamber filled by silica-saturated and extremely differentiated shoshonitic to calc-alkaline magmas of the Tuscan province. The interaction between the two magmas brought the extrusion of highly viscous crystal-rich Tuscan magmas together with mingled Roman magmas in which crystallization of leucite was suppressed by the interaction process with the high silica magmas (Conticelli *et al.*, 2010c). This explains the very recent time of extrusion, which is clearly associated with the Roman Magmatic Province volcanism, but also the high aspect ratios of lava flows and the exogenous dome formation (Ferrari *et al.*, 1996). A characteristic that has been never recorded in the volcanoes of the Roman Province, but recalling the Pliocene magmatism related with the Tuscan magmas such as the Tolfa-Manziana-Ceriti dome complexes and the Monte Cimino Volcanic complex.

Sr, Nd and Pb Isotopes

Italian ultrapotassic rocks and associated shoshonites, high-K calc-alkaline and calc-alkaline igneous rocks have extremely variable radiogenic isotope compositions (e.g., Tables 2-8), displaying a geographic variation firstly from West to East and later from North-West to South-West (see fig. 10 in Conticelli *et al.*, 2007).

The observed isotope variation covers almost the entire spectrum of mantle and upper crustal values, complicating the interpretation of the petrogenetic grid of Italian ultrapotassic and associated shoshonites and calc-alkaline rocks (e.g., Hawkesworth & Vollmer, 1979; Vollmer & Hawkesworth, 1981; Vollmer, 1989; Conticelli *et al.*, 2002, 2007; Gasperini *et al.*, 2002; Bell *et al.*, 2004; Martelli *et al.*, 2004; Peccerillo, 2004; Avanzinelli *et al.*, 2008).

$^{87}Sr/^{86}Sr_i$ values range from 0.70522 for a basanite at Monte Vulture Volcano (Avanzinelli *et al.*, 2008) to 0.71883 for the Rio Rechantez minette in the Western Alps Oligocene province (Owen, 2008); $^{143}Nd/^{144}Nd_i$ values range from 0.512712 for a basanite at Monte Vulture Volcano (D'Orazio *et al.*, 2007) to 0.511991 for the Rio Rechantez minette in the Western Alps Oligocene province (Prelevic *et al.*, 2008; Conticelli *et al.*, 2009a).

Initial $^{143}Nd/^{144}Nd$ values show a strong negative correlation with initial $^{87}Sr/^{86}Sr$ (Figs. 35, 36, and 37), although a decoupling of the correlation is observed between leucite-bearing and leucite-free trends (i.e., Conticelli *et al.*, 2002). The most primitive rocks of each magmatic province define trends with isotopic values that vary regularly passing from ultrapotassic mafic terms to calc-alkaline ones through shoshonites (Figs. 35 and 36), with the former having the most crust-like values. A strong correlation between isotopic values and the abundances of K, Rb, Sr, Ba and most incompatible trace elements is present (Cox *et al.*, 1976; Conticelli *et al.*, 2009a).

Figure 36. Nd-Sr isotopic variations for the Amiata Volcano, Roman and Lucanian Magmatic provinces.

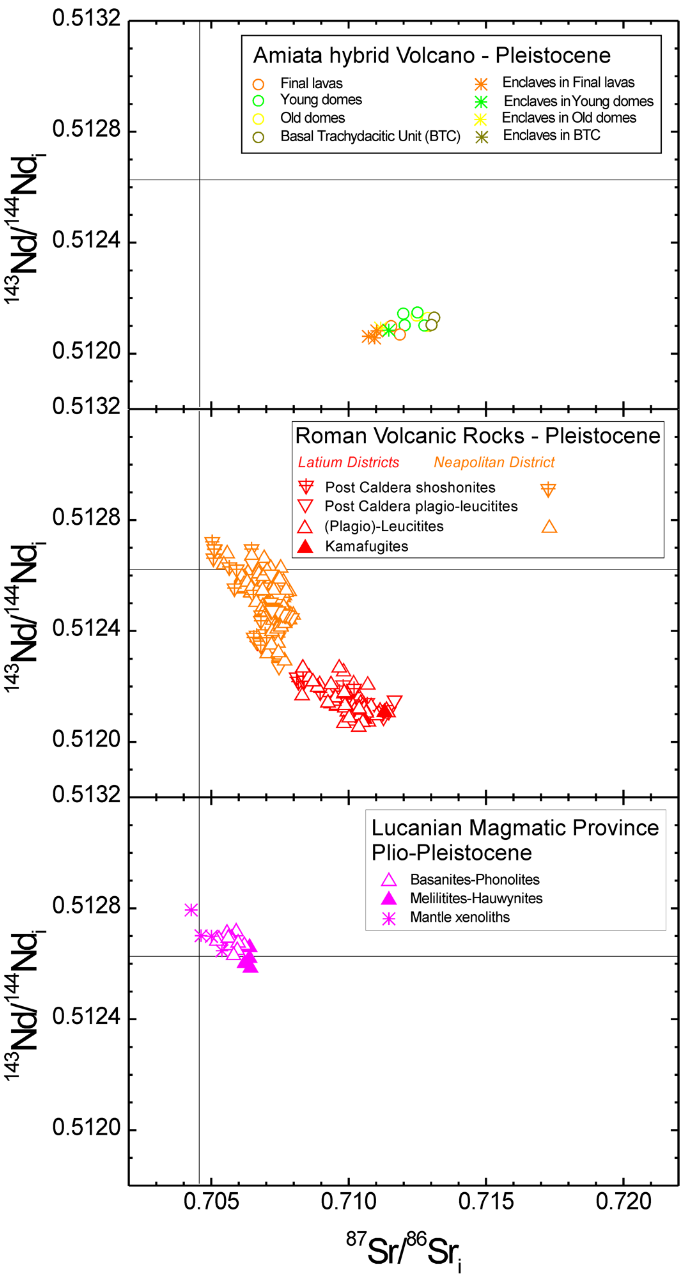

Data from Conticelli *et al.* (1987, 1991, 1997, 2002, 2007, 2009b), Ayuso *et al.* (1998), Pappalardo *et al.* (1999, 2002), D'Antonio *et al.* (1999b), Perini *et al.* (2000, 2003, 2004), Downes *et al.* (2002), Gasperini *et al.* (2002), De Astis *et al.* (2006), Di Rienzo *et al.* (2007), D'Orazio *et al.* (2007, 2008), Avanzinelli *et al.* (2008, 2010), Boari *et al.* (2009a,b), Conticelli's unpublished data; Melluso's unpublished data; Tommasini's unpublished data.

Within the Roman Magmatic Province two different sectors can be distinguished based on radiogenic isotopes: the rocks from the districts of the northern sector (i.e., Latian districts: Vulsini, Vico, Sabatini, Colli Albani, Middle Latin Valley, and Roccamonfina; Figs. 1 and 11) show higher $^{87}Sr/^{86}Sr_i$ and lower $^{143}Nd/^{144}Nd_i$ values relatively to the rocks of the Neapolitan district (Fig. 37), the southernmost cluster of volcanic apparata (Figs. 1 and 11). Post-caldera shoshonites and sub-alkaline rocks of the southernmost Latian district (i.e., Roccamonfina volcanoes) show intermediate values between Latian and Neapolitan rocks (Fig. 37).

Figure 37. Nd-Sr isotopic variations for the Roman Magmatic Provinces with fields for each single district.

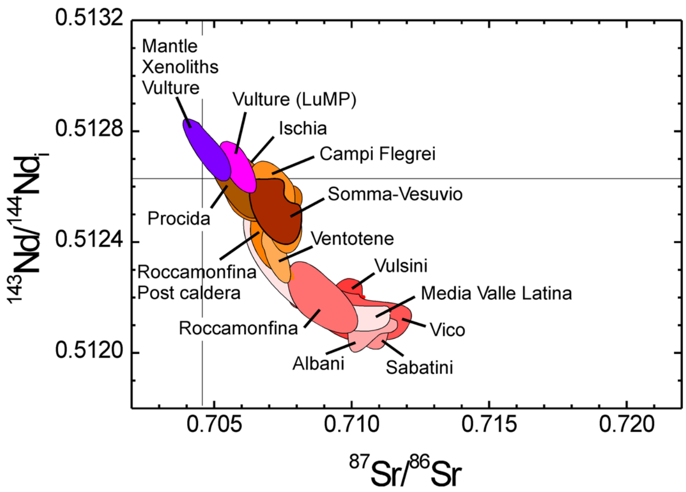

Data from Conticelli *et al.* (1987, 1991, 1997, 2002, 2007, 2009b), Ayuso *et al.* (1998), Pappalardo *et al.* (1999, 2002), D'Antonio *et al.* (1999b), Perini *et al.* (2000, 2003, 2004), Gasperini *et al.* (2002), Di Rienzo *et al.* (2007), Avanzinelli *et al.* (2008), Boari *et al.* (2009a,b), Tommasini's unpublished data.

The same geographic variation can be onserved in Pb, Hf, and He isotopes. Lead isotopes display single correlation trends for each magmatic province with the ultrapotassic terms, either leucite-bearing or –free, at the most radiogenic end. Each trend runs parallel to the other ones (e.g., Conticelli *et al.*, 2009b; Boari *et al.*, 2009b) (Fig. 38); the trend of Western Alps Oligocene magmatic province lies at the lowest $^{206}Pb/^{204}Pb_i$ values whilst that of the Lucanian Magmatic Province at the highest (Fig. 38).

Figure 38. $^{87}Sr/^{86}Sr_i$, $^{143}Nd/^{144}Nd_i$, and $^{208}Pb/^{204}Pb_i$ vs. $^{206}Pb/^{204}Pb_i$ for the Italian ultrapotassic rocks.

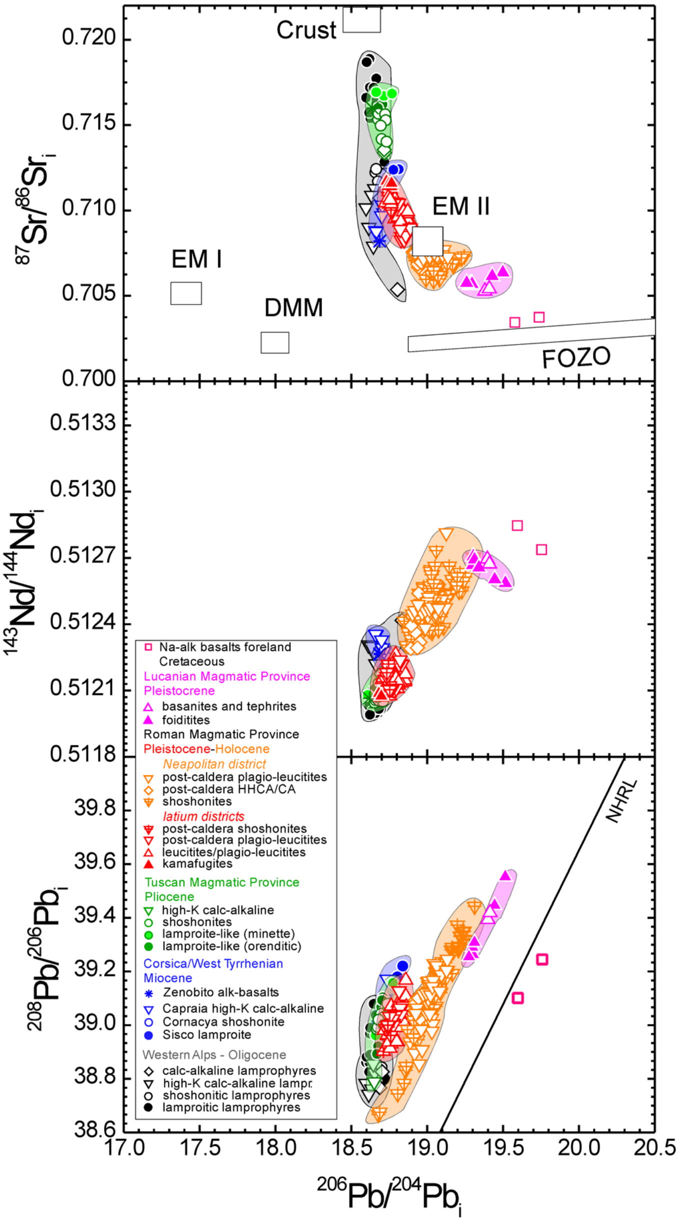

Data from Conticelli *et al.* (1987, 1991, 1997, 2002, 2007, 2009a, 2009b, 2010c, 2010d), Ayuso *et al.* (1998), Conticelli (1998), Pappalardo *et al.* (1999, 2002), D'Antonio *et al.* (1999b), Perini *et al.* (2000, 2003, 2004), Downes *et al.* (2002), Cadeaux *et al.* (2005), De Astis *et al.* (2006), Peccerillo & Martinotti (2006), Di Rienzo *et al.* (2007), D'Orazio *et al.* (2007, 2008), Owen (2007), Prelevic *et al.* (2008), Stoppa *et al.* (2008), Avanzinelli *et al.* (2008, 2010), Boari *et al.* (2009a,b), Cadeaux & Pinti (2009), Melluso's unpublished data; Tommasini's unpublished data.

The volcanic rocks of the of the Westrern Tyrrhenian Sea Magmatic Province (Corsican) represent an exception to the observed array of lead isotopes versus those of Strontium and Neodimium. Indeed the Corsican rocks depict opposite trends to those observed in the other magmatic provinces. Zenobito alkali basalts plot as an offset with respect to the Italian array (Fig. 38) toward the isotopic composition of Late/Middle Miocene-Quaternary volcanic rocks of Sardinia, and in general toward a depleted mantle source (e.g., Avanzinelli *et al.*, 2009, and references therein). Bell *et al.* (2004) argued that the general trend of the Italian rocks points toward a FOZO component in the $^{87}Sr/^{86}Sr_i$ vs. $^{206}Pb/^{204}Pb_i$ diagram (Fig. 38). Indeed, as a whole, Italian rocks fill the gap between upper crustal composition and FOZO (Hart *et al.*, 1992) passing through the isotopic composition of EM II end-member (Zindler & Hart, 1986), which is believed to represent a recycled sedimentary component. In figure 38 most of Italian potassic and ultrapotassic products plot between upper crustal composition and EM II with the most ultrapotassic compositions (i.e., lamproite, kamafugite and leucitite) closest to thye upper crustal composition. FOZO isotope compositions are only approached by volcanic rocks from magmatic suites south of the 41st parallel, which also points toward the isotope composition of anorogenic cretaceous alkali basalts occurring on the Apulian foreland (Fig. 38). A less-depleted asthenospheric mantle source has been proposed for the southernmost sector of Italian magmatism (e.g., Beccaluva *et al.*, 1991; Avanzinelli *et al.*, 2009). Similar isotopic compositions are also reported for calc-alkaline rocks from the Aeolian Arc (e.g., Francalanci *et al.*, 1993, 2007; Peccerillo, 2001, 2005a; Tommasini *et al.*, 2007).

Evidence for a strongly anomalously enriched upper mantle for the source of ultrapotassic magmas is also highlighted by the values of $^{176}Hf/^{177}Hf_i$ (Fig. 39), which vary from values typical of lamproitic magmatism (e.g., Prelevic *et al.*, 2010) to values similar to astenospheric mantle reservoir in the region below the 41st parallel (i.e. Neapolitan district). Indeed, eHf$_T$ values are as low as -13 in lamproitic rocks from Western Alps, Western Tyrrhenian Sea, and Tuscany (Prelevic *et al.*, 2010) increasing to values between -9 and -7 in shoshonitic rocks associated to lamproites (Gasperini *et al.*, 2002; Prelevic *et al.*, 2010), and between -8.1 and -6.2 in the leucite bearing rocks of the Latian districts of the Roman province (Gasperini *et al.*, 2002), up to values of -0.5 and -0.2 for the rocks of the Neapolitan district (Gasperini *et al.*, 2002; Tommasini's unpublished data). A strong negative correlation between $^{176}Hf/^{177}Hf_i$ and $^{87}Sr/^{86}Sr_i$ reinforce the hypothesis of the recycling of an upper crustal component in the mantle source of the ultrapotassic Italian magmas (e.g., Gasperini *et al.*, 2002; Prelevic *et al.*, 2010).

Figure 39. $^{176}Hf/^{177}Hf_i$ vs. $^{87}Sr/^{86}Sr_i$ for the Italian ultrapotassic rocks.

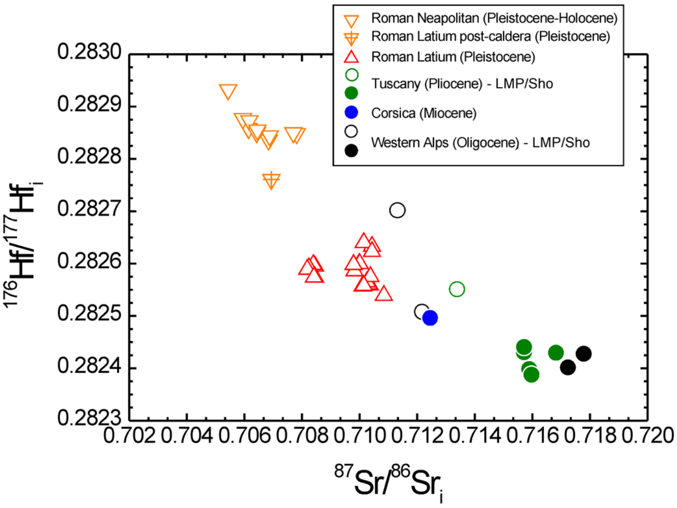

Data from Gasperini *et al.* (2002), Prelevic *et al.* (2010), Tommasini's unpublished data.

He isotopes performed on fluid inclusions within olivine and clinopyroxene crystals from rocks of the Tuscan and Roman magmatic provinces (Martelli *et al.*, 2004) add further constraints on the nature of the mantle sources of these magmas. $^{3}He/^{4}He$ values are significantly lower than MORB and display a negative correlation with $^{87}Sr/^{86}Sr$ (measured either on whole rocks or clinopyroxene crystals). Martelli *et al.* (2004) suggested the occurrence of a binary mixing between an asthenospheric component, similar to an HIMU ocean island basalt, and an enriched in radiogenic isotopes upper mantle component, metasomatised with recycled sediments.

Recycled sediments within the upper mantle source of ultrapotassic magmas has been also pointed out on the basis of $^{187}Os/^{188}Os_i$ vs. $^{87}Sr/^{86}Sr_i$ values (Fig. 40). Indeed, significant amounts of recycled crustal material (up to 65% for the most enriched lamproites of the Tuscan Magmatic Province) within the upper mantle source are required for the genesis of ultrapotassic lamproitic and kamafugitic magmas (Conticelli *et al.*, 2007).

Figure 40. $^{187}Os/^{188}Os_i$ vs. $^{87}Sr/^{86}Sr_i$ for the Italian ultrapotassic rocks.

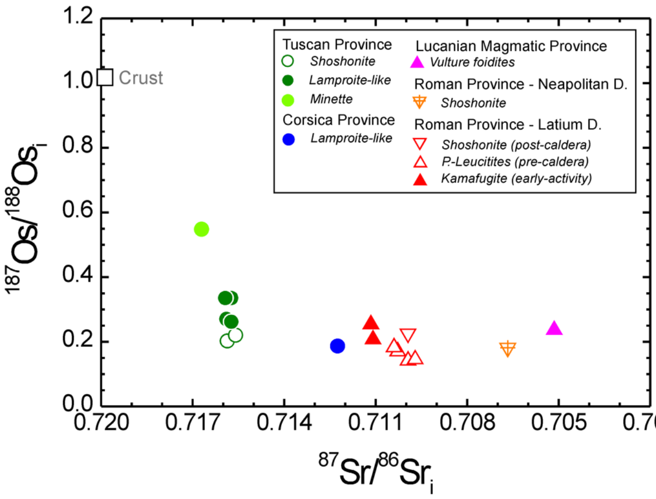

Data from Conticelli *et al.* (2007).

Origin of the Italian Magmatism

The origin of Italian potassic and ultrapotassic rocks and of their peculiar trace elements and isotopic signatures were the object of a scientific debate centered on two main possible mechanisms: a) within-plate origin, possibly linked to partial melting of an up-rising mantle plume (e.g., Vollmer & Hawkesworth, 1981; Vollmer, 1990; Ayuso *et al.*, 1998; Castorina *et al.*, 2000; Gasperini *et al.*, 2002; Bell *et al.*, 2004); b) orogenic to post-orogenic origin, related to partial melting of the sub-continental lithospheric metasomatised mantle at a destructive plate margin, with important contributions from recycled sediments (e.g., Cox *et al.*, 1976; Peccerillo, 1985, 2005a; Rogers *et al.*, 1986; Beccaluva *et al.*, 1991; Conticelli & Peccerillo, 1992; Downes *et al.*, 2002; Bianchini *et al.*, 2008).

Some of the authors suggesting the within-plate origin also point out the need for an increasing influence of an upper crustal geochemical component northward, although no convincing reasons have been provided to explain it in the frame of a within-plate, extensional geodynamic setting (e.g., Hawkesworth & Vollmer, 1979; Vollmer, 1990; Gasperini *et al.*, 2002; Bell *et al.*, 2004). In the anorogenic 'plume-related' model the crustal signature is generally attributed to shallow level magma contamination processes. The high extent of shallow level crustal contamination required to reproduce the Italian ultrapotassic magmas (> 70 vol. % to gives the lamproitic isotopic signatures) seems unlikely to occur at shallow level without suffering extensive crystallization of mafic phases. This would have decisely decreased the MgO, Ni, and Cr contents of the mafic rocks bringing them on the differentiated felsic side (Conticelli, 1998; Turner *et al.*, 1999; Murphy *et al.*, 2002). On the contrary, the most ultrapotassic rocks from each magmatic province (i.e. lamproites, kamafugites and lucitites), which also display the highest crustal signature, are the ones bearing the highest abundances in MgO and compatible trace elements (Tables 2-8). In addition these rocks have liquidus highly forsteritic olivine, which does show textural characteristics typical of extra olivine from cumulus processes. In addition, a proportion of assimilated crust higher than 40 vol. % would rapidly freeze the magma, stalling its ascent and causing it to crystallise completely. In summary, even a small amount of crustal contamination would result in rapid crystallization and fractionation of mafic minerals. MgO, FeO, Ni, Sc, and Cr contents would dramatic decrease in the contaminated magma with no further enrichment in K_2O (Conticelli, 1998; Turner *et al.*, 1999; Murphy *et al.*, 2002).

Avanzinelli *et al.* (2008) recently reported a comprehensive study of U-Th disequilibria on the youngest Italian rocks with the aim of investigating the mechanism of source melting. The authors excluded the possibility of the plume-related genesis, in particular of a plume upwelling from a slab window located under the Neapolitan area, on the strength of significant ^{238}U-excess measured in the volcanic rocks of the Neapolitan district of the Roman Province. In fact, ^{238}U-excess is widely accepted as one of the key evidence of subduction-related magma genesis (e.g., Elliott *et al.*, 1997; Hawkesworth *et al.*, 1997). The occurrence of such excesses only in Neapolitan rocks is ascribed to the recent addition of a U-rich fluid component, which is also expected to act as a trigger for magmatism. The lack of any significant disequilibria in the Latian districts (Roman Magmatic Province) and Amiata rocks (Tuscan Magmatic Province) is also inconsistent with adiabatic melting of a deep-seated mantle plume, which would produce significant ^{230}Th excesses (Avanzinelli *et al.*, 2008). On the other hand, significant ^{230}Th- excesses, an indicator of adiabatic melting, have only been measured in a sample from the Monticchio lakes volcanism, in the Lucanian Magmatic Province (Avanzinelli *et al.*, 2008, 2010).

Subduction-related metasomatism

The isotopic charateristics discussed above matches well with the incompatible trace element distributions ubiquitously shown by the volcanic rocks of each magmatic province. It is generally thought that fractionation of High Field Strength Elements (HFSE) with respect to Large Ion Lithophile Elements (LILE) is a typical characteristic beared by orogenic magmatic suites (e.g., Peccerillo, 1985; Hofmann, 1996, Hoefs, 2010) and that Pb peaks are generated by sediment recycling within the upper mantle (Avanzinelli *et al.*, 2008). The relative immobility in aqueous fluids of incompatible high field strength elements and Th with respect to large ion lithophile ones has long been used to distinguish between the roles of fluids and melts during metasomatism (e.g., Hawkesworth *et al.*, 1990; Keppler, 1996; Elliott *et al.*, 1997; Elliott, 2003; Kessel *et al.*, 2005). Conversely, the budget of other trace elements such as Th, is controlled in arc rocks by sediment recycling (e.g., Elliott *et al.*, 1997; Plank & Langmuir, 1998; Tommasini *et al.*, 2010). High Th concentrations, Th/Nb and Th/REE ratios in subduction-related volcanic rocks are interpreted as representative of recycled sediments. The comparison of these ratios with subducted sediments have suggested that the latter are recycled as melts (e.g., Elliott *et al.*, 1997; Hawkesworth *et al.*, 1997; Class *et al.*, 2000; Elliott, 2003; Plank, 2005) enriched in Th and incompatible trace elements, but still depleted in HFSE, probably due to the occurrence of residual rutile during sediment partial melting (e.g., Elliott *et al.*, 1997; Tommasini *et al.*, 2007).

At sub-arc temperatures and pressures the physical distinction between fluids and melts is lost above the 'second critical end point of saturation' (e.g., Kessel *et al.*, 2005; Hermann *et al.*, 2006) where they converge to a 'supercritical liquid', but 'fluid'-like and 'melt'-like liquids can still be distinguished using the relative proportion of H_2O and solute contents, depending upon the T°C of 'supercritical liquid' formation (e.g., Hermann *et al.*, 2006). Klimm *et al.* (2008) showed that the trace element budget of metasomatic agents released by the basaltic subducting crust at at 2.5 GPa, regardless of whether they are 'fluids' or 'supercritical liquids', depends upon the solubility of accessory phases such as allanite and monazite (controlling REE and Th and U) and rutile (determining the Ti and Nb contents). At normal slab/mantle interface temperatures these accessory phases are stabilised in the residuum during slab melting, strongly sequestering REE, Th, (in allanite and/or monazite) and Ti and Nb (in rutile) from the metasomatic liquids. The resulting metasomatic liquid is enriched only in the elements not hosted in the residual accessory phases (Cs, Rb, Ba, K, Pb, Sr and U over Th), perfectly reflecting the widely accepted composition of the slab derived aqueous ‘fluids’. With increasing temperature or/and pressure the metasomatic liquids incorporate higher amounts of solutes (i.e. ‘melts’), and the solubility of allanite, monazite and rutile increases until they are eventually eliminated from the residue with Th, and REE released into the melts (Hermann, 2002; Kessel *et al.*, 2005; Klimm *et al.*, 2008). However, until over-saturated, allanite and rutile will completely control the REE, Th, U (allanite) and Ti, Nb (rutile) content of the sedimentary ‘melts’. Similar conclusions have been reached by Skora & Blundy (2010) starting from radiolarian clay-rich sediments.

Allanite and monazite have partition coefficients for LREE and Th extremely higher than those for heavy REE (HREE) and U; thus allanite-saturated ‘melts’ from recycled pelitic sediments would have lower LREE/HREE and higher U/Th than their sedimentary protolith. On the contrary if temperatures are high enough keep the metasomatic liquids undersaturated in such minerals, then the Th, U and REE can be released in the liquids and their trace elements contents and ratios would be dependent on other mineral phases. The high Th/U and LREE/HREE of most Italian rocks (with the exception of the Neapolitan district) suggest that the dominant metasomatic agent is a ‘melt’ generated at temperatures where rutile was stable is still rutile-saturated, hence the HFSE depletion, but allanite and monazite were not, hence the high Th/U (Avanzinelli *et al.*, 2009). In this frame the high LREE/HREE of most of Italian ultrapotassic and associated shoshonitic rocks (Figs. 8, 10, 12, 14, 16, 24, 26, and 28) has been ascribed to the critical role of garnet during sediment melting (Avanzinelli *et al.*, 2008). This is consistent with the high amount of residual garnet observed during experiments of melting of both basaltic (Kessel *et al.*, 2005) and pelitic or carbonate rich (Kerrick & Connolly, 2005) sediments. The possibility of acquiring the garnet signature during by deep melting in the garnet stability filed (i.e. metasomatised mantle source deep enough to stabilise garnet) was ruled out by Avanzinelli *et al.* (2009) on the basis of the lack ^{230}Th excess (see also Asmerom, 1999).

Figure 41. Ba/Th vs. Th/Nb for the Italian ultrapotassic rocks.

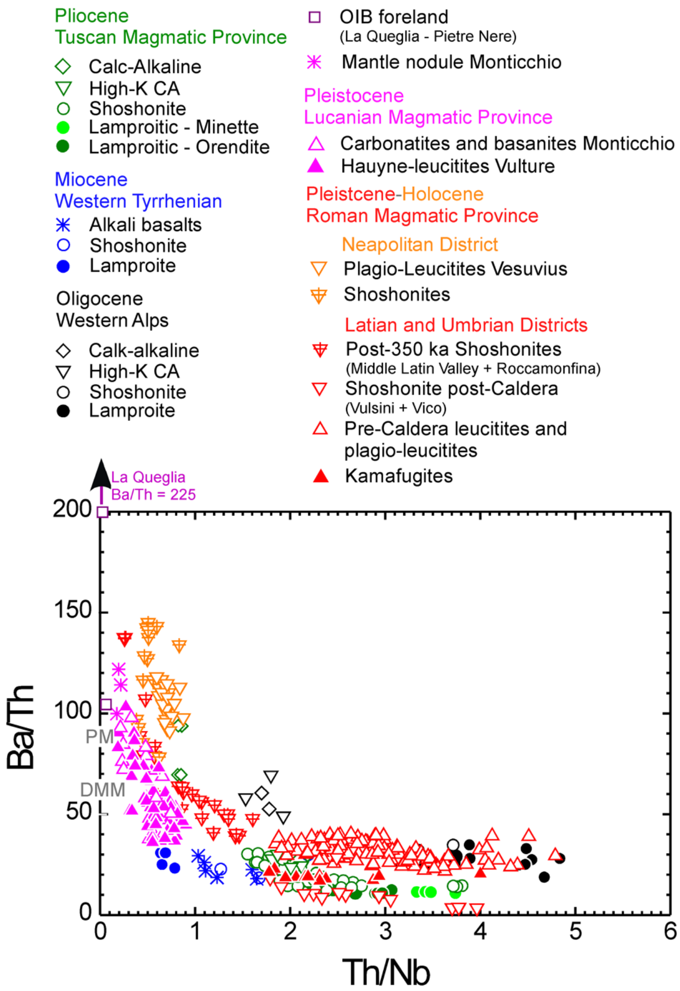

Plotted rocks with MgO > 4.5 wt. %. Data from Conticelli *et al.* (1987, 1991, 1997, 2002, 2007, 2009a, 2009b, 2010c, 2010d), Ayuso *et al.* (1998), Conticelli (1998), Pappalardo *et al.* (1999, 2002), D’Antonio *et al.* (1999b), Perini *et al.* (2000, 2003, 2004), Downes *et al.* (2002), Cadeaux *et al.* (2005), De Astis *et al.* (2006), Peccerillo & Martinotti (2006), Di Rienzo *et al.* (2007), D’Orazio *et al.* (2007, 2008), Owen (2007), Prelevic *et al.* (2008), Stoppa *et al.* (2008), Avanzinelli *et al.* (2008, 2010), Boari *et al.* (2009a,b), Cadeaux & Pinti (2009), Melluso’s unpublished data; Tommasini’s unpublished data.

The dominiant role of sediment derived ‘melts’ does not exclude the involvement of ‘fluids’ generated at lower temperature, but simply dimishes their possible effect on the final composition of the metasomatised mantle source, given their smaller ability of carrying trace elements with respect to ‘melts’ (Hermann *et al.*, 2006). In fact a widespread fluid-like component might have permeated the mantle source of Italian magmas in a more pervasive way than the melt-like metasomatism that generates the most enriched ultrapotassic products (see later discussion section).

The role of metasomatic 'fluids' vs. 'melts' is evident in a Ba/Th vs Th/Nb plot (Fig. 41). Negative correlation is ubiquitous, but the various magmatic provinces define different trends. The widest range is shown by the volcanic rock of the Roman Magmatic Province, where a decrese in Th/Nb, coupled with increasing Ba/Th, is evident passing from the oldest and northernmost districts (i.e. Latian districts) to the youngest and southernmost one, which is the Neapolitan district. Leucite-free (i.e., shoshonite) volcanic rocks from the post-caldera and the most recent periods of the Roccamonfina and Middle Latin Valley volcanoes, the two southermost of the Latian districts of the Roman Province (above the 41st parallel; Figs. 1 and 11), show Th/Nb vs Ba/Th values that ideally fill the gap. The occurrence of significant ^{238}U-excess in volcanic rocks from the Neapolitan distric (Avanzinelli *et al.*, 2008) confirms a major role for a young (few ka, see Avanzinelli *et al.*, 2008) fluid-like metasomatic component (i.e. allanite/monazite saturated); the position of the youngest products of Roccamonfina and Middle latin valley in Fig. 40, along with their vicinity in space and time with the Neapolitan districts might indicate a role for such a fluid component also in these magmas.

An increase of Ba/Th is also observed passing from ultrapotassic rocks (lamproites and minettes) to associated shoshonites and high-K calc-alkaline rocks within the products of the Tuscan Magmatic Province and Western Alps). As discussed above, this might suggest the presence of a pervasive fluid related metasomatism which is overshadowed by the recycled sediment melt component which dominates the geochemical composition of the most enriched magmas (see next section). The opposite occurs in the Western Tyrrhenian (i.e. Crosica province). Ultrapotassic magmas from Sisco (Corsica) display low Th/Nb and Ba/Th values (Fig. 41), with the latter even lower than upper mantle values (PM = 82.2, DMM = 48-60; Wood, 1979; Sun & McDonough, 1989), with little HFSE/LILE fractionation and lack of Pb peak (Fig. 10c). These characteristics suggest that the orogenic component in Corsica was significantly different than that responsible for the other provinces, less important or possibly even absent (Avanzinelli, 2009; Conticelli *et al.*, 2009a, 2010c).

In summary Italian ultrapotassic rocks, both leucite-free and –bearing, with the exclusion of the Sisco one (Corsica), were generated in a lithospheric upper mantle enriched in K and incompatible elements by pelitic sediments recycled mostly as 'melts' (e.g., Conticelli *et al.*, 2007, 2009a; Avanzinelli *et al.*, 2008, 2009).

Further issue to be addressed are: i) the time-related and geographic transition from Tuscan lamproite-like ultrapotassic magmas (silica-saturated, leucite-free) to Roman kamafugitic/leucititic-type ones (silica-understaurated, leucite-bearing); ii) the temporal and geochemical sequence from ultrapotassic products to shoshonites and high-K calc-alkaline rocks within each magmatic province.

Transition from leucite-free to leucite-bearing ultrapotassic rocks in the Italian peninsula

The shift from silica-saturated to silica-undersaturated (i.e., from leucite-free to leucite-bearing) ultrapotassic magmas with time is not only a compositional characteristic that controls the final mineralogical assemblages of the volcanic rocks, but it also seems to have a link with the rate of ultrapotassic magma production. Indeed in the Western Alps, Western Tyrrhenian Sea, and Tuscan Magmatic Provinces ultrapotassic rocks are strongly subordinate to shoshonitic mafic rocks and their derivative magmatic terms, whereas in the Roman Magmatic Province leucite-bearing ultrapotassic magmas dominate volumetrically over final shoshonites, which are confined to final stage activity and do not occur in all volcanic districts.

Silica-saturated lamproitic ultrapotassic magmas (leucite-free) are generated within a metasomatised lithospheric refractory upper mantle through incongruent melting of a phlogopite-bearing harzburgitic source under excess of H_2O, then low X_{CO2} (Foley, 1994). Experimental studies have shown that silica-rich lamproitic magmas are generated in a lithospheric mantle source originally depleted in the basaltic component and subsequently refertilised by metasomatism in a phlogopite-orthopyroxene-olivine paragenesis (e.g., Arima & Edgar, 1983a; Edgar, 1987; Foley, 1992b, 1994). Interaction with granitic melts from pelitic sediments is capable to stabilize modal phlogopite in a peridotitic mantle wedge (Sekine & Willie, 1982a, b, 1983; Wyllie & Sekine, 1982). Such metasomatic enrichment through melts from recycled pelitic sediments is also able to explain the higher Al_2O_3 content of ultrapotassic Italian magmatic rocks with respect to within-plate ones. Conticelli *et al.* (2007) have modelled for the source of Tuscan lamproite, the amount of recycled crustal component needed to produce the observed Sr, Nd, Pb, and Os isotopic characteristics (Fig. 40). These authors have estimated about 65 vol. % of a crustal-derived component, introduced as melts within the lithospheric depleted mantle. The partial melting of pelitic sediments at relatively high-pressure, within the stability field of garnet for pelitic sediments, following the model of Johnson & Plank (1999) gives a melt consistently enriched in SiO_2, Al_2O_3, and K_2O, and depleted in MgO, and FeO, but with an mg-# within the range of 0.85 and 0.80. The composition of this mixture is compatible with a mineralogy dominated by phlogopite/K-feldspar, with minor orthopyroxene and olivine, and possibly no clinopyroxene, as also shown by melting experiments on lamproitic rocks (e.g., Edgar, 1987; Foley, 1994, and references therein). Such a high proportion of metasomatic component is unrealistic to have pervasively patently modified the entire mantle wedge, but this might just represents the core of a peridotite-modified veinlet (Foley, 1992b). Indeed "melts" flowing through the lithospheric peridotite react with the wallrock and then freezing down in a newly formed metasomatized paragenesis, with most of the surrounding mantle unaffected by this reaction (Foley, 1992b; Perini *et al.*, 2004; Conticelli *et al.* 2007; Avanzinelli *et al.*, 2009). Then upper mantle will only be metasomatised along the main melt pathways thus generating a network of metasomatised veins surrounded by unreacted mantle (e.g., Suen & Frey, 1987; Menzies *et al.*, 1991; Foley 1992b).

Silica-undersaturated kamafugitic to leucititic ultrapotassic magmas (leucite-bearing) are conversely generated in a metasomatised upper mantle by partial melting of a phlogopite-bearing wherlite controlled by a CO_2 excess with respect to H_2O, then high X_{CO2} (e.g., Lloyd *et al.*, 1985; Edgar, 1987 and references thereins). Considering that the mantle beneath the Italian region is particularly depleted in the basaltic component (prior to metasomatism) as evidenced by the major and trace element contents of most primitive ultrapotassic magmas (e.g., lamproites, kamafugites and leucitites) and their olivine-spinel pairs compositions (Conticelli *et al.*, 2007, and references therein), a refertilization to produce a sub-lithospheric mantle source with modal clinopyroxene and phlogopite is needed (e.g., Edgar *et al.*, 1980; Arima & Edgar, 1983a; Lloyd *et al.*, 1985; Edgar, 1987 and refences thereins). Thus CaO-enrichment is required beside K and incompatible elements, as well as a source for CO_2. Such enriching agent might be consistent with the addition of $CaCO_3$ from the recycled sediments (Thomsen & Schmidt, 2008a; Franzolin *et al.*, 2009; Poli *et al.*, 2009). Reaction of such agent with depleted peridotite generates a re-fertilised phlogopite-bearing wehrlite or phlogopite-bearing lherzolite, with phlogopite and clinopyroxene formed at expenses of olivine and orthopyroxene within the metasomatised vein network. Partial melting of such metasomatised veins at relatively low pressure and high X_{CO2} is able to produce strongly silica-undersaturated ultrapotassic magmas, from kamafugitic to leucititic in composition (e.g., Wendlandt & Eggler 1980a, b). Arguments for the genesis of Italian kamafugites through the melting of a re-fertilised sub-continental lithospheric mantle at low pressure and under high X_{CO2} have been shown experimentally (Conticelli *et al.*, 1989). In addition, evidence for the occurrence of CO_2-mantle degassing beneath the Italian peninsula has been shown on the basis of geophysical data by Frezzotti *et al.* (2009, 2010, this volume).

Such a scenario also agrees with the trace element and isotopic distribution of Roman kamafugites and leucitites. Indeed the shift from leucite-free to leucite-bearing ultrapotassic rocks in Italy has been related with differences in the initial composition of the recycled sediments on the basis of isotope and trace element compositions of mafic terms. Conticelli *et al.* (2002) suggested that the decoupling of Sr and Nd isotopes between Tuscan and Roman magmatic provinces (Figs. 36-37) was caused by the change of the recycled sediment from pelitic to marly. Avanzinelli *et al.* (2008) suggested a southward increase of the $CaCO_3$ sedimentary fraction related to the composition of the pelitic sediment cropping out along the Apennine chain. Avanzinelli *et al.* (2009) suggested an increasing carbonate-rich sedimentary component on the basis of $^{87}Sr/^{86}Sr_i$ and trace element variations observed along the Italian peninsula. Indeed a negative correlation of $^{87}Sr/^{86}Sr_i$ vs. Sr/Ce and Sr/Rb is observed (Fig. 42) and it can also explain the disappearance of the negative Sr anomaly passing from mafic ultrapotassic rocks of Western Alps and Tuscan Magmatic Provinces to Roman mafic rocks (Figs. 8, 10, 12 vs. Figs 16, 18, 20, 22, 24, etc.). Sr and Ce are little fractionated when sediments are recycled as 'melts', although they are if the sediment is recycled as 'fluid'; Sr and Rb are both easily carried by fluids, but might be slightly fractionated during sediment or mantle melting. Therefore the combined use of Sr/Ce and Sr/Rb ratio should provide information about the original composition of the sediment end-member (i.e., carbonate- vs. clay-rich). In figure 42 the carbonate-rich component, characerised by high Sr/Ce and Sr/Rb, increases southward, with leucite-free rocks from the Tuscan Magmatic Province and Western alps plotting at low Sr/Rb and Sr/Ce close to the composition of clay-rich pelitic sediments. In the $^{87}Sr/^{86}Sr$ vs Sr/Ce diagram (Fig. 42) ultrapotassic rocks, from leucite-free lamproites to leucite-bearing kamafugites and plagio-leucitites, plot over and along the array connecting pelitic sediments to limestone. Rocks from the Lucanian Magmatic Province plot away from that array close to OIB-like compositions (Fig. 41). It is worth noting that Western Tyrrhenian (i.e. Corsica) rocks lie at mid way between Western Alps and Tuscan lamproites and the field of sedimentary compositions. Neapolitan district rocks and post-cladera shoshonites from Middle Latin valley and Roccamonfina also plot at lower $^{87}Sr/^{86}Sr$. This is consistent with the recent addition of a further component, as previously discussed to explain the increase of Ba and U contents in the same rocks (Fig. 41) and the ^{238}U-excess reported for the Neapolitan district (Avanzineli *et al.*, 2008).

Figure 42. Sr/Ce and Rb/Sr vs. $^{87}Sr/^{86}Sr_i$ for the Italian ultrapotassic rocks.

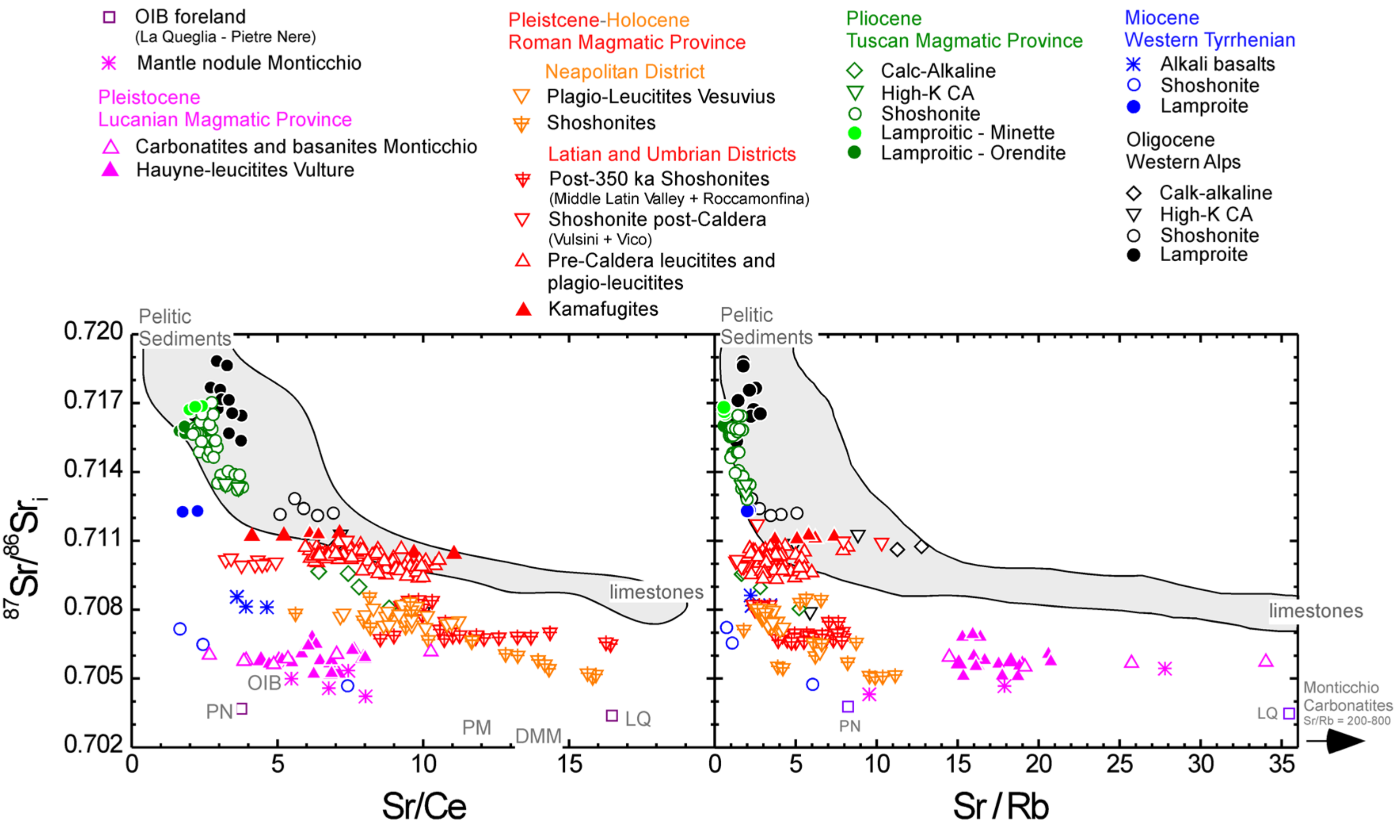

Plotted rocks with MgO > 4.5 wt. %. Data from Conticelli *et al.* (1987, 1991, 1997, 2002, 2007, 2009a, 2009b, 2010c, 2010d), Ayuso *et al.* (1998), Conticelli (1998), Pappalardo *et al.* (1999, 2002), D'Antonio *et al.* (1999b), Perini *et al.* (2000, 2003, 2004), Downes *et al.* (2002), Cadeaux *et al.* (2005), De Astis *et al.* (2006), Peccerillo & Martinotti (2006), Di Rienzo *et al.* (2007), D'Orazio *et al.* (2007, 2008), Owen (2007), Prelevic *et al.* (2008), Avanzinelli *et al.* (2008, 2010), Boari *et al.* (2009a,b), Cadeaux & Pinti (2009), Melluso's unpublished data; Tommasini's unpublished data.

The need for carbonate-rich sediment recycled as allanite-undersaturated melts in the source of the investigated magmas might provide some constraints on the condition of sediment melting. Carbonates are expected to behave as refractory phases at sub-arc depths (up to 180 km: Yaxley & Green 1994; Molina & Poli, 2000; Schmidt *et al.*, 2004). Recent experimental studies (Thomsen & Schmidt, 2008a, b; Poli *et al.*, 2009) have demonstrated that carbonate-saturated pelites (i.e. marls) might produce potassic granite or phonolite melts at temperatures from 900 °C, at 2.4 GPa, to 1070 °C, at 5.0 GPa. As already previously shown, when these melts are mixed with depleted mantle wedge they might represent suitable metasomatic agents for producing phlogopite-bearing wherlite/peridotite from which kamafugitic magma is produced by partial melting. Allanite and monazite solubility provides similar temperature constraints: in the same pressure range (2.5-4 GPa) the temperature required to exhaust allanite are >1000 °C (Hermann, 2002; Klimm *et al.*, 2008); admittedly this value could represent an over-estimate, given the doped composition of the experiments and the basaltic starting sediment composition; experiments on clay-rich sediments showed residual monazite up till 900°C (Skora & Blundy, 2010), whilst no studies are available for carbonate-rich sediment lithologies. The temperature range for sediment melting (900-1100°C) indicated by the geochemistry of the studied rocks is much higher than that estimated at the slab/mantle interface by thermal models of both ‘cold’ and ‘warm’ subduction (e.g., Peacock, 2003: Kelemen *et al.*, 2003). To explain this apparent inconsistency we suggest two possible scenarios; i) an increase in temperature of the slab/mantle interface due to locking of the subduction zone following continental collision; ii) the physical incorporation of portions of the subducted sediments from the top slab into the mantle, either by imbrication or via diapirs (e.g., Kelemen *et al.*, 2003; Klimm *et al.*, 2008), and their melting in the hot central region of the mantle wedge.

It is worth to note, however, that a recent study by Tommasini *et al.* (2011) indicates a more complex mechanism for the metasomatic enrichment of the mantle-source of Mediterranean lamproitic magmas. These authors have found that a multiple metasomatism event is needed to constrain the extreme enrichment in K and concomitant fractionation of Th and Sm with respect to La. This emerges from a widespread positive Th/La vs Sm/La correlation found in Tethyan Realm lamproites (including those from TMP, Corsica and Western Alps discussed in this study) and associated shoshonitic rocks (Tommasini *et al.*, 2010; Conticelli *et al.*, 2010b), which is opposite to what observed in subduction related magmas worldwide (Plank, 2005).

From ultrapotassic to potassic and sub-alkaline volcanic rocks.

Western Mediterranean ultrapotassic rocks are intimately associated in space and time to shoshonite and in some cases to high-K calc-alkaline suites: this association occurs in the Western Alps, Tuscan and Roman Provinces (Central Italy), but also in Murcia-Almeria (south-eastern Spain), Macedonia, Serbia, Montenegro, and Turkey (e.g., Conticelli *et al.*, 2002, 2007, 2009a; Altherr *et al.*, 2004; Peccerillo, 2004, 2005a; Prelevic *et al.*, 2004, 2005; Avanzinelli *et al.*, 2009). In the Western Alps correlation with time is not clear, also because the analytical error is sometimes greater than the possible time elapsed from one series to the other one. The best evidence of this time-dependent geochemical variation can be observed in the Tuscan and Roman magmatic provinces. In most cases above a single plumbing system, stratigraphy and geochronology testify the succession from either lamproite- or kamafugite-like rocks, to shoshonites and high-K calc-alkaline rocks, through high-K shoshonites or leucitites (e.g., Perini *et al.*, 2004; Conticelli *et al.*, 2007, 2009a, 2009b, 2010d; Frezzotti *et al.*, 2007; Boari *et al.*, 2009b). The opposite is observed at Somma-Vesuvius volcano where plagio-leucititites follow shoshonitic volcanic rocks (Cioni *et al.*, 2008, and references therein), similarly to the succession observed at Stromboli volcano in the Aeolian Arc (e.g., Ellam *et al.*, 1988; Peccerillo, 2001, 2005a; Alagna & Peccerillo, 2010, this volume).

The geochemical transition between magmatic series differently enriched in K and incompatible trace elements (i.e. from ultrapotassic to shoshonites or vice versa) has received at least three explanations: i) relaxation of isotherm that intercepts the solidus of variably metasomatized upper mantle levels, with the most strongly metasomatized mantle at deepest level (Peccerillo, 2005a; Frezzotti *et al.*, 2007); ii) either increase or decrease with time of shallow level carbonate assimilation, the former claimed to explain the Somma-Vesuvius case (Iacono-Marziano *et al.*, 2007, 2008); iii) incremental partial melting of a manle source metasomatized in a veined network and dilution of the vein end-member by interaction with surrounding peridotitic country-rocks (e.g., Foley, 1992b; Conticelli *et al.*, 2002, 2007, 2009a; Perini *et al.*, 2004; Avanzinelli *et al.*, 2009; Boari *et al.*, 2009b).

The first hypothesis fails to explain why earlier magmas, formed at deeper levels, did not interact with uppermost metasomatised levels. In addition, all primitive mafic magmas independently from their K_2O contents seem to have been in equilibrium with a mantle source characterized by the same depletion prior to metasomatism (Conticelli *et al.*, 2007). In fact, differences in the mantle source residuality are not observed within the same plumbing system, but rather between Latian and Neapolitan districts. Therefore the sources of ultrapotassic and shoshonitic magmas should not be too distant from each other.

Recently Iacono Marziano *et al.* (2007, 2008) have called for strong involvement of sedimentary carbonate assimilation in the Italian rocks to justify the derivation of ultrapotassic leucite-bearing rocks from shoshonite. Such a possibility was firstly postulated by several authors in the early twentieth century (e.g., Daly, 1910; Rittmann, 1933) and later discounted by Savelli (1967). Iacono Marziano *et al.* (2007, 2008), on the basis of experimental data, justify the passage from shoshonite to either leucititic or plagioclase leucititic magmas through limestone assimilation plus clinopyroxene crystallisation. Conticelli *et al.* (2009b) tackled this issue focusing on leucite-free shoshonites and leucite–bearing plagio-leucitites from Roccamonfina volcano. The authors attempted modelling of AFC processes able to drive the composition of magmas at Roccamonfina volcano from the post-cadera shoshonites to the pre-caldera leucitites and plagioleucitites and vice versa: they demonstrated that AFC processes, although important for the chemical evolution within each magmatic series, could not be responsible for the trasition from ultrapotassic leucite-bearing magmas to leucite-free shoshonites or vice versa. In the specific case of Somma-Vesuvius further evidence against a major role for crustal contamination are reported by Del Moro *et al.* (2001).

As previously discussed extremely high contribution from recycled crustal material are required in order to generate the most extreme composition of Italian lamproites and kamafugites. It is unlikely for such a high proportion of metasomatic component to pervasively modify the entire mantle wedge, whilst it have been proposed that it might affect only localised portions of the mantle in a network of metasomatic veins (Foley, 1992b). Indeed “melts” flowing through finite path trhough the lithospheric peridotite, react with the surrounding wallrock, freezing down as a newly formed metasomatized paragenesis, leaving most of the surrounding mantle unaffected by this reaction (Foley, 1992b; Perini *et al.*, 2004). The vein hypothesis is also consistent with most of the metasomatized peridotites observed in nature (e.g., Rivalenti *et al.*, 1995, 2007; Zanetti *et al.*, 1999; Rampone *et al.*, 2010). In the veined model, the mantle source reacts differently during upward migration of the isotherms. Initially, partial melting will affect the portion of the mantle with the lowest liquidus temperature, which is the inner portion of the veins characterized by pure metasomatic mineralogy (Foley, 1992b, 1994). The temperature increase, due to post-orogenic isotthrerm re-equilibrium, triggers partial melting also of the surrounding mantle alolowing the interaction between vein and country rock, thus diluting the metasomatised component (Conticelli *et al.*, 2007). Incompatible trace element and isotopic variations observed for the Western Alps, Tuscan and Roman Magmatic Province, with the exception of the Neapolitan district, which requires an additional U-rich ‘fluid’ component (Avanzinelli *et al.*, 2008), can be explained in terms of mixing between a strongly alkaline component, either lamproite for Western Alps and Tuscany leucite-free rocks or kamafugite for Roman leucite-bearing ones, and a probably sub-alkaline end member (i.e., high-K calc-alkaline). Indeed, it has been argued that the surrounding lithospheric mantle bear itself a sub-alkaline composition, possibly due to a pervasive ‘fluid’-like metasomatism, similar to that of many arc magmas worldwide, as opposed to the localised ‘melt’ metasomatism that give raise to the vein network (Conticelli *et al.*, 2009b; Conticelli *et al.*, 2010b). Passing from lamproites to shoshonites and high-K calc-alkaline rocks, the influence of the vein budget (i.e. high Th/Nb, low Ba/Th) over the composition of the erupted magmas becomes less important in favour of that of the surrounding mantle (Fig. 41). The increase of Ba/Th toward the less enciched terms (i.e. shoshonite and high-k calc-alkaine) suggests indeed that the surrounding mantle has been itself affected by a ‘fluid’-like component enriched in Ba with respect to Th. This pervasive metasomatism can also facilitate melting of the lithospheric mantle surrounding the vein that was deemed as highly depleted by previous basaltic extraction on the base of major elements and olivine-spinel pairs and that would result otherwise refractory.

The process of diluting the vein contribution by involving increasing proportion of the surrounding lithospheric mantle during partial melting produces isotopic mixing trends, which are not distinguishable from simple mixing between two end-member magmas. However, simple magma mixing at shallow level, within the upper crusts has to be ruled out on petrographic grond, since most of the high-MgO rocks can be confidently considered to be very close to primary magmas compositions. Most of the rocks under consideration have olivine on the liquidus, with compositions in equilibrium with the bulk rock. The latter is considered to be the composition of the magma from which olivine crystallises. If magma mixing occurred at shallow levels, olivine would have begun to crystallise and mixing would have altered the composition of the magma driving it away from equilibrium with olivine.

A further possibility is represented by the recent arrival of a fluid-like metasomatic agent that overprinted the old metasomatic signature and trigger partial melting also in the surrounding mantle. This is likely to be the case under the Neapolitan District, where such arrival is testified by the ^{238}U-excesses (Avanzinelli *et al.*, 2008). In general this process should imprint a different geochemical and isotopic signature in the most recent sub-alkaline magmas (e.g., De Astis *et al.*, 2006; Boari *et al.*, 2009b; Conticelli *et al.*, 2009b).

Within-plate component

The presence of this component and its origin is potentially the essence of the debate about plume vs. subduction-related origin of circum-Tyrrhenian magmatism. Namely, primordial mantle normalised incompatible trace elements patterns of the potassic rocks from the Lucanian Magmatic Province are clearly different from those of the other provinces (Fig. 34c). Troughs at Ta, Nb, and Hf as well as LIL vs. HFS elements fractionations are strongly reduced, especially in the most recent products of the Monticchio lakes. Isotopic signature resembles that of within-plate magmas (Figs. 35, 36, and 37) with values close to those of the OIB enriched terms, although a lithospheric orogenic signature appers to be still present in some way (e.g., Downes *et al.*, 2002; De Astis *et al.*, 2006; D'Orazio *et al.*, 2007, 2008). Indeed, Lucanian Province volcanic rocks also display the most radiogenic Pb and Nd and the least radiogenic Sr isotopic compositions with respect to all Western Mediterranean ultrapotassic and associated rocks (see references in Peccerillo, 2005a and Conticelli *et al.*, 2009a). A within-plate mantle component has been proposed to be involved, albeit in different style and extent, in the genesis of the southernmost Roman magmas, namely those of the Neapolitan district (Ellam & Hawkesworth, 1998; Beccaluva *et al.*, 1991; Ayuso *et al.*, 1998; Peccerillo, 2001; Gasperini *et al.*, 2002; De Astis *et al.*, 2006; Bianchini *et al.*, 2008), and at a still minor extent in the final activity of the southernmost Latian districts (Conticelli *et al.*, 2009b).

In the case of Roccamonfina volcano an abrut shift from pre- to post-caldera volcanic rocks is observed, with decrease of alkaline degree and total abundance of incompatible elements with time. All these characteristics might be consistent with the process of increasing interaction proportion of melts from surrounding mantle with respect to vein melts. In this case, however, the vein vs. wall-rock mantle interaction does not explain the large variation in Sr-Nd-Pb isotopes observed (Figs. 36, 37, and 38). Indeed, the expected isotopic composition of the surrounding mantle, which is low Sr and high Nd isotope ratios, respectively, would suite the versus of variation in the shoshonites; however, a depleted mantle is expected to have developed low U/Pb and Th/Pb and thus to have an unradiogenic signature, rather than the radiogenic one necessary to explain the increase in Pb isotopic ratios towards the shoshonites (Fig. 38). Early Roccamonfina ultrapotassic volcanic rocks (leucite-bearing) display Sr-Nd-Pb isotopes well within the range of values of the other Latian districts, whereas the rocks from the final stage of activity display values well within the field of the Neapolitan district and pointing to the isotopic compositions of the Lucanian Magmatic Province (Figs. 36, 37, and 38). The volcanoes of the Neapolitan district show a more abundant within-plate component with respect to Roccamonfina final activity both in terms of isotopic (Figs. 36, 37, and 38) and incompatible trace element compositions (Figs. 30, 31, and 32). To explain this within-plate component in the ultrapotassic and shoshonitic rocks of the Neapolitan district, Beccaluva *et al.* (1991) suggested the occurrence of a mantle wedge characterized by an OIB signature prior to metasomatism south of the 41st parallel. This possibility however, does not explain i) the occurrence of this component limited to the final stage activity of Roccamonfina, a volcano slightly north of the 41st parallel; ii) the observed geochemical trends from Roccamonfina to Lucanian rocks passing from Neapolitan ones; iii) the absence of the within plate component in the early Roccamonfina rocks; indeed if mantle wedge had an OIB signature prior to the metasomatism, it is conceivable that this signature would be at some extent preserved also within the veins producing early ultrapotassic rocks.

Geodynamic implications

Ultrapotassic and associated shoshonitic to high-K calc-alkaline volcanic rocks of the Italian region have been produced from anomalously enriched upper mantle source following sediment recycling at a denstructive plate boundary. Sediment-derived ‘melts’ represent the dominant metasomatic agent responsible for the establishment of a metasomatic vein network, but a more pervasive ‘fluid’-like metasomatism is also present. The extreme enrichment in Th and the fractionated REE pattern of the erupted rocks suggests the presence of garnet in the residuum during the partial melting of the recycled sediments brought into the mantle through subductionand crustal delamination. This implies that temperatures during sediment partial melting were high enough to exhaust other accessory phases, such as allanite and/or monazite. These temperatures are higher than those generally expected at the slab/mantle interface, indicating that sediment melting occurred in the hot, central regions of the mantle wedge rather than at the slab/mantle interface. Large HFSE negative anomalies and fractionated REE patterns require rutile and garnet in the residuum.

The first episode of magmatism occurred during the Oligocene within the Western Alps, and it was related to the Alpine collision. Lamproite-like ultrapotassic magmas were generated in strict association with shoshonitic, high-K calc-alkalic and possibly calc-alkalic magmas. Magmas were emplaced during the post-collisional stages of the Alpine chain. Peccerillo & Martinotti (2006), provides evidence that the same metasomatic Alpine event occurred also in Corsica, and Tuscany, well before than Apennine orogenic movements started. Reactivation of this old metasomatised should has promoted the partial melting and the formation of Corsica and Tuscan lamproites. Unfortunately, the Sisco lamproite (Corsica) has a within plate signature that dominate over the orogenic ones, whereas the Tuscan lamproitic rocks have a slightly different isotopic signature with respect to the Western Alps (Conticelli *et al.*, 2009a).

During Tortonian, shoshonitic and high-K calc-alkaline rocks were emplaced along the western margin of the Tyrrhenian Sea (Fig. 43) possibly related to a westward dipping Apennine subduction (e.g., Faccenna *et al.*, 1997; Jolivet *et al.*, 1998; Rosembaum *et al.*, 2002, 2004, 2008; Rosembaum & Lister, 2004). Backward migration of the subducted slab and consequent isotherm relaxation triggered the generation of lamproitic magmatism in the Italian peninsula after the beginning of continental collision. Shoshonites and high-K calc-alkaline rocks followed the eruption of lamproites (Fig. 43) as a consequence of the increasing heat flow that brought to melt larger portion of the mantle wedge, with surrounding mantle becoming dominant with respect to metasomatised veins. Magmatism progressively moved eastward.

The metasomatic event was possibly not generated during the Apennine subduction but through several events of subduction of the Tethys Ocean beneath the European plate (i.e., Tommasini *et al.*, 2010). During the upper Pliocene to lower Pleistocene the lamprotitic to shoshonitic magmatism furtherly migrated eastward with an arcuate distribution immediately back to the Apennine chain where post-orogenic extension started to produce NW-SE elongate basins (Fig. 43b).

After a hiatus of several hundred thousand years, during the Middle Pleistocene (Fig. 43c), magmatism shifted its composition from silica saturated and leucite-free to silica-undersaturated, with formation of kamafugitic to plagioclase leucititic and leucititic magmas, which were erupted along the same plumbing system used by the late Tuscan magmas. In some cases hybridism between Roman and Tuscan magmas took place during the early phases of the Roman volcanism (e.g., Palaeo-Bolsena, Rio Ferriera formation at Vico, Morlupo volcanic rocks at Sabatian district), in other cases reactivated old Tuscan crystallising magmatic reservoirs bringing hybrid rocks to form the Amiata volcano.

The newly arrived magma was silica undersaturated and was generated in response of the recycling of carbonate-rich pelitic sediments within the mantle wedge during last collisional phases. This carbonate-rich metasomatism produced phlogopite-bearing wehrlitic veins, which partial melting under high X_{CO2} generated kamafugites and leucitites. A further eastward migration of magmatism occurred at the passage from Middle to Upper Pleistocene with the formation of kamafugitic magmatism in intra-apennine area (Fig. 43c).

Figure 43. Schematic tectonic evolution of the circum-Tyrrhenian area since late Miocene.

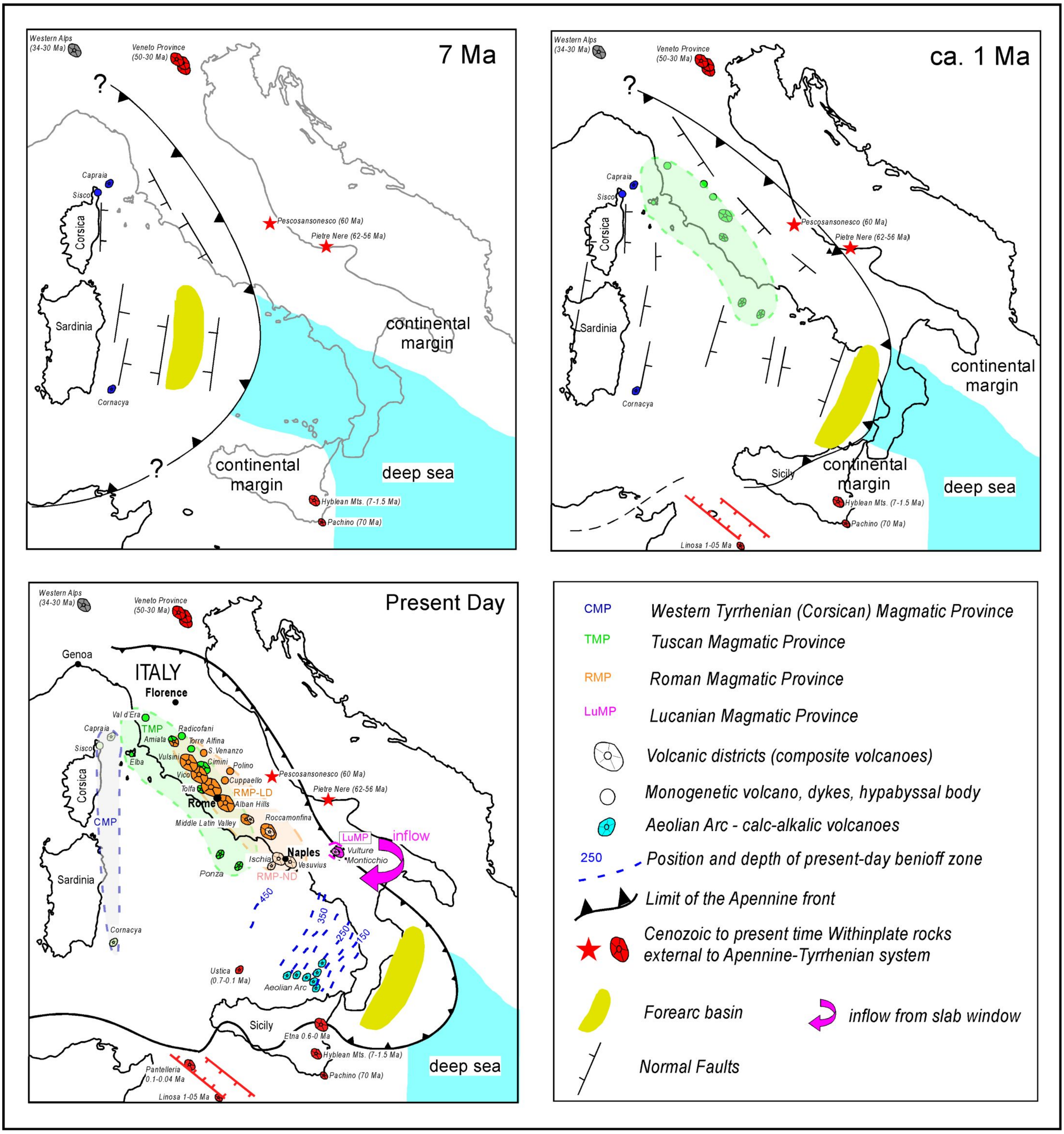

CMP = Corsica Magmatic Province; TMP = Tuscan Magmatic Province; RMP-LD = Roman Magmatic Province – Latian Districts; RMP-ND = Roman Magmatic Province, Neapolitan District; LuMP = Lucanian Magmatic Province; AA = Aeolian Arc Magmatic Province. Redrawn after Faccenna *et al.* (2004), Cifelli *et al.* (2007), and Avanzinelli *et al.* (2009).

During the late Pleistocene asthenospheric mantle from the foreland start to inflow within the mantle wedge through a slab-tear located close to the Bradanic trhough.located close to the bradanic through. Trace element ratios and isotopic values are consistent with the involvement of a within-plate mantle component similar to that of the asthenospheric mantle of the foreland, the Adria microplate. The Lucanian Magmatic Province with the nested Vulture and Monticchio volcanoes is located at the very extreme edge of the overriding plate (Fig. 11), where the mantle wedge is reduced or absent. Toroidal inflow of hot asthenospheric material into the mantle wedge will produce partial melting of the convecting mantle, which interacts with the small amount of metasomatised mantle wedge peridotite as recorded by Downes *et al.* (2002). This would results in magmatic rocks with intermediate geochemical characteristics between orogenic and within-plate. Inflow is favoured by the southeastward roll back and progressive fragmentation (i.e., detachment: Wortel & Spakman, 2000) of the subducting plate which is now reduced and segmented into narrow tongues from one original slab (Faccenna *et al.*, 2004; Rosembaum & Lister, 2004; Mattei *et al.*, 2007; Rosembaum *et al.*, 2008). The asthenosperic mantle flow through the tear within the subducted slab in correspondence of the Vulture volcano (Wortel & Spakman, 2000), with time moved into the southern Italian mantle wedge. The motion of the asthenospheric mantle from the foreland within the mantle wedge is recorded by the less evident within-plate signature observed from volcanoes of the Neapolitan district (e.g., Peccerillo, 2001; De Astis *et al.*, 2006), and at a less extent by the sub-alkaline recent volcanic rocks of the Roccamonfina, and even lesser extent of the Middle Latin Valley (Boari *et al.*, 2009b; Conticelli *et al.*, 2009b).

The location of the main tears are controlled by the presence of lateral heterogeneities in the subducting slab such as those represented by the transition from the Ionian oceanic lithosphere to the Apulia and Hyblean continental lithosphere. Such heterogeneities are responsible for the curvature of the Calabrian Arc and for the major fragmentation of the subducting plate. In the Vulture volcano area, the presence of a lateral tear in the subducting slab is suggested by the differing behaviours of the foreland areas southeast and northwest of the volcano. These areas correspond to the transition from the thick carbonate Mesozoic succession of the Apulian platform, which itself corresponds to the buoyant outcropping Apulia foreland, to the transitional and basinal facies outcropping in the Gargano area. The beginning of magmatism at Vulture volcano marks the vertical rupture of the subducted plate. In Lucanian Magmatic Province this scenario is also supported by a 230Th-excess measured in a sample from the Monticchio Lake maars, suggesting an important role for adiabatic melting in an up-welling asthenospheric mantle source (Avanzinelli *et al.*, 2008, 2010).

On the basis of the time of occurrence of the within-plate component we might suggest that the slab-tear in correspondance of the Vulture volcano formed before the middle Pleistocene, indeed the early Vulture volcanic products, which are as old as 0.7 Ma, show the presence of the within-plate component. However, the slab-tear opening northward occurred significantly later. Indeed the ultrapotassic magmatism during the Middle Pleistocene at Roccamonfina and Middle Latin Valley volcanoes was not affectetd by this component. The within plate component appears in these volcanoes at about 035 Ma. Since then the within-plate component invaded the Neapolitan mantle wedge.

Eventually, during the Holocene a further metasomatic agent arrived in the Neapolitan region to account the U-Th isotopic characteristics of Vesuvius, Ischia and Campi Flegrei magmas (Avanzinelli *et al.*, 2008). Indeed the U-Th disequilibria require the addition, shortly before the eruption of the magmas of the Neapolitan district (<10ka), of a U-rich component, which has affected neither the Latian district of the Roman Magmatic Province nor the Monticchio lakes volcanic products of the Lucanian Magmatic Province (Avanzinelli *et al.*, 2008).

Acknowledgements

The authors wish to thank D. Prelevic, S. Foley, Rob Ellam, K. Bell, F. Sani, G. Bianchini, C. Faccenna, V. Morra, and L. Morbidelli for stirring and focussing discussion and in some cases for suggestions at different stages of the manuscript preparation, L. Fedele for supplying the electronic base of figure 29. Financial support was provided by the Università degli Studi di Firenze (DST – ex 60% funds) issued to Sandro Conticelli, by the Italian Ministry of Education and Research (MIUR) through PRIN_2008 (research grants #: 2008HMHYFP_002; 2008HMHYFP_003; 2008HMHYFP_005).

References

Accordi, B., 1963. Lineamenti strutturali del Lazio e dell'Abruzzo meridionale. Memorie Soc. Geol. Italiana 4, 595-633.

Accordi, B., Angelucci, A., 1962. Un neck nel calcare cretacico di Monte Autore (Subiaco, Roma). Geologica Romana 2, 289-296.

Accordi, G., Carbone, F., 1988. Sequenze carbonatiche meso-cenozoiche. In: “Note illustrative alla carta delle litofacies del Lazio-Abruzzo ed aree limitrofe”, Accordi G., Carbone F., Civitelli G., Corda L., De Rita D., Esu D., Funiciello R., Kotsakis T., Mariotti G., Sposato A. (edts), Quaderni della Ricerca Scientifica del CNR 114(5), pp 11-92.

Acocella, V., Cifelli, F., Funiciello, R., 2001. The control of overburden thickness on resurgent domes: insights from analogue models. J. Volcanol. Geoth. Res. 111, 137-153.

Acocella, V., Faccenna, C., Funiciello, R., 1996. Elementi strutturali della Media Valle Latina. Bollettino Società Geologica Italiana 115, 501-518.

Acocella, V., Funiciello, R., 1999. The interaction between regional and local tectonics during resurgent doming: the case of the island of Ischia, Italy. J. Volcanol. Geoth. Res. 88, 109-123.

Acocella, V., Funiciello, R., 2006. Transverse systems along the extensional Tyrrhenian margin of central Italy and their influence on volcanism. Tectonics 25, 10.1029/2005TC001845

Acocella, V., Salvini, F., Funiciello, R., Faccenna, C., 1999. The role of transfer structures on volcanic activity at Campi Flegrei (Southern Italy). J. Volcanol. Geoth. Res. 91, 123-139.

Alagna, K.E., Peccerillo, A., Martin, S., 2010. Tertiary to present evolution of orogenic magmatism in Italy. In: “The Geology of Italy”, Beltrando M., Peccerillo, A., Mattei, M., Conticelli, S., Doglioni, C. (edts.), J. Virtual Explorer, paper 18.

Albore Livadie, C., Barra, D., Beneduce, G., Brancaccio, L., Cinque, A., Ortolani, F., Pagliuca, S., Russo, F., 1989. Evoluzione geomorfologica, neotettonica e vulcanica della pianura costiera del Fiume Sarno (Campania) in relazione agli insediamenti anteriori all'eruzione del 79 d.C.. Vulcan. Paleog. Archeol. PACT 10, 237-256.

Altaner, S.P., Ylagan, R.F., Savin, S.M., Aronson, J.L., Belkin, H.E., Pozzuoli, A., 2003. Geothermometry, geochronology, and mass transfer associated with hydrothermal alteration of a rhyolitic hyaloclastite from Ponza Island, Italy. Geochim. Cosmoch. Acta 67, 275-288.

Altherr, R., Meyer, H.-P., Holl, A., Volker, F., Alibert, C., McCulloch, M.T., Majer, V., 2004. Geochemical and Sr-Nd-Pb isotopic characteristics of late Cenozoic leucite lamproites from the East European Alpine belt (Macedonia and Yugoslavia). Contrib. Mineral. Petrol. 147, 58-73.

Alvarez, W., Ammerman, A.J., Renne, A.J., Karner, D.B., Terrenato, N., Montanari, A., 1996. Quaternary fluvial-volcanic stratigraphy and geochronology of the Capitoline Hill in Rome. Geology 24, 751-754.

Anderson, H., Jackson, J., 1987. Active tectonics of the Adriatic Region. Geophys. J. Royal Astron. Soc. 91, 937 – 983.

Angelucci, A., Brotzu, P., Civitelli, G., Morbidelli, L., Traversa, G., 1974. Il vulcanismo pleistocenico della Media Valle Latina (Lazio). Caratteristiche petrografiche e geologiche dei principali affioramenti lavici. Geologica Romana 13, 83-123.

Angelucci, A., Negretti, G., 1963. Una serie nelle vulcaniti pleistoceniche discordanti sul Miocene Medio-Superiore presso Pofi (Lazio Meridionale). Geologica Romana 2, 41-58.

Appleton, J.D., 1972. Petrogenesis of Potassium rich lavas from the Roccamonfina Volcano, Roman Region Italy. J. Petrol. 13, 425-456.

Arculus, R.J., 2003. Use and Abuse of the Terms Calcalkaline and Calcalkalic. J. Petrol. 44, 929-935.

Arima, M., Edgar, A.D., 1983a. A high pressure experimental study on a Magnesian-rich leucite-lamproite from a West Kimberley area, Australia: petrogenetic implication. Contrib. Mineral. Petrol. 84, 228-234.

Arima, M., Edgar, A.D., 1983b. High pressure experimental studies on a Katungite and their bearing on the genesis of some Potassium-rich magmas of the West branch of the African rift. J, Petrol. 24, 166-187.

Armienti, P., Barberi, F., Bizouard, H., Clocchiatti, R., Innocenti, F., Metrich, N., Rosi, M., Sbrana, A., The Phlegrean Fields: magma evolution within a shallow chamber. J. Volcanol. Geoth. Res. 17, 289-311.

Asmerom, Y., 1999. Th-U fractionation and mantle structure. Earth Placet. Sci. Lett. 166, 163-175.

Aurisicchio, C., Federico, M., Gianfagna, A., 1988. Clinopyroxene chemistry of the high-potassium suite from the Alban Hills, Italy. Mineral. Petrol. 39, 1-19.

Avanzinelli, R., Elliot, T., Tommasini, S., Conticelli, S., 2008. Constraints on the genesis of the potassium-rich Italian volcanics from U/Th disequilibrium. J. Petrol. 49. 195-223.

Avanzinelli, R., Lustrino, M, Mattei, M., Melluso, L., Conticelli, S., 2009. Potassic and ultrapotassic magmatism in the circum-Tyrrhenian region: the role of carbonated pelitic vs. pelitic sediment recycling at destructive plate margin. Lithos 113, 213-227.

Avanzinelli, R., Matturro, G., Schiattarella, M., Mattei, M., Conticelli, S., 2011. Partial melting mechanism and slab tears in the genesis of the haüyne-bearing alkaline magmas of the Lucanian Magmatic Province, Souther Italy: Sr-Nd-Pb and U/Th isotopic data. In preparation.

Ayuso, R.A., De Vivo, B., Rolandi, G., Seal, R.R. II, Paone, A., 1998. Geochemical and isotopic (Nd-Pb-Sr-O) variations bearing on the genesis of volcanic rocks from Vesuvius, Italy. J. Volcanol. Geoth. Res. 82, 53-78.

Baldi, P., Decandia, F.A., Lazzarotto, A., Calamai, A. 1974. Studio geologico del substrato della copertura vulcanica laziale nella zona dei laghi di Bolsena, Vico e Bracciano. Memorie Società Geologica Italiana 7, 575-603.

Ballini, A., Barberi, F., Laurenzi, M.A., Mezzetti, F., Villa, I.M., 1989a. Nuovi dati sulla stratigrafia del vulcano di roccamonfina. Bollettino Gruppo Nazionale Vulcanologia 5(2), 533-555.

Ballini, A., Frullani, A., Mezzetti, F., 1989b. La formazione piroclastica del tufo trachitico bianco del vulcano di roccamonfina. Bollettino Gruppo Nazionale Vulcanologia 5(2), 557-574.

Barberi, F., Borsi, S., Ferrara, G., Innocenti, F., 1967. Contributo alla conoscenza vulcanologica e magmatologica delle Isole dell'Archipelago Pontino. Memorie Società Geologica Italiana 6, 581-606.

Barberi, F., Buonasorte, G., Cioni, R., Fiordelisi, A., Foresi, L., Iaccarino, S., Laurenzi, M.A., Sbrana, A., Vernia, L., Villa, I.M., 1994. Plio-Pleistocene geological evolution of the geothermal area of Tuscany and Latium. Memorie Descrittive Carta Geologica d'Italia 49, 77-134.

Barberi, F., Innocenti, F, Landi, P., Rossi, U., Saitta, M., Santacroce, R., Villa, I.M., 1984. The evolution of Latera caldera (central Italy) in the light of subsurface data. Bull. Volcanol. 47, 125-141.

Barberi, F., Innocenti, F., Ricci, C.A., 1971. La Toscana meridionale. Il magmatismo. Rend. Soc. Ital. Mineral. Petrol., 27, 169-210.Marinelli G., 1961. Genesi e classificazione delle vulcaniti recenti Toscane. Atti Società Toscana di Scienze Naturali, Memorie (A), 68, 74-116.

Barberi, F., Ferrara, G., Franchi, F., Serri, G., Tonarini, S., Treuil, M., 1986. Geochemistry and geochronology of the Capraia Island volcanic Complex (North Tyrrhenian Sea, Italy). Terra Cognita abstract 6, 185.

Barbieri, M., Di Girolamo, P., Locardi, E., Lombardi, G., Stanzione D., 1979. Petrology of the Calc-Alkaline volcanics of the Parete 2 well (Campania) Italy. Periodico Mineralogia 48, 53-74.

Barbieri, M., Peccerillo, A., Poli, G., Tolomeo, L., 1988. Major, trace element and Sr isotopic composition of lavas from Vico volcano (Central Italy) and their evolution in an open system. Contrib. Mineral. Petrol. 99, 485-497.

Barchi, M., Amato, A., Cippitelli, G., Merlini, S., Montone, P., 2007. Extensional tectonics and seismicity in the axial zone of the Southern Apennines. Bollettino Società Geologica Italiana, Special volume 7, 47-56.

Barker, D.S., 1996. Carbonatite volcanism. In “Undersaturated alkaline rocks: mineralogy, petrogenesis, and economic potential”, R.H. Mitchell (edt.). Mineralogical Association of Canada, Short Course Series 24: 45-62.

Bartole, R. 1995. The North Tyrrhenian–Northern Apennines post-collisional system: constraints for a geodynamic model. Terra Nova 7, 7–30.

Barton, M., Varekamp, J.C., van Bergen, M.J., 1982. Complex zoning of clinopyroxenes in the lavas of vulsini, latium, Italy: Evidence for magma mixing. J. Volcanol. Geoth. Res. 14, 361-388.

Bear, A.N., Cas, R.A.F., Giordano, G., 2009a. Variations in eruptive style and depositional processes associated with explosive, phonolitic composition, caldera-forming eruptions: The 151 ka Sutri eruption, Vico Caldera, central Italy. J. Volcanol. Geoth. Res. 184, 225-255.

Bear, A.N., Cas, R.A.F., Giordano, G., 2009b. The implications of spatter, pumice and lithic clast rich proximal co-ignimbrite lag breccias on the dynamics of caldera forming eruptions: The 151 ka Sutri eruption, Vico Volcano, Central Italy. J. Volcanol. Geoth. Res. 181, 1-24.

Beccaluva, L., Bigioggero, B., Chiesa, S., Colombo, A., Fanti, G., Gatto, G.O., Gregnanin, A., Montrasio, A., Piccirillo, E.M., Tunesi, A., 1983. Post collisional orogenic dyke magmatism in the Alps. Memorie Socità Geologica Italiana 36, 341-359.

Beccaluva, L., Coltorti, M., Di Girolamo, P., Melluso, L., Milani, L., Morra, V., Siena, F., 2002. Petrogenesis and evolution of Mt.Vulture alkaline volcanism (Southern Italy). Mineral. Petrol. 74, 277-297.

Beccaluva, L., Di Girolamo, P., Morra, V., Siena F., 1990. Phlegrean fields volcanism revisited: A critical re-examination of deep eruptive systems and magma evolutionary processes. N. Jb. Geol. Paläont. Mh., 257-271.

Beccaluva, L., Di Girolamo, P., Serri, G., 1991. Petrogenesis and tectonic setting of the Roman Volcanic Province, Italy. Lithos 26, 191-221.

Beccaluva, L., Gabbianelli, G., Lucchini, F., Rossi, P.L., Savelli, C., 1985. Petrology and K/Ar ages of volcanics dredged from the Eolian Seamounts: implications for geodynamic evolution of the southern Tyrrhenian basin. Earth Planet. Sci. Lett. 74, 187-208.

Bell, K., Castorina, F., Lavecchia, G., Rosatelli, G., Stoppa, F., 2004. Is there a mantle plume beneath Italy ? EOS 85, 541-547.

Bellotti, P., Evangelista, S., Milli, S., Valeri, P., 1987. Un corpo lavico nelle marne ad orbulina di Ricetto (F° 145 Avezzano). Rendiconti Società Geologica Italiana 10, 67-70.

Bellucci, F., Grimaldi, M., Lirer, L., Rapolla, A. 1997. Structure and geological evolution of the island of Ponza, Italy: inferences from geological and gravimetric data. J. Volcanol. Geoth. Res. 79, 87-96.

Bellucci F., Lirer L., Munno R., 1999. Geology of Ponza, Ventotene and Santo Stefano. Acta Vulcanologica 11, 197-222.

Beneduce, P., Schiattarella, M, 1997. Realazioni tra tettonica regionale Quaternaria e deformazione vulcano genica nelle aree dei Campi Flegrei, Isola di Ustica e Monte Vulture (Italia meridionale). Il Quaternario 10: 583-588.

Bernardi, A., de Rita, A., Funiciello, R., Innocenti, F., Villa, I.M., 1982. Chronology and structutal evolution of the Alban Hills volcanic complex. In: Fifth International Conference on Geochronology, Cosmochronology, and Isotope Geology, Nikko, Japan, Abstracts, 23-24.

Bertagnini, A., De Rita, D., Landi, P., 1995. Mafic inclusions in the silica-rich rocks of the Tolfa-Ceriti-Manziana volcanic district (Tuscan Province, Central Italy): Chemistry and mineralogy. Mineral. Petrol. 54, 261-276.

Bertagnini, A., Sbrana, A., 1986. Il vulcano di Vico: stratigrafia del complesso vulcanico e sequenze eruttive delle formazioni piroclastiche. Memorie della Società Geologica Italiana 35, 699-713.

Bianchini, G., Beccaluva, L., Siena, F., 2008. Post-collisional and intraplate Cenozoic volcanism in the rifted Apennines/ Adriatic domain. Lithos 101, 125-140.

Bianco, F., Castellano, M., Milano, G., Ventura, G., Vilardo, G., 1998. The Somma–Vesuvius stress field induced by regional tectonics: evidences from seismological and mesostructural data. J. Volcanol. Geoth. Res. 82, 199-218.

Bigazzi, G., Bonadonna, F.P., Ferrara, G., 1973. Fission tracks ages of zircons and apatites from Northern Apennine ophiolites. Fortschr. Mineral. 50, 51-53.

Bigazzi, G., Bonadonna ,F.P., Ghezzo, C., Giuliani, O., Radicati di Brozolo, F., Rita, F.,1981. Geochronological study of the Monte Amiata lavas (Central Italy). Bull. Volcanol. 44(3), 455-465.

Bigazzi, G., Bonadonna, F.P., Iaccarino, S., 1979. Geochronological hypothesis on Plio-Pleistocene boundary in Latium region. Bollettino Società Geologica Italiana 92, 391-422.

Bindi, L., Cellai, D., Melluso, L., Conticelli, S., Morra, V., Menchetti, S., 1999. Crystal Chemistry of Clinopyroxene from Alkaline undersaturated rocks of the Monte Vulture Volcano, Italy. Lithos 46, 259-274.

Boari, E., 2005. Petrologia e magmatologia del vulcanismo Plio-Pleistocenico del Lazio meridionale e sue implicazioni geodinamiche (in Italian). Ph.D. Thesis Università degli Studi di Firenze, pp. 1-143.

Boari, E, Avanzinelli, R, Melluso, L, Giordano, G, Mattei, M, Morra, V, Conticelli, S, 2009b. Isotope geochemistry (Sr-Nd-Pb) and petrogenesis of leucite-bearing volcanic rocks from “Colli Albani” volcano, Roman Magmatic Province, Central Italy: inferences on volcano evolution and magma genesis. Bull. Volcanol. 71, 977-1005.

Boari, E., Conticelli, S., 2007. Mineralogy and Petrology of Mg-rich calc-alkalic, potassic, and ultrapotassic associated rocks: the Middle Latin Valley monogenetic volcanoes, Roman Magmatic Province, Southern Italy. Canad. Mineral. 45, 1443-1469.

Boari, E., Tommasini S., Laurenzi, M.A., Conticelli, S., 2009. Transition from ultrapotassic kamafugitic to sub-alkaline magmas: Sr, Nd, and Pb isotope, trace element and ^{40}Ar-^{39}Ar age data from the Middle Latin Valley volcanic field, Roman Magmatic Province, Central Italy. J. Petrol. 50, 1327-1357.

Bonadonna, F.P., Brocchini, D., Laurenzi, M.A., Principe, C., Ferrara, G., 1998. Stratigraphical and chronological correlations between Mt. Vulture volcanics and sedimentary deposits of the Venosa basin. Quat. Internat. 47/48, 87-96.

Bonardi, G., D'Argenio, B., Perrone, V., 1988. Carta Geologica dell'Appennino Meridionale. 74° Congresso della Società Geologica Italiana. Scala 1:250,000.

Borghetti, G., Sbrana, A., Sollevanti, F., 1981. Vulcano-tettonica dell'area dei Monti Cimini e rapporti cronologici tra vulcanismo Cimino e Vicano. Rendiconti Società Geologica Italiana 4, 253-254.

Borsi, S., Ferrara, G., 1971. Studio con il metodo K/Ar dei rapporti cronologici tra le rocce costituenti il complesso intrusivo dell'isola d'Elba. Rendiconti Società Italiana Mineralogia Petrologia 27, 323.

Borsi, S., Ferrara, G., Mazzuoli, R., 1965. Studio petrologico e datazione con i metodi K/Ar e Rb/Sr di una roccia granitica presso Roccastrada (Grosseto). Atti Società Toscana di Scienze Naturali 72, 1-24.

Borsi, S., Ferrara, G., Tongiorgi, E., 1967. Determinazione con il metodo K/Ar delle età delle rocce magmatiche della Toscana. Bollettino Società Geologica Italiana 86, 403-410.

Bosi, V., Giordano, G., 1997. Stress field evolution in central italy during middle late Pleistocene: new information from Southern Latium. Il Quaternario 10, 631-636.

Brancaccio, L., Cinque, A., Romano, P., Rosskopf, C., Russo, F., Santangelo, N., Santo A., 1991. Geomorphology and neotectonic evolution of a sector of the Tyrrhenian flank of the Southern Apennines (Region of Naples, Italy). Z. Geomorph. N. F. 82, 47-58

Branco, W., 1877. Die Vulkane des Hernikerlandes bei Frosinonen in Mittel-Italien. N. Jahrb. Mineral. Geol. Päleont.

Brocchini, D., 1993. Il Vulcano Vulture (Basilicata). Cronologia radiometrica ed evoluzione. M.Sc. thesis, Pisa, 1-70.

Brocchini, D., 1999. Cronologia ed evoluzione del vulcanismo nell'area del Somma-Vesuvio. Ph.D. thesis, Pisa, 1-168.

Brocchini, D., Di Battistini, G.D., Laurenzi, M.A., Vernia, L., Bargossi, G.M., 2000. New $^{40}Ar/^{39}Ar$ datings on the southeastern sector of the Vulsinian Volcanic District (Central Italy). Boll. Società Geol. Italiana 119, 113-120.

Brocchini, D., La Volpe, L., Laurenzi, M.A., Principe, C., 1994. Storia evolutiva del Monte Vulture. Plinius 12, 22-25.

Brocchini, D., Principe, C., Castradori, D., Laurenzi, M.A., Gorla, L., 2001. Quaternary evolution of the southern sector of the Campanian Plain and early Somma–Vesuvius activity: insights from the Trecase 1 well. Mineral. Petrol. 73, 67–91.

Brunamonte, F., Gaeta, M., Michetti, A.M., Mottana, A., Palladino, D.M., 1992. Caratterizzazione mineralogico-petrografica ed inquadramento stratigrafico preliminare di alcuni depositi vulcano clastici dell'area reatina. Studi Geologici Camerti 1992/1, 65-72.

Cadoux, A., Pinti, D.L., 2009. Hybrid character and pre-eruptive events of Mt Amiata volcano (Italy) inferred from geochronological, petro-geochemical and isotopic data. J. Volcanol. Geoth. Res. 179, 169-190.

Cadoux, A., Pinti, D.L., Aznar, C., Chiesa, S., Gillot, P.-Y., 2005. New chronological and geochemical constraints on the genesis and geological evolution of Ponza and Palmarola Volcanic Islands (Tyrrhenian Sea, Italy). Lithos 81, 121-151.

Caggianelli, A., De Fino, M., La Volpe, L., Piccarreta, G., 1990. Mineral chemistry of Monte vulture volcanics: petrological implications. Mineral. Petrol. 41, 215-227.

Callegari, E., Cigolini, C., Medeot, O., D'Antonio, M., 2004. Petrogenesis of Calc-alkaline and shoshonitic post-collisional Oligocene volcanics of the Cover Series of the Sesia Zone, Western Italian Alps. Geodin. Acta 17, 1-29.

Capaldi, G., Civetta, L., Gillot, P.Y., 1985. Geochronology of Plio-Pleistocene volcanic rocks from Southern Italy. Rendiconti Società Italiana di Mineralogia e Petrologia 40, 25-44.

Capitanio, F., Larocca, F., Improta, S., 2004. High-temperature rapid pyrometamorphism induced by a charcoal pit burning: The case of Ricetto, central Italy. Intern. J. Earth Sci. 93, 107-118.

Caprarelli, G., Togashi, S., De Vivo, B., 1993. Preliminary Sr and Nd isotopic data for a recent lavas from Vesuvius volcano. J. Volcanol. Geoth. Res. 58, 377-381.

Carmignani, L., Carosi, A., Di Pisa, A., Gattiglio, M., Musumeci, G., Oggiano, G., Pertusati P.C., 1994. The Hercynian chain in Sardinia, Italy). Geodin. Acta 7, 31-47.

Carminati, E., Negredo, A.M., Valera J.L., Doglioni, C., 2005. Subduction-related intermediate-depth and deep seismicity in Italy: insights from thermal and rheological modelling. Phys. Earth Planet. Interiors 149, 65-79.

Carraro, F., Ferrara, G., 1978. Alpine tonalite at Miagliano, Biella (zone diorite-kinzigitica). Schweiz. Mineral. Petrograp. Mitt. 48. 75-80.

Cassignol, C., Gillot, P.Y., 1982. Range and effectiveness of unspiked potassium-argon dating: experimental groundwork and applications. In: "Numerical Dating in Stratigraphy", (Odin G.S. Ed.), John Wiley & Sons, New York, 159-179.

Castorina, F., Stoppa, F., Cundari, A., Barbieri, M., 2000. An enriched mantle source for Italy's melilitite-carbonatite association as inferred by its Nd-Sr isotope signature. Mineral. Mag. 64, 625-639.

Cavinato, G.P., Carusi, C., Dall'Asta, M., Miccadei, G., Piacentini, T., 2002. Sedimentary and tectonic evolution of Plio–Pleistocene alluvial and lacustrine deposits of Fucino Basin (central Italy). Sed. Geol. 148, 29-59.

Cavinato, G.P., Chiaretti, F., Cosentino, D., Serva, L., 1989. Caratteri Geologico-Strutturali del margine orientale della Conca di Rieti. Bollettino Società Geologica Italiana 108, 207-218.

Cellai, D., Conticelli, S., Diella, V., 1993. Perrierite-chevkinite in igneous ultrapotassic rocks from Central Italy, chemical data and their petrological significence. Periodico Mineralogia 62, 57-66.

Cellai, D., Conticelli, S., Menchetti, S., 1994. Crystal-chemistry of clinopyroxenes in Italian Lamproites and Kamafugites, Implications on their genesis. Contrib. Mineral. Petrol. 116, 301-315.

Chelazzi, L., Bindi, L., Olmi, F., Peccerillo, A., Menchetti, S., Conticelli, S., 2006. A lamproitic component in the high-K calc-alkaline volcanic rocks of the Capraia Island, Tuscan Magmatic Province: evidence from clinopyroxene crystal chemical data. Periodico Mineralogia 75, 75-94.

Chiesa, S., Forcella, F., Pasquaré, G., Vezzoli, L. 1988. Geologic Map of the Island of Ischia. Consiglio Nazionale delle Ricerche, Progetto Finalizzato Geodinamica.

Chiodini, G., Cardellini, C., Amato, A., Boschi, E., Caliro, S., Frondini, F., Ventura, G., 2004. Carbon dioxide Earth degassing and seismogenesis in central and southern Italy. Geophys. Res. Lett. 31, L07615. 10.1029/2004GL019480

Cifelli, F., Mattei, M., Rossetti F., 2007. Tectonic evolution of arcuate mountain belts on top of a retreating subduction slab: The example of the Calabrian Arc. J.Geophys. Res. 112, B09101, 10.1029/2006JB004848

Cimarelli, C., De Rita, D., 2006. Structural evolution of the Pleistocene Cimini trachytic volcanic complex (Central Italy). Bull. Volcanol. 68, 538-548.

Cinque, A., Alinaghi, H.H., Laureti, L., Russo, F., 1987. Osservazioni preliminari sull'evoluzione geomorfologica della piana del Sarno (Campania, Appennino Meridionale). Geografia Fisica Dinamica Quaternaria 10, 161-174.

Cinque, A., Patacca, E., Scandone, P., Tozzi, M. 1993. Quaternary kinematic evolution of the Southern Apennines. Relationship between surface geological features and deep lithospheric structures. Annali Geofisica 36, 249-260.

Cioni, R., Bertagnini, A., Santacroce, R., Andronico, D., 2008. Explosive activity and eruption scenarios at Somma-Vesuvius (Italy): Towards a new classification scheme. J. Volcanol. Geoth. Res. 178, 331-346.

Cioni, R., Civetta, L., Marianelli, P., Metrich, N., Santacroce, R., Sbrana, A., 1995. Compositional layering and syn-eruptive mixing of a periodically refilled shallow magma chambre: the AD 79 Plinian eruption of Vesuvius. J. Petrol. 36, 739-776.

Cioni, R., Laurenzi, M.A., Sbrana, A., Villa, I.M., 1993. $^{40}Ar/^{39}Ar$ chronostratigraphy of the initial activity in the Sabatini volcanic complex (Italy). Bollettino Società Geologica Italiana 112, 251-263.

Cioni, R., Sbrana, A., Bertagnini, A., Buonasorte, G., Landi, P., Rossi, U., Salvati, L., 1987. Tephrostratigraphic correlations in the Vulsini, Vico and Sabatini volcanic successions. Periodico Mineralogia 56, 137-155.

Cipollari, P., Cosentino, D., 1995. Miocene unconformities in the central Apennines: geodynamic significance and sedimentary basin evolution. Tectonophysics 252, 375-389.

Cipollari, P., Cosentino, D., Guerrera, F., Laurenzi, M.A., Renzulli, A., Tramontana, M. 1995. Biostratigraphical correlation and geochronology of volcanoclastic horizons across the Tortonian/Messinian boundary in the Apennine foreland basin system. Annales Tectonicae 12, 113-132.

Civetta, L., Carluccio, E., Innocenti, F., Sbrana, A., Taddeucci, G., 1991a. Magma chambre evolution under the Phlegrean fields during the last 10 ka: trace element and isotop data. Europ. J. Mineral. 3, 415-428.

Civetta, L., D'Antonio, M., de Lorenzo, S., Di Renzo, V., Gasparini, P., 2004. Thermal and geochemical constraints on the 'deep' magmatic structure of Mt. Vesuvius. J. Volcanol. Geoth. Res. 133, 1-12.

Civetta, L., Del Carmine, P., Manetti, P., Peccerillo, A., Poli, G., 1984. Petrology, geochemistry and Sr-isotope characteristics of lavas from the area of Commenda (Mts. Vulsini, Italy). Bull. Volcanol. 47, 581-595.

Civetta, L., Galati, R., Santacroce, R. 1991b. Magma mixing and convective compositional layering within the Vesuvius magma chambre. Bull. Volcanol. 53: 287-300.

Civetta, L., Innocenti, F., Lirer, L., Manetti, P., Munno, R., Peccerillo, A., Poli, G., Serri, G., 1979. Serie potassica ed alta in potassio dei Monti Ernici (Lazio Meridionale): considerazioni petrologiche e geochimiche. Rendiconti Società Italiana di Mineralogia e Petrologia 35, 227-249.

Civetta, L., Innocenti, F., Manetti, P., Peccerillo, A., Poli, G., 1981, Geochemical characteristics of potassic volcanics from Mt. Ernici (Southern, Latium, Italy). Contrib. Mineral. Petrol. 78, 37-47.

Civetta, L., Orsi, G., Scandone, P., Pece, R., 1978. Eastward migration of the Tuscan Anatectic magmatism due to anticlockwise rotation of the Apennines. Nature 276, 604-606.

Class, C., Miller, D.M., Goldstein, S.L., Langmuir, C.H., 2000. Distinguishing nelt and fluid subduction components in Umnak volcanics, Aleutinian arc. Geochemistry Geophysics Geosystem 1: paper number 1999GC000010.

Clausen, C., Holm, M., 1990. Origin of the acidic volcanics of the Tolfa district, Tuscan Province, central Italy: an elemental and Sr-isotopic study. Contrib. Mineral. Petrol. 105, 403-411.

Cole, P.D., Guest, J.E., Duncan, A.M., 1993. The emplacement of intermediate volume ignimbrite: a case study from Roccamonfina volcano, Southern Italy. Bull. Volcanol. 55, 467-480.

Cole, P.D., Guest, J.E., Duncan, A.M., Chester, D.K., Bianchi, R., 1992. Post-collapse volcanic history of calderas on a composite volcano: an example from Roccamonfina, Southern Italy. Bull. Volcanol. 54, 504-520.

Cole, P.D., Scarpati, C. 1993. A facies interpretation of the eruption and emplacement mechanisms of the upper part of the Neapolitan Yellow Tuff, Campi Flegrei, southern Italy. Bull. Volcanol. 55, 311-326.

Collettini, C., Barch,i M., 2002. A low-angle normal fault in the Umbria region (Central Italy): a mechanical model for the related microseismicity. Tectonophysics 359, 97-115.

Collettini, C., De Paola, N., Holdsworth, R.E., Barchi, M.R., 2006. The development and behaviour of low-angle normal faults during Cenozoic asymmetric extension in the Northern Apennines, Italy. J. Struct. Geol. 28, 333-352.

Coltorti, M., Di Battistini, G., Nappi, G., Renzulli, A., Zeda, O., 1991. Structural setting and magmatic evolution of Montefiascone volcanic complex, vulsini district, central Italy. J. Volcanol. Geoth. Res. 46, 99-124.

Conte, A.M., Dolfi, D., 2002. Petrological and geochemical characteristics of Plio-Pleistocene Volcanics from Ponza Island (Tyrrhenian Sea, Italy). Mineral. Petrol., 74, 75-94.

Conticelli, S., 1989. Genesi del magmatismo alcalino-potassico dell'Italia centrale: evidenze Petrologiche, Geochimiche e Petrologico Sperimentali. Ph.D. Thesis, Università degli Studi di Firenze, Italy, 404 pp.

Conticelli, S, 1998, Effects of Crustal Contamination on Ultrapotassic Magmas with Lamproitic Affinity: Mineralogical, Geochemical and Isotope data from the Torre Alfina Lavas and Xenoliths, Central Italy. Chem. Geol. 149, 51-81.

Conticelli, S., Avanzinelli, R., Marchionni S., Tommasini, S., Melluso, L., 2011b. Mantle heterogeneities in a veined lithospheric upper mantle responsible of the shift from ultrapotassic to shoshonitic and high-K calc-alkaline magmatism: Sr-Nd-Pb study of the Radicofani monogenetic volcano, Tuscany, Central Italy. Mineral. Petrol. Submitted.

Conticelli, S., Boari, E., Avanzinelli, R., De Benedetti, A.A., Giordano, G., Mattei, M., Melluso, L., Morra, V., 2010. Geochemistry, isotopes and mineral chemistry of the Colli Albani volcanic rocks: constraints on magma genesis and evolution. In: Funiciello, R. & Giordano, G. (eds) The Colli Albani Volcano. Special Publications of IAVCEI, 3. The Geological Society of London, London, 107-139.

Conticelli, S, Boari, E, Braschi, E, Laurenzi, MA, Manetti, P, 2009c. Il Monte Amiata un vulcano quaternario con caratteristiche vulcanologiche, geochimiche e petrologiche controverse. Proc. Workshop “In Terra d’Amiata. Geologia, mineralogia, e patrimonio minerario”, Abbadia San Salvatore (Siena), Dicembre 2009, 21-23.

Conticelli, S, Bortolotti, V, Principi, G, Laurenzi, MA, Vagelli, G, D'Antonio, M, 2001. Petrology, mineralogy and geochemistry of a mafic dyke from Monte Castello, Elba Island, Italy. Ofioliti 26, 249-262.

Conticelli, S, Carlson, RW, Widom, E, Serri, G, 2007. Chemical and isotopic composition (Os, Pb, Nd, and Sr) of Neogene to Quaternary calc-alkalic, shoshonitic, and ultrapotassic mafic rocks from the Italian peninsula: Inferences on the nature of their mantle sources. In: Beccaluva L, Bianchini G, Wilson M (eds) Cenozoic Volcanism in the Mediterranean Area. Geol. Soc. Am., Special Paper 418, 171-202.

Conticelli, S, D’Antonio, M, Pinarelli, L, Civetta, L., 2002. Source contamination and mantle heterogenity in the genesis of Italian potassic and ultrapotassic volcanic Rocks: Sr-Nd-Pb Isotope data from Roman Province and Southern Tuscany. Mineral. Petrol. 74, 189-222.

Conticelli, S., Edgar, A.D., Manetti, P., Peccerillo A., 1989. Melting relationships on a Ultrapotassic olivine-melilitite composition (Venanzite) and their bearing on the genesis of Italian Alkaline-Potassic magmas. Plinius 1, 48-49.

Conticelli, S, Francalanci, L, Manetti, P, Cioni, R, Sbrana, A., 1997. Petrology and Geochemistry of the ultrapotassic rocks from the Sabatini Volcanic District, Central Italy: the role of evolutionary processes in the genesis of variably enriched alkaline magmas. J. Volcanol. Geoth. Res. 75, 107-136.

Conticelli, S., Francalanci, L., Manetti, P., Peccerillo, A., 1987. Evolution of Latera Volcano: evidence from major and trace element chemistry of pyroclastic rocks. Periodico Mineralogia 56, 175-199.

Conticelli, S., Francalanci, L., Manetti, P., Peccerillo, A., Santo, A.P. (1986). Caratteristiche composizionali dei prodotti dell'apparato di Latera (Monti Vulsini, Lazio Settentrionale) e loro significato vulcanologico. Memorie della Società Geologica Italiana 35, 715-726.

Conticelli, S, Francalanci, L, Santo, AP, 1991. Petrology of the final stage Latera lavas: Mineralogical, Geochemical and Sr-isotopic data and their bearing on the genesis of some potassic magmas in Central Italy. J. Volcanol. Geoth. Res. 46, 187-212.

Conticelli, S, Guarnieri, L, Farinelli, A, Mattei, M, Avanzinelli, R Bianchini, G, Boari, E, Tommasini, S, Tiepolo, M, Prelévic, D, Venturelli, G, 2009a. Trace elements and Sr-Nd-Pb isotopes of K-rich to shoshonitic and calc-alkalic magmatism of the Western Mediterranean region: genesis of ultrapotassic to calc-alkalic magmatic associations in post-collisional geodynamic setting. Lithos 107, 68-92.

Conticelli, S, Manetti, P, Menichetti, S, 1992. Petrology, Chemistry, Mineralogy and Sr-isotopic features of Pliocenic Orendites from South Tuscany: implications on their genesis and evolutions. Europ. J. Mineral. 4, 1359-1375.

Conticelli, S., Manetti, P., Peccerillo, A., Santo, A.P. 1986. Caratteri petrologici delle vulcaniti potassiche italiane: considerazioni genetiche e geodinamiche. Memorie della Società Geologica Italiana, vol. 35, pp. 775÷783.

Conticelli, S., Marchionni, S., Rosa, D., Giordano, G., Boari, E., Avanzinelli, R., 2009b. Shoshonite and sub-alkaline magmas from an Ultrapotassic Volcano: Sr-Nd-Pb isotope data on the Roccamonfina volcanic rocks, Roman Magmatic Province, Southern Italy. Contrib. Mineral. Petrol. 157, 41-63.

Conticelli, S., Melluso, L., Perini, G., Avanzinelli, R., Boari, E., 2004. Petrologic, geochemical, and isotopic characteristics of potassic and ultrapotassic magmatism in Central-Southern Italy: inferences on its genesis and on the nature of mantle sources. Periodico Mineralogia 73, 153-164.

Conticelli, S., Peccerillo, A., 1990. Petrological significance of high-pressure ultramafic xenoliths from ultrapotassic rocks of Central Italy. Lithos 24, 305-322.

Conticelli, S., Peccerillo, A., 1992. Petrology and geochemistry of potassic and ultrapotassic alkalic volcanism in Central Italy: petrogenesis and interferences on the mantle source. Lithos 28, 21-240.

Conticelli, S., Poli, G., Boni, S., Braschi, E., 2011a. Trace elements and Sr-Nd-Pb isotopes of Capraia and Zenobito Volcanoes, Corsica Magmatic Province: occurrence of within plate magmatism in a post-collisional geodynamic environment. Contrib. Mineral. Petrol., submitted.

Conticelli, S., Poli, G., Marchionni, S., 2011c. Transition from high-potassium calc-alkaline to shoshonite and lamproite-like rocks in post-collisional setting: petrologic and Sr-Nd-Pb isotopic data from Monte Cimino volcano, Central Italy. Europ. J. Mineral., in preparation.

Cortini, M., Hermes, O.D., 1981. Sr-isotopic evidence for a multi-source origino f the Potassic Magmas in the Neapolitan area (South Italy). Contrib. Mineral. Petrol. 77, 47-55.

Cortini, M., Roberti, N., Scandone, R., 1973. Geologia e paleomagnetismo del Vulcano Roccamonfina. Ann. Geofis. 28 (2-3), 129-138.

Cox, K., Hawkesworth, C.J., O'Nions, R.K., and Appleton, J.D., 1976. Isotopic evidence for the derivation of some Roman region volcanics from anomalously enriched mantle. Contrib. Mineral. Petrol. 56, 173-180.

Crisci, G.M., De Francesco, A.M., Mazzuoli, R., Poli, G., Stanzione, D., 1989. Geochemistry of recent volcanics of Ischia Island, Italy: Evidences for fractional crystallization and magma mixing. Chem. Geol. 78, 15-33.

Cross, W., 1897. Igneous rocks of the Leucite Hills and Pilot Butte, Wyoming. Am. J. Sci. 14, 115-141.

Cundari, A., 1979. Petrogenesis of Leucite-bearing lavas in the Roman volcanic region, Italy. The Sabatini Lavas. Contrib. Mineral. Petrol. 70, 9-21.

Cundari, A., Ferguson, A.K., 1982. Significance of the pyroxene chemi stry from Leucite-bearing and related assemblages. Tsch. Mineral. Petrol. Mitt. 30, 189-204.

Cundari, A., Ferguson, A.K., 1991. Petrogenetic relationships between melilitite and lamproite in the Roman Comagmatic Region: the lavas of San Venanzo and Cupaello. Contrib. Mineral. Petrol. 107, 343-357.

D'Agostino, N., Avallone, A., Cheloni, D., D'Anastasio, E., Mantenuto, S., Selvaggi, G., 2008. Active tectonics of the Adriatic region from GPS & earthquake slip vectors. J. Geophys. Res. 113, B12413 10.1029/2008JB005860

D'Agostino N., Cheloni, M., Selvaggi, G., Michelini, A., Zuliani F., 2005. Strain accumulation in the Southern Alps (NE Italy) and deformation at the north-eastern boundary of Adria observed by CGPS measurements. Geophys. Res. Lett. 32, 10.1029/2005GL024266

D'Agostino, N., Giuliani, R., Mattone, M., Bonci, L., 2001. Active crustal extension in the Central Apennines (Italy) inferred from GPS measurements in the interval 1994–1999. Geophys. Res. Lett. 28, 2121-2124.

D'Agostino, N., Selvaggi, G., 2004. Crustal motion along the Eurasia-Nubia plate boundary in the Calabrian Arc and Sicily and active extension in the Messina Straits from GPS measurements. J. Geophys. Res. 109, B11402, 10.1029/2004JB002998

Danese, E. Mattei, M., 2010. The sedimentary substrate of the Colli Albani volcano. In Funiciello, R. & Giordano, G. (eds): The Colli Albani Volcano. Special Publications of IAVCEI, 3. The Geological Society of London, London, 141–151.

D'Antonio, M., Civetta, L., Di Girolamo, P., 1999b. Mantle source heterogeneity in the Campanian Region (South Italy) as inferred from geochemical and isotopic features of mafic volcanic rocks with shoshonitic affinity. Mineral. Petrol. 67, 10.1007/BF01161520

D'Antonio M., Di Girolamo P., 1994. Petrological and geochemical study of mafic shoshonitic volcanics from Procida-Vivara and Ventotene Islands (Campanian Region, South Italy). Acta Vulcanologica 5, 69-80.

D'Antonio, M., Civetta, L., Orsi, G., Pappalardo, L., Piochi, M., Carandente, A., de Vita, S., Di Vito, M.A., Isaia, R., 1999a. The present state of the magmatic system of the Campi Flegrei caldera based on a reconstruction of its behavior in the past 12 ka. J. Volcanol. Geother. Res. 91, 247-268.

D'Antonio, M., Tilton, G.R., Civetta, L., 1996. Petrogenesis of Italian Akaline lavas deduced from Pb-Sr-Nd Isotope relationships. In: "Earth Processes: Reading the Isotope Code", Basu, A., and Hart S. (edts.) A.G.U., Geophysical Monograph 95, 253-267.

Dal Negro, A., Carbonin, S., Salviulo, G., Piccirillo, E.M., Cundari, A., 1985. Crystal-chemistry and site configuration of the clinopyroxene from leucite-bearing rocks and related genetic significance: The Sabatini lavas, Roman Region, Italy. J. Petrol., 26, 1027-1040.

Dal Piaz, G.V., Venturelli, G., Scolari, A., 1979. Calc-alkaline to ultrapotassic postcollosional volcanic activity in the internal Northwestern Alps. Memorie Società Geologica Università di Padova 32, 4-16.

Daly, R.A., 1910. Origin of the Alkaline Rocks. Bull. Geol. Soc. Am. 21, 87-118.

De Astis, G., Kempton, P.D., Peccerillo A., Wu T.W., 2006. Trace element and isotopic variations from Mt. Vulture to Campanian volcanoes: constraints for slab detachment and mantle inflow beneath southern Italy. Contrib. Mineral. Petrol. 151, 331-351.

De Astis, G., Pappalardo, L., Piochi, M., 2004. Procida volcanic history: new insights into the evolution of the Phlegraean Volcanic District (Campania region, Italy). Bull. Volcanol. 66, 622-641.

De Benedetti, A.A., Funiciello, R., Giordano, G., Diano, G., Caprilli, E., Paterne, M., 2008. Volcanology, history and miths of the Lake Albano maar (Colli Albani volcano, Italy). J. Volcanol. Geother. Res. 176, 387–406.

De Fino, M., La Volpe, L., Peccerillo, A., Piccarreta, G., Poli, G., 1986. Petrogenesis of Monte Vulture volcano (Italy): inferences from mineral chemistry, major and trace element data. Contrib. Mineral. Petrol. 92, 135-145.

Deino, A.L., Orsi, G., De Vita, S., Piochi, M., 2004. The age of the Neapolitan Yellow Tuff caldera-forming eruption (Campi Flegrei caldera, Italy) assessed by $^{40}Ar/^{39}Ar$ dating method. J. Volcanol. Geother. Res. 133, 157–170.

Dellino, P., Isaia, R., La Volpe, L., Orsi, G., 2001. Statistical analyses of textural data from complex pyroclastic deposits: inplications for fragmentation processo f the Aganano Monte Spina Eruption (4.1 ka). Phlegrean Fields, southern Italy. Bull. Volcanol., 63, 443-461.

Del Moro, A., Fulignati, P., Marianelli, P., Sbrana, A., 2001. Magma contamination by direct wall rock interaction: constraints from xenoliths from the walls of a carbonate-hosted magma chamber (Vesuvius 1944 eruption). J. Volcanol. Geother. Res. 112, 15-24.

De Rita, D., Di Filippo, M., Rosa, C., 1996. Structural evolution of the Bracciano volcano-tectonic depression, Sabatini volcanic district, Italy. In: “Volcano Instability on the Earth and other Planets”, W.J. McGuire, A.P. Jones and J. Neuberg (edts.), Geol. Soc. London, Spec. Pub. 110, 225-236.

De Rita, D., Di Filippo, M., Sposato, A., 1993b. Carta Geologica del Complesso Vulcanico Sabatino. In: "Sabatini Volcanic Complex", Di Filippo, M. (edt.), Quaderni de La Ricerca Scientifica, 114(11).

De Rita, D., Faccenna, C., Funicello, R., Rosa, C. 1995. Stratigraphy and Volcano-Tectonics. In: R. Trigila (ed.) The volcano of the Alban Hills. Roma, 33-71.

De Rita, D., Funiciello, R., Corda, L., Sposato, A., Rossi, U., 1993a. Volcanic Units. In: "Sabatini Volcanic Complex", Di Filippo, M. (edt.), Quaderni de La Ricerca Scientifica, 114(11), 33-79.

De Rita, D., Funiciello, R., Rossi, U., Sposato, A., 1983. Structure and evolution of the Sacrofano-Baccano Caldera, Sabatini Volcanic Complex, Rome. J. Volcanol. Geotherm. Res., 17, 219-236.

De Rita, D., Funiciello, R., Sposato, A., 1988. Complessi Vulcanici. In: "Carta delle Litofacies del Lazio-Abruzzo ed arewe limitrofe. Note Illustrative", Accordi, G., Carbone F. (edts.), Quaderni de La Ricerca Scientifica, 114, 201-215.

De Rita, D., Giordano, G., 1996. Volcanological and structural evolution of Roccamonfina volcano (southern italy). In: “Volcano instability on the Earth and other Planets”, Mc Guire, W.J., Jones, A.P., Neuberg J. (edts), Geol. Soc. London, Spec. Pub. 110, 209-224.

De Rita, D., Giordano, G., Cecili, A., 2001. A model for submarine rhyolite dome growth: Ponza Island (central Italy). J. Volcanol. Geother. Res. 107, 221-239.

De Rita, D., Giordano, G., Esposito, A., Fabbri, M., Rodani, S., 2002. Large volume phreatomagmatic ignimbrites from the Colli Albani volcano (Middle Pleistocene, Italy). J. Volcanol. Geotherm. Res. 118, 77-98.

De Rita, D., Giordano, G., Milli, S., 1998. Forestepping-Backstepping stacking pattern of volcaniclastic successions: Roccamonfina volcano (Italy). J. Volcanol. Geother. Res. 80, 155-178.

De Rita, D., Sposato, A., 1986. Correlazione tra eventi esplosivi ed assetto strutturale del substrato sedimentario del complesso vulcanico Sabatino. Memorie Società Geologica Italiana 35, 727-733.

De Rita, D., Zanetti, G., 1986. Caratteri vulcanologici e deposizionali selle piroclastiti di Stracciacappe (Sabatini Orientali, Roma). Memorie Società Geologica Italiana 35, 667-677.

de Vita, S., Orsi, G., Civetta, L., Carandente, A., D'Antonio, M., Deino, A., di Cesare, T., Di Vito, M.A.R., Fisher, V., Isaia, R., Marotta, E., Necco, A., Ort, M., Pappalardo, L., Piochi, M., Southon, J., 1999. The Agnano–Monte Spina eruption (4100 years BP) in the restless Campi Flegrei caldera, Italy. J.Volcanol.Geother. Res. 91, 269-301

De Vivo, B., Rolandi, G., Gans, P.B., Calvert, A., Bohrson, W.A., Spera, F.J., Belkin, H.E., 2001. New constraints on the pyroclastic eruptive history of the Campanian volcanic plain (Italy). Mineral. Petrol. 73, 47–65.

De Vivo, B.D., Scandone, R., Trigila R. (eds) 1993. Mount Vesuvius. J. Volcanol Geoth. Res. 58, 1-387.

Dewey, J.F., Helman, M.L., Turco, E., Hutton, D.H.W., Knott, S.D., 1989. Kinematics of the Western Mediterranean. In: Alpine Tectonics, Coward, M.P., Dietrich, D., Park, R.G. (eds.), Geol. Soc. London, Spec. Pub. 45, 265-283.

Di Battistini, G., Montanini, A., Vernia, L., Bargossi, G.M., Castorina, F., 1998. Petrology and geochemistry of ultrapotassic rocks from the Montefiascone Volcanic Complex (Central Italy): magmatic evolution and petrogenesis. Lithos 43. 169-195.

Di Battistini, G., Montanini, A., Vernia, L., Venturelli, G., Tonarini, S., 2001. Petrology of melilite-bearing rocks from the Montefiascone Volcanic Complex (Roman Magmatic Province): new insights into the ultrapotassic volcanism of Central Italy. Lithos 59, 1-24.

Di Bona, M., Lucente, F.P., Piana Agostinetti, N., 2008. Crustal structure and Moho depth profile crossing the central Apennines (Italy) along the N42 degree parallel. J. Geophys. Res. 113. 10.1029/2008JB005625

Di Girolamo, P., Franciosi, L., Melluso, L., Morra, V., 1996. The calc-alkaline rocks of the Campanian plain: new mineral chemical data and possible link with acidic rocks of the Pontine Island. Periodico Mineral. 65, 305-316.

Di Girolamo, P., Ghiara, M.R., Lirer, L., Munno, R., Rolandi, G., Stanzione, D., 1984. Vulcanologia e petrologia dei Campi Flegrei. Bollettino Società geologica Italiana, 103, 349-413.

Di Girolamo, P., Melluso, L., Morra, V., 1991, Magmatic activity of Roccamonfina volcano (Southern Italy): Petrology, geochemistry and relationships with campanian volcanics: Neus Jb. Mineral Petrol. Abh. 163, 271-289.

Di Girolamo, P., Melluso, L., Morra, V., Secchi, F.A.G., 1995. Evidence of interaction between mafic and intermediate magmas in the youngest activity phase at Ischia Island. Periodico Mineralogia 64, 393-411.

Di Girolamo, P., Nardi., G., Rolandi, G., Stanzione, D., 1976. Occurrence of calk-alkaline two-pyroxene andesites from deep bore-holes in the Phlegrean Fields. 1 – Petrographic and petrochemical data. Rend. Accademia Scienze Fisiche Matematiche XLIII, 1-29.

Di Renzo, V., Di Vito, M.A., Arienzo, I., Carandente, A., Civetta, L., D'Antonio, M., Giordano, F., Orsi, G., Tonarini, S., 2007. Magmatic history of Somma-Vesuvius on the basis of new geochemical and isotopic data from deep borehole (Camaldoli della Torre). J. Petrol. 48, 753-781.

Di Vito, M.A., Isaia, R., Orsi, G., Southon, J., de Vita, S., D'Antonio, M., Pappalardo, L., Piochi, M., 1999. Volcanic and deformational history of the Campi Flegrei caldera in the past 12 ka. J. Volcanol. Geoth. Res. 91, 221-246.

Doglioni, C., Harabaglia, P., Merlini, S., Mongelli, F., Peccerillo, A., 1999. Orogens and slabs vs. their direction of subductions. Earth Sci. Rev. 45, 167-208.

Dolfi, D., 1981. Considerazioni petrologiche su alcuni eietti a clinopirosseno e flogopite nelle vulcaniti della Media Valle Latina. Periodico Mineralogia 50, 199-214.

D'Orazio, M, Innocenti, F, Tonarini, S, Doglioni, C, 2007. Carbonatites in a subduction system: the Pleistocene Alvikites from Mt. Vulture (Southern Italy). Lithos 98. 313-334.

D'Orazio, M., Innocenti, F., Tonarini, S., Doglioni C., 2008. Reply to the discussion of "Carbonatites in a subduction system: the Pleistocene Alvikites from Mt. Vulture (Southern Italy)" by D'Orazio, M., Innocenti, F., Tonarini, S., Doglioni, C. (Lithos 98, 313-334) by F. Stoppa, C. Principe, and P. Giannandrea. Lithos 103, 557-561.

D'Orazio, M., Laurenzi, MA., Villa, IM., 1991. $^{40}Ar/^{39}Ar$ dating of a shoshonitic lava flow of the Radicofani volcanic center (Southern Tuscany). Acta Vulcanologica 1, 63-67.

D'Oriano, C., Poggianti, E., Bertagnini, A., Cioni, R., Landi, P., Polacci, M., Rosi, M., 2005. Changes in eruptive style during the A.D. 1538 Monte Nuovo eruption (Phlegrean Fields, Italy): the role of syn-eruptive crystallization. Bull. Volcanol. 67, 601-621.

Downes, H., Kostoula, T., Jones, A.P., Beard, A.D., Thirlwall, M.F., Bodinier, J.-L., 2002. Geochemistry and Sr–Nd isotopic compositions of mantle xenoliths from the Monte Vulture carbonatite–melilitite volcano, central southern Italy. Contrib. Mineral. Petrol., 144: 78–92.

Durazzo, A., Taylor, L.A., Sherwais, J.W., 1984. Ultramafic lamprophyres in a carbonate platform environment, Mt. Queglia, Abruzzo, Italy. N. Jahrb. Miner. Abh. 150, 199-217.

Edgar, A.D. 1987. The genesis of alkaline magmas with emphasis on their source regions: inferences from experimental studies. In: "Alkaline Igneous Rocks", Fitton, J.G., Upton, B.G.J. (eds.), London, Geol. Soc. Spec. Pub., 29-52.

Edgar, A.D., Condliffe E., Barnett, R.L., Shirran, R.J., 1980. An experimental study of an olivine Ugandite magma and mechanisms for the formations of its K-enriched derivatives. J. Petrol. 21, 475-497.

Ellam, R.M., Menzies, M.A., Hawkesworth, C.J., Leeman, W.P., Rosi, M., Serri, G., 1988. The transition from calc-alkaline to potassic orogenic magmatism in the Aeolian Islands, Southern Italy. Bull. Volcanol. 50, 386-398.

Ellam, R.M., Hawkesworth, C.J., 1988. Elemental and isotopic variations in subduction related basalts: evidence for a three component model. Contrib. Mineral. Petrol. 98, Number 1, 72-80.

Elliott, T. 2003. Tracers of the slab. In: Inside the Subduction Factory, Eiler, J. (edt.), Geophys. Monograph 138, Am. Geophys. Union, 23–45.

Elliott, T., Plank, T., Zindler, A., White, W., Bourdon, B., 1997. Element transport from slab to volcanic front at the Mariana arc. J. Geophys. Res. 102, 14991-15019.

Evernden, J.F., Curtis, G.H., 1965. The potassium-argon dating of late Cenozoic rocks in East Africa and Italy. Current Antropology 6, 343-385.

Faccenna, C., Funiciello, F., Giardini, D., Lucente, P., 2001. Episodic back-arc extension during restricted mantle convection in the Central Mediterranean. Earth Planet. Sci. Lett. 187, 105-116.

Faccenna, C., Funiciello, R., Bruni, A., Mattei, M., Sagnotti, L., 1994a. Evolution of a transfer-related basin: the Ardea basin (Latium, central Italy). Basin Research 6, 35-46.

Faccenna, C., Funiciello, R., Mattei, M. 1994c. Late Pleistocene N-S shear zones along Latium Tyrrhenian margin: structural characters and volcanological implications. Boll. Geofis. Teorica Applicata 36, 141-144.

Faccenna C., Funiciello R., Montone P., Parotto M., 1994b. An example of late Pleistocene strike-slip tectonics: the Acque Albule basin (Tivoli, Latium). Memorie Descrittive della Carta Geologica d'Italia 49, 37-50.

Faccenna, C., Mattei, M., Funiciello, R., Jolivet, L., 1997. Styles of back-arc extension in the Central Mediterranean. Terra Nova 9, 126-130.

Faccenna, C., Piromallo, C., Crespo-Blanc, A., Jolivet, L., Rossetti, F., 2004. Lateral slab deformation and the origin of the western Mediterranean arcs. Tectonics 23, TC1012 10.1029/2002TC001488

Fazzini, P., Gelmini, R., Mantovani, M.P., Pellegrini, M., 1972. Geologia dei Monti della Tolfa (Lazio Settentrionale; province di Viterbo e Roma. Memorie Società Geologica Italiana 11, 65-144.

Fedele, L., Scarpati, C., Lanphere, M., Melluso, L., Morra, V., Perrotta, A., Ricci G., 2008. The Breccia Museo formation, Campi Flegrei, southern Italy: geochronology, chemostratigraphy and relationship with the Campanian Ignimbrite eruption. Bull. Volcanol. 70, 1189-1219.

Fedele, L., Morra, V., Perrotta, A., Scarpati, C., 2006. Volcanological and geochemical features of the products of the Fiumicello eruption, Procida island, Campi Flegrei (southern Italy). Periodico Mineralogia 75, 43-72.

Fedele, L., Zanetti, A., Morra, V., Lustrino, M., Melluso, L., Vannucci, R., 2009. Clinopyroxene/liquid trace element partitioning in natural trachyte–trachyphonolite systems: insights from Campi Flegrei (southern Italy). Contrib. Mineral. Petrol. 158, 337-356.

Federico, M., Peccerillo., A., 2002. Mineral chemistry and petrogenesis of granular ejecta from the Alban Hills volcano (Central Italy). Mineral. Petrol. 74, 223-252.

Ferrara, G., Laurenzi, M.A., Taylor, H.P. Jr, Tonarini, S., Turi, B. 1985. Oxygen and Sr- Isotope studies of K-Rich volcanic rocks from the Alban Hills, Italy. Earth Planet. Sci. Lett. 75, 13-28.

Ferrara, G., Tonarini, S., 1985. Radiometric geochronology in Tuscany: results and problems. Rendiconti della Società Italiana di Mineralogia e Petrologia 40, 110-124.

Ferrari, L., Conticelli, S., Burlamacchi, L., Manetti, P., 1996. Volcanological Evolution of the Monte Amiata Volcanic Center, Southern Tuscany, Central Italy: New Geological and Petrochemical data. Acta Vulcanologica 8, 41-56.

Florindo, F., Karner, D.B., Marra, F., Renne, P.R., Roberts, A.P., Weaver, R., 2007. Radioisotopic age constraints for Glacial Terminations IX and VII from aggradational sections of the Tiber River delta in Rome, Italy. Earth Planet. Sci. Lett. 256, 61-80.

Fisher, R.V., Orsi, G., Ort, M., Heiken, G., 1993. Mobility of a large-volume pyroclastic flow -- emplacement of the Campanian ignimbrite, Italy. J. Volcanol. Geoth. Res. 56, 205-220.

Foley, S.F., 1992a. Petrological characterisation of the source components of potassic magmas: geochemical and experimental constraints. Lithos 28, 187-204.

Foley, S.F., 1992b. Vein-plus-wall-rock melting mechanisms in the lithosphere and the origin of potassic alkaline magmas. Lithos 28, 435-453.

Foley, S.F., 1994. Geochemische und experimentelle Untersuchungen zur genese der kalireichen Magmatite. N. Jahrb. Mineral. Abath. 167, 1-55.

Foley, SF, Venturelli G, 1989. High-K_2O rocks with high MgO, high SiO_2, affinities. In Boninites, edited by AJ Crawford, London, Unwin Hyman, 72-88.

Foley, SF, Venturelli, G, Green, DH, Toscani, L, 1987. The ultrapotassic rocks: characteristics, classification and constraints for petrogenetic models. Earth Sci. Rev. 24, 81-134.

Fornaseri, M., 1985a. Geochronology of Volcanic rocks from Latium (Italy). Rendiconti Società Italiana Mineralogia Petrologia 40, 73-105.

Fornaseri, M., 1985b. Geochronology of Volcanic rocks from Umbria (Italy). Rendiconti Società Italiana Mineralogia Petrologia 40, 107-110.

Fornaseri, M., Scherillo, A., 1963. Petrografia dei Colli Albani. In: M., Fornaseri, A., Scherillo, U., Ventriglia (eds.) La Regione Vulcanica dei Colli Albani, Consiglio Nazionale delle Ricerche, 340-550.

Fornaseri, M., Scherillo, A., Ventriglia, U. 1963. La regione vulcanica dei Colli Albani. Consiglio Nazionale delle Ricerche, 561 pp.

Francalanci, L., Avanzinelli, R., Tommasini, S., Heumann, A., 2007. A west-east geochemical and isotopic traverse along the volcanism of the Aeolian Island arc, southern Tyrrheninan Sea, Italy: Inferences on mantle source processes. In: “Cenozoic Volcanism in the Mediterranean Area”, L. Beccaluva and M. Wilson (eds.), GSA Special Paper 418, 235-264.

Francalanci, L., Peccerillo, A., Poli, G., 1987. Partition coefficients for minerals in potassium-alkaline rocks: Data from Roman Province (Central Italy). Geochem. J. 21, 1-10.

Francalanci, L., Taylor, S.R., McCulloch, M.T., Woodhead, J.D., 1993. Geochemical and isotopic variations in the calc-alkaline rocks of Aeolian arc, southern Tyrrhenian Sea, Italy: constraints on magma genesis. Contrib. Mineral. Petrol. 113, 300-313.

Franzolin, E., Schmidt, M.W., Poli, S., 2009. Subsolidus and melting phase relations in the system $CaCO_3$-$MgCO_3$-$FeCO_3$ at 35 kbar: from experiments to predictions based on a thermodynamic model. Am. Geophys. Union, Fall Meeting 2009, abstract #V11D-1989.

Freda, C., Gaeta, M., Karner, D.B., Marra, F., Renne, P.R., Taddeucci, J., Scarlato, P., Christensen, J.N., Dallai, L., 2006. Eruptive history and petrologic evolution of the Albano multiple maar (Alban Hills, Central Italy). Bull. Volcanol. 68, 567-591.

Freda, C., Gaeta, M., Misiti, V., Mollo, S., Dolfi, D., Scarlato, P., 2007. Magma-carbonate interaction: an experimental study on ultrapotassic rocks from Colli Albani (Central Italy). Lithos 101, 397-415.

Freda, C., Gaeta, M., Palladino, D.M., Trigila, R., 1997. The Villa Senni Eruption (Alban Hills, Central Italy): the role of H_2O and CO_2 on the magma chamber evolution and on the eruptive scenario. J. Volcanol. Geoth. Res. 78, 103-120.

Freda, C., Palladino, D.M., Pignatti, S., Trigila, R., Onorati, G., Poscolieri, M., 1990. Volcano-tectonic scenario of Vulsini volcanoes (Central Italy) from LANDSAT-MSS images and digital elevation data. ISPRS J. Photogrammetry Remote Sensing 45, 316-328.

Frezzotti, M.L., De Astis G., Dallai, L. Ghezzo, C., 2007. Corexisting calc-alkaline and ultrapotassic magmatism at Monti Ernici, Mid Latina Valley (Latium, central Italy). Europ. J. Mineral. 19, 479-497.

Frezzotti, M.L., Peccerillo, A., Panza, G., 2009. Carbonate metasomatism and CO_2 lithosphere–asthenosphere degassing beneath the Western Mediterranean: An integrated model arising from petrological and geophysical data. Chem. Geol. 262, 108-120.

Frezzotti, M.L., Peccerillo, A., Panza, G., 2010. Earth's CO_2 degassing in Italy. In: "The Geology of Italy", Beltrando, M., Peccerillo, A., Mattei, M., Conticelli, S., Doglioni, C., J. Virtual Explorer, paper 29.

Fuliganti, P., Marianelli, P., Metrich, N., Santacroce, R., Sbrana, A., 2004. Towards a reconstruction of the magmatic feeding system of the 1944 eruption of Mt. Vesuvius. Journal Volcanology and geothermal research 133, 13-22.

Funiciello, F., Faccenna, C., 2010. Unraveling the geodynamics of the Central Mediterranean in a tank. In: "The Geology of Italy", Beltrando, M., Peccerillo, A., Mattei, M., Conticelli, S., Doglioni, C., J. Virtual Explorer, paper 16.

Funiciello, R., Giordano, G., De Rita, D., 2003. The Albano maar lake (Colli Albani Volcani, Italy): recent volcanic activity and evidence of pre-Roman age catastrophic lahar events. J. Volcanol. Geoth. Res. 123, 43-61.

Funiciello, R., Parotto, M., 1978. Il substrato sedimentario nell'area dei Colli Albani: considerazioni geodinamiche e paleogeografiche sul margine tirrenico dell'appennino Centrale. Geologica Romana 17, 233-287.

Funiciello, R., Praturlon, A., Giordano, G., 2008. La Geologia di Roma. Dal centro storico alla periferia. Memorie Descrittive della Carta Geologica d'Italia, LXXX, volume 1, 1-443.

Gaeta, M., Fabrizio, G. & Cavarretta, G. 2000. F-phlogopite in the Alban Hills Volcanic District (Central Italy): indications regarding the role of volatiles in magmatic crystallisation. J. Volcanol. Geoth. Res. 99, 179-193.

Gaeta, M., Freda, C., Christensen, J.N., Dallai, L., Marra, F., Karner, D.B. & Scarlato, P. 2006. Time-dependent geochemistry of clinopyroxene from the Alban Hills (Central Italy): clues to the source and evolution of ultrapotassic magmas. Lithos, 86, 330-346.

Gaeta, M., Di Rocco, T., Freda, C. 2009. Carbonate Assimilation in Open Magmatic Systems: the Role of Melt-bearing Skarns and Cumulate-forming Processes. J. Petrol. 50, 361 – 385.

Gallo, F., Giammetti, F., Venturelli, G., Vernia, L., 1984. The kamafugitic rocks of San Venanzo and Cupaello, Central Italy. N. Jahrb. Mineral. Monat. 1984, 198-210.

Gagnevin, D., Daly, J.S., Poli, G., 2004. Petrographic, geochemical and isotopic contraints on magma dynamics and mixing in the Miocene Monte Capanne pluton (Elba Island, Italy). Lithos 78, 157-195.

Gagnevin, D., Daly, J.S., Poli, G., Morgan, D., 2005a. Microchemical and Sr isotopic investigation of zoned K-feldspar megacrysts: insights into the petrogenesis of a granitic system and disequilibrium crystal growth. J. Petrol. 46, 1689-1724.

Gagnevin, D., Daly, J.S., Waight, T.E., Morgan, D., Poli, G., 2005b. Pb isotopic zoning of K-feldspar megacrysts determined by laser ablation multiple-collector ICP-MS: insights into granite petrogenesis. Geochim. Cosmochim. Acta 69, 1899-1915.

Gagnevin, D., Waight, T.E., Daly, JS, Poli, G., Conticelli, S., 2007. Insights into magmatic evolution and recharge history in Capraia Volcano (Italy) from chemical and isotopic zoning in plagioclase phenocrysts. J. Volcanol. Geoth. Res. 168, 28-54.

Gasparon, M., Rosembaum, G., Wijbrans, J., Manetti, P., 2008. The transition from subduction arc to slab tearing: Evidence from Capraia Island, northern Tyrrhenian Sea. J. Geodyn. 47, 1 30-38.

Gasparini, P., and Adams, J.A.S., 1969. K-Ar dating of Italian Plio-pleistocene volcanic rocks. Earth Planet. Sci. Lett. 6, 225-230.

Gasperini, D., Blichert-Toft, J., Bosch, D., Del Moro, A., Macera, P., Albarede, F., 2002. Upwelling of deep mantle material through a plate window: evidence from the geochemistry of Italian basaltic volcanics. J. Geophys. Res. 107, 10.1029/2001JB000418

Ghiara, M.R., Lirer, L., 1978. Mineralogy and Geochemistry of the "Low Potassium" Series of the Roccamonfina volcanoc suite. Bull. Volcanol. 40/41, 39-56.

Ghiara, M.R., Lirer, L., Stanzione, L., 1973. Contributo alla conoscenza vulcanologica e petrografica del vulcano di Roccamonfina. Periodico Mineralogia 42, 267-293.

Giaccio, B., Marra, F., Hajdas, I., Karner, D.B., Renne, P.R., Sposato, A., 2009. $^{40}Ar/^{39}Ar$ and ^{14}C geochronology of the Albano maar deposits: Implications for defining the age and eruptive style of the most recent explosive activity at Colli Albani Volcanic District, Central Italy. J. Volcanol. Geotherm. Res. 185, 203-213.

Giannandrea, P., Principe, C., La Volpe, L., Schiattarella, M., 2006. Unità stratigrafiche a limiti inconformi e storia evolutiva del vulcano medio-pleistocenico di Monte Vulture (Appennino meridionale, Italia). Bollettino Societa Geologica Italiana 125, 67-92,

Giannetti, B., 1964. Carta Geopetrografica della caldera vulcanica di Roccamonfina. Grafica Editoriale Cartografica, Via Tiburtina 1099, Roma.

Giannetti, B., 1996. Volcanology of trachytic and associated basaltic pyroclastic deposits at Roccamonfina volcano, Roman region, Italy. J. Volcanol. Geoth. Res. 71, 229-248.

Giannetti, B., 2001. Origin of the calderas and evolution of Roccamonfina volcano (Roman Region, Italy). J. Volcanol. Geoth. Res. 106, 301-319.

Giannetti, B., De Casa, G., 2000. Stratigraphy, chronology and sedimentology of the White Trachytic Tuff, Roccamonfina volcano, Italy. J. Volcanol. Geotherm. Res. 96, 243-295.

Giannetti, B., De Casa, B., 2001. Origin of the calderas and evolution of Roccamonfina volcano (Roman Region, Italy). J. Volcanol. Geoth. Res. 71, 229-248.

Giannetti, B., Ellam, R., 1983. The primitive lavas of Roccamonfina volcano, Roman region, Italy: new constraints on melting processes and source mineralogy. Contrib. Mineral. Petrol. 116, 21-31.

Giannetti, B., Luhr, J.F., 1983. The white trachitic tuff of Roccamonfina volcano (Roman Region, Italy). Contrib. Mineral. Petrol. 84, 235-252.

Giannetti, B., Masi, U., 1929. Trace element behaviour during weathering of leucite in potassic rocks from the Roccamonfina volcano (Campania, Southern Italy) and environmental implications. Lithos 22, 317-324.

Giannetti, B., Nicoletti, M., Petrucciani, C., 1979. Datazioni K-Ar di lave leucitiche dello strato-vulcano di Roccamonfina. Rendiconti Società Italiana Minerogia Petrologia 35, 349-354.

Gillot, P.Y., 1988. Island of Ischia - 7. Geochronology. In: “Island of Ischia„, Vezzoli L. (edt.), , Quaderni de La Ricerca Scientifica 114(10), 93-95.

Gillot, P.Y., Chiesa, S., Pasquaré, G., Vezzoli, L., 1982. <33,000-yr K-Ar dating of the volcano-tectonic horst of the Isle of Ischia, Gulf of Naples. Nature 299, 242-244.

Giordano, G., 1998a. Facies characteristics and magma-water interaction of the White Trachytic Tuffs (Roccamonfina Volcano, Italy). Bull. Volcanol. 60, 10-26.

Giordano, G., 1998a. Facies characteristics and magma-water interaction of the White Trachytic Tuffs (Roccamonfina Volcano, Italy). Bull. Volcanol. 60, 10-26.

Giordano, G., 1998b. The effect of paleotopography on lithic distribution and facies associations of small volume ignimbrites: an insight into transport and depositional systems of WTT Cupa deposits (Roccamonfina volcano, Italy). J. Volcanol. Geother. Res. 87, 255-273.

Giordano, G. and C.A.R.G. team, 2010. Stratigraphy and volcano-tectonic structures of the Colli Albani volcanic field. In: “The Colli Albani Volcano” Funiciello, R., Giordano, G. (eds), Special Publications of IAVCEI, 3. Geol. Soc. London, London, 15-45.

Giordano, G., De Benedetti, A.A., Diana, A., Diano, G., Gaudioso, F., Marasco, F., Miceli, M., Mollo, S., Cas, R.A.F., Funiciello, R., 2006. The Colli Albani caldera (Roma, Italy): stratigraphy, structure and petrology. J. Volcanol. Geoth. Res. 155, 49-80.

Giordano, G., Scrocca, D., Naso, G., Funiciello, R., Catalani, F., 1995. Processi di estensione e circolazione di fluidi a bassa termalità nella piana di Riardo (Caserta). Bollettino Società Geologica Italiana 114, 361-371.

Goes, S., Giardini, D., Jenny, S., Hollenstein, C., Kahleb, H.G., Geigerb, A., 2004. A recent tectonic reorganization in the south-central Mediterranean. Earth Planet. Sci. Lett. 226, 335-345.

Gragnani, R., 1972. Le vulcaniti melilitiche di Cupaello (Rieti). Rendiconti Società Italiana di Mineralogia e Petrologia 28, 165-189.

Grapes, R.H., 2006. Pyrometamorphism. Springer-Verlag, Berlin, Heidelberg, 1-275.

Green T.H., Adam, J., Siel, S.H., 1992. Trace element partitioning between silicate minerals and carbonatite at 25 kbar and application to mantle metasomatism. Mineral. Petrol. 46: 179-184.

Guest, J.E., Duncan, A.M., Chester, D.K., 1988. Monte Vulture Volcano (Basilicata, Italy): an analysis of morphology and volcaniclastic facies. Bull. Volcanol. 50, 244–257.

Gurioli, L., Houghton, B.F., Cashman, K.V., Cioni, R., 2005. Complex changes in eruption dynamics during the 79 AD eruption at Vesuvius. Bull. Volcanol. 67, 144-159.

Hart, S.R., Hauri, E.H., Oschmann, L.A., Whitehead J.A., 1992. Mantle plumes and entrainment—Isotopic evidence, Science 256, 517–520.

Hawkesworth, C. J., Kempton, P.D., Rogers, N.W., Ellam, R.M., val Carlsteren, P.W., 1990. Continental mantle lithosphere and shallow level enrichments processes in Earth’s mantle. Earth Planet. Sci. Lett. 96, 256-268.

Hawkesworth, C. J., Turner, S. P., Peate, D. W., McDermott, F., van Calsteren, P., 1997. U-Th isotopes in arc magmas: implications for element transfer from the subducted crust. Science,276, 551-555.

Hawkesworth, C.J., Vollmer, R., 1979. Crustal contamination versus enriched mantle: $^{143}Nd/^{144}Nd$ and $^{87}Sr/^{86}Sr$ evidence from the Italian volcanics. Contrib. Mineral. Petrol. 69, 151-165.

Hermann, J., 2002. Allanite: thorium and light rare earth element carrier in subducted crust. Chem. Geol. 192, 289-306.

Hermann, J., Spandler, C., Hack, A., Korsakov, A.V., 2006. Aqueous fluids and hydrous melts in high-pressure and ultra-high pressure rocks: Implications for element transfer in subduction zones. Lithos 92, 399-417.

Hieke Merlin, O., 1964. Le vulcaniti del settore Nord-Orientale del Monte Vulture. Memorie degli istituti di geologia e Mineralogia dell'Università di Padova XXVI, 1-74.

Hieke Merlin, O., 1967. I prodotti vulcanici del Monte Vulture. Memorie degli istituti di geologia e Mineralogia dell'Università di Padova XXVI, 1-65.

Hoefs, J., 2010. Geochemical fingerprints: a critical appraisal. Europ. J. Mineral. 22, 3-16.

Holm, P.M., 1982. Mineral chemistry in perpotassic lavas of the Vulsinian District, the Roman Province, Italy. Mineral. Mag. 46, 379-386.

Holm, P.M., Lou, S., Nielsen, Å, 1982. The geochemistry and petrogenesis of the lavas of the Vulsinian District, Roman province, Central Italy. Contrib. Mineral. Petrol. 80, 367-378.

Holmes, A., 1940. Basaltic lavas of south Kivu, Belgian Congo. Geol. Mag. 77, 89-101.

Holmes, A., Harwood, H.F., 1932. Petrology of the volcanic fields East and South-East of Ruwenzori, Uganda. Quarter. J. Geol. Soc. of London, 88, 370-442.

Horvath, F., Berckheimer, H., 1982. Mediterranean backarc-basins. In: H. Berckheimer and K. Hsü (Edts), Alpine-Mediterranean-Geodynamics. AGU Geodynamics Series, 141-163.

Hunstad, I., Selvaggi, G., D'Agostino, N., England, P., Clarke, P., Pierozzi, M., 2003. Geodetic strain in peninsular Italy between 1875 and 2001. Geophys. Res. Lett. 30, 1181 10.1029/2002GL016447.

Hunziker, J.C., 1974. Rb-Sr age determination and the Alpine tectonic history of the Western Alps. Memorie Istituto Geologia e Mineralogia Università di Padova 31, 1-54.

Iacono-Marziano, G., Gaillard, F., Pichavant, M., 2007. Limestone Assimilation and the origin of CO_2 emissions at the Alban Hills (Central Italy): constraints from experimental petrology. J. Volcanol. Geoth. Res. 155, 719-738.

Iacono-Marziano, G., Gaillard, F., Pichavant, M., 2008. Limestone assimilation by basaltic magmas: an experimental re-assessment and application to Italian volcanoes. Contrib. Mineral. Petrol. 155, 719-738.

Innocenti, F, 1967. Studio chimico-petrografico delle vulcaniti di Radicofani. Rendiconti Società Italiana di Mineralogia Petrologia 13, 99-128.

Incoronato, A., Nardi, G., Ortolani, F., Pagliuca, S. 1985. The Plio-Quaternary Bagnoli Irpino-Calaggio torrent strike-slip fault. Campania-Lucania (southern apennines). Bollettino Società Geologica Italiana 104, 399-404.

Innocenti, F., Serri, G., Manetti, P., Ferrara, G., Tonarini, S., 1992. Genesis and classification of the rocks of the Tuscan Magmatic Province: Thirty years after Marinelli's model. Acta Vulcanologica 2, 247-265.

Ippolito, F., Ortolani, F., Russo, M. 1973. Struttura marginale tirrenica dell'appennino campano: reinterpretazioni dei dati di antiche ricerche di idrocarburi. Memorie Società Geologica Italiana 12, 227-250.

Isaia, R., D'Antonio, M., Dell'Erba, F., Di Vito, M., Orsi, G., 2004. The Astroni volcano: the only example of closely spaced eruptions in the same vent area during the recent history of the Campi Flegrei caldera (Italy). J. Volcanol. Geoth. Res. 133, 171-192.

Johnson, M.C., and T. Plank (1999), Dehydration and melting experiments constrain the fate of subducted sediments. Geochem. Geophys. Geosys., G3 7, 1999GC000014.

Jolivet, L., Faccenna, C., Goffé, B., Mattei, M., Rossetti, F., Brunet, C., Storti, F., Funiciello, R., Cadet, J.P., D'Agostino, N., Parra, T., 1998. Midcrustal shear zones in postorogenic extension: Example from the northern Tyrrhenian Sea. J. Geophys. Res. 103, 12123-12160.

Jones, A.P., Kostoula, T., Stoppa, F., Wolley, A.R. 2000. Petrography and mineral chemistry of mantle xenoliths in a carbonate-rich melilitic tuff from Mt. Vulture volcano, southern Italy. Mineral. Mag. 64, 34q1-361.

Joron, J.-L., Metrich, N., Rosi, M., Santacroce, R., Sbrana, A., 1987. 3. Chemistry and petrography. In: “Somma-Vesuvio”, Santacroce, R. (Ed.), Progetto Finalizzato Geodinamica, Monografie Finali, vol. 8, Consiglio Nazionale della Ricerca, Quaderni de la Ricerca Scientifica 114, 105-174.

Karner, D.B., Marra, F., Florindo, F., Boschi, E 2001b. Pulsed uplift estimated from terrace elevations in the coast of Rome: evidence for a new phase of volcanic activity? Earth Planet. Sci. Lett. 188, 135-148.

Karner, D.B., Marra, F., Renne, P.R., 2001a. The history of the Monti Sabatini and Alban Hills volcanoes: groundwork for assessing volcano-tectonic hazard for Rome. J. Volcanol. Geoth. Res. 107, 185-219.

Karner, D.B., Renne, P.R, 1998. $^{40}Ar/^{39}Ar$ geochronology of Roman volcanic province tephra in the Tiber River valley: Age calibration of middle Pleistocene sea-level changes. Geol. Soc. Am. Bull. 110, 740-747.

Karner, D.B., Renne, P.R., McDougall, I., Becker, T., 2001c. The viability of leucite for $^{40}Ar/^{39}Ar$ dating and as a Quaternary standard. Chem. Geol. 177, 473-482.

Kastens, K., Mascle, J., Auroux, C., Bonatti, E., Broglia, C., Channell, J., Curzi, P., Emeis, K.-C., Glaçon, G., Hasegawa, S., Hieke, W., Mascle, G., McCoy, F., McKenzie, J., Mendelson, J., Müller, C., Réhault, J.P., Robertson, A., Sartori, R., Sprovieri, R., Torii, M., 1988. ODP Leg 107 in the Tyrrhenian Sea: Insights into passive margin and back-arc basin evolution. Geol. Soc. Am. Bull. 100, 1140-1156.

Kelemen, P.B., Rilling, J.L., Parmentier, E.M., Mehl, L., Hacker, B.R., 2003. Thermal structure due to solid-state flow in the mantle wedge beneath arcs. In: “Inside the Subduction Factory”, J.M. Eiler (Ed.), Geophys. Monograph Serie, 138, AGU, Washington, 293– 311.

Keppler, H., 1996. Constraints from partitioning experiments on the composition of subduction-zone fluids. Nature 380, 237–240.

Kerrick, D.M., Connolly, J.A.D., 2001. Metamorphic devolatilization of subducted marine sediments and the transport of volatiles into the Earth's mantle. Nature 411, 293-296

Kessel, R., Schmidt, M.W., Ulmer, P., Pettke, T. 2005. Trace element signature of subduction-zone fluids, melts and supercritical liquids at 120-180 km depth. Nature 437, 724–727.

Kjarsgaard, B.A., Hamilton, D.L., Peterson, T.D., 1995. Peralkaline nepheline/carbonatite liquid immiscibility: comparison of phase compositions in experiments and natural lavas from Oldoynio L’Engai. In: “Carbonatite Volcanism: Oldiinyo Lengai and Petrogenesis of Natrocarbonatites”, Bell K. & Keller J. (edts.), Springer-Verlag, Berlin, 87-99.

Klimm, K., Blundy, J.D., Green, T.H., 2008. Trace element partitioning and accessory phase saturation during H_2O-saturated melting of basalt with implications for Subduction zone chemical fluxes. J. Petrol. 49, 523-553.

Krummenacher, D., Evernden, J.F., 1960. Determination d’age isotopique faites sur quelques roches des Alps par la méthode potassium-argon. Schweiz. Mineral. Petrograph. Mitt. 40, 267-277.

LaBerge, R.D., Giordano, G., Cas, R.A.F., Ailleres, L. 2006. Syn-depositional substrate deformation produced by the shear force of a pyroclastic density current: an example from the Pleistocene ignimbrite at Monte Cimino, northern Lazio, Italia. J. Volcanol. Geoth. Res. 158, 307-320.

La Berge, R.D., Porreca, M., Mattei, M., Giordano, G., Cas, R.A.F. 2009. Meandering flow of a pyroclastic density current documented by the Anisotropy of Magnetic Susceptibility (AMS): the case of the Pleistocene Peperino Tipico ignimbrite (Monte Cimino Volcanic Complex, Central Italy). Tectonophysics, 466, 64-68. 10.1016/j.tecto.2008.09.009

Laurenzi, M.A., 2005. Comment on “Recurrence of volcanic activity along the Roman Comagmatic Province (Tyrrhenian margin of Italy) and its tectonic significance” by F. Marra, J. Taddeucci, C. Freda, W. Marzocchi, & P. Scarlato. Tectonics, 24, TC5006, 10.1029/2004TC001780.

Laurenzi, M.A., Ballini, A., Barberi, F., Mezzetti, F., Oddone, M., Villa, I.M., 1990. High resolution chronostratigraphy of Roccamonfina volcano (Italy). ICOG VII, Geol. Soc. Australia 27, p. 57.

Laurenzi, M.A., Deino, A.L., 1996. $^{40}Ar/^{39}Ar$ single-crystal dating of Vulsinian Basal Ignimbrite (Central Italy). Eos, Transactions, AGU, 77 (46), F794.

Laurenzi, M.A., Stoppa, F.., Villa, I.M., 1994. Eventi ignei monogenetici e depositi piroclastici nel Distretto Ultra-alcalino Umbro-Laziale (ULUD): revisione, aggiornamento e comparazione dei dati cronologici. Plinius 12, 61–65.

Laurenzi, M.A., Villa, I.M., 1984. Datazione K–Ar dei centri vulcanici di Vicovaro e San Venanzo. Rendiconti Società Italiana Mineralogia Petrologia 40, 423–426.

Laurenzi, M.A., Villa, I.M., 1985. K/Ar chronology of the Vico volcano (Latium, Italy) - Abstract, International Association of Volcanology and Earth Interiors, Abstract Volume, Giardini Naxos, Catania.

Laurenzi, M.A., Villa, I.M., 1987. $^{40}Ar/^{39}Ar$ chronostratigraphy of Vico ignimbrites. Periodico Mineral. 56, 285-293.

Laurenzi, M.A., Villa, I.M., 1991. The age of the early volcanic activity of Mt. Amiata volcano, Tuscany: evidence for a paleomagnetic reversal at 300 ka bp. Plinius 6, 160-161.

Le Bas, M.J., 1987. Nephelinites and carbonatites. In: “alkaline igneous rocks”, Fitton J.G. & Upton B.G.J. (edts.), Geol. Soc. London, Spec. Pub. 30, 53-83.

Le Bas, M.J., 1999. Sövite and alvikite; two chemically distinct calciocarbonatites C1 and C2. South African J. Geol. 102, 109-121.

Le Maitre, R.W., 2002. Igneous Rocks. A Classification and Glossary of Terms. Recommendations of the International Union of Geological Sciences Subcommission on the Systematics of Igneous Rocks. Cambridge University Press, 236 pp.

Le Roex, A.P., Lanyon, R., 1998. Isotope and Trace Element Geochemistry of Cretaceous Damaraland Lamprophyres and Carbonatites, Northwestern Namibia: Evidence for Plume-Lithosphere Interactions. J. Petrol. 39, 1117-1146

Lloyd, F.E., Arima, M., Edgar, A.D., 1985. Partial melting of a phlogopite-clinopyroxenite nodule from south-west Uganda: an experimental study-bearing on the origin of a highly potassic continental rift volcanics. Contrib. Mineral. Petrol. 91, 321-329.

Locardi, E., Lombardi, G., Funiciello, R., Parotto, M., 1976. The main volcanic groups of the Latium (Italy): relations between structural evolution and petrogenesis. Geologica Romana 16, 279-300.

Lombardi, G., Nicoletti, M., Petrucciani, C., 1974. Età delle vulcaniti acide dei complessi Tolfetano, Cerite e Manziate (Lazio NordOccidentale). Periodico Mineralogia 43, 181-204.

Lonergan, L., White, N., 1997. Origin of the Betic–Rif mountain Belt. Tectonics 16, 504–522.

Luhr, J.F., Giannetti, B., 1987. The Brown Leucitic Tuff of Roccamonfina volcano (Roman Region, Italy). Contrib. Mineral. Petrol. 95, 420-436.

Lustrino, M., Morra, V., Melluso, L., Brotzu, P., D'Amelio, F., 2004. The Cenozoic igneous activity in Sardinia. Periodico Mineralogia 73, 105-134.

Magri, D., Sadori, L., 1999. Late Pleistocene and Holocene pollen stratigraphy at Lago di Vico, central Italy. Earth and Environmental Science Vegetation History and Archaeobotany 8, 247-260.

Malinverno, A., Ryan W.B.F., 1986. Extension in the Tyrrhenian Sea and shortening in the Apennines as result of arc migration driven by sinking of the lithosphere. Tectonics 5, 227-245.

Marani, M.P., Trua, T., 2002. Thermal constriction and slab tearing at the origin of a superinflated spreading ridge: Marsili volcano (Tyrrhenian Sea). J. Geophys. Res. 107, 2188, 15; 10.1029/2001jb000285

Marinelli, G., 1961. - Genesi e classificazione delle vulcaniti recenti toscane. Atti Società Toscana di Scienze Naturali,

Marinelli, G., 1967. Genèse des magmas du volcanisme Plio-Quaternarie des Apennines. Geolog. Rundschau 57, 127-141.

Marra, F., Freda, C., Scarlato, P., Taddeucci, J., Karner, D.B., Renne, P.R., Gaeta, M., Palladino, D.M., Trigila, R., Cavarretta, G. 2003. Post Caldera activity in the Alban Hills Volcanic district (Italy): $^{40}Ar/^{39}Ar$ geochronology and insights into the magma evolution. Bull. Volcanol. 65, 227-247.

Marra, F., Karner, D.B., Freda, C., Gaeta, M., Renne, P., 2008. Large mafic eruptions at Alban Hills Volcanic District (Central Italy): chronostratigraphy, petrography, and eruptive behaviour. J. Volcanol. Geotherm. Res., 10.1026/jvolgeores.2008.11.09

Marra, F., Taddeucci, J., Freda, C., Marzocchi, W., Scarlato, P. 2004. Recurrence of volcanic activity along the Roman Comagmatic Province (Tyrrhenian margin of Italy) and its tectonic significance. Tectonics, 23, TC4013, 10.1029/2003TC001600.

Martelli, M., Nuccio, P.M., Stuart, F.M., Burgess, R., Ellam, R.M., Italiano, F., 2004. Helium–strontium isotope constraints on mantle evolution beneath the Roman Comagmatic Province, Italy. Earth Planet. Sci. Lett. 224 295-308.

Mascle, G.H., Tricart, P., Torelli, L., Bouillin, J.P., Rolfo, F., Lapierre, H., Monié, P., Depardon, S. Mascle, J., Peis, D., 2001. Evolution of the Sardinia Channel (Western Mediterranean): new Constraints from a diving survey on Cornacya seamount off SE Sardinia. Marine Geology 179, 179-202.

Mascle, J., Kastens, K., Auroux, C., 1988. A land-locked back-arc basin: preliminary results from ODP Leg 107 in the Tyrrhenian Sea. Tectonophysics 146, 149-162.

Mattei, M., Cifelli, F., D'Agostino, N., 2007. The evolution of the Calabrian Arc: Evidence from paleomagnetic and GPS observations. Earth Planet. Sci. Lett. 263, 259-274.

Mattei, M., Cipollari, P., Cosentino, D., Argentieri, A., Rossetti, F., Speranza, F., Di Bella, L., 2002. The Miocene tectono-sedimentary evolution of the Southern Tyrrhenian Sea: stratigraphy, structural and paleomagnetic data from the on-shore Amantea basin (Calabrian arc, Italy). Basin Research 14, 147-168.

Mattei, M., Conticelli, S., Giordano, G., 2010. The Tyrrhenian margin geological setting: from the Apennine orogeny to the K-rich volcanism. In: Funiciello, R. & Giordano, G. (eds) The Colli Albani Volcano. Special Publications of IAVCEI, 3. Geol. Soc. London, London, 7-27.

Mattei M., Funiciello R., Kissel C., 1995. Paleomagnetic and structural evidence of Neogene block rotation in the Central Apennines, Italy, J. Geophys. Res., 100 17863-17883.

Mattei, M., Funiciello R., Parotto M., 2008. Roma e contesto geodinamico recente dell'Italia Centrale. Mem. Descr. della Carta Geologica d'Italia, LXX(1), 13-24.

Mattei, M., Petrocelli, V., Lacava, D., Schiattarella, M., 2004. Geodynamic implications of Pleistocene ultra-rapid vertical-axis rotations in the Southern Apennine (Italy). Geology 32, 9, 789–792.

Mattias, P.P., Ventriglia, U., 1970. La regione vulcanica dei Monti Sabatini e Cimini. Memorie Società Geologica Italiana 9, 331-384.

Mazzuoli, R., Pratesi, M., 1963. Rilevamento e studio chimico-petrografico delle rocce vulcaniche del Monte Amiata. Atti Società Toscana di Scienze Naturali, Memorie 70, 355-429.

McDowell, F.W., 1983. K-Ar dating: incomplete extraction of radiogenic Argon from alkali feldspar. Isotope Geosci. 1, 119-126.

McKenzie, D., 1972. Active Tectonics of the Mediterranean Region. Geophys. J. Royal Astronom. Soc. 30, 109-185.

Mele, G., Rovelli, A., Seber, D., Barazangi, M., 1997. Shear wave attenuation in the lithosphere beneath Italy and surrounding regions: tectonic implications. J. Geophys. Res. 103, 12529–12543.

Melluso L., Conticelli S., de' Gennaro R. (2010). Kirschsteinite in the Capo Bove melilite leucitite (cecilite), Alban Hills, Italy. Mineralogical Magazine, in the press.

Melluso, L., Conticelli, S., D'Antonio, M., Mirco, N., Saccani, E., 2003. Petrology and mineralogy of wollastonite-melilite-bearing pyrometamorphic rocks from Colle Fabbri and Ricetto, Central Apennines, Italy. Am. Mineral. 88, 1287-1299.

Melluso, L., Conticelli, S., D'Antonio, M., Mirco, N., Saccani, E., 2005a. Mineralogic and bulk rock composition of Italian wollastonite- and melilite-bearing paralavas and clinker: Further evidence for their pyrometamorphic nature. Am. Miner. 90, 1926-1933.

Melluso, L., Conticelli, S., D'Antonio, M., Mirco, N., Saccani, E., 2005b. Wollastonite- anorthite-gehlenite-and fassaite-bearing rocks: Igneous petrological oddity or paralavas? Am. Mineral. 90, 1940-1944.

Melluso, L., Morra, V., Di Girolamo, P., 1996. The M.te vulture volcanic complex (Italy): evidence for distinct parental magmas and for residual melts with melilite. Mineral. Petrol. 56, 225-250.

Melluso, L., Morra, V., Perrotta, A., Scarpati, C., Adabbo, M., 1995. The eruption of the Breccia Museo (Campi Flegrei, Italy): fractional crystallization processes in a shallow, zoned magma chamber and implications for the eruptive dynamics. J. Volcanol. Geotherm. Res., 68, 325-339.

Menzies, M.A., Dupuy, C., Nicolas, A., 1991. Orogenic Lherzolites and Mantle Processes. Terra Nova 3, 6-8.

Metrich N., Santacroce R., Savelli C. (1986) Ventotene, a potassic quaternary volcano in central Tyrrhenian Sea. Rendiconti Società Italiana di Mineralogia e Petrologia 43, 1195-1213.

Metzeltin, S., Vezzoli, L., 1983. Contributi alla geologia del Vulcano di Latera (Monti Vulsini, Toscana Meridionale-Lazio Settentrionale). Mem. Soc. geol. It. 25, 247-271.

Michetti, A., 1990. Nuovi dati sulle vulcaniti della "Cava dell'Oro" presso Polino (Terni). Rendiconti Società Geologica Italiana 13, 240-241.

Michetti, A., Serva, L., 1990. New data on the seismotectonic potential of the Leonessa fault area (Rieti, Central Italy). Rendiconti Società Geologica Italiana 13, 37-46.

Miller, S.A., Collettini, C., Chiaraluce, L., Cocco, M., Barchi, M.R. & Kaus, B. 2004. Aftershocks driven by a high pressure CO_2 source at depth. Nature 427, 724–727.

Mirco, N., 1990. Rapporti tra rocce alkaline e per alcaline potassiche nell'area Laziale-Abruzzese. B.Sc. Thesis, University of Florence, 65 pp.

Mittempergher, M., 1965. Vulcanismo e petrogenesi nella Zona di San Venanzo. Atti Società Toscana di Scienze Naturali LXXII, 437-479.

Molina, J.F., Poli, S., 2000. Carbonate stability and fuid composition in subducted oceanic crust: an experimental study on H_2O-CO_2-bearing basalts. Earth Planet. Sci. Lett. 176, 295-310.

Mongelli, F., Zito, G., Cataldi, R. et al. 1991. Geothermal regime of Italy and surrounding seas, in Terrestrial Heat Flow and the Lithosphere Structure (eds. V. Cermák and L. Rybach). Springer-Verlag, Berlin/Heidelberg, pp. 381–394.

Montone, P., Mariucci, M.T., Pondrelli, S., Amato, A., 2004. An improved stress map for Italy and surrounding regions (central Mediterranean). J. Geophys. Res. 109, B10410. 10.1029/2003JB002703.

Morgan, D.J., Blake, S., Rogers, N.W., De Vivo, B., Rolandi, G., Davidson, J.P., 2006. Magma chambre recharge at Vesuvius in the century prior to the eruption of A.D. 79. Geology 34, 845-848.

Murphy, D.T., Collerson, K.D., Kamber, B.S., 2002. Lamproites from Gaussberg, Antarctica: possible transition Zone melts of Archean Subducted Sediments. J. Petrol. 43, 981-1001.

Nappi, G., Antonelli, F., Coltorti, M., Milani, L., Renzulli, A., Siena, F., 1998. Volcanological and petrological evolution of the Eastern Vulsini District, Central Italy. J. Volcanol. Geoth. Res. 87, 211-232.

Nappi, G., Capaccioni, B., Mattioli, M., Mancini, E., Valentini, L., 1994. Plinian fall deposits from Vulsini Volcanic District (Central Italy). Bull. Volcanol. 56, 502-515.

Nappi, G., Renzulli, A., Santi, P., 1987. An evolutionary model for the Paleo-Bolsena and Bolsena Volcanic Complexes: a structural and petrographic study. Periodico Mineralogia 56, 241-267.

Nappi, G., Renzulli, A., Santi, P., 1991. Evidence of incremental growth in the Vulsinian calderas (central Italy). J. Volcanol. Geoth. Res. 47. 13-31.

Nappi, G., Renzulli, A., Santi, P., Gillot, P.-Y., 1995. Geological evolution and geochronology of the Vulsini Volcanic District (Central Italy). Bollettino Società Geologica Italiana 114, 599-613.

Nicoletti, M., 1969. Datazioni argon potassio di alcune vulcaniti delle Regioni vulcaniche Cimina e Vicana. Periodico Mineralogia 38, 1-20.

Nicoletti, M., Petrucciani, C., Piro, M., Trigila, R., 1981a. Nuove datazioni Vulsinee per uno schema di evoluzione dell'attività vulcanica: Il quadrante nord-occidentale. Periodico Mineralogia 48, 153-165.

Nicoletti, M., Petrucciani, C., Piro, M., Trigila, R., 1981b. Nuove datazioni Vulsinee per uno schema di evoluzione dell'attività vulcanica: nota II. Il quadrante sud-occidentale. Periodico Mineralogia 50, 141-169.

Nicolosi, I., Speranza, F., Chiappini, M., 2006. Ultrafast oceanic spreading of the Marsili Basin, southern Tyrrhenian Sea: Evidence from magnetic anomaly analysis. Geology 34, 717-720.

Nikogosian, I.K., van Bergen, M.J., 2010. Heterogeneous mantle sources of potassium-rich magmas in central-southern Italy: Melt-inclusion evidence from Roccamonfina and Ernici (Mid Latina Valley). J. Volcanol. Geoth. Res. 10.1016/j.jvolgeores.2010.06.014

Orsi, G., Civetta, L., D'Antonio, M., Di Girolamo, P., Piochi, M., 1995. Step-filling and development of a three-layer magma chamber: the Neapolitan Yellow Tuff case history. J. Volcanol. Geoth. Res. 67, 291-312.

Orsi, G., D'Antonio, M., de Vita, S., Gallo, 1992b. The Neapolitan Yellow tuff, a large magnitude trachytic phreatoplinian eruption: eruptive dynamics, magma withdrawal and caldera collapse. J. Volcanol. Geoth. Res. 53, 275-287.

Orsi, G., de Vita, S., Di Vito, M., 1996a. The restless, resurgent Campi Flegrei nested caldera (Italy): constraints on its evolution and configuration. J. Volcanol. Geoth. Res. 74, 179-214.

Orsi, G., Gallo, G., Heiken, G., Wohletz, K., Yu, E., Bonani, G., 1992a. A comprehensive study of pumice formation and dispersal: the Cretaio Tephra of Ischia (Italy). J. Volcanol. Geoth. Res. 53, 329-354.

Orsi, G., Gallo, G., Zanchi, A., 1991. Simple shearing block-resurgence in caldera depressions. A model from Pantelleria and Ischia. J. Volcanol. Geoth. Res. 47, 1-11.

Orsi, G., Piochi, M., Campaiola L., D'Onofrio, A. Gialanella, L., Terrasi, F., 1996b. 14C geochronological constraints for the volcanic history of the island of Ischia (Italy) over the last 5000 years. J.Volcanol.Geoth.Res. 71, 249-257

Ort, M., Orsi, G., Pappalardo, L., Fisher, R.V., 2003. Anisotropy of magnetic susceptibility studies of depositional processes in the Campanian Ignimbrite, Italy. Bull. Volcanol., 65, 55-72.

Owen, J.P., 2008. Geochemistry of lamprophyres from the Western Alps, Italy: implications for the origin of an enriched isotopic component in the Italian mantle. Contrib. Mineral. Petrol. 155, 341-362.

Pantosti, D., Schwartz, D.P., Valensise, G., 1993. Paleoseismology Along the 1980 Surface Rupture of the Irpinia Fault: Implications for Earthquake Recurrence in the Southern Apennines, Italy. J. Geophys. Res. 98, 6561-6577.

Palladino, D.M., Agosta, E., Freda, C., Spaziani, S. Trigila, R., 1994. Studio geo-petrografico dei Vulsini Meridionali, settore Valentano-Marta-La Rocca. Memorie Descrittive Carta Geologica d'Italia XLIV: 255-276.

Palladino, D.M., Gaeta, M., Marra, F. 2001. A large K-foiditic hydromagmatic eruption from the early activity of the Alban Hills Volcanic District, Italy. Bulletin of Volcanology 63, 345-359.

Palladino, D.M., Simei, S., Sottili, G., Trigila, R., 2010. Integrated approach for the reconstruction of stratigraphy and geology of Quaternary volcanic terranes: an example from the Vulsini volcanoes. Geol. Soc. Am., Spec. Papers 464, 63-84.

Paone, A., 2004. Evidence for crustal contamination, sediment and fluid components in the Campanian volcanic rocks. J. Volcanol. Geoth. Res. 138, 1-26.

Paone, A., 2006. The geochemical evolution of the Mt. Somma-Vesuvius volcano. Mineral. Petrol. 87, 53-80.

Pappalardo, L., Civetta, L., D'Antonio, M., Deino, A., Di Vito, M., Orsi, G., Carandente, A., de Vita, S., Isaia, R., Piochi, M., 1999. Chemical and Sr-isotopical evolution of the Phlegraean magmatic system before the Campanian Ignimbrite and the Neapolitan Yellow Tuff eruptions. J. Volcanol. Geoth. Res. 91, 141-166.

Pappalardo, L., Piochi, M., D'Antonio, M., Civetta, L., Petrini, R., 2002. Evidence for Multi-stage Magmatic evolution during the past 60 kys at Campi Flegrei (Italy) deduced from Sr, Nd, and Pb isotope data. J. Petrol. 43, 1415-1434.

Parker, R.J., 1989. Geochemical and petrographic characteristics of potassium-rich pyroclastic and lava samples from Vulsini Volcano, Roman Magmatic region, Italy. J. Volcanol. Geoth. Res. 39, 297-314.

Pasquaré, G., Chiesa, S., Vezzoli, L., Zanchi A., 1983. Evoluzione paleogeografica e strutturale di parte della Toscana meridionale a partire dal Miocene superiore. Memorie Società Geologica Italiana 25, 145-157.

Pasquaré, G., Serri, G., Vezzoli, L., 1985. Carta geologica dell'area della Media Valle Latina. Scala 1:50000. Progetto finalizzato geodinamica. Sottoprogetto: sorveglianza dei vulcani e rischio vulcanico. In: Carte tematiche sul vulcanismo recente. Istituto di Geologia, Università di Milano.

Peacock, S.M. 2003. Thermal structure and metamorphic evolution of subducting slab. In: J.M. Eiler (Ed.), Inside the Subduction Factory, Geophysical Monograph Series 138, AGU, Washington, 293– 311.

Peccerillo, A., 1985. Roman Comagmatic Province (Central Italy): Evidence for subduction related magma genesis. Geology 13, 103-106.

Peccerillo, A., 1998. Relationships between ultrapotassic and carbonate-rich volcanic rocks in Central Italy: petrogenetic and geodynamic implications. Lithos 43, 267-279.

Peccerillo, A., 1999. Multiple mantle metasomatism in Central-Southern Italy: Geochemical effects, timing and geodynamic implications. Geology 27, 315-318.

Peccerillo, A., 2001. Geochemical similarities between the Vesuvius, Phlegraean Fields and Stromboli volcanoes: petrogenetic, geodynamic and volcanological implications. Mineral. Petrol., 73, 93-105.

Peccerillo, A., 2004a. Carbonate-rich pyroclastic rocks from central Apennines: carbonatites or carbonated rocks? A commentary. Periodico Mineralogia 73. 183-194.

Peccerillo, A., 2004b. Plio-Quaternary magmatism in Italy. Episodes 26, 222-226.

Peccerillo, A., 2005a. Plio-Quaternary Volcanism in Italy: Petrology, Geochemistry, Geodynamics. Springer-Verlag. Berlin, 365 pp.

Peccerillo, A., 2005b. On the nature of carbonate-rich volcanic rocks in Central Italy. A reply to comments by Woolley et al., p.195-204. Periodico Mineralogia 74, 195-204.

Peccerillo, A., Conticelli S., Manetti P., 1987. Petrological characteristics and the genesis of the recent magmatism of South Tuscany and North Latium. Periodico Mineralogia 56, 167-183.

Peccerillo, A., Federico, M., Barbieri, M., Brilli, M., Tsai-Wan Wu, 2010. Interaction between ultrapotassic magmas and carbonate rocks: Evidence from geochemical and isotopic (Sr, Nd, O) compositions of granular lithic clasts from the Alban Hills Volcano, Central Italy. Geochim. Cosmoch. Acta 74, 2999-3022.

Peccerillo, A., Martinotti, G., 2006. The Western Mediterranean lamproitic magmatism: origin and geodynamic significance. Terra Nova 18, 109-117.

Peccerillo, A., Poli, G., L. Tolomeo, L. 1984. Genesis, evolution and tectonic significance of K-rich volcanics from the Alban Hills (Roman comagmatic region) as inferred from trace element geochemistry. Contrib. Mineral. Petrol. 86, 230-240.

Peccerillo, A., Poli, G., Serri, G., 1988. Petrogenesis of orenditic and kamafugitic rocks from Central Italy. The Canad. Mineral. 26, 45-65.

Peccerillo, A., Taylor, S.R., 1976. Geochemistry of the calc-alkaline volcanic rocks from the kastamonu area, Northern Turkey. Contrib. Mineral. Petrol. 58, 63-81.

Perini, G., Conticelli, S. (2002). Crystallization conditions of Leucite-Bearing magmas and their implications on the magmatological evolution of ultrapotassic magmas: The Vico Volcano, Central Italy. Mineral. Petrol. 74, 253-276.

Perini, G., Conticelli, S., Francalanci, L., 1997. Inferences on the volcanic history of the Vico volcano, Roman Magmatic Province, Central Italy: stratigraphic, petrographic and geochemical data. Mineralogica et Petrographica Acta, vol. 40, pp. 1÷27.

Perini, G., Conticelli, S., Francalanci, L., Davidson, J. P., 2000. The relationship between potassic and calc-alkaline post-orogenic magmatism at Vico volcano, central Italy. J. Volcanol. Geoth. Res. 95, 247-272.

Perini, G., Francalanci, L., Davidson, J.P., Conticelli S., 2004. Evolution and genesis of magmas from Vico Volcano, Central Italy: multiple differentiation pathways and variable parental magmas. J. Petrol. 45, 139-182.

Perini, G., Tepley, F. J. III, Davidson, J. P., Conticelli, S., 2003. The origin of K-feldspar megacrysts hosted in alkaline potassic rocks: track for low scale mantle heterogeneity. Lithos 66, 223-240

Perrotta, A., Scarpati, C., Giacomelli, L., Capozzi, A.R., 1996. Proximal depositional facies from a caldera-forming eruption: the Parata Grande Tuff at Ventotene Island (Italy). J. Volcanol. Geoth. Res. 71, 207-228.

Plank, T. 2005. Constraints from Thorium/Lanthanum on Sediment Recycling at Subduction Zones and the Evolution of the Continents. J. Petrol. 46, 921-944.

Plank, T., Langmuir, C.H., 1998. The chemical composition of subducting sediments and its consequence for the crust and mantle. Chem. Geol. 145, 325-394.

Pialli, G., Barchi, M.R., Minelli, G., 1998. Results of the CROP03 deep seismic reflection profile. Memorie della Societa` Geologica Italiana 52, 657pp.

Piana Agostinetti, N., Lucente, F.P., Selvaggi, G., Di Bona, M., 2002. Crustal Structure and Moho Geometry beneath the Northern Apennines (Italy). Geoph. Res. Lett. 29, 1999-2002.

Pierattini, D., 1978. Geochronological and paleomagnetic data from volcanic rocks of the isle of Capraia. Boll. Geof. Teorica Applicata 21, 46-77.

Pinarelli, L., 1991. Geochemical and isotopic (Sr, Pb) evidence of crust-mantle interaction in acidic melts - The Tolfa-Cerveteri-Manziana volcanic complex (Central Italy): a case history. Chem. Geol. 92, 177-195.

Pinarelli, L., Poli, G., Santom A.P., 1989. Geochemical characterisation of recent volcanism from the Tuscan magmatic province (Central Italy): the Roccastrada and San Vincenzo centers. Periodico Mineralogia 58, 67-96.

Poli, G., 1992. Geochemistry of Tuscan Archipelago Granitoids, Central Italy: The Role of Hybridisation processes in their genesis. J. Geol. 100, 41-56.

Poli, G., 2004. Genesis and evolution of Miocene-Quaternary intermediate acid-rocks from the Tuscan Magmatic Province. Periodico Mineralogia 73-1, 187-214.

Poli, G., Frey, F.A., Ferrara, G., 1984. Geochemical characteristics of the South Tuscany (Italy) magmatic province: constraints on lava petrogenesis. Chem. Geol. 43, 203-221.

Poli, G., Manetti, P., Tommasini, S., 1989. A petrological review on Miocene-Pliocene intrusive rocks from southern Tuscany and Tyrrhenian Sea (Italy). Periodico Mineralogia 58, 109-126.

Poli, G., Tommasini, S., Halliday, A.N., 1996. Trace element and isotopic exchange during acid-basic magma interaction processes. Transaction of the Royal Society of Edinburgh, Earth Sciences 87, 225-232.

Poli, S., Chiesa, S., Gillot, P.Y., Gregnanin, A., Guichard, F., 1987. Chemistry versus time in the Volcanic Complex of Ischia (Gulf of Naples, Italy): evidence of Successive magmatic cycle. Contrib. Mineral. Petrol. 95, 322-335.

Poli, S., Chiesa, S., Gillot, P.Y., Guichard, F., Vezzoli, L. 1989. Time dimension in the Geochemical approach and hazard estimates of a volcanic area: the isle of Ischia case (Italy). J. Volcanol. Geoth. Res. 36, 327-335.

Poli, S., Franzolin, E., Fumagalli, P., Crottini, A., 2009. The transport of carbon and hydrogen in subducted oceanic crust: An experimental study to 5 Gpa. Earth Planet. Sci. Lett. 278, 350-360.

Pondrelli, S., Morelli, A., Boschi, E., 1995. Seismic deformation in the Mediterranean area estimated by moment tensor summation. Geophys. J. Internat. 122, 938 – 952.

Prelevic, D., Foley, S.F., Cvetkovic, V., Romer, R.L., 2004. Origin of minette by mixing of lamproite and dacite magmas in Veliki Majdan Serbia. J. Petrol. 45, 759-792.

Prelevic, D., Foley, S.F., Cvetkovic, V., Romer, R.L., Downes, H., 2005. Tertiary Ultrapotassic Volcanism in Serbia: Constraints on Petrogenesis and Mantle Source Characteristics. J. Petrol. 46, 1443-1487.

Prelevic, D., Foley, S.F., Romer, R.L., Conticelli, S., 2008. Mediterranean Tertiary Lamproites: Multicomponent melts in post-collisional geodynamics. Geochim. Cosmochim. Acta 72, 2125-2156.

Prelevic, D., Stracke, A., Foley, S.F., Romer, R.L., Conticelli, S., 2010. Hf isotope compositions of Mediterranean lamproites: mixing of melts from asthenosphere and crustally contaminated mantle lithosphere. Lithos, 10.1016/j.lithos.2010.07.007.

Principe, C., 2006. La geologia del Monte Vulture. Regione Basilicata. Grafiche Finiguerra, Lavello. 217 p.

Principe, C., Giannadrea, P., 2006. Monte Vulture volcano evolution history. In: “La Geologia del Monte Vulture”, C. Principe (edt.), Regione Basilicata, Lavello (PZ) 2006, 49-53.

Principe, C., Tanguy, J.-C., Arrighi, S., Paiotti, A., Le Goff, M., Zoppi, U., 2004. Chronology of Vesuvius’ activity from A.D. 79 to 1631 based on archeomagnetism of lavas of historical sources. Bull. Volcanol. 66, 703-724.

Puxeddu, M., 1971. Studio chimico e petrografico delle vulcanite del Monte Cimino (Viterbo). Atti Società Toscana di Scienze Naturali, Serie A 78, 329-394.

Quidelleur, X., Gillot, P.Y., Grove, M., Harrison, T.M., Deino, A., 1997. The White Trachytic Tuff Sanidine: a potential age standard for $^{40}Ar/^{39}Ar$ dating of Pleistocene-Pliocene samples. Terra Cognita, p. 69.

Radicati di Brozolo, F., di Girolamo, P., Turi, B., Oddone, M., 1988. $^{40}Ar/^{39}Ar$ e K-Ar dating of K-rich rocks from the Roccamonfina volcano, Roman Comagmatic Region, Italy. Geoch. Cosmoch. Acta 52, 1435-1441.

Radicati di Brozolo, F., Huneke, J.C., Papanastassiou, D.A., Wasserburg, G.J., 1981. $^{40}Ar/^{39}Ar$ and Rb-Sr age determinations on Quaternary volcanic rocks. Earth Planet. Sci. Lett. 53, 445-456.

Rampone, R., Vissers, R.L.M., Poggio, M., Scambelluri, M., Zanetti, A., 2010. Melt Migration and Intrusion during Exhumation of the Alboran Lithosphere: the Tallante Mantle Xenolith Record (Betic Cordillera, SE Spain). J. Petrol. 51, 295-325.

Rittmann, A., 1933. Die Geologische Bedingte Evolution und Differentiation des Somma-Vesuvius magmas. Z Vulkanol 15, 1-2

Rivalenti, G., Mazzucchelli, M., Vannucci, R., Hofmann, A.W., Ottolini, L., Bottazzi, P., Obermiller, W., 1995. The relationship between websterite and peridotite in the Balmuccia peridotite massif (NW Italy) as revealed by trace element variations in clinopyroxene. Contrib. Mineral. Petrol. 121, 275-288.

Rivalenti, G., Mazzucchelli, M., Zanetti, A., Vannucci, R., Bollingerd, C., Hémond, C., Bertotto, G.W., 2007. Xenoliths from Cerro de los Chenques (Patagonia): An example of slab-related metasomatism in the backarc lithospheric mantle. Lithos 99, 45-67.

Rock, NMS, 1986. The nature and origin of lamprophyres: an overview. Geol. Soc. London, Spec. Pub. 30. 191 - 226.

Rodolico, F., 1934. Ricerche sulle rocce eruttive recenti della Toscana. II. - Le rocce di Orciatico e Montecatini Val di Cecina. Memorie Società Toscana Scienze Naturali 44, 61-86.

Rodolico, F., 1934. Inclusi scistoso-cristallini nella trachite del Monte Amiata. Periodico Mineralogia 5, 1-23.

Rodolico, F., 1935. On the Chemistry of the igneous effussive rock of Cupaello (Rieti). (In Italian). Rendiconti Regia Accademia Nazionale Lincei 22, 469-472.

Rodolico, F., 1935. Ricerche sulle rocce eruttive recenti della Toscana. III. - Le rocce del Monte Amiata. Memorie Società Toscana Scienze Naturali 45, 89-142.

Rodolico, F., 1937. Le zone vulcaniche di San Venanzo e Cupaello. Bollettino Società Geologica Italiana 56, 33-66.

Rodolico, F., 1938. Ricerche sulle rocce eruttive recenti della Toscana. VII. - Sguardo d'insieme. Memorie Società Toscana Scienze Naturali 48, 281-288.

Rogers, N.W., Hawkesworth, C.J., Parker, R.J., Marsh, J.S., 1985. The geochemistry of potassic lavas from Vulsini, Central Italy, and implications for mantle enrichment processes beneath the Roman region. Contrib. Mineral. Petrol. 90, 244-257.

Rolandi, G., Bellucci, F., Heizler, M.T., Belkin, H.E., De Vivo, B., 2003. Tectonic controls on the genesis of ignimbrites from the Campanian Volcanic Zone, souther Italy. Mineral. Petrol. 79, 3-31.

Romano, P., 1992. La distribuzione dei depositi marini lungo le coste della Campania. Stato delle conoscenze e prospettive di ricerca. Studi Geologici Camerti (spec vol) 1992/1, 265-269.

Rosatelli, G., Stoppa, F., Jones, A.P., 2000. Intrusive calcite-carbonatite occurrence from Mt. Vulture volcano, southern Italy. Mineral. Mag. 64, 341-361.

Rosenbaum, G., Gasparon, M., Lucente, F.P., Peccerillo, A. Miller, M.S., 2008. Kinematics of slab tear faults during subduction segmentation and implications for Italian magmatism, Tectonics, 27, TC2008, 10.1029/2007TC002143.

Rosenbaum, G., Lister, G. S., 2004. Neogene and Quaternary rollback evolution of the Tyrrhenian Sea, the Apennines and the Sicilian Maghrebides, Tectonics, 23, TC1013, 10.1029/2003TC001518.

Rosenbaum, G., Lister, G.S., Duboz, C., 2002. Reconstruction of the tectonic evolution of the western Mediterranean since the Oligocene. Journal of the Virtual Explorer, 8, 107-130.

Rosenbaum, G., Lister, G. S., Duboz, C., 2004. The Mesozoic and Cenozoic motion of Adria (central Mediterranean): constraints and limitations, Geodinamica Acta, 17, 125-139.

Rosi, M., Principe, C., Vecci, R., 1993. The 1631 Vesuvius eruption. A reconstruction based on historical and stratigraphical data. J. Volcanol. Geoth. Res. 58, 151-182.

Rosi, M., Sbrana, A., 1987. Phlegrean Fields. In: “Progetto Finalizzato Geodinamica, Monografie Finali, vol.9”, Consiglio Nazionale della Ricerca, Quaderni de la Ricerca Scientifica 114, 1-175.

Rosi, M., Sbrana, A., Principe, C., 1983. The Phlegrean Fields: structural evolution, volcanic history, and eruptive mechanisms. J. Volcanol. Geoth. Res. 17, 273-295.

Rosi, M., Vezzoli, L., Aleotti, P., De Censi, M., 1996. Interaction between caldera collapse and eruptive dynamics during the Campanian Ignimbrite eruption, Phlegraean Fields, Italy. Bull. Volcanol. 57, 541-554.

Rouchon, V., Gillot, P.Y., Quidelleur, X., Chiesa, S., Floris, B., 2008, Temporal evolution of the Roccamonfina volcanic complex (Pleistocene), Central Italy. J. Volcanol. Geoth. Res. 177, 500-514.

Sabatini, V., 1899. I vulcani di San Venanzo. Rivista di Mineralogia e Cristallografia Italiana 22: 3-34.

Sahama, Th.G., 1952. Leucite, potash nepheline, and clinopyroxene from volcanic lavas from volcanic lavas from Southwestern Uganda and Adjoining Belgian Congo. In: Bowen Volume, pt. II, Am. J. Sci., 457-470.

Sahama, Th.G., 1960. Kalsilite in the lavas of Mt. Nyiragongo (Belgian Congo). J. Petrol. 1, 146 - 171.

Sahama, Th.G., 1974. Potassium Rich Alkaline Rocks. In: The Alkaline Rocks, Sorensen G. (editor), John Wiley & Son, New York, 355-389.

Santacroce, R. (Ed.) 1987. Somma-Vesuvio. In: “Progetto Finalizzato Geodinamica, Monografie Finali, vol. 8”, Consiglio Nazionale della Ricerca, Quaderni de la Ricerca Scientifica 114, 1-251.

Santacroce, R., Bertagnini, A., Civetta, L., Landi, P., Sbrana, A. 1993. Eruptive dynamics and petrogenetic processes in a very shallow magma reservoir: the 1906 eruption at Vesuvius. J. Petrol. 34, 383-425.

Santacroce, R., Cioni, R., Marianelli, P., Sbrana, A., Sulpizio, R., Zanchetta, G., Donahue, D.J., Joron J.-L., 2008. Age and whole rock–glass compositions of proximal pyroclastics from the major explosive eruptions of Somma-Vesuvius: A review as a tool for distal tephrostratigraphy. J. Volcanol. Geoth. Res. 177, 1-18.

Sartori, F., 1965. Su di una tufite della zona di San Venanzo (Umbria). Atti Società Toscana di Scienze Naturali LXXII, 25-48.

Sartori, R., 1990. The main results of ODP Leg 107 in the frame of Neogene to Recent geology of perityrrhenian areas, in Proceedings ODP ScientificResults, 107 (eds. K.A. Kastens, J. Mascle, C. Auroux et al.), College Station, Texas, (Ocean Drilling Program), 715–730.

Savelli, C., 1967. The Problem of rock assimilation by Somma-Vesuvius magma. I. Composition of Somma and Vesuvius lavas. Contrib. Mineral. Petrol. 16, 328-353.

Savelli, C., 1983. Età K/Ar delle principali manifestazioni riolitiche dell’Isola di Ponza. Rendiconti Società di Mineralogia Petrologia 6. 39-42.

Savelli, C., 1988. Late Oligocene to Recent episodes of magmatism in and around the Tyrrhenian Sea: implications for the processes of opening in a young inter-arc basin of intra-orogenic (Mediterranean) type. Tectonophysics 146, 163-181.

Scaillet, B., Pichavant, M., Cioni, R., 2008. Upward migration of Vesuvius magma chamber over the past 20,000 years. Nature 455, 216-219.

Scaillet ,S., Vita-Scaillet, G., Guillou, H., 2008. Oldest human footprints dated by Ar/Ar. Earth Planet. Sci. Lett. 275, 320-325.

Scandone, R., Bellucci, F., Lirer, L., Rolandi, G., 1991. The structure of the Campanian Plain and the activity of the Neapolitan volcanoes (Italy). J. Volcanol. Geoth. Res. 48, 1-31.

Scarpati, C., Cole, P., Perrotta, A. 1993. The Neapolitan Yellow Tuff — A large volume multiphase eruption from Campi Flegrei, Southern Italy. Bull. Volcanol. 55, 343-356.

Schmidt, M.W., Vielzeuf, D., Auzanneau, E. (2004) Melting and dissolution of subducting crust at high pressures: the key role of white mica. Earth Planet. Sci. Lett. 228, 65–84.

Schiattarella, M., Beneduce, P., 2006. Tectonics and morphostructural evolution of Monte Vulture. In: “La Geologia del Monte Vulture”, C. Principe (edt.), Regione Basilicata, Lavello (PZ) 2006, 17-24.

Scutter, C.R., Cas, R.A.F., Moore, L., De Rita, D. 1998. Voluminous submarine rhyolitic volcanism, Island of Ponza, Italy. J. Geophys. Res. 103, 27551-27566.

Sekine, T., Wyllie, P.J., 1982a. Phase relationships in the system $KAlSiO_4$-Mg_2SiO_4-SiO_2-H_2O as a model for hybridization between hydrous siliceous melts and peridotite. Contrib. Mineral. Petrol. 79, 368-374.

Sekine, T., Wyllie, P.J., 1982b. The system granite-peridotite-H_2O at 30 kbar, with applications to hybridization in subduction zone magmatism. Contrib. Mineral. Petrol. 81, 190-202.

Sekine, T., Wyllie, P.J., 1983. Experimental Simulation of Mantle Hybridization in Subduction Zones. J. Geology 91, 511-528.

Sella, G.F., Dixon, T.H. Mao, A., 2002. REVEL: A model for Recent plate velocities from space geodesy. J. Geophys. Res. 107, 2081-3010.

Selvaggi, G., Amato, A., 1992. Subcrustal Earthquakes in the Northern Apennines (Italy): Evidence for a Still Active Subduction. Geophys. Res. Lett. 19, 21, 2127-2130.

Skora, S., Blundy, J., 2010. High pressure hydrous phase relations of radiolarian clay and implication for the involvement of subducting sediment in arc magmatism. J. Petrol., submitted.

Sigurdsson, H, Carey, S., Cornell, W., Pescatore, T., 1985. The eruption of Vesuvius in 79 AD. National Geographic Res. 1, 332-387.

Sollevanti, F., 1983. Geologic, Volcanologic and tectonic of the Vico-Cimino Area, Italy. J. Volcanol. Geoth. Res. 17, 203-217.

Sottili, G., Palladino, D.M., Marra, F., Jicha, B., Karner D.B., Renne, P., 2010. Geochronology of the most recent activity in the Sabatini Volcanic District, Roman Province, central Italy. J. Volcanol. Geoth. Res. 196, 20-30.

Sparks, R.S.J., 1975. Stratigraphy and geology of the ignimbrites of Vulsini Volcano, Central Italy. Geol. Rundschau 64, 497-523.

Speranza, F., Villa, I.M., Sagnotti, L., Florindo, F., Cosentino, D., Cipollari, P., Mattei M., 2002. Age of the Corsica-Sardinia rotation and Liguro-Provencal Basin spreading: New paleomagnetic and Ar/Ar evidences, Tectonophysics 347, 231– 251.

Steiger, R.H., Jäger, E., 1977. Subcommission on geochronology: Convention on the use of decay constants in geo- and cosmochronology. Earth Planet. Sci. Lett. 36, 359-362.

Stoppa, F., 1988. L’Euremite di Colle Fabbri (Spoleto): un litotipo ad affinità carbonatitica in Italia. Bollettino della Società Geologica Italiana 107, 239-248.

Stoppa, F., 1996. The San Venanzo maar and tuff ring, Umbria, Italy: eruptive behaviour of a carbonatite-melilitite volcano. Bull. Volcan. 57, 563-577.

Stoppa, F., Cundari A., 1995. A new Italian carbonatitic occurrence at Cupaello (Rieti) and its genetic significance. Contrib. Mineral. Petrol. 122: 275-288.

Stoppa, F. Lavecchia, G., 1992. Late Pleistocene ultra-alkaline magmatic activity in the Umbria-Latium region (Italy): An overview. J. Volcanol. Geoth. Res. 52, 277-293.

Stoppa, F., Lupini, L., 1993. Mineralogy and petrology of the Polino monticellite calciocarbonatite (Central Italy). Mineral. Petrol. 49, 213-231.

Stoppa, F., Principe, C., 1997. Eruption style and Petrology of a new carbonatitic suite from the Mt. Vulture Southern Italy/: The Monticchio Lakes formation. J. Volcanol. Geoth. Res. 78, 251-265.

Stoppa, F., Principe, C., Giannandrea, P., 2008. Comments on: Carbonatites in a subduction system: The Pleistocene alvikites from Mt. Vulture (southern Italy) by d'Orazio et al., (2007). Lithos 103, 550-556.

Stoppa, F., Woolley, A.R., 1997. The Italian carbonatites: field occurrence, petrology and regional significance. Mineral. Petrol. 59, 43-67

Suen, C.J., Frey, F.A., 1987. Origins of the mafic and ultramafic rocks in the Ronda peridotite. Earth Planet. Sci. Lett. 85, 183-202.

Sun, S.S., McDonough, W. F., 1989. Chemical and isotopic systematics of oceanic basalts: implications for mantle composition and processes. Geological Society, London, Special Publications 42. 313-345.

Tallini, M., Magaldi, D., Loré, A., Reale, E., Scozzafava, M., 2002. Geologia del Quaternario e pianificazione territoriale della piana in tramontana L’Aquila-Scoppito (Italia-Centrale). GEAM, Ambiente e Sviluppo Sostenibile, Marzo 2002, 55-67.

Taylor. jr J.R., Turi, B., 1976. High-^{16}O igneous rocks from the Tuscan Magmatic Province, Italy. Contrib. Mineral. Petrol. 55, 33-54.

Taylor. jr J.R., Turi, B., 1984. $^{18}O/^{16}O$ and chemical relationships in K-rich volcanic rocks from Australia, East Africa, Antarctica, and San Venanzo-Cupaello, Italy. Earth Planet. Sci. Lett. 69, 33-54.

Thomsen, T.B., Schmidt, M.W. 2008a. Melting of carbonated pelites at 2.5–5.0 GPa, silicate–carbonatite liquid immiscibility, and potassium–carbon metasomatism of the mantle. Earth Planet. Sci. Lett. 267, 17–31.

Thomsen, T.B., Schmidt, M.W. 2008b. Control of the Products of Serpentinization by the $Fe^{2+}Mg^{-1}$ Exchange Potential of Olivine and Orthopyroxene. J. Petrol. 2008 49, 1873-1887.

Tilley, C.E., 1952. Some trends of Basaltic magmas in limestone sintexis. In: Bowen Volume, Am. J. Sci. 529-545.

Traversa, G., Bellotti, P., Evangelista, S., Milli, S., Ronca, S., Traversa, F., Valeri, P., 1991. Preliminary data on melilititic lavas from Carseolani Mountains (Rieti). Periodico Mineralogia, 60, 81-82.

Treves, B., 1984. Orogenic belts as accretionary prisms: the example of the Northern Apennines. Ofioliti 9, 577-618.

Trigila, R., Agosta, E., Currado, C., De Benedetti, A.A., Freda, C., Gaeta, M., Palladino, D.M., Rosa, C., 1995. IV. Petrology. In: “The Volcano of the Alban Hills”, Trigila R. (ed.), Roma 1995, 95-165.

Tommasini, S., Avanzinelli, R., Conticelli, S., 2011. The Th/La and Sm/La conundrum of the Tethyan realm lamproites. Earth Planet. Sci. Lett. 301, 469-478.

Tommasini, S., Heumann, A., Avanzinelli, R., Francalanci, L., 2007. The Fate of High-Angle Dipping Slabs in the Subduction Factory: an Integrated Trace Element and Radiogenic Isotope (U, Th, Sr, Nd, Pb) Study of Stromboli Volcano, Aeolian Arc, Italy. J. Petrol. 48, 2407-2430.

Tropeano, M., Sabato, L., Pieri, P., 2002. Filling and cannibalization of a foredeep: the Bradanic Trough, Southern Italy. Geological Society, London, Special Publications 191, 55-79.

Turbeville, B.N., 1992. $^{40}Ar/^{39}Ar$ Ages and Stratigraphy of the Latera caldera, Italy. Bull. Volcanol. 55, 110-118.

Turbeville, B.N., 1993. Petrology and Petrogenesis of the Latera Caldera, Central Italy. J. Petrol. 34, 77-124

Turi, B., Taylor, H.P. jr., 1976. Oxygen Isotope study of Potassic Volcanic Rocks of the Roman Province, Central Italy. Contrib. Mineral. Petrol. 55, 1-31.

Turi, B., Taylor, H.P. jr., Ferrara, G., 1991. Comparison of $^{18}O/^{16}O$ and $^{87}Sr/^{86}Sr$ in volcanic rocks from the Pontine Islands, M. Ernici, and Campania with other areas in Italy. In: "Stable Isotope Geochemistry: A tribute to Samuel Epstain", H.P. Taylor Jr., J.R. O'Neal and I.R. Kaplan, edts., The Geochemical Society, Special Publication 3, 307-324.

Turner, F.J., Verhoogen, J., 1960. Igneous and metamorphic petrology, New York, McGraw-Hill, 695p.

Turner, S.P., Platt, J.P., George, R.M.M., Kelley, S.P., Pearson, D.G., Nowell, G.M., 1999. Magmatism associated with orogenic collapse of the Betic-Alboran domain, SE Spain. J. Petrol. 40, 1011-1036.

Valensise, G., Pantosti, D., 2001. The investigation of potential earthquake sources in peninsular Italy: A review. J. Seismol. 5, 287-306.

van Bergen, M.J., 1984. Magmas and inclusions of Monte Amiata Volcano, Tuscany, Italy. Geologica Ultraiectina 37, 1- 172.

van Bergen, M.J., Ghezzo, C., Ricci, C.A., 1983. Minette inclusions in the rhyodacitic lavas of Monte Amiata (Central Italy): mineralogical and chemical evidence of mixing between Tuscan and Roman type magmas. J. Volcanol. Geoth. Res. 19, 1-35.

Van der Voo, R, 1993. Paleomagnetism of the Atlantic, Tethys, and Iapetus oceans. Cambridge University Press, 1-413.

Varekamp, J.C., 1980. Vulsinian area, Lazio, Italy. Bull. Volcanol. 43. 489-503.

Varekamp, J.C., Kalamarides, R.I., 1989. Hybridization Processes in Leucite Tephrites From Vulsini, Italy, and the Evolution of the Italian Potassic Suite. J. Geophys. Res. 94: 4603-4618.

Velde, D., 1967. Sur un lamprophyre hyperalkaline potassique: la minette de Sisco (Ile de Corse). Bulletin Societè Francaise Mineralogique et Cristallographique 90, 214-223.

Venturelli, G., Thorpe, R.S., Dal Piaz, G.V., Del Moro, A., Potts, P.J., 1984. Petrogenesis of calc-alkaline, shoshonitic and associated ultrapotassic Oligocene volcanic rocks from Northwestern Alps, Italy. Contrib. Mineral. Petrol. 86, 209-220.

Vezzoli, L., 1988. Island of Ischia - 3. Stratigraphy. In: “Island of Ischia„, Vezzoli L. (edt.), Quaderni de La Ricerca Scientifica 114(10), 93-95.

Vezzoli, L., Conticelli, S., Innocenti, F., Landi, P., Manetti, P., Palladino, D.M., Trigila, R., 1987. Stratigraphy of the Latera Volcanic complex: proposal for a new nomenclature. Periodico Mineralogia 56, 85-110.

Vilardo, G., Terranova, C., Bronzino, G., Giordano, S., Ventura, G., Alessio, G., Gabriele, M., Mainolfi, R., Pagliuca, E., Veneruso, M., 2001. SISCam: Sistema Informativo Sismotettonico della Regione Campania. Laboratorio di Geomatica e Cartografia INGV-OV.

Villa, I.M., 1988. Excess Ar in K-rich volcanites: the role of fluids. Rendiconti Società Italiana di Mineralogia e Petrologia 43, 95-104.

Villa, I.M., 1992. Datability of Quaternary volcanic rocks: an $^{40}Ar/^{39}Ar$ perspective on age conflicts in lavas from the Alban Hills, Italy. Eur. J. Mineral. 4, 369-383.

Villa, I.M., Buettner, A., 2009. Chronostratigraphy of Monte Vulture volcano (southern Italy): secondary mineral microtextures and $^{39}Ar/^{40}Ar$ systematics. Bull. Volcanol. 71, 1195-1208.

Villa, I.M., Calanchi, N., Dinelli, E., Lucchini, F., 1999. Age and evolution of the Albano crater lake (Roman Volcanic Province). Acta Vulcanologica 11 (2), 305-310.

Villa, I.M., Giuliani, O., De Grandis, G., Cioni, R., 1989. Datazioni K/Ar dei vulcani di Tolfa e Manziana (in Italian). Bollettino Gruppo Nazionale di Vulcanologia 5, 1025-1026.

Villa, I.M., Serva, L., Quercioli, C., 1991. Verso una datazione della lava di Cupaello (Rieti). Plinius 4, 102-102.

Villemant, B., 1988. Trace element evolution in the Phlegrean Fields (Central Italy) : fractional Crystallization and selective enrichment. Contrib. Mineral. Petrol. 98. 169-183.

Villemant, B., Fléhoc, C., 1989. U/Th fractionation by fluids in K-rich magma genesis: the Vico volcano, Central Italy. Earth Planet. Sci. Lett. 91, 312-326.

Villemant B., Palacin P. (1987). Différenciation magmatique et mécanismes de concentration de l'uranium: exemple du volcanisme du Latium (Italie centrale). Bullétin Mineralogique.

Villemant, B., Trigila, R., De Vivo, B., 1993. Geochemistry of Vesuvius volcanics during 1631-1944 period. J. Volcanol. Geoth. Res. 58, 291-313.

Viola, C., 1896. Mineralogische und Petrographische Mittheilungen aus dem Hernikerlande in der Provinz Rom (Italien). N. Jahrb. Mineral. Geol. Päleont.

Viola, C., 1902. I principali tipi di lave dei vulcani Ernici (Prov. Di Roma). Tipografia Nazionale di G. Bertero e C., Via Umbria, Roma. 1-24.

Vollmer, R. 1976. Rb-Sr and U-Pb-Th systematics of alkaline rocks: the alkaline rocks from Italy. Geoch. Cosmochim Acta 40, 283-295.

Vollmer, R., 1977. Isotopic evidence for Genetic Relations between Acid and Alkaline Rocks in Italy. Contrib. Mineral. Petrol. 60, 109-118.

Vollmer, R., 1989, On the Origin of the Italia Potassic Magmas. 1. a discussion contribution. Chem. Geol. 74, 229-239.

Vollmer, R., Hawkesworth, C.J., 1980. Lead isotopic composition of the potassic rocks from Roccamonfina (South Italy). Earth Planet. Sci. Lett. 47, 91-101.

Vollmer, R., Johnston, K., Ghiara, M.R., Lirer, L., Munno, R., 1981. Sr-isotope geochemistry of megacrysts from continental rift and converging plate margin alkaline volcanism in South Italy. J.Volcanol.Geoth.Res. 11, 317-327.

Voltaggio, M., Andretta, D., Taddeucci, A., 1994. 230Th-238U data in conflict with $^{40}Ar/^{39}Ar$ leucite ages for quaternary volcanic rocks of the Alban Hills, Italy. Eur. J. Mineral. 6, 209-216.

Von Blanckenburg, F., Kagami, H., Deutch, A., Oberli, F., Meier, M., Wiedenbeck, M., Barth, S., Fische,r H, 1998. The origin of the Alpine plutons along the periadriatic lineament. In Zingg A., Hunziker, J.C., Frey M., Arendt H. (1976) Age and degree of metamorphism of the Canavese Zone and the Sedimentary cover of the Sesia Zone. Schweiz. Mineral. Petrograp. Mitt. 78, 55-66.

Wade, A., Prider, R.T., 1940. The Leucite bearing-rocks of West Kimberley area, Western Australia. Quart. J. Geol. Soc. London 96, 39-98.

Wagner, C., Velde, D., 1986. The mineralogy of K-richterite bearing lamproite. Am. Mineral. 71, 17-37.

Ward, S.N., 1994. Constraints on the seismotectonics of the Central Mediterranean from Very Long-Base-Line Interferometry. Geophys. J. Intern. 117, 441-452.

Washington, H.S., 1906. The Roman Comagmatic Region. Carnegie Institution of Washington 36, 1-220.

Watkins, S.D., Giordano, G., Cas, R.A.F., De Rita, D., 2002. Emplacement processes of the mafic Villa Senni Eruption Unit (VSEU) ignimbrite succession, Colli Albani volcano, Italy. J. Volcanol. Geoth. Res. 118, 173-203.

Watts, M.D., 1987. Geothermal exploration of Roccamonfina volcano, Italy. Geothermics 16, 527-528.

Wendlandt, R.F., Eggler, D.H., 1980a. The origin of potassic magmas: 1. Melting relations in the systems $KAlSiO_4$-Mg_2SiO_4-SiO_2 and $KAlSiO_4$-MgO-SiO_2-CO_2 to 30 kb. Am. J. Sci. 280, 385-420.

Wendlandt, R.F., Eggler, D.H., 1980b. The origin of potassic magmas: 2. Stability of phlogopite in natural spinel lherzolite and in the system $KAlSiO_4$-MgO-SiO_2-H_2O-CO_2 at high pressure and high temperature. Am. J. Sci. 280, 421-458.

Westerman, D.S., Innocenti, F., Tonarini, S., Ferrara G., 1993. The pliocene intrusions of the island of Giglio. Memorie Società Geologica Italiana 49, 345-363.

Westaway, R., Jackson, J., 1984. Surface faulting in the southern Italian Campania-Basilicata earthquake of 23 November 1980. Nature 312, 436 – 438.

Wohletz, K., Orsi, G., de Vita, S. 1995. Eruptive mechanisms of the Neapolitan Yellow Tuff interpreted from stratigraphie, chemical, and granulometric data. J. Volcanol. Geoth. Res. 67, 263-290.

Wood, D.A., 1979. A variably veined suboceanic upper mantle —Genetic significance for mid-ocean ridge basalts from geochemical evidence. Geology 7, 499-503.

Woolley, A.R., Bailey, D.K., Castorina, F., Rosatelli, G., Stoppa, F., Wall, F., 2005. Reply to: "Carbonate-rich pyroclastic rocks from central Apennines: carbonatites or carbonated rocks? A commentary". A. Peccerillo, p.183-194. Periodico Mineralogia 74, 195-204.

Wortel, M.J.R., Spakman W., 2000. Subduction and Slab Detachment in the Mediterranean-Carpathian Region. Science 290, 1910-1917.

Wulf, S., Kraml, M., Brauer, A., Keller, J., Negendank, J.F.W., 2004. Tephrochronology of the 100 ka lacustrine sediment record of Lago Grande di Monticchio (Southern Italy). Quaternary International 122, 7-30.

Wyllie, P.J., Sekine, T., 1982. The formation of mantle phlogopite in subduction zone hybridization. Contrib. Mineral. Petrol. 79, 375-380.

Yaxley, G.M., Green, D.H., 1994. Experimental demonstration of refractory carbonate-bearing eclogite and siliceous melt in the subduction regime. Earth Planet. Sci. Lett. 128, 313-325.

Yoder, H.S. Jr, 1973. Melilite stability and paragenesis. Fortschritte der Mineralogie 50, 140-173.

Yoder, H.S. Jr., 1979. Melilite-bearing rocks and related lamprophyres. In: The Evolution of the Igneous rocks: fiftieth anniversary perspective, Princeton University Press, 391-411.

Yoder, H.S. Jr., 1986. Potassium-rich Rocks: Phase Analysis and Heteromorphic Relations. J. Petrol. 27, 1215-1228.

Zanetti, A., Mazzucchelli, M., Rivalenti, G., Vannucci, R., 1999. The Finero phlogopite-peridotite massif: an example of subduction-related metasomatism. Contrib. Mineral. Petrol. 134, 107-122,

Zanon, V., 2005. Geology and Volcanology of San Venanzo volcanic field (Umbria, Central Italy). Geol. Mag. 142, 683-698.

Zindler, A., Hart S., 1986. Chemical geodynamics, Annu. Rev. Earth Planet. Sci. 14, 493–571.